UNIVERSITY OF LONDON THESIS

Degree PhD Year 2007 Name of Author SUTTON, Liza Marie

TOWARDS THE DEVELOPMENT OF A CELL LINE STABLY PROPAGATING HUMAN PRIONS

by
Liza Marie Sutton

Department of Neurodegenerative Disease
Institute of Neurology
University College London

May 2007

A thesis presented in partial fulfilment of the requirements for the degree of Doctor of Philosophy to the University of London

Supervisors: Dr Sarah Tabrizi
Professor Parmjit Jat

ProQuest LLC
789 East Eisenhower Parkway
P.O. Box 1346
Ann Arbor, MI 48106-1346

ABSTRACT

Prion diseases are neurodegenerative disorders affecting both animals and humans. They may be sporadic, infectious or genetic in origin. Variant CJD (vCJD) is a novel form of human prion disease, experimentally proven to be acquired from the consumption of bovine prion-infected material. The causative transmissible agent of prion disease is thought to consist predominantly of an abnormal isoform of the host-encoded prion protein (PrP^{C}), designated PrP^{Sc}. To date, most prion research has been undertaken in animal models since transmitting the disease in cell culture has proved difficult. Nevertheless, a number of prion-propagating mammalian cell lines do exist but despite world-wide effort, no cell lines have shown susceptibility to human prion infection. The aim of this thesis was to develop a cell line that stably propagated vCJD prions.

First, a high-throughput screening methodology for detection of human prions in cells was established. This involved subcloning of vCJD prion-infected cell lines, in order to isolate a rare susceptible clone, followed by detection of PrP^{Sc} using the scrapie cell assay or cell blot assay. A panel of cell lines was selected to best mimic *in vivo* disease and screened for susceptibility to vCJD prion infection, but mammalian neuroblastoma, neuroglial, and epithelial cell lines were unable to stably propagate human prions. Transient vCJD prion propagation (between one and six passages) was observed in two human neuroblastoma lines (SKN-SH and SHSY5Y) and a rabbit epithelial kidney line (RK13) overexpressing human PrP^{C}. Attempts to prolong prion propagation in a human neuroblastoma cell line with retroviral infection, to mimic the intercellular spread of prions via exosomes, were unsuccessful. The second approach involved the humanisation of a mouse prion-propagating cell line, N2a. To eliminate dominant-negative inhibition of human prion propagation by murine PrP^{C}, the endogenous PrP^{C} was knocked-out using RNAi technology. Greater than 90% murine PrP^{C} knockout was achieved in several N2a-derived lines and exogenous expression of mouse PrP^{C} demonstrated that these cells were still susceptible to mouse prion infection. Human PrP^{C} was subsequently expressed in these murine PrP^{C} knockout lines to various levels. Following infection with vCJD prions, no long-term vCJD prion propagation was observed in these lines. A single murine PrP^{C} knockout line overexpressing human PrP^{C} (two-fold) transiently propagated vCJD prions but this was not stable. The third approach used a v-myc immortalised human foetal neural stem cell (NSC) line derived from human ventral mesencephalon (ReNcell 197VM). These undifferentiated 197 cells were resistant to vCJD prion infection. Upon differentiation, the 197 cultures acquired a neuronal phenotype. Infection with a purified vCJD prion-infected brain homogenate yielded propagation of vCJD prions in these differentiated human neurons for >40 days *in vitro*. This work has improved understanding of the complex factors underlying cellular susceptibility to prion infection. The primary human

neuronal model will be invaluable for the study of the pathophysiology of human prion disease.

DECLARATION

I, Liza Sutton, hereby declare that this thesis is a presentation of my own research work. However, the development of a cellular model of human prion disease was a team project on which I worked with two other research assistants headed by Dr Sarah Tabrizi and funded by a Department of Health program grant. Therefore, in order to present a complete story I have included several experiments carried out by other team members and collaborators. Whenever this was the case, I have made every effort to acknowledge it in the text but key contributions are highlighted below:

In chapter 3, Jennifer Podesta (DND) and I worked equally on SCA of vCJD prion-infected RK13 cells.

In chapter 4, Parineeta Arora (DND) performed siRNA transductions to knockout murine PrP in PK1 cells, the subsequent exogenous murine PrP transductions of these KO cells and RML prion infections. Jennifer Podesta (DND) performed the real-time PCR assays to quantify *Prnp* knockdown.

In chapter 5, electrophysiological study of differentiated 197 cells was performed by Dr. Roberta Donato (UCL) and their ultrastructural analysis by transmission electron microscopy was performed by Dr Alison Wood-Kaczmar (DND).

ACKNOWLEDGEMENTS

First and foremost, I would like to thank my supervisor, Dr Sarah Tabrizi, for both academic and personal support over the last five years. The "human cell model" project has certainly been challenging but we would not have made such progress without Sarah's unfailing enthusiasm and drive! Jennifer Podesta and Dr Ralph Andre, past and present members of the "human cell model" group, deserve a special mention for their hard work and dedication to the project and for some of the data presented in this thesis. I would like to acknowledge other members of the MRC Prion Unit/Department of neurodegenerative disease (DND) for their intellectual and practical support of work presented in this thesis: Professor Parmjit Jat and Parineeta Arora for their contribution to the RNAi project (chapter 4), Dr Jonathan Wadsworth and Dr Peter Klohn for experimental advice and reading drafts of my thesis. I would also like to acknowledge ReNeuron Ltd. for the provision of the ReNcell 197VM neural stem cell line and to thank Dr Erik Miljan, in particular, for sharing his stem cell expertise. Thanks also to the Department of Health for funding and to the kindness of the vCJD patients and families for tissue donation, without both of which this project would not have been possible. I am also very grateful to Ray Young for his very capable and calm assistance with the figures in this thesis.

My gratitude extends to the many members of the "Prion Unit", who over the years have provided me with support and distraction to cope with the trauma of studying for a PhD. A special mention goes to the fabulous "Team Tabrizi"- Dr Ralph Andre, Pelagia Deriziotis, Dr Mark Kristiansen, Dr Alison Wood-Kaczmar and Dr Sonia Gandhi. Kevin Williams, of course, warrants acknowledgement for gallantly letting me beat him at tennis *every* time!

I certainly would not have maintained my sanity through this period of my life without the love and support of my very precious friends and family. Particular thanks to Kev, for your pragmatic advice and superb distraction techniques, to Lucy for our cake rendez-vous' and to my amazing Mum, Dad and sister, Zoe, for always believing in me.

For my beautiful Mummy for teaching, inspiring and loving me

INDEX **PAGE**

TABLE OF CONTENTS

CHAPTER 1 - Introduction

CHAPTER 2 – Materials and methods

LIST OF TABLES

LIST OF FIGURES

ABBREVIATIONS

°C	degrees Celsius
Ab	antibody
AEBSF	4-(2-aminoethyl)-benzonase sulfonyl fluoride
AP	alkaline phosphatase
ATCC	American Type Culture Collection
bFGF	basic fibroblast growth factor
bp	base pairs
BSA	bovine serum albumin
BSE	bovine spongiform encephalopathy
CBA	cell blot assay
cDNA	complementary deoxyribose nucleic acid
CJD	Creutzfeldt-Jakob disease
cm	centimetre
CNS	central nervous system
CNTF	ciliary neurotrophic factor
CWD	chronic wasting disease
DAPI	4', 6-diamino-2-phenylindole
ddH_2O	double distilled water
DMEM	Dulbecco's modified eagle medium
DMSO	dimethylsulphoxide
DNA	deoxyribose nucleic acid
DND	Department of Neurodegenerative Disease, UCL
dNTP	deoxynucleotide triphosphates
ECACC	European Collection of Cell Cultures
ECL	enhanced chemiluminescence
EDTA	ethylene diamine tetra-acetic acid
EEG	electroencephalogram
EGF	epidermal growth factor
ELISA	enzyme-linked immunosorbant assay
ER	endoplasmic reticulum
ERAD	ER-associated degradation (of proteins)
FBS	fetal bovine serum
FGF	fibroblast growth factor
FITC	fluoroscein isothiocyanate
g	gram
GABA	gamma-aminobutyric acid

GAPDH	glyceraldehyde-3-phosphate dehydrogenase
GFAP	glial fibrillary acidic protein
GPI	glycophosphatidylinositol
h	hour(s)
HBSS	Hank's Balanced Salt Solution
HIV	Human immunodeficiency virus
HRP	horseradish peroxidase
HSC	haemopoietic stem cell
iCJD	iatrogenic CJD
IFN	interferon
Ig	immunoglobulin
kb	kilobase
kDa	kilodalton
KO	knockout
L or l	litre
log	logarithm to base 10
M	molar
m	metre
min	minute(s)
MM	homozygous at codon 129 *PRNP* for methionine
mRNA	messenger ribonucleic acid
MuLV	Moloney murine leukaemia virus
MV	heterozygous at codon 129 *PRNP* for methionine and valine
MW	molecular weight
NGF	nerve growth factor
NGS	normal goat serum
NMR	nuclear magnetic resonance
NSC	neural stem cell
Nt	nucleotide
OD	optical density
ORF	open reading frame
P	probability
p-	phospho-
PAGE	polyacrylamide gel electrophoresis
PBS	phospho-buffered saline
PCR	polymerase chain reaction
PFA	paraformaldehyde
pH	hydrogen ion concentration

PK	Proteinase K
PMSF	phenylmethylsulphonyl fluoride
PNS	peripheral nervous system
PrP	prion protein
PrP^{C}	cellular prion protein
PrP^{Sc}	disease-associated prion protein
PRNP	gene encoding human prion protein
Prnp	gene encoding mouse prion protein
PVDF	polyvinylidene difluoride
qRT-PCR	quantitative real-time PCR
RML	Rocky Mountain Laboratory (mouse-adapted scrapie prion strain)
RNA	ribonucleic acid
rcf	relative centrifugal force
RNAi	RNA interference
rpm	revolutions per minute
RT	room temperature
SCA	scrapie cell assay
sCJD	sporadic Creutzfeldt-Jakob disease
SD	standard deviation
SDS	sodium dodecyl sulphate
sec	second(s)
SEM	standard error of the mean
STI1	stress-inducible protein-1
TAB	Tropix assay buffer
TME	transmissible mink encepahlopathy
TSE	transmissible spongiform encephalopathy
UCL	University College London
UTR	untranslated region
V	volts
vCJD	variant Creutzfeldt-Jakob disease
v/v	volume/volume
w/v	weight/volume
<u>prefixes</u>	
k-	kilo
m-	milli-
µ-	micro-
n-	nano-
p-	pico

Chapter 1

Introduction

1 Introduction

Prion diseases or transmissible spongiform encephalopathies (TSEs) are fatal, currently incurable neurodegenerative conditions affecting both humans and animals. Although these diseases are rare, they have attracted much attention due to the unique biology of the transmissible agent. The transmissible agent, designated the prion (PrP^{Sc}), is unlike other infectious pathogens since it is composed either exclusively or principally of proteinacious material devoid of nucleic acid. The prion is believed to be a conformational isomer of the host-encoded prion protein (PrP^{C}), and is self-propagating. Neuropathological hallmarks shared by these diseases are spongiform vacuolation of cerebral grey matter, neuronal loss, astrocytic proliferation and often, amyloid deposition of disease-associated prion protein (PrP^{Sc}). The diseases are characterised clinically by long incubation times and a combination of dementia and neurological symptoms.

1.1 Prion diseases in animals

1.1.1 Scrapie

Scrapie is the prototypic animal prion disease, which naturally affects both sheep and goats. It was first described in the UK over 250 years ago but is now present worldwide (with the exception of Australasia). In the 18th and 19th centuries, scrapie was suspected to be hereditary because of a strong genetic element to the disease, for example, scrapie affects only certain breeds (Parry, 1979). However, the contagious nature of scrapie was first demonstrated experimentally by inoculation into goats (Cuillé and Chelle, 1936). Since then it has been experimentally transmitted to other species, including mice (Chandler, 1961). The mode of natural transmission is thought to be lateral, perhaps via shedding in faeces and saliva (Ryder et al., 2004).

Scrapie derives its name from one of the main symptoms, pruritis or itching, which causes animals to scrape themselves against objects leading to wool loss and skin damage. Additional early symptoms include excitability and apprehension. As the disease progresses, the animals develop gait disorders, tremor of the head and neck and eventual prostration. Death usually occurs six weeks to six months after symptom onset.

1.1.2 Transmissible mink encephalopathy

Transmissible mink encephalopathy (TME) was first detected in farmed mink at a ranch in Winsconsin in 1947. This outbreak was attributed to a BSE-contaminated food source but it can also occur as a result of scrapie-infected feed (Marsh et al., 1991). The disease has been observed in the US, Canada, Russia, Finland and Germany. Symptoms include aggression, loss of muscle

coordination and increased tendency to bite. The disease course is rapid, lasting at most six weeks before death.

1.1.3 Chronic wasting disease

Chronic wasting disease (CWD) was first recognised as a clinical syndrome in elk, mule deer and white-tail deer in the 1960s. It affects both captive and wild cervid populations across North America and Canada and, like scrapie, transmission is thought to be lateral, through saliva and blood (Miller and Williams, 2003;Mathiason et al., 2006). Symptoms include weight loss, somnolence and excessive drinking (polydypsia). The disease course ranges from days to months. Despite considerable concern in the USA and Canada, there is no current evidence of transmission to humans.

1.1.4 Bovine spongiform encephalopathy

The most notorious TSE to emerge to date is bovine spongiform encephalopathy (BSE) or "mad cow disease". It was probably present in the UK cattle population in the 1970s and early 1980s, however, due to long incubation times of prion disease, the first case was not recognised until November 1986. This marked the onset of an epidemic that devastated the British cattle industry, with an estimated one million cows affected (Anderson et al., 1996). The BSE epidemic peaked in 1992 when 850 cattle were being diagnosed every week; currently (2007) fewer than 4 cattle a week are affected by BSE (http://www.BSE review.org.uk). The origin of BSE remains elusive but two theories have been proposed. (1) It arose from the consumption by cattle of scrapie-infected sheep carcasses, though this is unlikely because scrapie and BSE are caused by different prion strains (Bruce et al., 1994) or (2) from sporadic BSE as a result of a stochastic conformational change in the bovine prion protein (Weissmann and Aguzzi, 1997). The epidemic was sustained by use of meat and bone meal (MBM) from BSE-infected cattle in their feed. The reason the BSE epidemic was confined to the UK may be due to changes in farming practices between 1970 and 1988. A reduction in solvent concentration was used in the rendering process, which may have lead to increased infectivity in MBM. Furthermore, artificially-reared dairy calves were fed MBM at a particularly susceptible age; 1-2 weeks (Wilesmith et al., 1988). The epidemic was halted by implementation of stringent control measures in 1988. Affected and at-risk herds were culled on a huge scale and a ban preventing the feeding of ruminant-derived proteins back to ruminants was introduced. Since its description in the UK, BSE has been reported in cattle throughout Europe, in the US, Canada, Israel and Japan (http://www.BSE review.org.uk).

1.1.5 Feline and ungulate spongiform encephalopathy

The emergence of feline spongiform encephalopathy (FSE) in cats, spongiform encephalopathies of exotic ungulates (including nyala and oryx) at zoological parks (Bruce et al., 1994) and new variant CJD in humans (Collinge and Rossor, 1996;Bruce et al., 1997;Hill et al., 1997a) has been attributed to BSE. The ability of the BSE prion strain to transmit to several different species has identified it as a highly promiscuous prion strain.

1.2 Human prion diseases

Human prion diseases are rare disorders with an incidence of approximately 1-2 per million worldwide per annum, with an equal incidence of disease in men and women. They have the unique characteristic of being inheritable, sporadic or acquired in origin, and all are transmissible. The most common human prion disease is Creutzfeldt-Jakob disease (CJD), named after the two doctors who independently first described the disorder; Creutzfeldt in 1920 and Jakob in 1921. The disease is characterised clinically by a rapid onset neurological degeneration causing chronic decline in motor and cognitive function. Definitive diagnosis of prion disease across species can be made from post-mortem examination of brain tissue showing spongiform degeneration of the grey matter (resulting from neuronal vacuolation and loss), gliosis and absence of an immune reaction. Although it is by no means a constant feature, some prion diseases including kuru and GSS, are characterised by deposition of amyloid plaques composed of insoluble aggregates of the disease-associated prion protein, PrP^{Sc}. Fatal familial insomnia (FFI) is characterised neuropathologically by the absence of PrP^{Sc} plaque deposition (Collinge et al., 1995b). The human PrP gene (PRNP) exists in two major allelic forms that encode either methionine or valine. There is marked genetic susceptibility for the development of human prion disease at this polymorphic codon 129 of the prion protein. The majority of human prion disease cases are homozygous for either methionine (129MM) or valine (129VV), which occur in 37% and 12% of the Caucasian population, respectively (Owen et al., 1990). Codon 129 heterozygotes (129MV), which make up 51% of the Caucasian population, are relatively protected from protecting prion disease (Palmer et al., 1991;Collinge et al., 1991;Windl et al., 1996). The susceptibility of methionine homozygotes may be explained by increased propensity of PrP to form PrP^{Sc}-like structures *in vitro* (Tahiri-Alaoui et al., 2004). Codon 129 heterozygosity is thought to confer resistance to prion disease by inhibiting homologous prion protein-protein interactions (Palmer et al., 1991).

1.2.1 Sporadic prion disease

85% of human prion diseases are sporadic in origin. The most common is sporadic CJD (sCJD), of which there are 50-60 cases in the UK every year. The cause of sCJD is unknown but the theory

favours a spontaneous change in PrP structure or a somatic *PRNP* mutation that leads to production of the abnormal form of the prion protein. It remains possible, but less likely, that sCJD is an acquired illness due to unidentified environmental prion protein exposure, since two case-control studies have reported prior surgery as a risk factor for sCJD (Collins et al., 1999;Ward et al., 2002). The disease affects adults mostly commonly aged between 45 to 75 years, with the median age of death being 67 years (Will RG et al., 2004). The majority of cases follow a relatively uniform and aggressive course. Patients present with a rapidly progressive dementia, accompanied by symptoms including myoclonus, cerebellar ataxia and cortical blindness. Median duration of illness is 4 months. The disease culminates in an akinetic mute state and death is typically caused by a pulmonary or systemic infection.

1.2.2 Inherited Prion Disease

10-15% of human prion diseases are Mendelian autosomal dominantly inherited conditions with high penetrance, which cause five deaths in the UK per year. Inherited prion diseases are associated with mutations in the gene encoding the prion protein, *PRNP*, of which more than thirty have been described (**figure 1.1**) leading to a wide range of clinical syndromes between and within kindreds (Collinge, 2001). The fact that a single *PRNP* mutation can elicit different disease phenotypes underscores the importance of factors additional to the prion protein sequence in prion disease pathogenesis, such as environmental and epigenetic factors. Pre-symptomatic genetic diagnosis of inherited prion disease is possible from DNA sequencing of *PRNP* from blood samples.

Inherited prion disease includes syndromes such as fatal familial insomnia (FFI), a rare disorder observed in several Italian kindreds (Medori et al., 1992). It is caused by the substitution of asparagine with an aspartate residue at codon 178 of the prion protein (D178N). The disease affects adults from 30-50 years of age. It causes focal neuronal degeneration in the thalamus resulting in progressive insomnia, panic attacks, hallucinations, weight loss, dementia, and eventually ending in an akinetic mute state over the course of seven months to three years. The most common cause of inherited prion disease is a *PRNP* point mutation at codon 200, which results in the substitution of glutamate (E) with lysine (K) (Kahana and Zilber, 1991). This E200K *PRNP* mutation has been identified in families from Slovakia (Goldfarb et al., 1990), Chile (Goldfarb et al., 1991) and the US (Bertoni et al., 1992). The high incidence of CJD in a group of Israeli Jews of Libyan origin was mistakenly attributed to the consumption of lightly cooked sheep brain and eyeballs until the E200K mutation was eventually identified (Kahana et al., 1974).

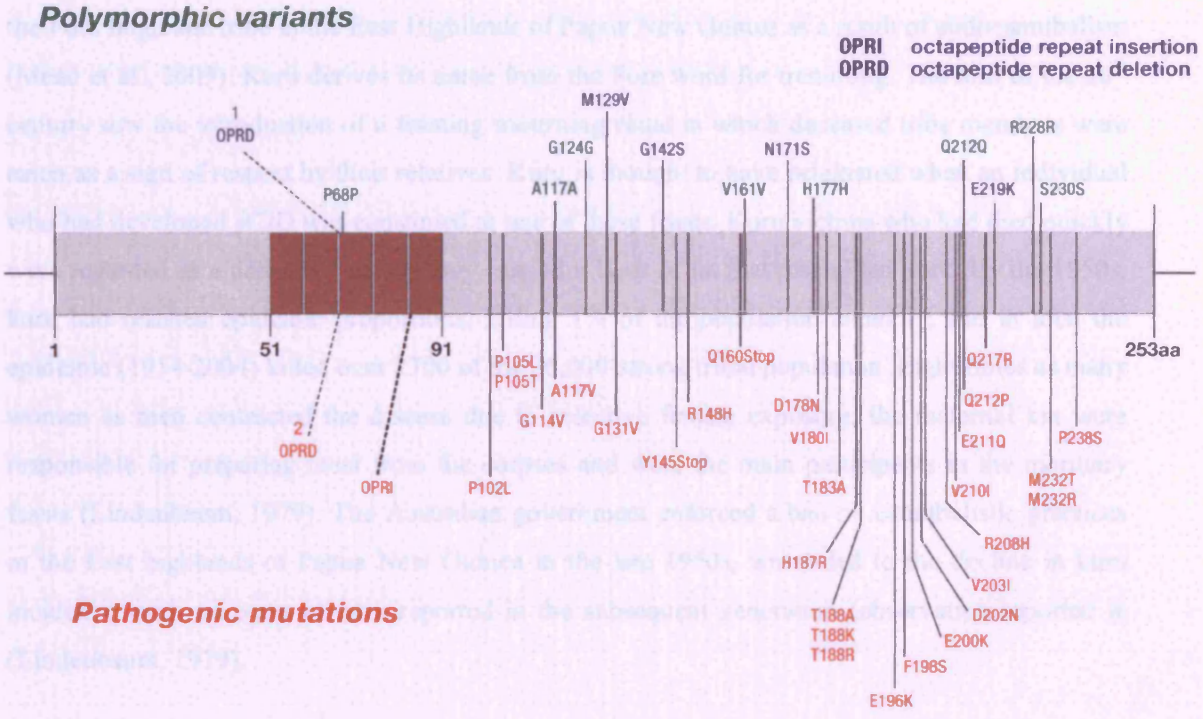

Figure 1.1 Pathogenic mutations and polymorphic variants of human PrP

Definite or suspected pathogenic mutations are shown below the representation of the prion protein. Neutral (green) and disease modifying/susceptibility (blue) polymorphisms are shown above. *Figure modified from Mead, 2006.*

1.2.3 Acquired prion diseases

1.2.3.1 Kuru

Kuru represents the largest group of acquired human prion diseases. It emerged in about 1920 in the Fore linguistic tribe in the East Highlands of Papua New Guinea as a result of endocannibalism (Mead et al., 2003). Kuru derives its name from the Fore word for trembling. The turn of the 20th century saw the introduction of a feasting mourning ritual in which deceased tribe members were eaten as a sign of respect by their relatives. Kuru is thought to have originated when an individual who had developed sCJD was consumed at one of these feasts. Kuru victims who had died quickly were regarded as a delicacy because they carried a layer of fat that resembled pork. By the 1950s, kuru had reached epidemic proportions, killing 1% of the population annually, and in total the epidemic (1954-2004) killed over 2700 of the 36,000-strong tribal population. Eight times as many women as men contracted the disease due to selective female exposure; the maternal kin were responsible for preparing meat from the corpses and were the main participants in the mortuary feasts (Lindenbaum, 1979). The Australian government enforced a ban on cannibalistic practices in the East highlands of Papua New Guinea in the late 1950s, which led to the decline in kuru incidence, with no cases of kuru reported in the subsequent generation (observation reported in (Lindenbaum, 1979).

Kuru is a cerebellar syndrome progressing through several clinical stages, involving ataxia, dysarthria and dementia in terminal stages with a mean clinical duration of 12 months (Alpers, 1987). Neuropathologically, the disease is characterised by kuru-like plaques in the brain, which are PrP^{Sc}-positive plaques with a dark eosiniphilic centre and pale periphery. The mean incubation period of kuru is estimated to be 12 years (Collinge, 1999). However, in the most susceptible genotype (codon 129 MM), the shortest disease incubation time estimates were between 4 and 5 years (Collinge et al., 2006), and disease onset was estimated to occur 11 years earlier than in heterozygotes (Cervenakova et al., 1999). Some individuals of the most resistant genotype (codon 129 MV) exhibited incubation times of over 50 years (Collinge et al., 2006). Kuru is the only known example of a major human prion disease epidemic and therefore serves as an important model on which to study acquired human prion disease (see vCJD section - **1.2.3.3**).

The kuru epidemic has had a strong genetic effect on the present-day Fore population, essentially eliminating *PRNP* codon 129 homozygotes (who are most susceptible to prion disease). A study of surviving elderly Fore women (over the age of 50), found that *PRNP* codon 129 heterozygotes

were more common in those who had attended multiple mortuary feasts than those who remained unexposed to kuru (Mead et al., 2003). Since heterozygosity at the codon 129 polymorphism in *PRNP* confers resistance to prion disease, there was selection pressure in favour of these alleles in the Fore tribe. Studies of global haplotype diversity and allele frequency of coding and non-coding polymorphisms of *PRNP* (in which there is more variability than expected because of heterozygote advantage) suggest balancing selection pressure at this locus may have been imposed by several prion disease epidemics in human prehistory (King et al., 2003).

1.2.3.2 Iatrogenic CJD

Iatrogenic CJD (iCJD) arises when human prion disease, of any form, is transmitted from one person to another accidentally by medical or surgical intervention. The infectious nature of CJD and kuru was confirmed in the 1960s when both were transmitted experimentally to chimpanzees (Gajdusek et al., 1966;Gibbs, Jr. et al., 1968). Over 200 cases of iCJD have been reported to date, most commonly following dura mater implants and human growth hormone injections. Other sources of infection include contaminated human cadaveric corneal transplants and gonadotrophin injections. Prions are not inactivated by normal hospital sterilisation procedures, therefore inadequately sterilised surgical and medical equipment, such as intracerebral EEG electrodes, can also cause iCJD (Brown et al., 2000). Preventative measures include use of recombinant growth hormone and incineration of surgical instruments from confirmed CJD patients.

1.2.3.3 Variant CJD

The most recent TSE to be described is variant CJD (vCJD): a novel clinicopathological form of CJD that emerged in the UK in 1996 as a result of dietary exposure to BSE (Will et al., 1996). To date there have been 158 deaths from vCJD in the UK, and nearly 30 cases identified overseas, including France, USA and Spain (http://www.cjd.ed.ac.uk/figures.htm: March 2007).

The age of onset of vCJD varies considerably from 12-74 years and notably affects young individuals. The typical presenting symptoms are psychiatric or behavioural in nature, often involving depression, social withdrawal and anxiety. Painful sensory symptoms may also be present, possibly as a result of thalamic damage. Cognitive impairment, ataxia and myoclonus, often early symptoms in classical CJD, occur towards the later stages of the disease. Like sCJD the disease terminates with an akinetic mute state. Mean survival is 13.5 months, longer than for sCJD, and median age of death is 28.5 years.

Distinguishing neuropathological features of vCJD are spongiform degeneration, predominantly in the basal ganglia and cerebellum, and concentrated PrP^{Sc} accumulation in so-called "florid

plaques" (Will et al., 1996). The florid plaques of vCJD are similar to dense PrP^{Sc}-positive kuru plaques but they are surrounded by vacuolated tissue (**figure 1.2**). Unlike other human prion diseases, PrP^{Sc} can be also detected outside the CNS, most notably in lymphoreticular tissue (tonsils, spleen and lymph nodes etc.), but also in ocular tissue and skeletal muscle (Wadsworth et al., 2001;Peden et al., 2006). vCJD has also recently been transmitted from human rectal tissue to transgenic mice (Wadsworth et al., 2006).

Several lines of evidence support the fact that vCJD is caused by dietary exposure of humans to BSE. First, epidemiological data demonstrate that those affected by vCJD were resident in the UK during the BSE epidemic (Will et al., 1996;Collinge and Rossor, 1996). Second, transmission studies in both humanised transgenic and wild-type mice showed a close correlation in disease pathology between vCJD and BSE (Bruce et al., 1997;Hill et al., 1997a). Third, molecular strain typing analysis of the disease-associated prion protein, which involves assessment of SDS-PAGE migration patterns of PrP following protease digestion (see section **1.5.3.1**), demonstrated that vCJD prions are a distinct strain of prion compared to other forms of CJD; type 1-3 (**figure 1.3**). The novel vCJD prion strain was designated type 4 and exhibited the same SDS-PAGE signature as BSE; with the majority of PrP being glycosylated at two sites (Collinge et al., 1996). Premortem diagnosis of vCJD is determined from tonsil biopsy by the presence of type 4 PrP^{Sc} on immunoblot (Hill et al., 1999).

The incidence of vCJD remains low and appears to be in decline following control of the BSE epidemic and BSE-infected foodstuff entering the human food chain. The number of deaths per year peaked at 28 in 2000 and fell to 5 in 2005. However, basing estimations of the eventual size of a vCJD epidemic on the number of current cases may be misleading for several reasons. First, almost all individuals who have developed vCJD to date are of the most susceptible genotype; methionine homozygous at codon 129 of *PRNP* (Collinge, 2005). Evidence derived from iCJD cases (Huillard d'Aignaux et al., 1999), the kuru epidemic (Collinge et al., 2006) and humanised transgenic mice (Poulter et al., 1992;Lloyd et al., 2002) indicates BSE may transmit to other *PRNP* codon 129 genotypes (MV and VV), albeit with longer incubation periods. The mean incubation period for human-to-human prion transmission, based on kuru and iatrogenic CJD data, is estimated to be around 12 years (Brown et al., 1992;Collinge, 1999). Since human infection with BSE prions involves a species barrier (see section **1.5.4**), one would expect an increased mean and range of incubation period for vCJD. Based on a three-fold increase in incubation period

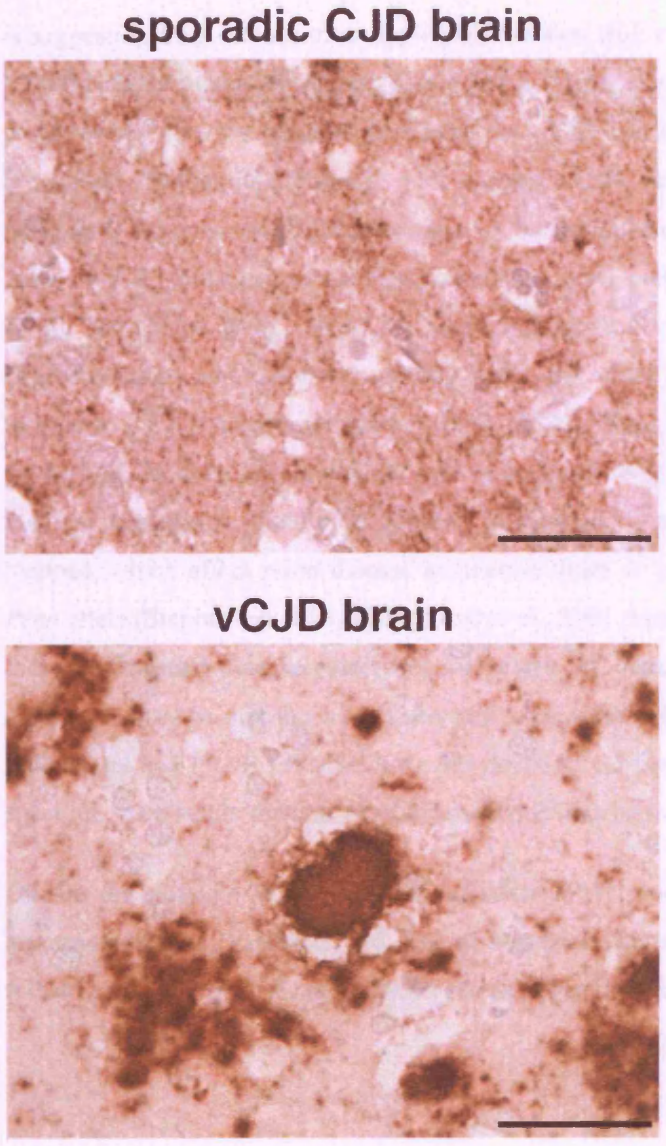

Figure 1.2 PrP^{Sc} deposition in vCJD and sCJD patient brains

Brains from patients with sCJD and vCJD show abnormal PrP immunoreactivity following immunohistochemistry using anti-PrP monoclonal antibody. **Top panel**: abnormal PrP deposition in sCJD most commonly presents as diffuse synaptic staining. **Bottom panel**: vCJD brain is distinguished by the presence of PrP "florid plaques" consisting of a round amyloid core of PrP surrounded by a ring of spongiform vacuoles. Scale bar: 50 µm. *Figure courtesy of Dr J.Wadsworth, MRC Prion Unit*

between cows and mice, a mean vCJD incubation period of 30 years has been suggested, with a maximum incubation period approaching a normal human lifespan (Collinge, 1999). Second, there is suggestion from murine strain typing studies that BSE may also transmit as sCJD in humans of 129MM *PRNP* genotype (Asante et al., 2002). Third, secondary iatrogenic transmission of vCJD is of serious concern because asymptomatic vCJD carriers have been detected within the UK population. Studies in transgenic mice suggest vCJD may transmit relatively easily to humans because of the substantially reduced species barrier (Bishop et al., 2006). Already three probable cases of vCJD transmission via blood transfusion have been reported (Llewelyn et al., 2004;Peden et al., 2004;Wroe et al., 2006). A recent anonymised study of human lymphoid tissue (from appendicectomy and tonsillectomy) suggested that vCJD was present at a prevalence of 237 per million in the UK population (Hilton et al., 2004). Though it is unclear if these individuals will develop vCJD, they pose a risk for secondary transmission through blood products, surgical and medical instruments. Finally, in addition to the prion gene, several other genetic loci have been mapped, which affect prion disease incubation times in inbred mouse lines expressing the same *Prnp* allele (Stephenson et al., 2000;Lloyd et al., 2001;Asante et al., 2002). Human homologues of these unidentified disease-modifying loci could be important in human susceptibility to prion disease. It may be that the most genetically susceptible individuals (those with short incubation time alleles and *PRNP* 129MM) have developed vCJD thus far and the other genotypes are still to succumb. As a result, the human vCJD epidemic may be multiphasic.

Due to the possible vCJD infection of other *PRNP* codon 129 genotypes, the prevalence of asymptomatic vCJD carriers and risk of secondary transmission, contrary to some estimations (Ghani et al., 2003), vCJD still poses a serious threat to public health in the UK.

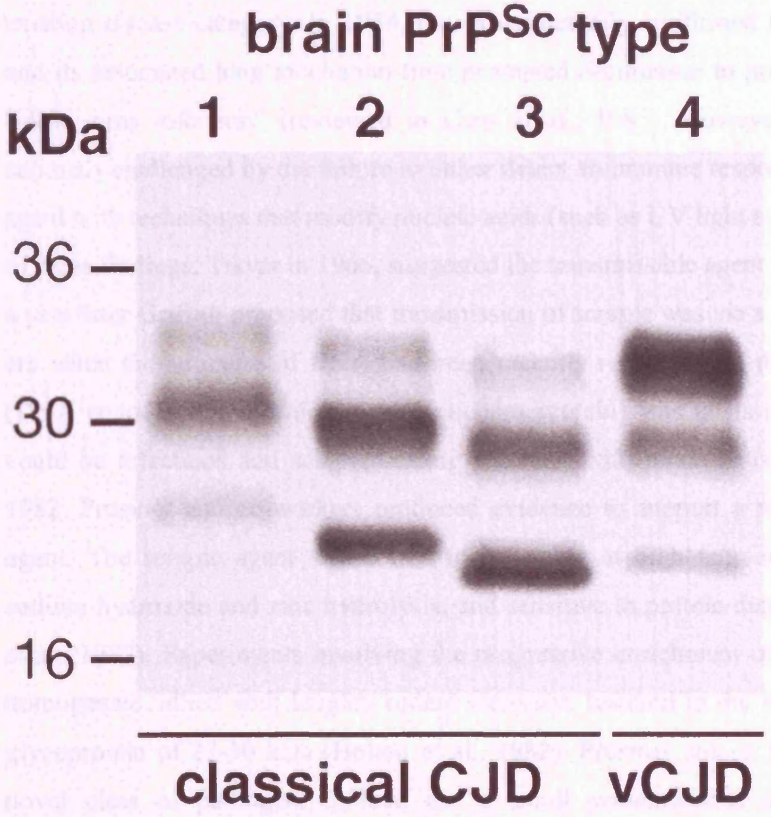

Figure 1.3 Molecular strain typing of human prions

Immunoblot for PrP in CJD-infected brain homogenates after treatment with Proteinase K. Each strain type possesses its own biochemical signature on polyacrylamide gel determined by tertiary conformation and glycosylation patterns. PrP has 3 different glycosylation states represented by the 3 bands; the top band is diglycosylated, the middle is monoglycosylated and the bottom is unglycosylated. vCJD represents a novel prion strain, type 4, since like BSE, it is predominantly diglycosylated. Other human prions, such as sporadic CJD and iatrogenic CJD, fall into strain types 1-3. *Modified from Collinge, 2005.*

1.3 Protein-only hypothesis of prion transmission

For the last hundred years, the nature of the causative agent of TSEs has been the subject of substantial research. The unique characteristics of the diseases defy their placement into any existing disease category. In 1954, the experimentally confirmed transmissible nature of scrapie and its associated long incubation time prompted Sigurdsson to propose scrapie was caused by a "slow virus infection" (reviewed in Carp et al., 1985). However, the slow virus theory was seriously challenged by the failure to either detect an immune response, or to inactivate the scrapie agent with techniques that modify nucleic acids (such as UV light and nuclease treatment). In view of these findings, Tikvar in 1966, suggested the transmissible agent was devoid of nucleic acid and a year later Griffith proposed that transmission of scrapie was via a protein-only mechanism. In an era when the structure of DNA had been recently resolved and the "central dogma" of biology (DNA encodes RNA, which in turn encodes protein) was in its prime, the theory that proteins could be infectious and self-replicating was met with much resistance. Over a decade later, in 1982, Prusiner and co-workers produced evidence to support a protein-only theory of the TSE agent. The scrapie agent was found to be stable at high temperatures, resistant to nucleases, sodium hydroxide and zinc hydrolysis, and sensitive to protein denaturants and proteases (Bolton et al., 1982). Experiments involving the progressive enrichment of infectivity from scrapie brain homogenate, allied with lengthy rodent bioassays resulted in the isolation of a protease-resistant glycoprotein of 27-30 kDa (Bolton et al., 1982). Prusiner coined the term prion to describe this novel class of pathogen, defined as "a small *pr*oteinaceous *in*fectious particle that resists inactivation by procedures that modify nucleic acids". Oligonucleotides derived from the partial sequence of the isolated prion protein$^{27\text{-}30}$ were used to screen cDNA libraries from scrapie-infected hamsters. To much surprise, rather than being virally encoded, the prion protein was found to be encoded by a single copy host chromosome (Oesch et al., 1985). The normal product of the prion gene is a 33-35 kDa protein called the cellular prion protein, (PrP^{C}). The disease-associated isoform of the prion protein, PrP^{Sc}, results from a post-translational template-induced conformational change of PrP^{C} and is the central event in prion disease. PrP^{C} and PrP^{Sc} do not differ in amino acid sequence. There are currently no antibodies that clearly discriminate these two isoforms, therefore, PrP^{Sc} is currently operationally distinguished from PrP^{C} by its partial resistance to Proteinase K (PK) and its insolubility in detergents. PK fully digests PrP^{C} but just cleaves 60-70 residues from the amino terminal of PrP^{Sc} to produce $PrP^{27\text{-}30}$.

Nowadays, it is almost indisputable that the causative agent of prion disease is composed primarily of disease-associated PrP^{Sc}. Some of the most convincing evidence is the recent generation of synthetic prions: recombinant mouse truncated prion protein (89-230) was polymerised into fibrils

in vitro and found to be infectious. When intracerebrally inoculated into transgenic mice, these fibrils produced neurological dysfunction at 380-660 days, which was further transmissible to both transgenic mice and wild-type mice (Baskakov et al., 2004) Nonetheless, investigations are in progress to disprove the theory these mice develop spontaneous disease due to overexpression of PrP (16-fold). The fact that mutations in the *PRNP* gene underlie inherited prion disease further substantiates the protein-only hypothesis.

1.4 Cellular prion protein - PrP^C

The normal or cellular form of the prion protein, PrP^C, is a sialoglycoprotein of 30-35 kDa, attached to the external surface of the membrane via a glycosylphosphatidylinositol (GPI) anchor. It is ubiquitously expressed, though the highest expression is present in the nervous and immune systems (Dodelet and Cashman, 1998a). The prion gene is highly conserved across mammalian species and present in other vertebrates including birds, amphibians and marsupials (Windl et al., 1995;Wopfner et al., 1999;Calzolai et al., 2005;Cotto et al., 2005). In humans, PrP^C is composed of 253 amino acids and is encoded by a single exon of the *PRNP* gene located on the short arm of chromosome 20 (20p).

1.4.1 Maturation and cellular processing of PrP^C

Following translation, PrP^C is processed through the endoplasmic reticulum (ER) where the N-terminal and C-terminal regions of the protein are removed. The N-terminal signal peptide is cleaved at lysine residue 22 and C-terminal truncation occurs between 2 serine residues at positions 230 and 231 for the GPI anchor to be attached (**figure 1.4A**).

The GPI anchor consists of a phospholipid chain that spans the cellular membrane and a head group composed of a phosphodiester-linked inositol group attached to the top of the chain. The inositol is linked to a chain of glucosamine, three mannose sugars and a phosphoethanolamine which links sugars to protein. Phosphatidylinositol-specific phospholipase C (PIPLC) is able to selectively cleave PrP^C (but not PrP^{Sc}) from the cell surface membrane at the GPI moiety (Stahl et al., 1990) indicating that the conformation of PrP^{Sc} hinders accessibility of the enzyme. Sialic acid is added to the GPI anchor of both PrP^C and PrP^{Sc} in the ER. PrP^C contains two asparagine-linked glycosylation sites (at Asn181PheThr and Asn197 PheThr of human PrP). Glycosylation occurs as PrP^C is processed in the Golgi, where neither, either or both sites can be modified with carbohydrate so that *in vivo* PrP^C exists as a mixture of unglycosylated, monoglycosylated and diglycosylated moieties. A disulphide bond is formed between the two cysteine residues (174 and 214 in human PrP) near the C-terminus between the two glycosylation sites in the ER. Finally, PrP^C is transported to the cell surface where it is tethered to the outer leaflet of the membrane via

its GPI anchor. The 3-dimensional conformation of recombinant mouse PrP^C (soluble PrP without glycan chain or membrane anchor) was established by NMR spectroscopy (Riek et al., 1996) and found to be essentially the same in all mammalian species (**figure 1.4B**) (James et al., 1997;Lysek et al., 2005;Gossert et al., 2005). The C-terminal domain is composed predominantly of alpha-helical structure (three α-helices and a short anti-parallel β-sheet), stabilised by a single disulphide bond linking helices 2 and 3. The N-terminal domain is unstructured in solution and contains a highly conserved octapeptide repeat region (containing five repeats in mice) with two copper binding sites (Jackson et al., 2001).

1.4.2 PrP^C function

The amino acid sequence of mammalian PrP^C is highly conserved between mammalian species suggestive of an important cellular function. However, mice lacking PrP^C as a result of gene knockout show no overt phenotype, probably due to compensatory pathways (Bueler et al., 1993b;Mallucci et al., 2002). A plethora of functions for PrP^C have been proposed but its precise physiological role remains unclear.

Putative functions of PrP^C are based on its localisation and on PrP^C-interacting molecules generated from *in vitro* binding assays with recombinant PrP (reviewed in Lee et al., 2003). As a GPI-anchored cell surface glycoprotein, PrP^C is located in lipid rafts, which are associated with an abundance of signalling proteins. Therefore, PrP^C has been proposed to play a role in signal transduction. In addition, PrP^C is continually cycled from the cell surface through the endocytic pathway into endosomes (Shyng et al., 1994). This cycling occurs through the association of PrP^C with clathrin-coated pits, invaginations of the cell membrane that bud off into the cytoplasm to form endosomes. This aspect of its cell biology lends credence to the idea that PrP^C is acting as a receptor of some kind (Lee et al., 2003). Since PrP^C resides on the external surface of the membrane, for PrP^C to perform the above functions, it would require a binding partner with a transmembrane domain. It is also proposed PrP^C is involved in cellular adhesion since PrP^C ligands identified have included adhesion molecules: N-CAMS (Schmitt-Ulms et al., 2001), laminin receptors (Gauczynski et al., 2001) and glycosaminoglycans (Pan et al., 2002). PrP^C has been implicated in a numerous physiological processes which are outlined below.

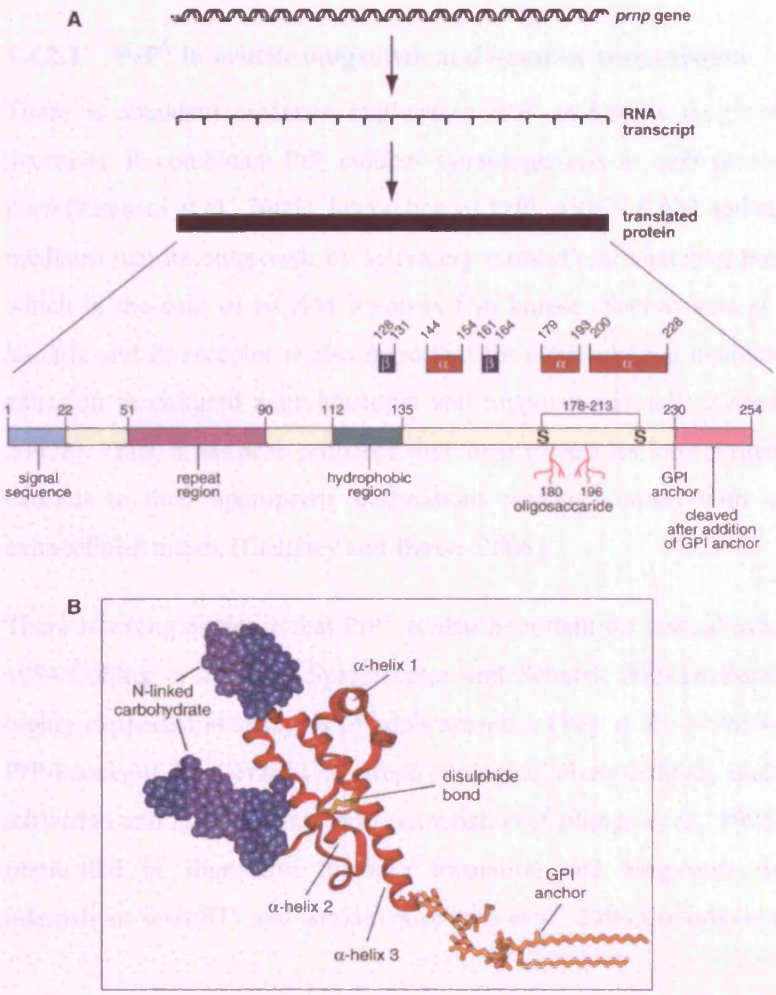

FIGURE 1.4 (A) Cellular processing of prion protein (PrP^C) - Processing of PrP from its genetic transcript to the primary protein sequence. Post-translational modifications include cleavage of N- and C-terminal signal sequences, attachment of a GPI anchor to residue 231, glycosylation of asparagine residues 180 and 196 and disulphide bond formation (S) between cysteines at 178 and 213 stabilising α-helices 2 and 3. Known regions of secondary structure (α-helix and β-sheet) are also shown in the C-terminal domain. Amino acid numbers refer to mouse PrP but processing is essentially the same for the human form. **(B) Three-dimensional structure of mouse PrP^C** - Representation of 3D structure derived from data determined by NMR of recombinant mouse PrP^{21-231} (Hosszu et al., 1999) shows the positions of the post-translational modifications, α-helix and β-sheet secondary structure. Globular structure of the protein with the three α-helices (red), glycosylations at residues 180 and 196 (blue), disulphide bond (yellow) and GPI anchor (gold).

1.4.2.1 PrP^C in neurite outgrowth and synaptic transmission

There is abundant evidence implicating PrP^C in neurite outgrowth and synapse formation in neurones. Recombinant PrP induces synaptogenesis in embryonic rat hippocampal neurones *in vitro* (Kanaani et al., 2005). Interaction of PrP^C with N-CAM and stress-inducible protein 1 (ST1) mediates neurite outgrowth by activating intracellular signaling pathways (Kanaani et al., 2005), which in the case of NCAM involves Fyn kinase (Santuccione et al., 2005). PrP^C binding with laminin and its receptor is also important for extension and maintenance of neurites and neuronal adhesion in cultured neuroblastoma and hippocampal cells (Graner et al., 2000a;Graner et al., 2000b). Thus, it has been proposed that these molecules form protein complexes to guide growing neurites to their appropriate destinations making contact with neurones, other cells and the extracellular matrix (Caughey and Baron, 2006).

There is strong evidence that PrP^C is also important for normal synaptic function (Collinge et al., 1994;Colling et al., 1996;Spielhaupter and Schatzl, 2001;Mallucci et al., 2002). First, PrP^C is highly expressed at synapses of adult neurones (Vey et al., 1996;Naslavsky et al., 1997). Second, PrP-knockout mice exhibit electrophysiological abnormalities, such as impaired GABAergic fast inhibition and reduced long-term potentiation (Collinge et al., 1994). Furthermore, PrP^C has been implicated in short-term memory formation and long-term memory consolidation via its interactions with ST1 and laminin (Coitinho et al., 2006;Coitinho et al., 2007).

PrP^C is also crucial in neuronal development; it increases cell proliferation in neurogenic regions (dentate gyrus of the hippocampus and along the rostral migratory stream, adjacent to the subventricular zone) and directs multipotent neural precursors to differentiate into neurones (Steele et al., 2006).

1.4.2.2 PrP^C in copper homeostasis and neuroprotection

The octapeptide repeat motif at the N-terminus of PrP^C enables it to strongly bind metal ions, particularly copper, with high affinity (Brown et al., 1997a). The ability of PrP^C to both bind and internalise copper and zinc has lead to the proposal that PrP^C is involved in their neuronal metabolism or transport (Brown et al., 1997b;Pauly and Harris, 1998;Brown, 1999;Kretzschmar et al., 2000;Watt and Hooper, 2003).

Although data are conflicting, there is evidence copper-bound PrP^C possesses SOD-1 (super oxide dismutase 1)-like activity and is neuroprotective against oxidative stress (Brown et al., 1999;Vassallo and Herms, 2003). For example, PrP^C-deficient neurones are more susceptible to

oxidative stress and serum deprivation *in vitro* (Brown et al., 1997b). PrP^C is thought to play a role in cell survival and neuroprotection through its interaction with STI-1 and apoptotic pathways though the exact mechanism remains unclear (reviewed in Roucou and LeBlanc, 2005). PrP^C can bind the anti-apoptotic factor Bcl-2 (Kurschner and Morgan, 1995) and it can protect neurones from Bax-mediated cell death with the same potency as Bcl-2.

1.4.2.3 PrP^C in the immune system

PrP^C is highly expressed in cells of the immune system via its signalling and adhesion properties, PrP^C is thought to induce cellular differentiation of leukocytes and follicular dendritic cells (Dodelet and Cashman, 1998b) and regulate the immune response by recruitment of leukocytes to the site of inflammation, T-cell activation and inhibition of phagocytosis (Cashman et al., 1990;de Almeida et al., 2005).

PrP^C has also been implicated in long-term renewal of haematopoietic stem cells (HSC) since PrP^C-expressing HSCs were significantly more effective at repopulating blood than PrP^C-null cells when transplanted into irradiated mice. The exact mechanism by which PrP^C promotes long-term renewal is unclear but it may transduce cell survival signals, act as a co-receptor for hormones affecting HSC activity or interact with the extracellular matrix allowing homing of the stem cells to the appropriate environment (Zhang et al., 2006).

Better understanding of the physiological function and interactions of PrP^C may be important in the development of prion disease therapeutics. Alterations in the structure and expression level of PrP^C can cause neurological disease (reviewed in Chiesa and Harris, 2001), suggesting that aberrant interactions of PrP^{Sc} with PrP^C contribute to pathogenesis in prion disease.

1.5 Disease-associated prion protein - PrP^{Sc}

1.5.1 Properties of PrP^{Sc}

In contrast to PrP^C, which is mainly monomeric, sensitive to proteolysis, readily soluble in mild detergents and rich in α-helical structure, PrP^{Sc} is detergent and partially protease-resistant (carboxyl segment of about 140 residues), with a propensity to aggregate. Fourier transform infrared spectroscopy suggests PrP^{Sc} is richer in β-sheet content than PrP^C; comprising 45% of PrP^{Sc} compared to 3% of PrP^C (Pan et al., 1993). Use of high-resolution techniques, such as NMR, to study the precise atomic structure of the native conformation of PrP^{Sc} is precluded by its insolubility and aggregation state. The nature of the self-propagating infectious agent is not known

but a recent study revealed that mid-sized PrP oligomers of 14-28 molecules were maximally infective when compared to monomeric or fibrillar PrP (Silveira et al., 2005).

1.5.2 Conversion of PrP^C to PrP^{Sc}

The conversion of PrP^C to PrP^{Sc} is the central molecular event in prion disease, however the exact events involved in this conversion are unresolved. The most current theory proposes that PrP fluctuates between a predominant native state, PrP^C, and a series of minor conformations, some of which can self-associate to form a stable supramolecular structure, PrP^{Sc}, made up of misfolded PrP monomers (β-PrP; **figure 1.5**). Further aggregation of β-PrP occurs until it reaches a critical size at which point a stable "seed" structure is formed. At this stage, explosive autocatalytic formation of PrP^{Sc} ensues involving the recruitment of unfolded PrP and β-PrP monomers. This proposed mechanism of prion propagation could account for the acquired, sporadic and inherited aetiologies of prion disease. Initiation of this pathogenic self-propagating conversion reaction with accumulation of aggregated β-PrP may be induced by exposure to a "seed" of aggregated β-PrP following prion inoculation, or as a rare stochastic conformational change, or as an inevitable result of expression of a pathogenic mutant form of PrP^C that is prone to form β-PrP. Whether the PrP itself, through its fluctuating conformations can adopt PrP^{Sc} conformation, or whether it requires other co-factors has not been confirmed. Possible co-factors for conversion include STI1, which not only binds to PrP^C but also localises in a chaperone complex (Lassle et al., 1997) and Hsp60, the bacterial homologue of which catalyses prion aggregation (Edenhofer et al., 1996;Stockel and Hartl, 2001). There is evidence to suggest nucleic acids may also play a role in prion propagation *in vivo*. First, PrP avidly binds nucleic acids (Cordeiro et al., 2001;Gabus et al., 2001a;Gabus et al., 2001b;Moscardini et al., 2002;Nandi et al., 2002) and second, single-stranded mammalian RNA molecules (of about 300 nucleotides) stimulate prion conversion *in vitro*. This work is still consistent with the protein-only hypothesis because the RNA molecules are host-encoded and do not form part of the infectious agent.

The exact sub-cellular site of prion propagation is also the subject of debate. Considerable evidence points to late-endosome-like organelles or lysosomes (Laszlo et al., 1992;Mayer et al., 1992;Taraboulos et al., 1992;Arnold et al., 1995). These organelles are favoured because the acidic environment induces protein unfolding and may facilitate the conversion of PrP^C to PrP^{Sc}.

1.5.3 Prion strains

Different prion strains exist and give rise to prion disease that varies markedly in neuropathology (presence of plaques and spongiform degeneration), brain region and cell type affected, incubation

time and disease length. Prion strains are not encoded by a nucleic acid genome, which conventionally encodes strains of viruses and bacteria. Neither are they encoded by differences in PrP primary structure since dinstinct strains can be serially propagated in lines of inbred mice with the same *Prnp* genotype (Scott et al., 1997). Molecular strain typing studies, in which prion-infected material is Proteinase K treated and immunoblotted for PrP, show that different strains of PrP^{Sc} display distinctive migration patterns on polyacrylamide gels, reflecting their different glycosylation pattern and proteolytic cleavage sites. Therefore, it is a combination of protein conformation and glycosylation that encodes strain diversity.

1.5.3.1 Human prion strains

Four distinct human PrP^{Sc} types have been identified (type 1-4), which are associated with different phenotypes of CJD (**figure 1.3**). An alternative molecular classification system has identified six sub-types (Gambetti et al., 2003). As displayed in figure 1.3, following limited proteolysis (cleavage of the N-terminus), CJD isolates show different PrP fragment sizes and ratios of the three glycoforms by immunoblotting. These signatures can be maintained when passaged into both human transgenic mice and wild-type mice, fulfilling the definition of strains. Classical CJD is associated with PrP^{Sc} types 1-3, while type 4 human PrP^{Sc} is uniquely associated with vCJD. Molecular strain typing of prion isolates from tonsil is now used for diagnosis of vCJD (Hill et al., 1997b).

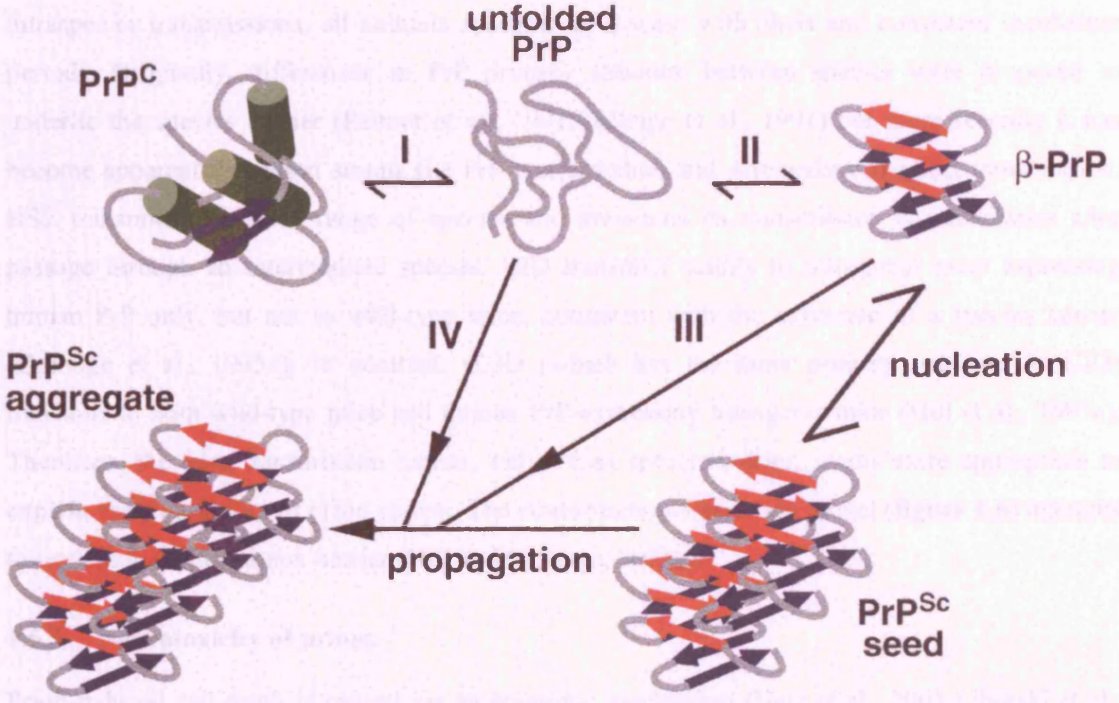

Figure 1.5 Putative mechanism for prion propagation

Predominantly α-helical PrP^C reversibly refolds, via an unfolded state (Hosszu et al., 1999). (i), to a largely β-sheet form, β-PrP (ii), which has a propensity to aggregate under physiological conditions. Once β-PrP has aggregated to a critical "seed" size, prion propagation is an essentially irreversible process (driven thermodynamically by intermolecular interactions) involving the further recruitment of unfolded PrP (iii) or β-PrP monomers (iv). *Modified from (Collinge, 2005).*

1.5.4 Species barrier

When prions from species A are transmitted to species B, not all animals of species B develop disease and those that do have longer and more variable incubation times; this phenomenon is referred to as the species barrier of prion transmission. On secondary passage of infectivity, as intraspecies transmissions, all animals succumb to disease with short and consistent incubation periods. Originally, differences in PrP primary structure between species were proposed to underlie the species barrier (Palmer et al., 1991;Collinge et al., 1991) but more recently it has become apparent that prion strains (i.e PrP conformation and glycosylation) affect transmission. BSE transmits to a wide range of species and maintains its transmission characteristics after passage through an intermediate species. CJD transmits readily to transgenic mice expressing human PrP only, but not to wild-type mice, consistent with the existence of a species barrier (Collinge et al., 1995c). In contrast, vCJD (which has the same primary structure as CJD) transmits to both wild-type mice and human PrP-expressing transgenic mice (Hill et al., 1997a). Therefore, the term transmission barrier, rather than species barrier, seems more appropriate to explain transmissibility of prion strains. The conformational selection model (**figure 1.6**) attempts to explain the transmission barrier (Hill and Collinge, 2003a).

1.5.5 Neurotoxicity of prions

Prion-induced cell death is caused via an apoptotic mechanism (Hetz et al., 2003;Liberski et al., 2004;Cronier et al., 2004;Carimalo et al., 2005) but exactly how the accumulation of PrP^{Sc} is related to cellular toxicity, neuronal loss and eventual host death in prion disease is the subject of intense research. In order to exert its toxic effect PrP^{Sc} requires PrP^{C} since PrP knockout mice are resistant to infection with scrapie prions (Bueler et al., 1993a) but regain susceptibility on reintroduction of a murine PrP transgene (Fischer et al., 1996). However, it is unclear if PrP^{Sc} causes cell death due to a toxic gain of function. On the one hand, PrP^{Sc} and PrP^{Sc} fragments (encompassing residues 106-126) exhibit direct toxicity in primary cultured neurones (Forloni et al., 1993). On the other hand, the level of PrP^{Sc} *in vivo* often does not correlate with disease severity. For example, in FFI, there is very little PrP^{Sc} deposition observed in patient brains and some prion-inoculated mice remain asymptomatic in their lifespan despite high prion titres in their brains; a phenomenon termed sub-clinical prion disease (Hill and Collinge, 2003b).

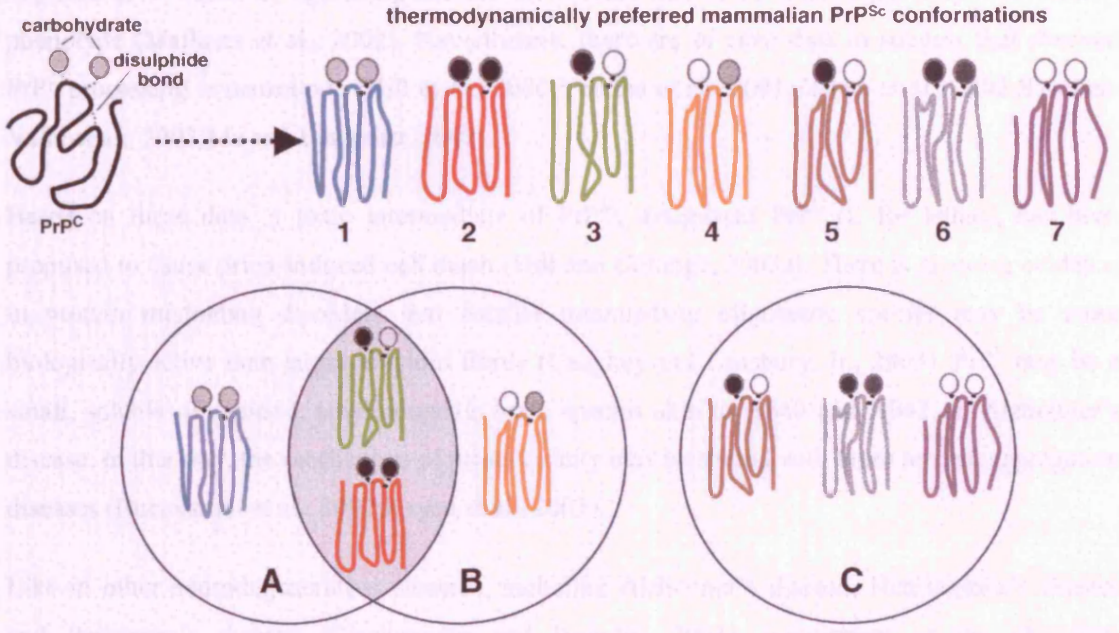

Figure 1.6 Conformational selection model of prion transmission barriers

Since mammalian PrP genes are highly conserved, this hypothesis proposes that only a limited number of different PrP^{Sc} conformations or strains are permissible thermodynamically and are stable enough to be serially propagated in prion disease. For each species only a certain subset of these conformations (or strains) will be allowed. Transmission between species may occur if there is an overlap between the subset of permissible PrP^{Sc} conformations; red and green strains may be transmissible between species A and B, but not the yellow and blue strains. But a large barrier to transmission will exist between species with no PrP^{Sc} conformations in common, for example, species C and species A or B. *Modified from (Hill and Collinge, 2003a).*

It seems unlikely that prion-induced cell death is due to loss of normal PrP^C function because PrP^C-knockout mice develop normally (Bueler et al., 1993a) and the absence of neuronal PrP^C in adulthood is also well tolerated; a *Prnp* conditional knockout mouse, in which PrP^C is post-natally depleted at 9 weeks of age using the cre-lox system, shows no neurodegeneration or clinical phenotype (Mallucci et al., 2002). Nevertheless, there are *in vitro* data to suggest that aberrant PrP^C processing is neurotoxic (Hill et al., 2000;Yedidia et al., 2001;Zanata et al., 2002;Sanchez-Valle et al., 2002;Ma and Lindquist, 2002).

Based on these data, a toxic intermediate of PrP^{Sc}, designated PrP^L (L for lethal), has been proposed to cause prion-induced cell death (Hill and Collinge, 2003a). There is growing evidence in protein misfolding disorders that smaller intermediate oligomeric species may be more biologically active than larger amyloid fibrils (Caughey and Lansbury, Jr., 2003). PrP^L may be a small, soluble oligomeric, amyloidogenic toxic species akin to Aβ40 and Aβ42, in Alzheimer's disease. In this way, the mechanism of prion toxicity may be shared with other protein aggregation diseases (Bucciantini et al., 2002;Kayed et al., 2003).

Like in other neurodegenerative diseases, including Alzheimer's disease, Huntingtons's disease and Parkinson's disease (Ciechanover and Brundin, 2003), impairment of the ubiquitin-proteasome system has also been implicated in the pathogenesis of prion disease (Hooper, 2003;Kristiansen et al., 2005). The ubiquitin-proteasome system (UPS) is responsible for the non-lysosomal degradation and clearance of short-lived, misfolded, mutant and damaged proteins in eukaryotic cells (Goldberg, 2003). Whether inhibition of this system by protein aggregates is primary or a secondary effect is presently unclear (Hetz et al., 2007).

1.6 Therapeutic strategies for treatment of prion disease

Currently, there are no effective drugs for patients with prion disease but strategies for the development of prion disease therapeutics attempted to-date are presented in a systematic review (Trevitt and Collinge, 2006).

As discussed above, although PrP^{Sc} is associated with prion disease pathology and infectivity, it is unlikely to be the neurotoxic species. Consistent with these observations, therapies aimed at preventing PrP^{Sc} accumulation, including Congo red, have produced only modest effects in experimental models. They often need to be administered at the time of infection and are only effective against peripheral prion inoculation (Aguzzi et al., 2001). Exceptions to this are

intracerebroventricular pentosan polysulphate for intracerebrally inoculated mice (Doh-ura et al., 2004) and amphotericin, of which late administration is effective (Demaimay et al., 1997).

The main thrust of current prion therapeutic research is to target PrP^{C} and prevent its conversion to PrP^{Sc}. Since the generation of PrP^{Sc} is thought to involve almost complete unfolding of PrP^{C} (Hosszu et al., 1999) one approach under investigation is the prevention of prion conversion using small PrP^{C} binding ligands to stabilise ordered structure of PrP^{C}. High throughput screening of large compound libraries is being pursued to identify such ligands. Already antibodies that bind PrP (mainly at the N-terminus) have been effective in preventing prion propagation in chronically prion-infected cell cultures (Enari et al., 2001;Peretz et al., 2001;Gilch et al., 2003) possibly by sequestering PrP^{C} and preventing its incorporation into prions. Passive immunisation of peripherally inoculated animals with anti-PrP monoclonal antibodies was very effective in curing prion disease; there was reduced splenic infectivity and animals lived over 300 days longer than their untreated counterparts (White et al., 2003). Humanised anti-PrP antibodies may have a role in post-peripheral exposure prophylaxis to stop neuroinvasion. However, because antibodies do not cross the blood brain barrier they would have to be administered intracerebroventricularly to treat CNS disease and this would require optimisation; not only is tissue penetration inconsistent, there is suggestion that delivery of high dose antibodies into the CNS may induce extensive neuronal apoptosis (Solforosi et al., 2004).

Development of the *Prnp* conditional knockout mouse model (Mallucci et al., 2002) strongly validates the depletion of PrP^{C} as a safe and effective therapeutic strategy for prion disease and challenges the dogma that neurodegeneration is irreversible. Following prion infection of this model one week after birth, depletion of neuronal PrP^{C} at 12 weeks, halted neurological disease progression and reversed pathology (early hippocampal spongiform changes), allowing animals to survive almost to their natural lifespan (Mallucci et al., 2003). For therapeutic purposes PrP^{C} would need to be depleted by extrinsic means. The RNA interference (RNAi) technique of gene silencing has been successfully implemented for the inhibition of PrP^{C} expression in N2a cells (Tilly et al., 2003) and curing scrapie-infected cell cultures (Daude et al., 2003). Although therapeutic benefit of RNAi for prion disease has yet to be demonstrated *in vivo*, the approach has been successful for animal models of Alzheimer's disease and frontotemporal dementia (Davidson and Paulson, 2004).

Active immunisation is, of course, limited by immune tolerance to PrP but has proved effective in animal models (Sigurdsson et al., 2002). Vaccination with recombinant mouse prion protein, before or after intraperitoneal inoculation of prions in mice, demonstrated delayed disease onset in

both groups but was more prolonged in animals immunised before prion exposure (Sigurdsson et al., 2002). Vaccines may be useful for treatment of larger scale animal prion diseases, such as scrapie. Furthermore, several immunomodulatory approaches are also being pursued for prevention of prion diseases. For example, inhibition of follicular dendritic cell maturation by interference with cytokines signalling prevents splenic PrP^{Sc} accumulation and prion neuroinvasion (Montrasio et al., 2000).

A key research goal is to develop an early diagnostic blood-based test for PrP^{Sc} or specific prion biomarkers (Castilla et al., 2005) so that treatment can be offered prior to significant neurodegeneration. The prolonged peripheral phase of prion propagation, characteristic of many forms of prion disease, which takes place in the lymphoreticular system and/or peripheral nerves also offers an opportunity for therapeutic intervention prior to neuroinvasion and precludes the need to use drugs that cross the blood-brain barrier.

To-date several drugs have been tested in relatively few patients, with no clear efficacy of any agent demonstrated; controlled clinical trials are desperately needed. However, such trials are problematic because prion diseases are very rare, the use of placebo is unethical due to the fatal nature of the disease, the disease course is rapid and there is an absence of biomarkers with which to monitor disease progression. A clinical trial protocol for prion disease has been developed and quinacrine, an anti-malarial acridine derivative, is currently being assessed in an MRC-funded trial.

1.7 Cell models of prion disease

Early studies into prion disease were conducted in experimental rodent models of scrapie (reviewed in Collinge et al., 1995a;Weissmann C, 1999). However, in view of the long prion disease incubation times (between 3 months and >2 years in mice), cell culture models represent a faster and cheaper alternative to rodent models, and entail fewer ethical constraints. Moreover, the easier manipulation of the genome and proteome of cells facilitates the study of cellular and molecular disease pathogenesis. Cellular models are also more physiologically relevant than the available cell-free *in vitro* assays of mammalian prion propagation (Kocisko et al., 1994;Saborio et al., 2001;Lucassen et al., 2003).

In light of the benefits of cell culture, attempts to propagate prions from animal models in cultured neuronal cells began in the 1960s, with the first cell models reported in the 1970s (Clarke and Haig, 1970b;Gajdusek et al., 1972). The last two decades has seen the emergence of a number of

cell culture models of infectious and inherited forms of prion disease, in which prions are stably propagated (reviewed in Solassol et al., 2003).

1.7.1 Methods for development of prion-propagating cell lines

The simplest procedure for development of a cell line stably replicating prions is first to expose a PrP^{C}-expressing line to PrP^{Sc}, usually in the form of brain homogenates from prion-infected animals. Next, cell cultures are washed and passaged extensively in order to remove the original inoculum and are then assayed for the presence of *de novo* infectivity over numerous passages (Beranger et al., 2001). Prior to the discovery of PrP^{Sc}, the gold-standard surrogate marker for prion infection, successful prion transmission to cell culture was assessed by the presence of infectivity using the mouse bioassay (prion-susceptible strains of mice). Nowadays, the presence of PrP^{Sc} is assessed by biochemical methods, including immunoblotting, or the 10-fold more sensitive cell blot assay (CBA; Bosque and Prusiner, 2000). These methods involve the detection of protease-resistant PrP using antibodies targeting the carboxyl terminus of PrP. To further verify infectivity, infected cells are homogenised and inoculated into either prion-susceptible mice or identical uninfected cells (Cronier et al., 2004). Culture medium of infected cells often harbours infectivity and can also be used to test if the cell line is infectious (Schatzl et al., 1997;Cronier et al., 2004;Baron et al., 2006). An alternative approach for the development of cell models of prion disease is the isolation of primary cultures from prion-susceptible mouse models (see section **1.7.4**).

Mutant PrP molecules have been expressed in cells to improve understanding of the pathogenic process occurring in inherited prion disease. Expression of octapeptide repeat mutations, associated with CJD, have revealed an altered membrane association of PrP that is resistant to PIPLC cleavage (Lehmann and Harris, 1995) and has an increased tendency to aggregate and gain PK resistance (Priola and Chesebro, 1998). Expression of the D178N mutant PrP, associated with both FFI (codon 129MM) and CJD (codon 129VV), indicates only glycosylated forms of this mutated protein are attached to the cell membrane (Petersen et al., 1996).

1.7.2 Increasing susceptibility of cells to prion infection

The refractory nature of most cell lines to prion infection has prompted strategies to increase likelihood of cell infection with the transmissible agent. One such strategy is the use of sub-cloning. Using techniques such as the CBA (Bosque and Prusiner, 2000) and the post-embedded method (Vilette et al., 2001), it is apparent that not all cells within a susceptible cell line become infected. N2a mouse neuroblastoma cells are permissive to the RML mouse-adapted scrapie strain

(Race et al., 1987), though only 1% of these cells appear to be susceptible and become infected (Race, 1991). More efficient cell culture models do exist; 47% of L929 cells become infected with 22L mouse-adapted scrapie (Vorberg et al., 2004a) and 30% of Rov cells become infected with sheep scrapie (Vilette et al., 2001). Dilution subcloning of the parent N2a population, prior to RML infection, allows the isolation of the most susceptible clones, producing the highest amounts of PrP^{Sc} (Bosque and Prusiner, 2000). This work validates subcloning as a method for isolating the most prion-susceptible cells in a population and has subsequently been used to isolate a cell line propagating CWD (Raymond et al., 2006).

Increasing PrP^{C} expression levels reduces disease incubation times in animal models (Prusiner et al., 1990;Raeber et al., 1998). In accord with this finding, PrP^{C} overexpression can also improve prion transmission to cells. In their endogenous state N2a neuroblastoma cell lines are only permissive to RML prions but up to six-fold overexpression of PrP^{C} renders them permissive to two further mouse-adapted scrapie strains; 22L and 139A (Nishida et al., 2000). Mouse embryonic neurosphere cultures overexpressing mouse PrP^{C} (four- to eight-fold) are more susceptible than wild-type cultures to RML prion infection, establishing high PrP^{Sc} levels much sooner than the wild-type cultures. Indeed, overexpression of PrP^{C} has been important for successful development of many of the cell models of prion disease (Archer et al., 2004;Giri et al., 2006). However, it is clear that cellular susceptibility to prion infection is dependent on factors other than PrP^{C} levels. When attempting to render N2a cells more susceptible to prion infection by transfection of PrP^{C}, Enari *et al.* found that it was the vector-only clone (with wild-type PrP^{C} expression level) that was most susceptible to prion infection (Enari et al., 2001).

A further strategy for improving prion infection efficiency in cells is to use different PrP^{Sc} preparations. First, microsomal preparations of scrapie-infected brain homogenate (Baron et al., 2002) have recently been identified as a very efficient way of initiating prion infection in cultured cells (mouse cholinergic septal neurones and N2a neuroblastoma cells) compared to detergent purified PrP^{Sc} (Baron et al., 2006). Microsomal fractions contain PrP^{Sc} associated with membrane vesicles (from all types of cellular membrane). These preparations may be more infectious because the PrP^{Sc} aggregates appear more diffuse than detergent-purified preparations, providing a greater number of seeds for replication. Alternatively, PrP^{Sc} microsomes may improve uptake of PrP^{Sc} into target cells, either by membrane fusion or association of microsomal molecules with target cell ligands. Second, scrapie-associated fibrils (SAFs), prepared by treatment of prion-infected brain homogenate with proteinase K and sarkosyl, are often used to improve efficiency of prion infection in cells (Race et al., 1987).

1.7.3 Immortalised cell lines supporting prion propagation

There are only a limited number of cell lines permissive to mammalian prion propagation, reflecting the inefficiency of prion infection of cells and the lack of knowledge regarding cellular susceptibility factors. Moreover, there is restricted strain propagation for each cell line. Of the available cell models of prion disease, the majority are permissive to mouse-adapted scrapie strains, but there are some cell models of sheep scrapie, hamster scrapie and CWD (**table 1.1**). Most notably, no cell lines have been reported that can stably propagate human prions. Any claims of cell lines replicating human prions have proved unfounded (Ladogana et al., 1995;Kikuchi et al., 2004).

In order to eliminate the prion species barrier, the majority of cell models of prion disease are homologous; that is, the species origin of the cells and PrP^{C} expressed are the same as the PrP^{Sc} in the inoculum. In addition, the development of prion cell models originally focussed on cell lines of neural origin since prion disease targets the central nervous system and neuronal cells highly express PrP^{C}. Thus, the most extensively studied cell lines in prion research are the N2a mouse neuroblastoma cell line (Race et al., 1987) and the ScGT1 cell line (Schatzl et al., 1997), developed from a T-antigen immortalised mouse hypothalamic (gonadotropin hormone-releasing hormone) neuronal line. Unfortunately, these two lines are only able to stably propagate the RML mouse-adapted scrapie strain in their endogenous state. Like most other cell culture models of prion disease, scrapie-infected N2a cells (ScN2a) do not exhibit a disease phenotype. Minor changes have been reported in ScN2a cells, including increased intracellular catecholamine levels and increased proliferative rate (Markovits et al., 1983) but these may be due to clonal differences or factors in the inoculum (Solassol et al., 2003). The chronically prion-infected ScGT1 line was the first prion-infected cell line to exhibit a pathological phenotype. The cultures exhibit apoptosis, signs of vacuolation (Schatzl et al., 1997) and reduced viability in response to oxidative stress (Milhavet et al., 2000). Prion infection of cell lines is not restricted to those of neuronal origin, non-neuronal cells derived from fibroblast and epithelial lines are reported to support prion replication (**table 1.1**). Although PrP^{Sc} has not been detected in fibroblasts *in vivo* (Meiner et al., 1992), several fibroblast cells lines can replicate prions *in vitro* (Vorberg et al., 2004b;Raymond et al., 2006). The murine L929 fibroblast cell line is a highly prion permissive line. Despite its low PrP expression, it can propagate three strains of mouse-adapted scrapie (ME7, RML and 22L; Raymond et al., 2006).

There are several heterologous cell models of prion propagation, in which there is a mismatch between the species origin of PrP^{Sc} and the species origin of either the PrP^{C} expressed or the cell

line. The first cross-species transmission of prions in culture was reported in 1984 when a NGF-differentiated PC12 rat phaeochromocytoma line was found to support replication of the mouse-adapted scrapie strain, 139A (Rubenstein et al., 1984). A rabbit epithelial kidney cell line (RK13) was rendered susceptible to sheep scrapie by heterologous overexpression of ovine PrP (homozygous for the most susceptible V^{136} R ^{154} Q^{171} polymorphism; Vilette et al., 2001). Most commonly, cell models propagate prions which have been passaged through rodents but this Rov model propagates naturally-occurring prion disease (scrapie from a VRQ homozygous sheep) and clearly demonstrates the importance of PrP polymorphisms in disease susceptibility and in establishing prion infection. It has been suggested that although the epithelial cells (like Rov) are non-neuronal, they may share some susceptibility factors of neurones because the nervous system is developmentally derived from an epithelium and both cell types are polarised. Moreover, the presence of PrP^C-expressing epithelial cells in skin, the digestive tract and reticuloendothelial system suggests this cell type may be important in the prion disease pathogenesis and transmission (Vilette et al., 2001).

1.7.4 Primary cultures supporting prion propagation

Cell models of prion disease have been derived by primary culture from either prion-infected or prion-susceptible animal models. The first such model, and first ever model of prion disease, was the scrapie mouse brain cell line (SMB) derived from the brain of a RML prion-infected mouse (Clarke and Haig, 1970a). Recently, primary culture has been employed to establish a number of prion-propagating cell lines. These evidently represent a more accurate disease model than tumour cell lines and allow the role of different cell types in prion disease pathogenesis to be assessed.

Two prion-propagating peripheral neuroglial cell lines have been developed: Schwann cells isolated from transgenic mice overexpressing ovine PrP^C (Mov) can sustain mouse-adapted sheep scrapie prion propagation (Archer et al., 2004) and a mouse Schwann cell line (MSC-80) propagates RML prions (Follet et al., 2002). These cell lines suggest Schwann cells play a role in peripheral prion disease pathogenesis and their study may allow better understanding of prion neuroinvasion. Furthermore the recent development of a microglial cell line from PrP-overexpressing mice may allow the role of microglia in prion disease pathogenesis to be elucidated (Iwamaru et al., 2007).

Sheep scrapie-propagating primary cerebellar cultures derived from a transgenic mouse line (overexpressing ovine PrP^C on a mouse *Prnp* knockout background) have been established (Cronier et al., 2004). This system demonstrated that both neuronal and astrocyte cultures could sustain prion propagation. Prion disease was faithfully recapitulated since the accumulation of *de*

novo PrP^{Sc} was neurotoxic to cerebellar granule neurones, which underwent delayed apoptotic cell death, but the cerebellar astrocyte cultures remained healthy.

Until very recently, a cell line permissive to CWD was lacking. An SV40-immortalised brain fibroblast line was cultured from a mule deer brain with the most common and susceptible PrP genotype (Raymond et al., 2006). It was isolated by dilution cloning and stably propagates CWD prions of the same genotype, following infection with a microsomal preparation of homogenate. Due to the widespread nature of CWD in the USA and Canada, treatment for the disease is of utmost importance. This model will be useful for the screening of potential CWD therapeutics.

RML prion-propagating embryonic neurospheres have been isolated from prion-susceptible mice overexpressing mouse PrP^{C} (Giri et al., 2006). Neurospheres are free-floating spherical aggregates of proliferating neural stem cells. The close-packed nature of cells in neurospheres is proposed to facilitate cell-to-cell transmission of prions in this model. The prion susceptibility of these neurosphere cultures reflects that of the mice from which they were derived, suggesting this system may be useful for the development of cellular prion models of different species, with a range of genotypes. Due to their stem cell component, neurospheres also have the potential to differentiate into the three brain cell types, neurones, astrocytes and oligodendrocytes, to allow the study of prion neuropathophysiology (Giri et al., 2006). Differentiated embryonic and adult mouse neural stem cells have been found to propagate several mouse prion strains (Milhavet et al., 2006). The close resemblance of this *in vitro* model to the brain environment has been suggested as the basis for its prion susceptibility.

1.7.5 Applications of cell models of prion disease

These prion-propagating cell lines have been valuable in the study of of PrP^{Sc} biology and the putative molecular mechanisms of prion conversion (Lehmann and Harris, 1997), subcellular localisation and neurotoxicity of PrP^{Sc} (Vey et al., 1996;Naslavsky et al., 1997;Cronier et al., 2004;Carimalo et al., 2005;Kristiansen et al., 2005) and the species barrier of prion transmission (Priola et al., 1994;Kaneko et al., 1997). They have also contributed to the evaluation of putative therapeutic agents (Caughey and Raymond, 1993;Doh-ura et al., 2000). For research purposes, a quantitative infectivity assay for mouse RML prions has been developed from highly susceptible N2a clones as a cheaper and faster alternative to mouse bioassay of prion infectivity (Klohn et al., 2003).

Cell line	Species of cell	Cell type / tissue origin	Prion strain propagated	Reference
NEURAL				
N2a	mouse	neuroblastoma	RML	(Race et al., 1987)
N1E-115	mouse	neuroblastoma	RML	(Race et al., 1987)
GT1	mouse	hypothalamic neurone	RML	(Schatzl et al., 1997)
HaB	hamster	brain	hamster strain	(Taraboulos et al., 1990)
Mov	mouse + ovine PrP	dorsal root ganglia	sheep scrapie	(Archer et al., 2004)
SN56	mouse	cholinergic septal neurone	RML/ 22L/ ME7	(Baron et al., 2006)
Neurosphere	mouse	embryonic NSC	RML	(Giri et al., 2006)
Differentiated neurone	mouse	embryonic NSC	22L/ RML/ C506M3	(Milhavet et al., 2006)
CGN	mouse + ovine PrP	cerebellar granule neurone	mouse-passaged sheep scrapie	(Cronier et al., 2004)
NON-NEURAL				
SMB	mouse	brain-mesodermal origin	RML	(Clarke and Haig, 1970b)
L929	mouse	fibroblast	RML/ 22L/ ME7	(Vorberg et al., 2004b)
NIH-3T3	mouse	fibroblast	22L	(Vorberg et al., 2004b)
NS1	mouse	fused spleen & scrapie-infected NS1 cell	RML	(Elleman, 1984)
MG20	mouse	microglia	RML/ME7/Obihiro/BSE	(Iwamaru et al., 2007)
PC12	rat	phaeochromocytoma	139A/ME7	(Rubenstein et al., 1984)
Glial cell	rat	gasserian ganglia	RML	(Roikhel et al., 1987)
Rov	rabbit + ovine PrP	kidney epithelial	sheep scrapie	(Vilette et al., 2001)
CAS	mouse + ovine PrP	cerebellar astrocyte	mouse-passaged sheep scrapie	(Cronier et al., 2004)
MDB	deer	mule deer brain fibroblast	CWD	(Raymond et al., 2006)
MSC-80	mouse	Schwann cell	RML	(Follet et al., 2002)
Schwann cell	mouse	Schwann cell	mouse-passaged sheep scrapie	(Archer et al., 2004)

Table 1.1 Cell lines capable of stably propagating animal prion strains

1.8 Aims of this project

The principal aim of this project was to develop a cell line stably propagating human vCJD prions. Currently, only primates and transgenic mouse models are available for the study of human prion disease (Telling et al., 1994;Brown et al., 1994;Telling et al., 1995;Collinge et al., 1995a;Asante et al., 2002;Korth et al., 2003) because despite worldwide effort, no cell model of human prion disease exists. Human prion-propagating cell lines are criticially needed for both basic and applied research of human prion disease. Progress in prion biology made by mouse prion cell models may not be relevant to human prion disease and would need to be verified in human prion-propagating cell lines.

Stable human prion-propagating cell lines will allow the study of cellular and molecular aspects of human prion disease in an efficient manner. Fundamental questions of prion cell biology remain to be answered. Human cell models may facilitate the elucidation of PrP^{C} function, the mechanism of PrP^{Sc} conversion, the identification of cellular factors conferring susceptibility to prion infection, the mechanisms of prion-induced cell death and the basis of prion strain cell tropism. Better understanding of these aspects of prion biology will improve prospects for therapeutic research specific to human prion disease.

A human prion-propagating cell line will also be a rapid, cost-effective bioassay for detection of human prions in tissue, not only for research purposes but also for diagnosis. Pre-mortem early diagnosis of human disease would allow early therapeutic intervention prior to any significant neurodegeneration. With the more recent emergence of vCJD and the fact that it is clearly transmitted by blood transfusion (Llewelyn et al., 2004; Peden et al., 2004; Wroe et al., 2006), identification of anti-prion therapeutics for human disease is all the more urgent. A human prion-propagating cell line will be a powerful tool for screening potentially therapeutic agents.

In the attempt to develop a cell line stably propagating human prions, the following strategies were pursued:

- The development of methodology to assay human prion infectivity in cells.
- The investigation of human PrP^{C}-expressing immortalised mammalian cell lines, of both neuronal and non-neuronal origin, for susceptibility to human prion infection.
- Humanisation of existing N2a mouse prion-propagating cell lines and the investigation of their susceptibility to human prion infection.

- The investigation of human foetal neural stem cells for susceptibility to human prion infection.

Here I present evidence to support the fact that transmission of human prions to cells *in vitro* is more difficult than *in vivo*. The cellular expression of human prion protein (PrP^{C}) of the same sequence as the disease-associated prion protein (PrP^{Sc}) in the vCJD inoculum was insufficient to establish human prion propagation in immortalised mammalian cell lines. From work on the humanisation of a mouse prion-propagating cell line, it is also evident that cell lines are permissive to restricted strains, and that perhaps cellular prion propagation factors are prion strain-specific. This thesis describes the first report of a cell line able to propagate human prions. The finding that a differentiated human foetal neural stem cell is able to propagate human vCJD prions suggests a human neuronal phenotype is critical for the propagation of human prions *in vitro*.

Chapter 2

Materials and Methods

2.1 Materials

2.1.1 Equipment

- Biomat class I microbiological safety cabinet (medical air technology.com)
- Biomat class II microbiological safety cabinet (medical air technology.com)
- Nuaire™ DH autoflow CO_2 air-jacketed incubator
- Zeiss Axiovert 25 inverted light microscope
- Zeiss Axioplan 2 MOT fluorescence microscope
- Zeiss Confocal microscope LSM510 META
- Zeiss KS ELISPOT system (Stemi 2000-C stereomicroscope with KL1500 LCD scanner, Hitachi HV-C20A colour camera, WELLSCAN software (Imaging Associates, UK)
- Tecan Spectra Image spectrophotometer
- Universal 32R Hettich benchtop centrifuge
- Eppendorf centrifuge 5415D
- Biorad power pac 200
- Eppendorf comfort thermomixer

2.1.2 Laboratory reagents

Unless stated otherwise, chemicals were supplied by Sigma (UK) and cell culture reagents by Invitrogen (UK).

2.2 Mammalian cell culture

2.2.1 Cell lines

Cell lines were acquired from ATCC (via LGC promochem), ECACC or as gifts as detailed below.

2.2.1.1 BE(2)M17

BE(2)M17 (ATCC) is a human neuroblastoma cell line derived from a bone marrow metastasis with neuroblast morphology.

2.2.1.2 H4

H4 (ATCC) is a human neuroglioma cell line with epithelial morphology.

2.2.1.3 HEK293

HEK293 (ECACC) is a human embryonic kidney cell line with epithelial morphology.

2.2.1.4 iPK1

iPK1 was a kind gift from Dr Peter Klohn (MRC Prion Unit, London). It is a chronically RML prion-infected PK1 cell line derived from the RML infection of PK1 cells as described in (Klohn et al., 2003).

2.2.1.5 L929

L929 (ECACC) is a mouse fibroblast cell line derived from adipose tissue.

2.2.1.6 Mink lung retroviral producer cell line (mink-ampho)

Mink-ampho was a kind gift from Professor Robin Weiss (University College London, UK). This is a Moloney murine leukaemia virus (MuLV) producer cell line that generates competent amphotropic retroviral particles.

2.2.1.7 N2a

N2a (ATCC) is a mouse neuroblastoma cell line with neuronal and amoeboid morphology.

2.2.1.8 N2aG

N2aG cell line was a kind gift from Dr Peter Klohn (MRC Prion Unit). It is an RML prion-susceptible cell line, derived from N2a cells by one round of subcloning and exhibits more than 100-fold susceptibility to RML compared to parent N2a cells (Klohn et al., 2003).

2.2.1.9 NP2

NP2 was a kind gift from Dr Hiroo Hoshino (Gunma University, Maebashi, Japan). It is a human glioma cell line.

2.2.1.10 PhiNX- ecotropic and PhiNX-amphotropic packaging cell lines

These were a kind gift from Professor Parmjit Jat. PhiNX-eco and PhiNX-ampho cell lines are second-generation retroviral producer lines (MuLV-based) for the generation of helper-free ecotropic and amphotropic retroviruses.The lines are based on the 293T cell line; a human embryonic kidney line transformed with adenovirus E1a, carrying a temperature sensitive T antigen co-selected with neomycin (Pear et al., 1993). These were used for gene transfer into cells. Virus packaging lines express genes required for the formation of viral particles (gag-pol-env), which are deleted from the retroviral vectors. PhiNX-eco cells produce virus particles able to

infect mouse cells whereas PhiNX-ampho cells package virus particles that can infect all species of cells.

2.2.1.11 PK1

PK1 (N2aPK1) was a kind gift from Dr Peter Klohn (MRC Prion Unit). It is an RML prion-susceptible cell line, derived from N2a cells by successive rounds of subcloning and exhibits more than 1000-fold susceptibility to RML prions compared to parent N2a cells (Klohn et al., 2003).

2.2.1.12 PrP null embryonic neurospheres

Primary neurosphere cultures were isolated at embryonic day 13.5 from the brains of FVB mice with a targeted null mutation in the PrP gene (F5_FVB/PrP null) as outlined in section **2.2.5.1**.

2.2.1.13 ReNcell 197VM

ReNcell 197VM (referred to throughout as 197 NSC) was acquired via a collaboration with ReNeuron Ltd. (Guildford, UK). It is a human foetal neural stem cell line (NSC) derived from the ventral mesencephalon of a 10-week foetus, immortalised by the retroviral transduction and overexpression of v-myc oncogene.

2.2.1.14 RG6

RG6 was a kind gift from Dr Miratul Muqit (Institute of Child Health, London). It is a rat neuroglial cell line with fibroblast morphology.

2.2.1.15 RK13

RK13 (ECACC) is a rabbit epithelial kidney cell line with epithelial morphology.

2.2.1.16 SHSY5Y

SHSY5Y (ATCC) is a human neuroblastoma line of epithelial morphology, cloned from SKN-SH.

2.2.1.17 SHSY5Y_A

SHSY5Y_A was a kind gift from Dr Konstantin Chumakov (FDA, Maryland, USA). It was derived from the retroviral transduction of SHSY5Y with the human prion gene (*PRNP*), encoding the methionine allele at codon 129, with CD25 as a selective marker.

2.2.1.18 SKN-SH

SKN-SH (ATCC) is a human neuroblastoma cell line derived from a bone marrow metastasis with epithelial morphology.

2.2.1.19 U87 MG

U87 MG was a kind gift from Professor Robin Weiss (UCL). It is a human astrocytoma cell line.

2.2.2 Cell culture maintenance

Cell cultures were handled as potentially bio-hazardous material under BioSafety Level 2 containment, and incubated in a humidified 37°C incubator aerated with 5% CO_2. Cells were cultured in tissue-culture treated plasticware; 10 cm dish (Falcon), T25 and T75 vented flasks (Nunc), 6-well plates, 24-well plates or 96-well plates (Costar).

Details of culture conditions for each cell line, including culture medium, freeze medium and passage details, are outlined in **table 2.1**. All cell lines grew as adherent monolayers and were passaged twice a week, when confluent, either by trituration or trypsinisation, as described below. Prior to passaging, reagents were pre-warmed to 37°C. Spent medium was aspirated and cells washed with 5 ml PBS (volumes are provided for a 10 cm dish). For trituration, PBS was replaced with 5 ml fresh medium and cells gently triturated with a 1 ml Gilson pipette tip until all cells were detached from the dish. For trypsinisation, PBS was replaced with 1 ml 1x trypsin-EDTA (0.25% trypsin-EDTA.4Na in HBSS) and cells incubated at 37°C until all cells had rounded up and detached (2-15 minutes). As soon as cells had detached, the trypsin was neutralised with 4 ml 10% FBS-containing medium. Following detachment, cells were harvested and pelleted at 160 rcf for 5 minutes. The cell pellet was resuspended in fresh medium and passaged at the appropriate ratio.

197 NSC and PrP null neurospheres required modified culturing procedures, which are outlined in sections **2.2.4** and **2.2.5**, respectively.

2.2.3 Freezing and defrosting cell cultures

Cells were harvested as described for passaging (section **2.2.2**) and pelleted at 160 rcf for 5 minutes at 4°C. The pellet was resuspended in ice-cold DMSO-containing freeze medium (**table 2.1**) at 1-2 x10^6 cells/ml. 1 ml aliquots of this cell suspension were dispensed into cryovials with an O-ring (Corning) and placed directly into an isopropanol-containing freezing vessel (Nalgene), which slowly cools cells by 1°C per minute to prevent cell lysis. The cells were frozen at - 80°C overnight and then deposited into liquid nitrogen for long-term storage.

Cells were defrosted by rapidly thawing vials in a 37°C water bath, resuspending in 14 ml pre-warmed culture medium and pelleting at 160 rcf for 5 minutes. The cell pellet was resuspended in fresh culture medium, deposited in tissue-culture plates and placed in a humidified incubator at 37°C, with 5% CO_2 overnight. The culture medium replaced the following day to remove dead cells from the culture.

Species	Cell Line	Cell Type	Culture medium	Passage method	Passage ratio	Passage frequency (per week)	Freeze medium	G418 selection concentration (ug/ml)
human	BE(2)M17	neuroblastoma	1:1 H+F,15% F, P/S, L, N	trypsin	1/5	2x	culture medium, 8% DMSO	800
	SKN-SH	neuroblastoma	M,15% F, P/S, L, N, Pyr	trypsin	1/5	2x	culture medium, 8% DMSO	n/a
	SHSY5Y	neuroblastoma	1:1 H+F,15% F, P/S, L, N	trypsin	1/3 - 1/5	2x	culture medium, 8% DMSO	400
	H4	neuroglioma	D, 10% F, P/S	trypsin	1/10	2x	culture medium, 10% DMSO	400
	U87 MG	astrocytoma	D, 10% F, P/S	trypsin	1/5	2x	culture medium, 10% DMSO	n/a
	NP2	glioma	D, 10% F, P/S	trypsin	1/5	2x	culture medium, 10% DMSO	n/a
	HEK 293	embryonic kidney	D, 10% F, P/S, N	trypsin	1/10	2x	culture medium, 10% DMSO	500
	Phx-NX eco	retroviral packaging line	D, 10% F, P/S, N	trituration	1/8	3x	NSC culture medium, DMSO	n/a
	ReNcell VM (197)	neural stem cell	DF12, B,L, Hep, G, FGF, EGF	trypsin	~1x10^4/ cm2	2-3x	10% DMSO	150
mouse	N2a	neuroblastoma	O, 10% F, P/S	trituration	1/10	2x	O, 30% F, 8% DMSO	500
	N2aG	neuroblastoma	O, 10% F, P/S	trituration	1/8	2x	O, 30% F, 8% DMSO	700
	PK1	neuroblastoma	O, 10% F, P/S	trituration	1/8	2x	O, 30% F, 8% DMSO	400
	iPK1	neuroblastoma	Opti, 10% FBS, 1x P/S	trituration	1/8	2x	O, 30% F, 8% DMSO	n/a
	L929	epithelial	D, 10% F, P/S, N	trypsin	1/10	2x	culture medium, 10% DMSO	1200
	PrP null neurosphere	neural stem cell	DF12, B,L, Hep, G, FGF, EGF	collagenase	1/4	1x	NSC culture medium, 30% F, 8% DMSO	n/a
rat	RG6	neuroglial	D, 10% F, P/S, N	trypsin	1/10	2-3x	culture medium, 10% DMSO	1000
rabbit	RK13	epithelial kidney	M,10% F, P/S, L	trypsin	1/8	2x	culture medium, 20% F, 8% DMSO	800

Abbreviation	Reagent (Invitrogen)
B	1x B27 supplement
D	Dulbecco's modified Eagle's medium with 4500mg/ml glucose and L-glutamine
DF12	DMEM:F12
EGF	20ng/ml EGF
F	fetal bovine serum
FGF	10ng/ml bFGF
G	50ug/ml gentamycin
H	Hams F12
Hep	10U/ml heparin
L	2mM L-glutamine
M	Minimum essential medium Eagle
N	1mM non-essential amino acids
O	OptiMEM
P/S	1x penicillin (100 U/ml) and Streptomycin (100 ug/ml)
Pyr	sodium pyruvate
trypsin	1x trypsin-EDTA (0.25% trypsin-EDTA 4Na in HBSS)

Table 2.1 Culturing information for cell lines

2.2.4 197 neural stem cell culture

2.2.4.1 Laminin coating of tissue culture plasticware

197 NSC were grown on laminin-coated tissue culture plastic. 1 mg/ml mouse laminin-1 (Trevigen) was thawed at 4°C and diluted in cold DMEM/F12 to 20 µg/ml final concentration. The appropriate volume of laminin (**table 2.2**) was used to generously cover the bottom of the culture vessels and vessels were coated for 2-24 hours at 37°C. The laminin was aspirated and the vessels washed with double the original laminin volume of DMEM/F12. Flasks were used immediately or stored at 4°C for 2-3 days.

culture vessel	volume of laminin to coat
T75	5 ml
T25	2.5 ml
6-well	2 ml
96-well	60 µl

Table 2.2 Volumes of laminin required to coat tissue culture vessels

2.2.4.2 Passage of 197 NSC

Cells were passaged at 80-90% confluency. Spent medium was aspirated from a T25 and cells washed with 5 ml Hank's balanced salt solution (HBSS) for 2 minutes. 1 ml trypsin was added to the flask and incubated at 37°C until cells were detached. The trypsin was neutralised with 2.5 ml trituration solution (see **appendix 1.3**). Cells were harvested and pelleted at 160 rcf for 5 minutes. The cell pellet was resuspended in fresh NSC culture medium (see **appendix 1.1**) supplemented with 20 ng/ml EGF (Sigma) and 10 ng/ml bFGF (Peprotech) and passaged $1x10^6$ into a T75 flask, $2.5x10^5$ into T25 flask, $5x10^4$ in 6-well, $5x10^3$ in 96-well. Culture medium, with fresh growth factors (see **appendix 1.2**), was replenished every other day and cells passaged 2-3 times a week. Reagents were not kept for more than 2 weeks at 4°C. 197 NSC were frozen as described in **2.2.3** in 90% NSC culture medium supplemented with 10% DMSO.

2.2.4.3 Differentiation of 197 NSC

Differentiation of 197 NSC cultures was initiated at 50% confluency by removal of growth factors, EGF and bFGF, from the culture medium. 50% of culture medium was replenished every 5-7 days.

2.2.5 PrP null neurosphere culture

2.2.5.1 Neurosphere isolation

Isolation of neurosphere lines used methods similar to those described previously (Reynolds et al., 1992;Reynolds and Weiss, 1992). Embryos from F5_FVB/PrP null mice were harvested at embryonic day 13.5. The brains were removed, transferred to a 35-mm plate containing HBSS and mechanically dissociated roughly with a scalpel. The tissue was then enzymatically dissociated to a single cell suspension with 3% collagenase II-S (Sigma) for 10 minutes at 37°C, followed by trituration with a 200 µl Gilson pipette, and a further 3 minutes incubation at 37°C. The collagenase was neutralised with 10% FBS-containing NSC culture medium. The cells were centrifuged at 100 rcf for 5 minutes and the pellet resuspended in 10 ml NSC culture medium supplemented with EGF, bFGF and 1x antibiotic/antimycotic (Sigma; containing 100U/ml penicillin, 100ug/ml streptomycin, 250 ng/ml amphotericin). The cells were cultured in a T25 flask placed vertically in a humidified incubator at 37°C with 5% CO_2. After 2 days, non-adherent cell aggregates were harvested and placed into a new T25 flask. After 4-7 days of culture, distinct spheres of cells containing CNS stem cells (neurospheres) were observed.

2.2.5.2 Neurosphere maintenance

Neurosphere cultures underwent a 50% media change every 3-4 days. Neurospheres were passaged every 7-10 days with 0.3% collagenase II-S at a ratio of 1:4. Neurospheres from a T25 were pelleted at 100 rcf, resuspended in 200 µl 0.3% collagenase II-S and incubated at 37°C for 10-15 minutes. Neurospheres were gently triturated with a 200 µl Gilson pipette, and the collagenase neutralised with 10% FBS-containing NSC culture medium. The cells were centrifuged at 100 rcf for 5 minutes and the pellet resuspended in NSC culture medium supplemented with EGF and FGF and passaged. To prevent attachment of neurospheres to the culture vessel, the flasks were gently tapped every other day. Neurospheres were harvested and frozen, 2-3 days after passage as small neurospheres, in NSC culture medium supplemented with 30% FBS and 8% DMSO.

2.2.5.3 Growth of PrP null neurospheres as adherent stem cells

PrP null cells were cultured as adherent stem cells and could be differentiated as described for 197 cells (section **2.2.4.3**).

2.2.6 Determining plating efficiency for cell lines

10 cells per well were seeded in a 96-well plate and colonies counted under the microscope 3-4 days later. The plating efficiency was calculated by taking the average number of colonies per well divided by 10 and expressing as a percentage.

2.3 General molecular biology

2.3.1 Preparation of agar plates

For growth of transformed *E.coli*, Luria Bertani (LB) agar was prepared (see **appendix 2.2**) in ddH_2O, autoclaved and cooled to 50°C before the addition of filter-sterilised ampicillin to 100 µg/ml final concentration. The warm LB agar was poured carefully into 10 cm petri dishes and allowed to set overnight.

2.3.2 Transformation of competent *E.coli*

JM109 competent *E.Coli* cells (Promega) were thawed on ice; 100 µl was mixed quickly with 50 ng plasmid DNA in a 12ml round-bottomed tube and placed on ice for 10 minutes. Control mock-transformation was performed using JM109 cells alone. Transformation was achieved by heat-shock at 42°C for exactly 50 seconds, after which cells were transferred back to ice for a further 2 minutes. 900 µl filtered pre-warmed LB medium (see **appendix 2.1**) without antibiotics was added and the suspension incubated at 37°C for 45 minutes, whilst shaking at 150 rpm. Cells were concentrated by pulsing for 5 seconds and 100 µl and 400 µl of transformed cell suspension were spread onto LB agar-ampicillin plates (section **2.3.1**). These plates were inverted and incubated overnight at 37°C. The resultant transformed colonies were prepared for plasmid DNA extraction (section **2.3.3**).

2.3.3 Maxi-prep of plasmid DNA

5 ml LB ampicillin medium was inoculated with a successfully transformed *E.Coli* colony from plates prepared above (section **2.3.2**) and the culture grown for 8 hours at 37°C, whilst shaking at 180 rpm. 1 ml of this *E.Coli* starter culture was used to inoculate 500 ml LB-ampicillin medium and grown overnight on a shaker at 37°C. Plasmid DNA was extracted using QIAGEN maxi-prep kit according to manufacturer's instructions. This system employs a modified alkaline lysis in conjunction with patented QIAGEN anion-exchange resin, which selectively binds plasmid DNA under appropriate low salt and pH conditions. Saturated overnight LB cultures were centrifuged for 15 minutes at 4°C at 6000 rcf. The supernatant was discarded and the bacterial pellet resuspended completely in buffer P1 (50 mM Tris-HCl, pH 8, 10 mM EDTA, 100 µg/ml RNase A). Cells were lysed under alkaline conditions by addition of buffer P2 (1% SDS, 200 mM NaOH) at RT for 5 minutes. To precipitate genomic DNA, chilled buffer P3 (3 M potassium acetate, pH 5.5) was added and incubated on ice for 20 minutes. The lysate was centrifuged at 4°C, at 20,000 rcf for 30 minutes and the supernatant promptly removed and loaded onto an equilibrated QIAGEN 500-tip. Any residual impurities were removed by washing the tip twice with buffer QC (1 M NaCl, 50 mM MOPS). Pure plasmid DNA was eluted in high salt buffer QF (1.25 M NaCl,

50 mM Tris-HCl pH 8.5), precipitated and desalted by mixing with 0.7 volumes of isopropanol, followed by centrifugation at 15000 rcf at 4°C for 30 minutes (the cold temperature encourages flocculation of DNA). The DNA pellet was washed in 15 ml 70% ethanol, re-centrifuged, air-dried and resuspended in molecular biology grade H_2O.

2.3.4 Preparation of glycerol stocks

For long-term storage, 1ml fresh log-phase *E.coli* cultures (from starter cultures) were mixed with sterile glycerol to a final concentration of 20% (v/v) glycerol. The glycerol culture was transferred to cryotubes, snap frozen in dry ice and stored at -70°C.

2.3.5 Spectrophotometric determination of DNA concentration and purity

DNA in solution has an absorption spectrum at 260 nm wavelength of light (OD_{260}), which can be used to calculate its concentration with the following formula:

DNA concentration (µg/ml) = OD_{260} x dilution factor x 50µg/ml

The ratio of absorbance readings at 260 nm and 280 nm (OD_{260}/OD_{280}) can be used to estimate the purity of DNA in solution. 500 µl ddH_2O was transferred to a clean quartz cuvette to set the reference point to zero on the spectrophotometer at both 260 nm and 280 nm. 5 µl of the DNA sample solution was diluted in ddH_2O to a total volume of 500 µl and transferred to a second cuvette. Absorbance readings were taken at 260 nm and 280 nm. (OD_{260} and OD_{280}). OD_{260} readings of less than 0.15 were considered unreliable. If this occurred, the dilution factor was reduced and a repeat measurement taken. The ratio of OD_{260}/OD_{280} for pure DNA preparations is from 1.8. Only sufficiently pure DNA, with an OD_{260}/OD_{280} ratio of between 1.8 and 2, was used for transfection.

2.3.6 Ethanol precipitation of DNA

This procedure was used to remove contaminants (e.g. protein) from the DNA preparation to ensure it was of sufficient purity for transfection. To equalise the ion concentration, 1:10 volume 3M sodium acetate (pH 5.2) was added to the DNA solution. 3 volumes of cold 100% ethanol were added, the mixture vortexed and incubated at -80°C for 1 hour or -20°C overnight. The DNA was pelleted at 13,000 rcf at 4°C for 15 minutes. The supernatant was fully removed with a pipette and the DNA pellet washed with 70% ethanol. The DNA was repelleted at 13,000 rcf at 4°C for 5 minutes, the supernatant removed and the pellet left to dry on a tissue before resuspending in molecular biology grade H_2O.

2.3.7 DNA sequence analysis

This technique was kindly carried out by Gary Adamson, James Uphill and John Beck, to determine siRNA and human *PRNP* sequence. Human *PRNP* primers for PCR and sequencing are shown in **appendix 5**. SiRNA sequences were determined using pSuper.retro vector-specific primers (Oligoengine).

2.3.7.1 Polymerase chain reaction (PCR)

PCRs were carried out in 15 µl reactions containing 13.7 µl MegaMix Blue (Microzone), 0.15 µl forward primer (50 pM/µl), 0.15 µl reverse primer (50 pM/µl) and 1 µl template (genomic) DNA (~50 ng/µl). Cycling conditions on the Tetrad thermal cycler were polymerase activation step of 95°C for 3 minutes and then 34 cycles of DNA template denaturation at 95°C for 30 seconds, primer annealing at 55°C (or relevant temperature) for 40 seconds, 72°C extension step for 45 seconds, and a final extension step of 72°C for 5 minutes and 15°C for 2 minutes.

2.3.7.2 Purification of PCR amplicons for sequencing

PCR products were purified using *micro*CLEAN (Microzone), to remove reaction buffers, enzymes, primer dimers and unincorporated primers and dNTPs, following the manufacturer's protocol. Briefly, an equal volume of *micro*CLEAN was added to a 96-well plate containing PCR products and incubated at RT for 5 minutes. The plate was centrifuged at 3000 rcf for 40 minutes and then inverted onto absorbent paper and pulsed at 100 rcf to discard the supernatant. The purified DNA pellet was then resuspended in 20 µl sterile distilled water.

2.3.7.3 Sequencing of purified templates and vectors

Automated fluorescent sequencing was carried out with the BigDye Terminator Ready Reaction Kit (Applied Biosystems) and internal *PRNP* sequence primers. For the BigDye Terminator Ready Reaction Kit, a sequencing master-mix was made containing (per reaction) 1µl BigDye terminators, 5µl BetterBuffer (Microzone), 0.5 µl forward/reverse primer (1 µM), and 7 µl sterile distilled water. A Gilson Distriman repeater-pipette was used to aliquot 13.5 µl BigDye master-mix into wells of a skirted 96-well plate, to which 1.5 µl purified PCR products were added, for a total reaction volume of 15 µl. Cycling conditions were 96°C for 30 seconds, followed by 30 cycles of 50°C for 15 seconds and 60°C for 3 minutes and a final hold step of 15°C for 5 minutes.

2.3.7.4 Post-reaction clean-up with ethanol/salt precipitation

Sequencing products were precipitated to remove reaction buffers and unincorporated terminators to avoid tall early peaks, often termed "terminator blobs". 55 µl 100% absolute ethanol and 1 µl

3M sodium acetate was added to 20 µl reaction and the mixture was chilled on ice for 15 minutes. The plate was centrifuged at 3000 rcf for 45 minutes to pellet the DNA and the supernatant discarded by inverting onto absorbent tissue paper and pulse-centrifuging at 100 rcf for 1 minute. 150 µl 70% ethanol was added to wash the pellets and the plate was centrifuged at 3000 rcf for 10 minutes. Again, the plate was inverted onto absorbent tissue paper, pulse-centrifuged at 100 rcf for 1 minute to remove the supernatant and the pellet was allowed to air dry for 10 minutes.

2.3.7.5 DNA sequencing on the MegaBACE 1000 DNA Analysis System

The automated MegaBACE 1000 DNA Analysis System (Amersham Pharmacia) was used to sequence DNA. The MegaBACE uses capillary array electrophoresis to perform fragment size separation of fluorescently labelled DNA samples with a confocal optical system to collect data. The manufacturer's guidelines and protocols were followed unless otherwise stated. Precipitated DNA with fluorescently labelled terminators, was resuspended in 10 µl MegaBACE Loading Buffer (Amersham Pharmacia), vortexed thoroughly to ensure the complete solubilisation of the DNA and then pulse-centrifuged to return the liquid to the bottom of the 96-plate wells.

MegaBACE Long Read Sequencing Matrix (Amersham Pharmacia) was used to pressure-fill the capillary array with sieving matrix to separate DNA fragments of varying sizes. Sequencing products were electrokinetically injected into the capillary array by a potential difference of 3 kV for 40 seconds and electrophoresis was carried out in 1x LPA Buffer (Amersham Pharmacia) at 9 kV for 100 minutes. Laser excitation of the fluorescently-labelled samples yielded data as an electropherogram for each capillary/sample which were analyzed in forward and reverse directions using the Sequence Analyser v3.0 package (Molecular Dynamics), and inspected by eye.

2.4 Human PrP expression

2.4.1 Human PrP expression vectors

Human *PRNP* 1 kb open reading frame (ORF) was cloned into BamH1 and Not1 restriction sites of pcDNA3.1(+).neo (Invitrogen, UK; **appendix 4.1A**) and into Bgl II and Not1 of retroviral vector, pLNCX2.neo (Clontech, USA; **appendix 4.1B**), by Professor Parmjit Jat. Following cloning, the human PrP ORF was checked for mutations by DNA sequence analysis (**2.3.7**).

2.4.2 Plasmid DNA transfection of human PrP

BE(2)M17, H4, HEK293, RG6 and N2aG cells were transfected with pcDNA3.1 human PrP expression vector using GeneJammer transfection reagent (Stratagene), according to manufacturer's instructions. The reagent is a cationic polyamine which binds negatively charged

DNA in micelles, the non-polar lipids on the outer layer of the micelles allow DNA entry into the cell by fusion with the plasma membrane. Briefly, cells were seeded in 6-well plates, 24 hours prior to transfection to reach exponential growth phase (~50% confluency). 100 µl unsupplemented, serum-free medium was incubated with 6 µl GeneJammer reagent for 10 minutes at RT. 3 µg plasmid DNA was added to the transfection mix and incubated for a further 10 minutes. 900 µl FBS-containing culture medium was added to cells in a 6-well, the transfection mix added dropwise to the cells and the plate rocked back and forth gently to mix. Control wells without DNA were set up. Cells were incubated overnight and the transfection mix replaced with 1 ml fresh culture medium in the morning. 24 hours later, cells were passaged; each 6-well transferred to three 10 cm dishes. About 12 hours later, cells were selected with the appropriate concentration of G418 (**table 2.1**) until stable colonies became visible (after 2-3 weeks *in vitro*). The appropriate G418 selection concentration for each cell line was determined by performing a G418 kill curve (section **2.4.5**). Either stable clones were pooled to produce "mixed clones" or single cell clones were isolated by picking colonies or by limiting dilution subcloning (as described in **2.4.2.1**).

2.4.2.1 Isolation of single cell clonal lines

Two methods were used for the isolation of single cell clones: colony picking and limiting dilution subcloning. For colony picking, medium was removed from the 10 cm dish and single discrete colonies expressing sequence of interest were picked from 10 cm dishes with a sterile 200 µl Gilson tip and transferred to 96-well plate containing culture medium (150 µl per well). For dilution subcloning, the stable mixed transfected population, expressing the sequence of interest, was seeded at 3 cells per well in a 96-well plate. 24-48 hours after plating, wells were examined and those with 1 cell or a small colony derived from one cell were marked and expanded.

2.4.3 Packaging of human PrP into retroviral producer cell line

Human PrP expression vector, pLNCX2, was transiently transfected into the PhiNX cell line to produce retroviral particles containing human *PRNP* ORF. PhiNX-eco cells were used to produce supernatant to infect mouse lines and PhiNX-ampho for infection of cell lines of other species. PhiNX cells were seeded at $1x10^6$ cells per 10 cm dish 24 hours prior to transfection to achieve exponential growth phase. Transfection was performed with FuGene 6 (Roche) according to manufacturer's instructions; 10 µg plasmid DNA and 12 µl FuGene were used per transfection reaction. 10 ml retroviral human PrP supernatant was harvested from each culture dish 48 hours and 72 hours after transfection and passed through a 0.45 µm filter to remove cells. Supernatant was used fresh or 5-10 ml aliquots made for storage at -80°C.

2.4.4 Retroviral transduction of human PrP

Retroviral transduction is more efficient than plasmid transfection because the gene of interest becomes integrated into the genome and it is also less harsh on the cells (Blanton, Jr. et al., 2000). Cells for human PrP transduction (RK13, L929, N2a and *Prnp* knockout PK1 clones) were seeded in 6-well plates to achieve exponential growth phase 24 hours later. In 72 hours, three rounds of human PrP retroviral transduction were performed. Cells were incubated overnight with 50% retroviral supernatant (prepared as described in section **2.4.3**) in culture medium, supplemented with 8 µg/ml polybrene (a cationic polymer, which improved viral infection efficiency by facilitating membrane fusion). Cells were also transduced using pLNCX2 vector-only control supernatants. Cells were allowed to recover for 24 hours before plating at a low density (25,000 cells per 10 cm dish in quintuplicate) and allowed to adhere. Cells successfully transduced with the human PrP expression vector were selected with the appropriate concentration of G418 (see **table 2.1**). Stable human PrP-expressing clones (mixed and single) were isolated as described in **2.4.2.1**. PrP^C expression level was assessed by immunoblotting.

2.4.5 Antibiotic kill curves

Selection antibiotics used were G418, puromycin, and hygromycin, which all kill cells not expressing the relevant resistance gene by inhibiting different stages of protein synthesis. The antibiotic selection concentration for each cell line was determined by performing a "kill curve" as follows. Two 6-well plates, with cells at 40% confluency, were treated with a titration of selection antibiotic in culture medium. Five concentrations of antibiotic were added to wells in duplicate, 2 control wells were set up with no antibiotic. Selection medium was replenished every 3-4 days and the percentage of surviving cells assessed by direct visualisation with light microscopy. The optimum selection concentration was the one resulting in 100% cell death after 3-14 days (depending on antibiotic). Kill curves for G418 lasted for 7-10 days, for puromycin for 3-4 days and for hygromycin B for 10-14 days. For G418, 200, 400, 600, 800 and 1000 µg/ml were tested, for puromycin, 1, 2, 5, 7.5 and 10 µg/ml were tested and for hygromycin B 50, 100, 250, 500 and 1000 µg/ml were tested

2.4.6 Isolation of human PrP-expressing single cell clones for vCJD prion infection

Prnp knockout PK1 clones were transduced with human PrP as described in section **2.4.4** and single cell clones isolated by colony picking (**2.4.2.1**). Clones were grown to confluency and passaged 1:8 to two replica 96-well plates. One plate of the pair was infected with vCJD prion-infected brain homogenate (section **2.7.2**), the other plate was grown to confluency and frozen in 100 µl freeze medium, wrapped in tissue and aluminium foil and stored at -80°C. If the infected

plate revealed any vCJD prion-infected clones, it was planned the replica plate would be thawed and the vCJD prion-susceptible clones expanded and re-infected.

2.5 Knockout of *Prnp* using RNA interference

2.5.1 SiRNA sequence design for mouse *Prnp* knockout

Short hairpin RNAs were designed to selectively knockdown mouse *Prnp* expression but not human *PRNP* expression. Eight 19-mer siRNA duplexes were designed to exactly targeting mouse *Prnp* mRNA and contained a 3'UU overhang (to prevent nuclease digestion; **table 2.3**). Sequences #1, #2, #3 and #4 were designed by Professor Parmjit Jat using a set of empirical design rules (see **4.4.1.1**). Briefly, these included targeting sequences 50-100 base pairs upstream of *Prnp*, starting with an AA dimer and using the next 19 nucleotides, avoiding stretches of more than four A and T (a termination signal for polymerase III) and ensuring the GC content was between 30 and 50%. Sequences #5, #6, #7 and #8 were designed by Dharmacon Inc. (USA) using SMART Selection™ technology, which employs an algorithm to select functional siRNAs (Reynolds et al., 2004). siRNA #1 targeted the mouse *Prnp* open reading frame (containing four mismatches with human cDNA sequence) and siRNA #2 to #8 targeted the 3'UTR of mouse *Prnp*.

siRNA number	Location in mouse prion protein mRNA	Base pair	Sequence
1	coding region	470 - 490	AACCAACCTCAAGCATGTGGC
2	3' UTR	1072 - 1092	AATGTACAGTAGACCAGTTGC
3	3' UTR	1392 - 1412	AACGATAGCTGATTGAAGGCA
4	3' UTR	2039 - 2059	AATCTGCATGTACTTCACGTT
5	3' UTR	1693 - 1711	GAGAGACAATCTAAACATT
6	3' UTR	1695 - 1713	GAGACAATCTAAACATTCT
7	3' UTR	1760 - 1778	GAAATTCTGCTAGCATTGT
8	3' UTR	1512 - 1530	TAGGAGATCTTGACTCTGA

Table 2.3 Location of siRNA target sequences in mouse *Prnp* mRNA

siRNAs #1-4 (black) were designed by Professor Parmjit Jat using empirical design rules. Dharmacon Inc (blue) designed siRNAs #5-8 using *in silico* technology.

2.5.2 Cloning of siRNA into pSuper.retro.puro expression vector

SiRNA oligonucleotides #1-#8 were cloned into the pSUPER.retro.puro expression vector (OligoEngine Inc., USA; **appendix 4.2A**) by Professor Parmjit Jat, according to the manufacturer's instructions. Briefly, 64-mer duplexes (comprising the siRNA target sequence in sense and anti-sense orientations, separated by a 9-nucleotide spacer sequence) were ligated into the vector cloning site between Bgl II and Hind III, under control of the RNA polymerase III H1 promoter. This system transcribes a short hairpin RNA, which is processed intracellularly by the enzyme, Dicer, to functional siRNA (**figure 2.1**). This system allowed stable expression of siRNA and the potential for long-term knockdown of target *Prnp* gene expression. Vector-specific primers were used to verify the correct sequences of siRNA #1-#8.

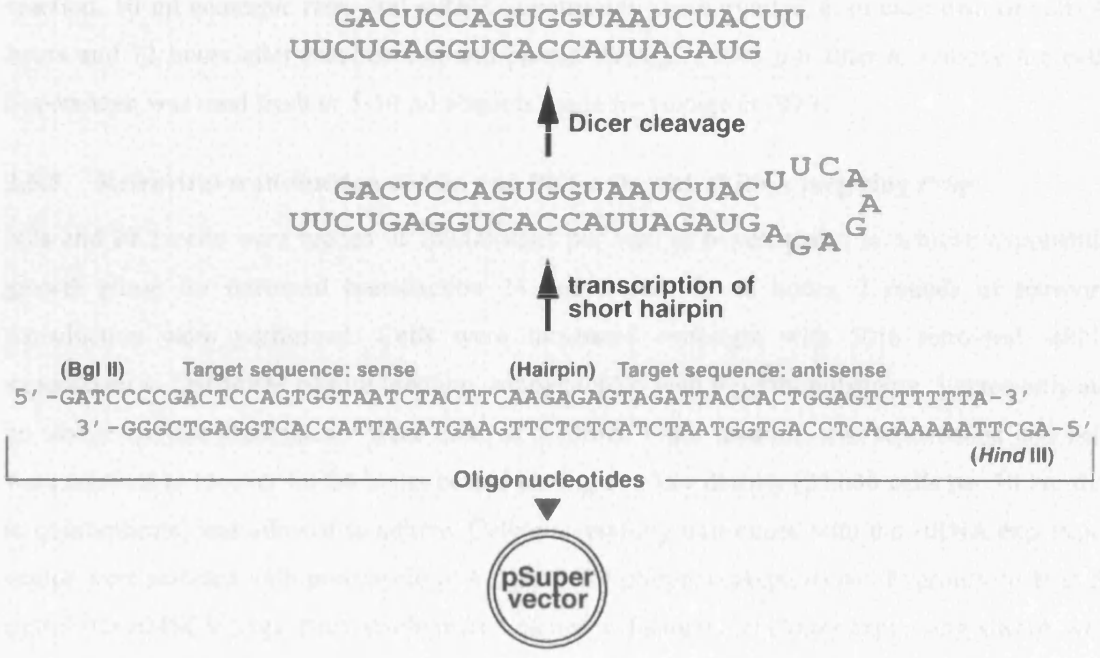

Figure 2.1 Shorthairpin RNA processing

60-nucleotide sequences are transcribed to form to hairpin RNA and processed intracellularly by Dicer to functional siRNAs. *Figure modified from www.oligoengine.com.*

2.5.3 Cloning of siRNA into pMSCV.hyg expression vector

To allow for co-expression of two siRNA sequences in the same cell, siRNAs #2-#5 expression cassettes were cleaved from the pSuper.retro vector, at the Xho I and EcoRI sites, and cloned into another retroviral vector: pMSCV, with a hygromycin B selectable marker (Clontech, USA; **appendix 4.2B**).

2.5.4 Packaging of siRNA expression vector into retroviral producer cells

siRNA expression vectors (pSUPER.retro.puro_siRNA or pMSCV.hyg_siRNA) were transiently transfected into the PhiNX-eco retroviral producer line to produce ecotropic retroviral supernatant. Cells were seeded at 1x 10^6 cells per 10 cm dish, 24 hours prior to transfection to achieve exponential phase of growth. Transfection was performed with FuGene 6 (Roche) according to manufacturer's instructions; 10 µg plasmid DNA and 12 µl FuGene were used per transfection reaction. 10 ml ecotropic retroviral siRNA supernatant was harvested from each dish of cells 48 hours and 72 hours after transfection, and passed through a 0.45 µm filter to remove the cells. Supernatant was used fresh or 5-10 ml aliquots made for storage at -80°C.

2.5.5 Retroviral transduction of N2a and PK1 cells with shRNA targeting *Prnp*

N2a and PK1 cells were seeded at 70,000 cells per well in 6-well plates to achieve exponential growth phase for retroviral transduction 24 hours later. In 48 hours, 2 rounds of retroviral transduction were performed. Cells were incubated overnight with 50% retroviral siRNA supernatant in OptiMEM culture medium, supplemented with 8 µg/ml polybrene. Vector-only and no vector control supernatants were used as controls. Fresh medium was replenished and cells were allowed to recover for 24 hours before plating at a low density (25,000 cells per 10 cm dish in quintuplicate) and allowed to adhere. Cells successfully transduced with the siRNA expression vector were selected with puromycin at 4 µg/ml (for pSuper.retro.puro) and hygromycin B at 50 µg/ml (for pMSCV.hyg). Both stable mixed clones and single cell clones expressing siRNA were established. Single cell clones were isolated as described in **2.4.2.1**. The effect of stable *Prnp*-specific siRNA expression on PrP^C expression levels was assessed by immunofluorescence and immunoblotting of both clonal and mixed populations.

2.5.6 Quantitation of *Prnp* mRNA in cell lines

2.5.6.1 RNA extraction from cell lines

Cells were harvested from 6-well plates at 80% confluency. Culture medium was aspirated from the plates and cells washed with PBS. 750 µl Trizol reagent (Invitrogen) was added per well and plates placed on a shaker for 5 minutes at RT. Each well of Trizol-lysed cells was transferred to one 1.5ml eppendorf tube, shaken vigorously by hand for 15 seconds and left to stand at RT for 5 minutes. 200 µl chloroform was added to each tube, shaken for 15 seconds and left to stand at RT for 5 minutes. Tubes were then centrifuged at 12,000 rcf for 10 minutes at 4°C to separate into aqueous and organic phases. Transfer the upper colourless aqueous phase (containing RNA) into a fresh eppendorf tube. RNA was precipitated by addition of 750 µl isopropanol to each tube. Tubes were shaken for 15 seconds and left to stand at RT for 10 minutes. RNA was pelleted by centrifugation at 12,000 rcf for 15 minutes at 4°C and tubes placed on ice. The RNA pellet was washed with 180 µl 100% ethanol, vortexed and re-pelleted by centrifugation 13,000 rcf for 5 minutes at 4°C. The ethanol was carefully aspirated, the pellet air-dried for 10 minutes and dissolved in water. RNA concentration and purity were determined spectrophotometrically in a similar way to DNA, as described in section **2.3.5.** RNA was diluted 300-fold and absorbance readings taken at 260 nm and 280 nm. The RNA concentration of the solution was calculated using the following formula:

RNA concentration (µg/ml) = OD_{260} x dilution factor x 40µg/ml

Only RNA of purity (OD_{260}/OD_{280} ratio) greater than 1.9 was used for PCR reactions.

2.5.6.2 cDNA synthesis

All reagents obtained for the cDNA synthesis step were acquired from Invitrogen. The cDNA synthesis assays were performed in 20 µl reaction volumes, as described. First, 1 µg RNA was combined with 2.5 µl random primers (100 ng/ul) and RNAse-free water to a total reaction volume of 11 µl, and denatured by heating to 70°C for 10 minutes. The tube was immediately cooled on ice and briefly centrifuged (30 seconds at 13,000 rcf). The following mixture was added to each reaction and heated to 25°C for 10 minutes: 4 µl 5X First Strand Buffer, 2 µl 0.1 M DTT, 1 µl dNTP and 1 µl RNAase out. Finally 1 µl SuperScript II reverse transcriptase was added to the reaction mix and stirred with a pipette tip. The reverse transcriptase reaction conditions were as follows: 25°C for 10 minutes, 42°C for 10 minutes and 70°C for 10 minutes.

2.5.6.3 Quantitative real-time PCR (qRT-PCR)

Prnp mRNA expression levels in *Prnp* knockout PK1 and N2a clones were quantified compared to wild-type by qRT-PCR and data normalised against GAPDH house-keeping gene. The mouse

Prnp FAM-labeled probe and primer set (ABI# Mm00448389_m1) and rodent GAPDH VIC-labeled probe and primer set (ABI# 4308313) used were acquired from ABI and made up according to the manufacturer's instructions. The multiplex qRT-PCR assay was performed in 25 µl reaction volumes. A qRT-PCR master mix was prepared on ice consisting of 12.5 µl QuantiTect Probe PCR master mix (2x), 1 µl mouse *Prnp* probe/primer, 1 µl GAPDH probe/primer and 8.5 µl ddH_20. The 23 µl qRT-PCR master-mix was aliquoted using a Gilson Distriman repeater-pipette into a MicroAmp Optical 96-well reaction plate on ice and 2 µl cDNA added (~50 ng/µl; prepared as described in **2.5.6.2**). Plates were sealed using MicroAmp optical adhesive seals with particular attention paid to sealing around the edges of the plate to prevent evaporation. Plates were then vortexed briefly at medium speed for 2 seconds and pulse centrifuged at 3000 rcf. Plates were run on an ABI 7000 detection system, following the manufacturer's protocol. A rubber evaporation mat supplied with the machine was used to prevent evaporation. Cycling conditions were as follows: 95°C for 10 minutes, 40 cycles of 94°C for 15 seconds and 60°C for 1 minute. Data were analysed using ABI sequence detection software v1.3.1 (Applied Biosystems)

2.5.6.4 Quantitation of relative *Prnp* gene expression using the comparative threshold method

Comparative threshold ($\Delta\Delta C_T$) method was used to determine relative *Prnp* gene expression levels of knockout clones (Heid et al., 1996). In order to apply the $\Delta\Delta C_T$ method, it was necessary to determine that the amplification efficiencies of both target (*Prnp*) and normaliser (GAPDH) probes were equal. This was done by generating a standard curve: five 1:2 serial dilutions (1:2 – 1:32) of PK1 wild-type template cDNA were prepared and run in quintuplicate on qRT-PCR (as described in **2.5.6.3**). A plot of log dilution of cDNA against cycle threshold (C_T; cycle number at which fluorescence emission exceeds a fixed threshold) for each probe was drawn and slopes of the lines determined. Equal slope values (within 0.1 of each other) indicated the probe efficiencies were equal and that the $\Delta\Delta C_T$ method could be applied.

Briefly the $\Delta\Delta C_T$ method involved the following calculations:

- The difference in C_T values between target and normaliser were calculated
  ΔC_T= C_T (sample) - C_T (GAPDH)
- The comparative $\Delta\Delta C_T$ calculation found the difference between the samples ΔC_T and a baseline ΔC_T
  $\Delta\Delta C_T$ = ΔC_T (sample) - ΔC_T (PK1 wild-type)
- These values were then transformed to absolute values with the following formula:
  $2^{-\Delta\Delta CT}$

2.6 Protein detection techniques

Table 2.4 shows anti-PrP monoclonal antibodies and the detection technique in which they were used.

antibody	epitope (human PrP)	PrP species detected	technique
ICSM18	143-153	mouse, human, ovine, bovine, hamster	immunofluorescence, SCA, curing of prion-infected cells
ICSM35	93-102	mouse, human, ovine, bovine, hamster	immunoblotting, FACS
3F4	109 – 112	human, hamster, feline	immunoblotting

Table 2.4 PrP-specific monoclonal antibodies

2.6.1 Protein quantitation assay

All protein assays were performed using the Pierce BCA™ protein assay reagent. This system uses the reaction of protein with Cu^{2+} in an alkaline environment to form Cu^{1+}, which is then detected by the reagent bicinchoninic acid (BCA). The purple reaction product of BCA and Cu^{1+} is water-soluble and exhibits a strong absorbance at 562 nm. For each assay a set of protein standards was made using dilutions of bovine serum albumin (BSA) in the same diluent as the unknown samples (1x sample buffer or PBS). The BSA standards were made at the following protein concentrations to cover expected concentration of samples: 0, 25, 125, 250, 500, 750, 1000, 1500, 2000, 3500, 5000 µg/ml. The assays were performed in a microplate format according to the manufacturer's instructions. 10 µl of each sample was pipetted into a 96-well plate to which 200 µl working reagent (50 parts BCA reagent A to 1 part BCA reagent B) was added. The plate was kept in the dark and incubated at 37°C for 30 minutes. The plate was cooled to RT before reading absorbance at 570 nm. Each assay was performed in duplicate and 2 dilutions of each sample were used. The protein concentration of each sample was determined from the BSA standard curve, using the regression feature of GraphPad Instat software.

2.6.2 Protein extraction for immunoblotting

2.6.2.1 Extraction of protein from cell culture for PrP^C detection

A confluent 10 cm dish of cells was washed in ice-cold PBS (without Ca^{2+} and Mg^{2+}) and the cells harvested using a cell scraper. The cells were collected by centrifugation at 160 rcf for 5 minute at 4°C and the cell pellet washed a further two times in ice-cold PBS to remove all traces of serum.

The cell pellet was then resuspended in 100-250 µl of ice-cold 1x Complete EDTA-free protease inhibitor cocktail (Roche), supplemented with 1 mM $MgCl_2$ and 50 units/ml Benzonase (VWR). The cells were then lysed by three freeze-thaw cycles in liquid nitrogen. Samples were incubated on ice for 15 minutes to allow Benzonase to digest nucleic acids and reducing sample viscosity. Samples were solubilised by boiling for 10 minutes at 100°C in final concentration 1x sample buffer (final concentration; see **appendix 3.1** for 2x recipe), without bromophenol blue or β-mercaptoethanol, which would interfere with the subsequent BCA assay. Samples underwent centrifugation at 16,000 rcf for 10 minutes and the supernatant was collected. A BCA protein quantitation assay (section **2.6.1**) was performed using 1x sample buffer as the diluent. Samples were subsequently adjusted to 1 mg/ml protein with PBS, supplemented with 0.013% bromophenol blue and 2% β-mercaptoethanol reducing agent and boiled for 10 minutes at 100°C to fully denature the protein. Samples underwent centrifugation at 16,000 rcf for 2 minutes to pellet any insoluble material prior to SDS-PAGE.

2.6.2.2 Deglycosylation of PrP^C

Protein extraction from cells was performed (section **2.6.2.1**) and cell lysates adjusted to 2 mg/ml protein concentration. Following the protein denaturation step and clarification of the lysate with a short spin, 30 µg of sample was taken for deglycosylation. Cell lysates, originally containing 4% SDS, were diluted in fresh deglycosylation buffer (see **appendix 3.2**) to a final 0.1% SDS concentration and treated with 30 units/ml *N*-glycosidase F (PNGase; Roche) for 4 hours at 37°C in a thermomixer. Protein precipitation of samples was achieved by adding 6 volumes of ice-cold methanol and centrifugation at 16,000 rcf for 30 minutes. The supernatant was removed and pellets air-dried before dissolving in 1x sample buffer and analysis by immunoblotting.

2.6.2.3 Extraction of protein from cultured cells for PrP^{Sc} detection

Cell lysates were prepared in a similar way to those for PrP^C detection (section **2.6.2.1**). However, after harvesting the cell pellet was resuspended in ice-cold PBS instead of the protease inhibitor cocktail, which would have interfered with subsequent proteinase K (PK) digestion. Two wells of a 6-well plate were harvested and resuspended in 30 µl ice-cold PBS. The BCA protein quantitation assay (section **2.6.1**) was performed prior to boiling in 1x sample buffer, using PBS as the diluent. Cell lysates were adjusted to 2.5 mg/ml with PBS prior to PK digestion.

2.6.2.4 Proteinase K digestion of cultured cells and brain tissue

Cell lysates (as prepared in section **2.6.2.3**) were digested with Proteinase K (PK; Roche) at 5 µg/mg protein for 30 minutes at 37°C on a thermomixer. 10% brain homogenate was first treated

with 50 units/ml Benzonase for 30 minutes at 37°C, followed by 10 µg/mg PK digestion for 1 hour at 37°C. To halt PK digestion, samples were mixed 1:1 with 2x sample buffer (**see appendix 3.1**) supplemented with 4 mM AEBSF protease inhibitor (from 100mM stock in DMSO) and 2% β-mercaptoethanol. Samples were boiled for 10 minutes at 100°C, centrifuged at 16,000 rcf for 2 minutes to pellet any insoluble material prior to SDS-PAGE.

2.6.2.5 PrP^{Sc} precipitation from cell lysates with sodium phosphotungstic acid (NaPTA)

Sodium phosphotungstic acid (NaPTA) is a lead containing compound, which is used in this protocol to pull down aggregated material, i.e PrP^{Sc} and not monomeric PrP^{C} (Safar et al., 1998). The protocol is adapted from Wadsworth and colleagues (Wadsworth et al., 2001). vCJD prion-infected cell lysates were prepared using the same protocol described in **2.6.2.3** and diluted 1:1 with 4% (w/v) sarkosyl in PBS (pH 7.4), followed by incubation at 37°C for 10 minutes on a thermomixer. Following centrifugation at 500 rcf for 1 minute, pre-warmed 4% (w/v) NaPTA/170mM $MgCl_2$ (prepared in ddH_2O titrated to pH 7.4) was added to the sample to a final concentration of 0.3% NaPTA. The sample was incubated at 37°C for 30 minutes on a thermomixer, followed by centrifugation at 15,000 rcf for 30 minutes. The supernatant was discarded and the pellet resuspended in 20 µl final volume with 0.1% sarkosyl in PBS (pH 7.4). 5 µg/mg PK (final concentration) was added to the 20 µl resuspended NaPTA pellet and the sample incubated at 37°C for 1 hour on thermomixer. Centrifugation of the sample at 15,000 rcf for 1 minute was followed by addition of AEBSF and boiling in 1x sample buffer as described in **2.6.2.4**.

2.6.2.6 Immunoblotting

2.6.2.7 SDS-Polyacrylamide gel electrophoresis (SDS-PAGE) of protein extracts

Protein samples (prepared as in section **2.6.2**) and 10 µl SeeBlue pre-stained markers (Invitrogen, UK) were loaded onto pre-cast 16% Tris-Glycine 1.5 mm SDS-PAGE mini-gels (Novex, UK) set up in an XCell *Surelock*™ mini-cell tank (Invitrogen, UK) containing running buffer (see **appendix 3.4**). Unless stated otherwise, 25 µg protein was loaded per lane. Gels were electrophoresed at 200 V for 80 minutes.

2.6.2.8 Protein transfer

Following SDS-PAGE, gels were electroblotted onto Immobilon PVDF membrane (Millipore). The hydrophobic membrane was first wet in 100% methanol (BDH), followed by a 5 minute soak in blotting buffer (**see appendix 3.5**). Three pieces of Whatman No.1 filter paper (Whatman Ltd,

Kent) and 5 sponges were also soaked in blotting buffer. A piece of filter paper was laid on top of a sponge, followed by the gel. The membrane was laid onto the gel, taking care to exclude air bubbles, followed by two sheets of filter paper. This was then sandwiched between 5 sponges and laid inside a Novex blot module and placed into an XCell *Surelock*™ mini-cell tank (Invitrogen, UK). The tank was filled with blotting buffer. Electroblotting was performed at 35 V for 90 minutes.

2.6.2.9 Immunodetection of PrP

After electroblotting, membranes were transferred to square tissue culture dishes (Falcon) and washed in PBST (see **appendix 3.7**) to remove excess blotting buffer. The membrane was blocked for 1 hour at RT with gentle agitation in 5% non-fat milk powder (Marvel Premier Brands, UK) in PBST and washed 4 times in PBST. Overnight incubation at RT of the membrane in anti-PrP primary antibody (biotinylated-ICSM35; D-Gen Ltd., UK, or 3F4; Covance) diluted as appropriate in PBST (0.25 μg/ml or 1:5000, respectively) was followed by 5 washes in PBST over 45 minutes. An avidin-biotin alkaline phosphatase (AP)-conjugated complex (DAKO) was used for secondary labeling of the biotinylated primary antibody. The complex was prepared according to manufacturer's instructions in PBST. AP-conjugated goat anti-mouse IgG and IgM secondary antibody (Biosource) was used in conjunction with 3F4 primary antibody. The membrane was incubated for 45 minutes at RT with secondary antibody and then washed for 1 hour in PBST, followed by two 5 minute washes in Tropix Assay Buffer (see **appendix 3.8**). It was developed using Tropix CDP-Star chemiluminescent AP-substrate (Applied Biosystems). The membrane was placed between 2 pieces of acetate paper and visualized by exposure to Biomax MR film (Anachem) before development and fixation. Western blots presented in this thesis are representative of at least 3 replicates.

2.6.2.10 Coomassie staining of protein on tris-glycine gel

Following SDS-PAGE, gels were stained for 30 minutes with 0.1% (w/v) Coomassie brilliant blue R in 30% (v/v) methanol and 10% (v/v) acetic acid. Subsequently gels were washed with destain (40% [v/v] methanol, 10% [v/v] acetic acid) until protein bands were visible. Bands were visualised on a light box and photographed using 677 Polaroid gel cam (Sigma). This procedure was used to check successful protein transfer and equal protein loading in PK-digested samples when reprobing with β-actin was not possible.

2.6.2.11 Densitometric analysis of immunoblot for quantitation of PrP^C expression levels

Densitometry analysis was performed from film using a Kodak Image Station 440CF with Kodak 1D 3.6 image analysis software. The net intensity values for the PrP^C bands were determined for

Prnp PK1 KO clones transduced with human PrP^C and then expressed as a fold increase in PrP^C expression compared to the wildtype PK1 cell line.

2.6.3 Immunofluorescence staining

2.6.3.1 Preparation of coverslips for immunofluorescence

Poly-L-lysine is a non-specific attachment factor for cells and functions to enhance electrostatic interaction between negatively charged ions of the cell membrane and the culture surface. When adsorbed to the culture surface, poly-L-lysine increases the number of positively charged sites available for cell binding. For immunofluorescence experiments, sterile 22 mm glass coverslips (BDH) were coated with 1 mg/ml poly-L-lysine hydrobromide (Sigma P1399; in sterile water). Briefly, one coverslip was placed in each well of 6-well plates. 400 µl poly-L-lysine was pipetted onto the coverslip surface and left to coat for at least 30 minutes at RT. Coverslips were then washed three times in sterile distilled water and air-dried in a laminar flow hood before use. Depending on cell lines, 30-50,000 cells were seeded onto each coverslip and grown to 75% confluency before immunocytochemistry. Sufficient coverslips were set up to allow for secondary antibody-only controls and for each condition to be tested in duplicate.

2.6.3.2 Immunofluorescence staining protocol

Cells were fixed onto glass coverslips (prepared as in section **2.6.3.1**) using 4% (w/v) paraformaldehyde (pH 7.4) for 20 minutes at RT, washed three times with PBS, and then permeabilised in 100% methanol at -20°C for 15 minutes. Following another three PBS washes, cells were incubated in 10% normal goat serum (NGS) for 30 minutes at 37°C in a humidified chamber. The primary antibody for the desired target protein (see **table 2.5**) was diluted to the appropriate concentration in 1% NGS in PBS and applied to coverslips for 1 hour at 37°C in a humidified chamber. The secondary antibody-only controls were incubated in 1% NGS in PBS during this period to determine if primary antibody binding was specific for the target protein. After washing with PBS, cells were incubated for 45 minutes with the desired fluorescent-tagged goat anti-mouse or anti-rabbit secondary antibody (Molecular Probes Inc), diluted to the appropriate concentration in 1% normal goat serum in PBS (see **table 2.5**) at 37°C in a humidified chamber. The coverslips were then washed three times in PBS and mounted in antifade medium (DAKO) containing either 1 µg/ml 4',6-diamidino-2-phenylindole (DAPI) or 1 µg/ml Hoechst for nuclear counterstaining.

Primary antibody	Antibody host	Supplier	Concentration	Secondary antibody	Concentration
anti-PrP ICSM18	mouse	D-Gen UK, Ltd	10 ug/ml	AlexaFluor 488	1:1000
nestin	mouse	Chemicon	1:500	AlexaFluor 555	1:500
BIII-tubulin	mouse	Sigma	1:1000	AlexaFluor 488	1:200
GFAP	rabbit	DAKO	1:5000	AlexaFluor 568	1:2500

Table 2.5 Antibodies used for immunofluorescence

2.6.3.3 Immunofluorescence image acquisition and analysis

Images were obtained using a Zeiss Axioplan 2 MOT microscope and Plan Neofluar 10x/0.30 Ph1 objective at RT. A Zeiss AxioCam MRm camera controlled by Axiovision Control software was used. Dr Mark Kristiansen helped to obtain fluorescent images using a confocal microscope (Zeiss microscope LSM510 META). The microscope was equipped with a "plan-Apochromat" 63x/1.40 Oil DIC objective and is controlled by Zeiss LSM software. Fluorescence was recorded at 488 nm using 30 mW argon laser for excitation. Zeiss immersol™ 518 F was used as imaging medium. At least 5 random fields of view were studied from duplicate coverslips and assessed for target protein expression, specificity was determined by comparison with secondary antibody only controls. Results were corroborated blind by a second operator.

2.6.4 Fluorescence activated cell sorting (FACS)

FACS was used for isolation of human PrP^C over-expressing cells. Stable human PrP^C clones were transduced with human PrP^C by three overnight rounds of retroviral infection (section **2.4.4**). FACS sorting was performed 48 hours later.

2.6.4.1 Harvesting cells and PrP immunostaining for FACS

Cells were maintained on ice and kept in sterile conditions throughout the procedure. Cells were washed twice in ice-cold PBS, harvested by trituration and counted. Cells were pelleted by centrifugation at 160 rcf for 5 minutes at 4°C and resuspended at 2 x 10^6 cells per ml. 400,000 cells of each cell line were set aside for secondary antibody-only controls. The remaining cells were incubated for 45 minutes at 4°C with ICSM35 anti-PrP antibody diluted to 2.5 µg/ml in PBS containing 0.01% sodium azide preservative. Following two washes in PBS, cells were incubated for 45 minutes at 4°C in the dark with FITC-conjugated anti-mouse IgG Fab (Sigma) diluted 1:50 in PBS containing 0.01% sodium azide. Following a wash with PBS, cells were resuspended in 3

ml OptiMEM medium with 5% serum, placed in capped sterile FACS tubes (Falcon) and maintained on ice until sorting.

2.6.4.2 Isolation of cells with high human PrP^C expression by FACS

Sorting was performed on a Beckman Coulter Epics Altra sorter with Expo2 software (Institute of Child Health, London) with FACS technician, Joanne Buddle. Cells were excited by a 488 nm argon laser, and PrP FITC-positive cells collected using 525 nm +/- 20 nm bandpass filter. Forward scatter and side scatter characteristics were used to gate out dead cells, debris and clumps. Cells expressing greater than endogenous PrP^C levels (outside secondary antibody-only control and wild-type gates) were sorted. Cells were sorted on the basis of purity. Human PrP^C over-expressing cells were sorted into culture medium with 20% FCS and pelleted by centrifugation, resuspended in conditioned medium as quickly as possible after the sorting procedure (to increase viability). They were plated at about 50,000 cells per 6-well and left in the 37°C incubator to recover for at least 24 hours.

2.7 Prion infection of cells

Prion-infected material was handled as biohazardous under Biosafety level 3 containment. Work with prion-infected material was performed in a containment level III facility within a Biomat class I microbiological safety cabinet, which protects the user from air-borne particulate contamination by inward air flow at the front aperture of the cabinet and filtration of exhaust air.

2.7.1 Homogenisation of prion-infected brain tissue

This task was performed by assigned members of staff, Dr Jonathan Wadsworth and Katie Fox. Prion-infected brain specimens in sealed pots were partially thawed from -80°C and transferred to a petri dish. A suitable quantity of tissue was excised using a disposable scalpel and forceps, sealed in a disposable plastic pot and weighed. A 10% (w/v) brain homogenate was prepared in sterile Dulbecco's PBS (without Ca^{2+} and Mg^{2+}). The tissue was disrupted by repeated aspiration through disposable needles of decreasing diameter (commencing with 19-gauge needle, through 21-gauge and 23-gauge needles) until homogenate eventually passed easily through 25-gauge needle without blocking. Brain homogenate aliquots were stored in sterile screw-top tubes at -80°C.

2.7.1.1 Human prion-infected brain homogenate

Appropriate consent and ethical approval were obtained for use of vCJD prion-infected brain material in the development of a cell model of human prion disease (LREC refs: 03/N113 and

03/N006). Tissue from the frontal cortex of vCJD donors, PDG 2946, PDG 3140 and PDG 5063, was used to prepare 10% vCJD brain homogenate (as described in **2.7.1** above) and assigned inocula numbers I2811, I3139 and I4618, respectively (see **table 2.6**). I2811 vCJD inoculum was used for infection of cells unless stated otherwise. 12811 transmissibility was demonstrated in wild-type mice (**appendix 6**).

patient identifier	inoculum number
PDG 2946	I2811
PDG 3140	I3139
PDG 5063	I4618

Table 2.6 vCJD inocula

2.7.1.2 Mouse prion-infected brain homogenate

Brains from scrapie-sick CD-1 mice infected with Rocky Mountain Laboratory (RML) prions were used to prepare 10% RML brain homogenate (as described in **2.7.1**).

2.7.2 Standard method for prion infection of cell lines

Cells were seeded in 96-well plates to yield 50% confluency the following day. 10% (10^{-1}) prion-infected crude brain homogenate (prepared as described in **2.7.1**) was diluted in pre-warmed culture medium to the desired concentration (0.0001% and 2%), mixed thoroughly by vortexing and added to cells for 72 hours. After 72 hours, the prion-infected inoculum was removed and cells washed with PBS. Cells were either sib-selection subcloned (see **2.7.2.1**), or passaged normally, and assayed for the presence of PrP^{Sc} by cell blot assay or scrapie cell assay (**sections 2.7.5.1** and **2.7.5.2**) after at least the equivalent of 1:1000 passage to dilute out the original inoculum. Cells exposed to culture medium only were used as uninfected negative controls. Prion-resistant cell lines with similar doubling times to candidate lines were exposed to prion-infected brain homogenate in parallel to monitor the presence of original inoculum in the cultures. These were called "particle monitor" cell lines and they allowed the detection of PrP^{Sc} in the cultures, which derived from inoculum. Once these cultures were clear of PrP^{Sc}, it was concluded *de novo* (newly produced) PrP^{Sc} was being produced in candidate cells.

2.7.2.1 Sib-selection subcloning of prion-infected cells

Following 72 hour prion infection (**section 2.7.2**), cells from four 96-wells were resuspended, pooled and viable cells counted using a haemocytometer. 150-400 cells per well (depending on plating efficiency of cell line) were distributed into three 96-well plates to yield 100 colonies and

grown to confluency. Cells were passaged normally and assayed for PrP^{Sc} by SCA (**section 2.7.5.2**) after the first passage.

2.7.3 vCJD prion infection of differentiating 197 NSC

197 NSC were seeded to yield approximately 60% confluency the following day (~3000 cells per 96-well; ~ 80,000 cells per 6-well). Cells were differentiated by removal of growth factors (EGF, bFGF) from the culture medium. 197 NSCs were prion-infected at day 0 or day 4 differentiation with 0.1% (unless otherwise stated) or 0.01% semi-purified vCJD prion-infected brain homogenate (preparation of which is described in **2.7.3.2.2**). In parallel, they were mock-infected with semi-purified normal human brain homogenate. Differentiating NSCs were exposed to brain homogenate for 96 hours, followed by a wash with HBSS and replacement of the differentiating culture medium. 50% media changes were subsequently performed every 5-7 days.

2.7.3.1 Anti-PrP antibody treatment of differentiated 197 NSC as particle monitor control for prion infections

Anti-PrP antibody treatment cures prion-propagating cells, this is thought to be due to antibody binding to cell surface PrP^{C} and preventing its conversion to PrP^{Sc} (Enari et al., 2001). Differentiated neurons cannot be passaged, therefore, prion-infected inoculum cannot be diluted out in this way. In order to determine if the PrP^{Sc} signal detected in cells was derived from the active replication of PrP^{Sc} or from the original inoculum, actively prion-propagating cells were cured with anti-PrP antibody treatment. Cells were treated for five days with 5 µg/ml ICSM18 antibody diluted in culture medium before being assayed for PrP^{Sc} by immunoblotting.

2.7.3.2 Inoculum preparation for infection of cell lines

2.7.3.2.1 *Washed vCJD inoculum*

This procedure was carried out to remove soluble toxic factors from brain homogenate. 10% (w/v) brain homogenate (see **section 2.7.1**) was pelleted by centrifugation at 16,000 rcf for 30 minutes in an eppifuge. The supernatant was removed and the wash step involved the pellet being resuspended in 1 ml sterile PBS. The inoculum was then re-pelleted at 16,000 rcf for 30 minutes and the pellet resuspended in culture medium to the appropriate concentration for infection

2.7.3.2.2 *Semi-purification of vCJD prion-infected brain homogenate with detergent*

A 10% (w/v) brain homogenate was thawed and diluted 1:10 in sterile lysis buffer (see **appendix 3.9**), vortexed and centrifuged at 16,000 rcf for 15 minutes. The supernatant was discarded. The

pellet was resuspended by vortexing in warmed cell culture medium, to a final concentration of 0.1%, and then directly added to cells.

2.7.3.2.3 *Sonication of prion-infected brain homogenate*

Semi-purified inoculum was prepared as described in section **2.7.3.2.2**. Following the final spin of the semi-purified inoculum, the pellet was roughly resuspended in culture medium to final concentration of 1% and transferred to a 15 ml tube. This volume was sonicated for a continuous 1 second pulse at 40% power output, using a MS73 probe. Inoculum was immediately diluted to the desired concentration in pre-warmed culture medium and added to cells.

2.7.4 Replication-competent Moloney MuLV retroviral infection of cells

MuLV supernatant was harvested from milk lung amphotropic retroviral producer cells and passed through a 0.45 µm filter to remove cells. Cells were incubated overnight with 33% amphotropic MuLV viral supernatant in culture medium, supplemented with 4 µg/ml polybrene. Cells were replenished with fresh culture medium the following day. Cells were cultured normally in the presence of 2 µg/ml polybrene to enhance retroviral infection within the population. MuLV infection of cells was determined by immunoblotting for viral capsid protein (CAp30) with anti-Rauscher p30 goat polyclonal antibody (1:10,000; a kind gift from Dr Peter Klohn) and anti-goat HRP secondary antibody (1:5000; DAKO). Antibodies were diluted in 1% non-fat milk and 1% normal goat serum. Blots were developed with ECL reagent (West Pico Supersignal, Pierce).

2.7.5 Assaying for PrP^{Sc} in cells

2.7.5.1 Cell blot assay (CBA)

The CBA procedure, developed by Bosque (Bosque and Prusiner, 2000), is briefly described in (Klohn et al., 2003). Following prion infection, 80,000 cells were seeded onto 25 mm Thermanox coverslips (Nunc) in 6-well plates. After growth for 4-5 days at 37°C with 5% CO_2, cells were blotted onto nitrocellulose membrane (0.45 µm Bio-Rad) soaked in lysis buffer (see **appendix 3.9**). This involved placing lysis buffer-soaked Whatman filter paper onto a glass plate and placing coverslips on top cell-side up. Nitrocelluose membrane, first wet with water and then soaked for 5 minutes in lysis buffer, was laid on top of the coverslips followed by dry filter paper. The sandwich was pressed together for 2 minutes using a second glass plate. The nitrocellulose membrane, to which the cells had adhered, was peeled away carefully and dried for 1 hour at 37°C. The membrane was then incubated with 5 µg/ml PK (specific activity 30millianson units/mg, Merck Pharmaceuticals) in lysis buffer for 90 minutes at 37°C, rinsed twice with ddH_2O,

and incubated in 2 mM phenyl methyl sulfonyl fluoride (PMSF) for 10 minutes. The membrane was placed into denaturing buffer, 3 M guanidinium thiocyanate (GSCN) in 10 mM Tris-HCl (pH 8.0), for 10 minutes, rinsed five times with water, incubated in Superblock (Pierce) for 1 hour. The membrane was shaken with 0.3 µg/ml ICSM18 monoclonal anti-PrP antibody in TBST (see **appendix 3.6**) with 1% non-fat milk powder (Marvel, Premier Brands, UK) for 1 hour and washed in TBST four times for 5 minutes. The membrane was then incubated with HRP-conjugated anti-mouse IgG1 antibody (Zymed; 1:30,000 in TBST 1% non-fat dry milk) for 45 minutes. After washing five times for 5 minutes with TBST, membranes were dried at RT on filter paper (protein side up), soaked for 3 minutes with ECL reagent (West Pico Super Signal, Pierce) and exposed to X-ray film (Hyperfilm ECL, Amersham Pharmacia).

2.7.5.2 Scrapie cell assay (SCA)

The SCA is an ELISA-based assay that was developed in the MRC Prion Unit as a quantitative, highly sensitive *in vitro* assay for RML mouse prions (Klohn et al., 2003). It can detect single PrP^{Sc}-positive cells. It was used to detect infectivity in cells following infection with both the RML strain of mouse-adapted prions and human prions. Unless otherwise stated all steps were carried out at RT. All steps were undertaken in class I microbiological safety cabinet in containment level III laboratory. Solutions were aspirated by a vacuum pump into trap containing sodium hypochlorite (20% final concentration) for decontamination (**figure 2.2A**). GSCN-containing solutions were decontaminated with 2N NaOH because GSCN-containing solutions react with sodium hypochlorite to produce chlorine gas.

Prion-infected cells were transferred to an Elispot plate (Enzyme-Linked Immunospot Multiscreen Immobilon-P 96-well Filtration Plates, Millipore; **figure 2.2B**). Elispot plates were activated by wetting the 0.45 µm PVDF membrane of each well with 70% ethanol, aspirating and washing once with PBS. 100 µl PBS was added to keep the membrane moist. An average cell number per well was calculated from five wells of 96-well prion infection plate and 25,000 cells were transferred to the membrane of an Elispot plate. SCA controls were always seeded onto the same plate: uninfected cells as negative controls (25,000 cells per well) and chronically RML prion-infected PK1 cells (iPK1) as positive controls (5000 and 15,000 cells per well). Cells were seeded onto the membrane by applying a vacuum and drying them onto the membrane in a 50°C oven in biocontainment boxes. PK concentration to digest PrP^{C} was determined for each cell line. 50 µl PK (Roche) diluted in lysis buffer was added to each well for 90 minutes at 37°C before it was aspirated. The plate was washed twice with PBS, exposed to 160 µl per well 2 mM PMSF for 10 minutes to inhibit the action of the PK, washed once with PBS before incubation with 160 µl of 3

M guanidinium thiocyanate (GSCN) in 10 mM Tris-HCl (pH 8.0) for 10 minutes to expose the PrP^{Sc} epitopes. GSCN was discarded into 2N NaOH and the wells washed five times with PBS.

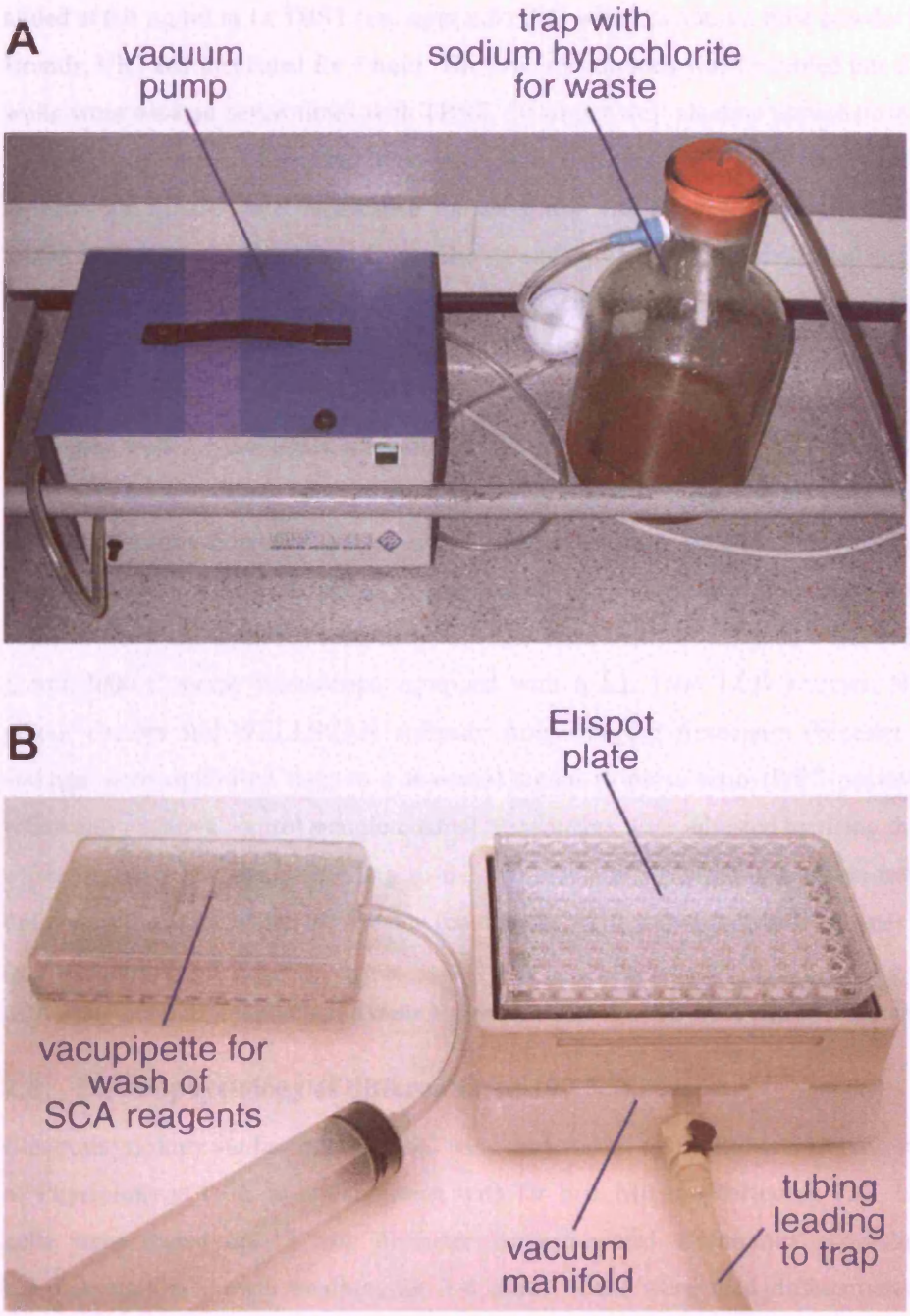

Figure 2.2 SCA equipment

A Vacuum pump and trap containing 100% sodium hypochlorite for decontamination of SCA solutions

B Vacuum manifold holding Elispot plate

For immunoprobing of PrP^{Sc}, 160 µl per well Superblock blocking buffer (Pierce) was added to plates for 1 hour and aspirated. 50 µl per well anti-PrP ICSM18 monoclonal anti-PrP antibody was added at 0.6 µg/ml in 1x TBST (see **appendix 3.6**) with 1% non-fat milk powder (Marvel, Premier Brands, UK) and incubated for 1 hour. The primary antibody was discarded into 2N NaOH and the wells were washed seven times with TBST. 50 µl per well alkaline phosphatase (AP)-conjugated anti-IgG1 (Southern Biotechnology Associates) diluted in TBST/1% non-fat milk powder (appropriate dilution was established for each new vial of secondary antibody by titration) was added and plates incubated for 1 hour. The secondary antibody was discarded and the plate washed eight times with TBST. The underdrains of the plates were removed and plates dried under airflow and taken to containment level II laboratory.

50 µl per well AP-conjugate substrate (prepared as recommended by Bio-Rad) was added until there was a clear colour change in the positive controls (approximately 20 minutes). The AP-substrate was discarded and the plates were washed twice with de-ionised water before being dried under airflow. Plates were stored in the dark at –20°C until analysed. PrP^{Sc}-positive cells were counted using the Zeiss KS Elispot system and each well was assigned a SCA value (**figure 2.3**): Stemi 2000-C stereo microscope equipped with a KL 1500 LCD scanner, Hitachi HV-C20A colour camera and WELLSCAN software from Imaging Associates (Bicester, UK). Detection settings were optimised to give a maximal signal to noise ratio (PrP^{Sc}-positive sample counts relative to negative control sample counts). Parameters were adjusted by using the training feature of the software program according to the manufacturer's instructions. Prion-infected wells were defined as those for which SCA value (counts per well) was significantly greater than background (particle monitor):

SCA value of vCJD prion-infected wells > mean particle monitor SCA value + 5 x standard deviation

2.8 Electrophysiology of differentiated 197 NSC

Electrophysiology studies on 197 NSC were undertaken by Dr Roberta Donato in the Department of Physiology at UCL in collaboration with Dr Erik Miljan (ReNeuron Ltd., UK). Briefly, 197 cells were plated on 13 mm diameter laminin-coated Thermanox coverslips (Nalge Nunc International) in growth medium for 3-4 days. Cells were then differentiated by removal of growth factors from the medium for 7-14 days. At specified times (days of differentiation), coverslips were placed in a recording chamber on an upright microscope (Olympus). Cells were perfused with an extracellular solution containing (in mM): 125 NaCl, 2.4 KCl, 2 $CaCl_2$, 1 $MgCl_2$, 26 $NaHCO_3$, 1.1 NaH2PO_4, 10 glucose, and bubbled with 95% O_2, 5% CO2. The conventional

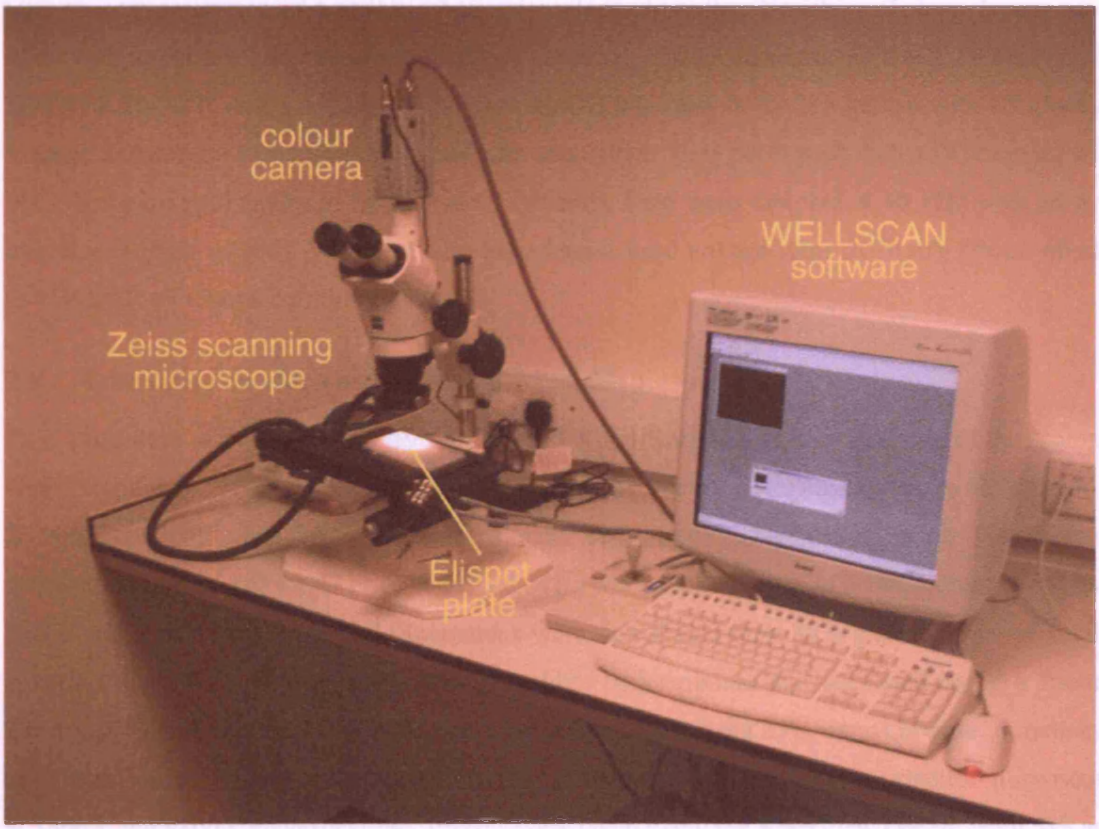

Figure 2.3 Zeiss KS Elispot system

Stemi 2000-C stereo microscope equipped with a KL 1500 LCD scanner, Hitachi HV-C20A colour camera and WELLSCAN software from Imaging Associates (Bicester, UK).

whole cell patch clamp technique was employed by using an Axopatch 1-D patch-clamp amplifier (Axon Instruments, Foster City, CA) both for current clamp and voltage clamp recordings. Electrodes were pulled from thick walled borosilicate glass (World precision Instruments, Herts, UK) to a tip resistance of 4-6MΩ (PP-83 microelectrode puller; Narishige, Tokyo, Japan) when filled with an intracellular solution containing (in mM); 130 KGluconate, 10 NaCl, 10 HEPES, 10 EGTA, 2 MgATP, and 1 $MgCl_2$, pH7.4 with NaOH and osmolality 298 mOsm with 25 glucose. Voltage and current pulse generation and data acquisition were performed with a PC running with WCP software (University of Strathclyde, Scotland). Data were sampled at 10 kHz with an A/D interface (Digidata 1200). Voltage clamp experiments used voltage steps of 10 mV (from -60 mV to + 30 mV) of 400 ms duration.

2.9 Transmission electron microscopy (TEM)

This procedure was performed by Dr Alison Wood-Kaczmar at the Institute of Neurology. Undifferentiated 197 cells were plated on 13 mm Thermanox coverslips coated with laminin at 20,000 cells per coverslip. When confluent, cells were differentiated using the standard differentiation protocol for 47 days and fixed using 3% glutaraldehyde in 0.1M sodium cacodylate buffer and 5 mM CaCl2, pH 7.4. Specimens were dehydrated through a graded series of Analar ethanol (70%, 90%, 100%), embedded in araldite resin mixture and sectioned using a Richert Ultracut S microtome diamond knife. Sections were stained using 25% uranyl acetate in methanol and Reynolds lead citrate. Images were taken on a Philips CM10 transmission electron microscope at 3800X and 9800X magnification. Images were taken using the KeenView system from SIS and processed in Adobe Photoshop.

2.10 Statistical analysis

Data were expressed as mean plus standard error of mean (SEM; $sd/\sqrt{n}$). Data were compared by 2-tailed *t*-tests and considered significantly different when $P<0.05$. Degree of significance was expressed as follows: $*P<0.05$, $**P<0.005$, $***P<0.0005$, unless stated otherwise.

Chapter 3

Screening neuronal and non-neuronal mammalian tumour cell lines for susceptibility to vCJD prion infection

3.1 Introduction

As outlined in chapter 1, cell lines replicating several non-human mammalian prion strains have been developed (**table 1.1**) but a much needed cellular model of human prion disease is still lacking. Since a number of the existing mammalian prion cell models are derived from immortalised tumour cell lines (Rubenstein et al., 1984;Race et al., 1987;Vilette et al., 2001b;Vorberg et al., 2004b;Baron et al., 2006), this chapter describes how this strategy was pursued for the development of a cellular model of human prion disease. There is considerable evidence supporting a principal role for neurones in prion propagation and disease pathogenesis (Race et al., 1995;Jeffrey et al., 2003), particularly the fact that disease progression can be halted by neuronal depletion of murine PrP^{C} in adulthood (Mallucci et al., 2003). Glia also play a consistent role in prion disease in the form of gliosis and there is also evidence they actively propagate prions (Mallucci et al., 2003;Cronier et al., 2004). Existing prion permissive cell lines suggest that non-neural cells also have the capacity to propagate prions *in vitro*. As a result, in this project human and other mammalian tumour cell lines, of both neural and non-neural origin, were screened for susceptibility to human prion infection. Non-human cell lines were transfected with human PrP^{C} to eliminate the species barrier of prion transmission. An ovine scrapie-propagating cell line, in which ovine PrP^{C} was overexpressed in a rabbit cell line, set a precedent for this heterologous approach (Vilette et al., 2001b).

The criterion for a prion-propagating cell line is the persistent detection of *de novo* PrP^{Sc} (the gold-standard surrogate marker for prion infection) in cells following exposure to prion-infected brain homogenate. In the development of the majority of prion-propagating cell models, immunoblotting was used for the detection of PrP^{Sc} in cells but other techniques do exist (Butler et al., 1988;Schatzl et al., 1997;Nishida et al., 2000;Mangé et al., 2000;Cronier et al., 2004;Vorberg et al., 2004b;Milhavet et al., 2006). The cell blot assay (CBA), developed by Bosque and Prusiner, is 10-fold more sensitive than immunoblotting for the detection of PrP^{Sc}-positive cells and requires fewer cells to be assayed (Bosque and Prusiner, 2000). The assay involves growing prion-infected cells on thermanox coverslips, blotting them onto nitrocellulose membrane and immunodetection of PK-resistant PrP (see **2.7.5.1**). PrP^{Sc}-positive colonies are visualised and counted relative to the number of plated cells. The CBA was used in combination with immunoblotting in the development an ovine scrapie-propagating Schwann cell line and the murine prion-propagating cholinergic neuronal cell line (Archer et al., 2004;Baron et al., 2006). A more recent innovation for the detection of PrP^{Sc} in cell culture was the scrapie cell assay (SCA;Klohn et al., 2003), which was developed as a faster, cheaper,

in vitro alternative to the mouse bioassay for the quantitation of prion infectivity. The assay is a high-throughput version of the CBA in a 96-well format. Prion-infected cells are transferred to an Elispot plate and immunoprobed for PK-resistant PrP (see **2.7.5.2**). The proportion of PrP^{Sc}-containing cells is determined using automated counting equipment (**figure 2.3 and 3.1**). The SCA was used to isolate a highly RML prion-susceptible N2a subclone, called PK1, which is greater than 1000-fold more sensitive to RML prion infection than the N2a parent population (Klohn et al., 2003). In my research project, both the CBA and SCA were employed for the detection of vCJD prion infection in cells.

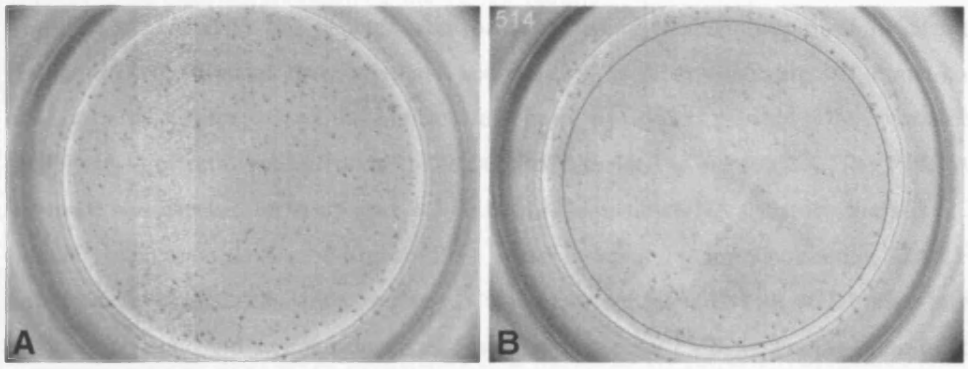

Figure 3.1 Example SCA well showing PrP^{Sc}-positive RML prion-infected PK1 cells

1000 chronically RML prion-infected PK1 (iPK1) cells have been spiked into 24,000 uninfected PK1 cells and assayed for PrP^{Sc} by SCA. (**A**) PK-resistant PrP^{Sc}-positive cells are detected as purple spots by the SCA. (**B**) The Elispot plate is read by a scanning microscope associated with WELLSCAN software, which quantifies the PrP^{Sc}-positive cells per well (yellow circles); in this case 514. *Figure courtesy of Dr P.Klohn.*

3.2 Aims of this study

- To select candidate cell lines based on cell types involved in vCJD pathogenesis or cell types of existing prion-propagating cell lines.
- To determine the status of *PRNP* codon 129 polymorphism in selected human cell lines and to ectopically express human PrP ORF (129 MM) in non-human cell lines.
- To optimise methodology for vCJD prion infection and PrP^{Sc} screening to isolate vCJD prion-susceptible clones from candidate cell lines.
- To screen candidate cell lines for susceptibility to vCJD prion infection.
- To infect a vCJD prion-susceptible cell line with retrovirus to prolong vCJD prion propagation.

3.3 Methods

The data presented in this chapter were produced using methods described in chapter 2. Human PrP^{C} (methionine homozygous at codon 129; 129 MM) was expressed in non-human cell lines or overexpressed in human cell lines by either plasmid DNA transfection (pCDNA3.1) or retroviral infection (pLNCX2) as described in section **2.4**. The *PRNP* ORF sequence was checked for mutations and codon 129 status by DNA sequence analysis (**2.3.7**). Cellular expression levels of human PrP^{C} were assessed by immunoblotting (**2.6.2**) and immunofluorescence (**2.6.3**), respectively. Cell lines were infected with vCJD prion-infected brain homogenate and then subcloned as described in section **2.7.2**. Following prion infection and passaging, the presence of PrP^{Sc} in cell lines was determined using either the cell blot assay (CBA; **2.7.5.1**) or the scrapie cell assay (SCA; **2.7.5.2**). In some experiments, cell lines were infected with amphotropic murine leukaemia virus (MuLV) to test whether prion propagation could be enhanced (**2.7.4**).

3.4 Results

3.4.1 Selection of candidate cell lines to screen for vCJD prion susceptibility

A panel of eleven candidate cell lines was selected on the basis of cell types involved in vCJD pathogenesis and cell lines susceptible to non-human prion strains *in vitro* (see **table 3.1**). Since prions target the central nervous system, where PrP^{C} is highly expressed, six human and two non-human neuroblastoma and neuroglial cell lines were selected. The human neuroblastoma cell lines selected were BE(2)M17, SHSY5Y and SKN-SH; the human neuroglial lines selected were, H4, U87 and NP2; the mouse neuroblastoma line, N2aG, and rat neuroglial line, RG6, were also selected. The CNS is not the only target of prions and non-neural cell types are also permissive to non-human prions *in vitro*. Therefore, one human and

one rabbit epithelial cell line, and a mouse fibroblast were also selected: HEK293, RK13 and L929, respectively. Some existing non-human prion-propagating cell lines were included within this panel of candidate cell lines (asterisked in **table 3.1**): the mouse neuroblastoma N2aG cell line is highly susceptible to RML prions, the mouse fibroblast L929 cell line is permissive to three mouse-adapted scrapie strains (Vorberg et al., 2004b), the rabbit epithelial kidney RK13 cell line is permissive to sheep scrapie (Vilette et al., 2001b) and a mouse-adapted CJD strain, FU-1 (A.Hill, Melbourne University, unpublished data).

cell type	human cell line	non-human cell line
neuroblastoma	BE(2)M17	N2aG*
	SHSY5Y	-
	SKN-SH	-
neuroglial	H4	RG6
	U87	-
	NP2	-
epithelial	HEK293	RK13*
fibroblast	-	L929*

Table 3.1 Candidate cell lines selected for vCJD prion susceptibility screening

* indicates cell lines permissive to non-human prion strains

3.4.2 Suitability of candidate cell lines for vCJD prion infection

As previously mentioned, factors conferring susceptibility to prion infection are poorly characterised. However, it is apparent that susceptibility to prion infection absolutely requires PrP^C expression (Bueler et al., 1993). On occasions, overexpression of PrP^C has enhanced susceptibility to prion infection in cells (Nishida et al., 2000;Giri et al., 2006) and reduced prion disease incubation time in mice (Prusiner et al., 1990;Carlson et al., 1994). Furthermore, methionine homozygosity at codon 129 of *PRNP* (129 MM) is a major determinant of susceptibility to vCJD since it is the genotype of all vCJD cases to date (Collinge, 2005). Therefore, the expression of human PrP^C and codon 129 status was determined in the candidate human cell lines by immunoblotting, immunofluorescence and DNA sequence analysis. To remove the species barrier of prion transmission in non-human cell lines, human PrP ORF (129 MM) was ectopically expressed.

3.4.2.1 *PRNP* codon 129 genotype of candidate human cell lines

The *PRNP* codon 129 genotype of all but one of the human candidate cell lines was methionine homozygous, the genotype of all vCJD cases to date. The BE(2)M17 cell line was heterozygous at codon 129 (129MV) but it was included in the screen because methionine homozygosity at codon 129 of PrP may not be the only susceptible genotype; pre-clinical vCJD was reported at autopsy in a heterozygous individual (MV) (Peden et al., 2004).

human cell line	PrP codon 129 polymorphism
BE(2)M17	MV
H4	MM
HEK293	MM
NP2	MM
SHSY5Y	MM
SKN-SH	MM
U87	MM

Table 3.2 PrP codon 129 polymorphism present in human candidate cell lines
The *PRNP* ORF of human candidate cell lines was sequenced to check for mutations in the coding region and to determine the codon 129 status. No mutations were found in the sequence and all cell lines were codon 129 methionine homozygous (129 MM), except the neuroblastoma BE(2)M17 cell line, which was heterozygous (129 MV).

3.4.2.2 Endogenous PrP^C expression in human candidate cell lines

The expression of human PrP^C was detected in all the human cell lines studied. There was high endogenous human PrP^C expression in BE(2)M17, SKN-SH, U87 and HEK 293 cell lines and relatively low expression in NP2 cell line compared to mouse PK1 cells and normal human brain (**figure 3.2**). The lowest endogenous expression of human PrP^C was observed in the SHSY5Y and H4 cell lines (**figure 3.3**). Since overexpression of PrP^C has been hypothesised to result in increased cellular susceptibility to prion infection (Nishida et al., 2000;Giri et al., 2006), these two lowest PrP^C-expressing cell lines were transfected with human PrP^C to increase expression levels. Two human PrP^C-overexpressing H4 clones were isolated from plasmid transfection (A and B; **figure 3.3**). We acquired a human PrP^C-overexpressing SHSY5Y clone (clone A) derived by retroviral transfection from K.Chumakov (FDA, USA) because the wild-type cells failed to transfect with the plasmid construct (**figure 3.3**). Because conversion of PrP^C to PrP^{Sc} is proposed to occur at the cell surface (Caughey and Raymond, 1991), expression of PrP^C was determined for cell lines by immunofluorescence and all cell lines showed PrP^C expression at the cell surface (**figure 3.4**).

3.4.2.3 Heterologous human PrP^C expression in non-human candidate cell lines

For the development of heterologous prion cell models, non-human cell lines were transfected with human PrP ORF (129 MM) construct. N2aG and RG6 were transfected with a plasmid human PrP ORF construct, which generated two human PrP^C-expressing RG6 clones (A and B) and one human PrP^C-expressing N2aG clone (A) with high expression levels (**figure 3.5A**). Two human PrP^C-overexpressing L929 clones (A and B) and four human PrP^C-overexpressing RK13 clones (A-D) were generated by retroviral infection (**figure 3.5B**). High human PrP^C expression levels were observed in three RK13 clones, A, C, D, and one L929 clone, B, and intermediate expression levels were observed in RK13 clone B and L929 clone A.

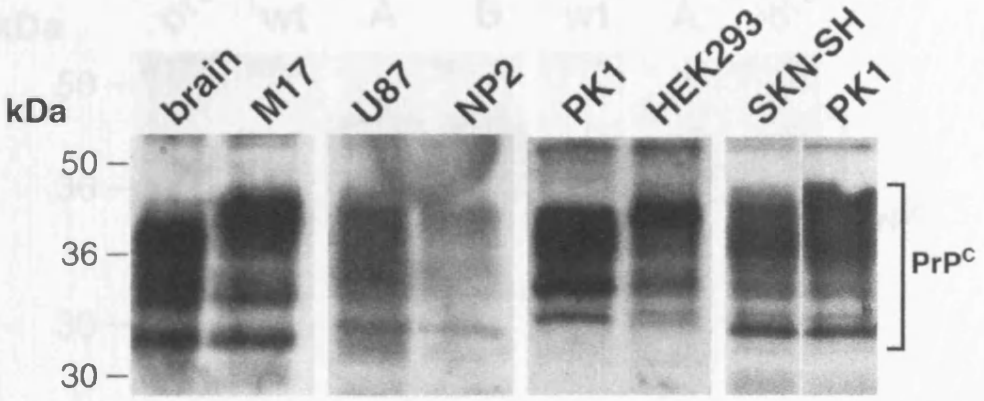

Figure 3.2 Endogenous PrP^C expression in human candidate cell lines

Cell lysates of human cell lines BE(2)M17, U87, NP2, SKN-SH, HEK 293, mouse control cell line, PK1, and normal human brain homogenate (brain) were immunoblotted using anti-PrP antibody, biotinylated ICSM35. 25 µg protein from cell lysates and 50 µg human brain homogenate was loaded per lane. PrP^C runs between 50-30 kDa in its 3 glycosylation states (di-, mono- and un-glycosylated). The endogenous human PrP^C expression in BE(2)M17, HEK293, U87 and SKN-SH cell lines was significant compared to normal human brain and comparable to PK1 PrP^C expression. However, that of NP2 was relatively low.

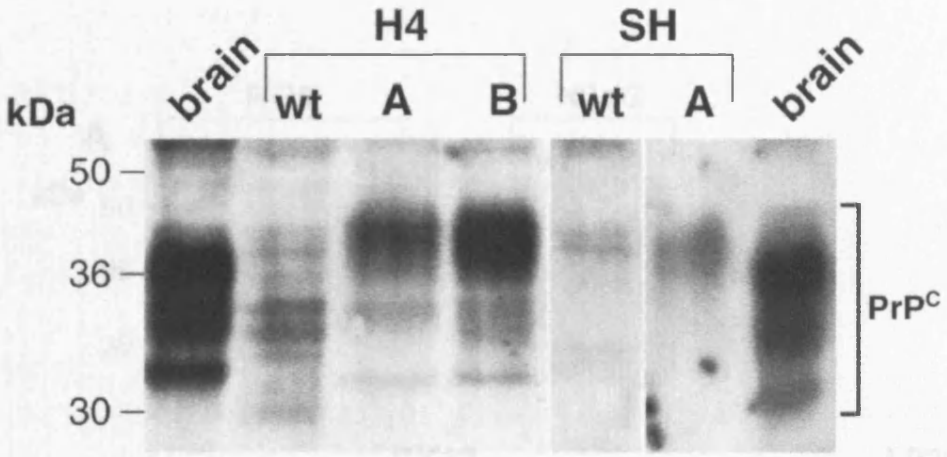

Figure 3.3 Human PrP^C overexpression in low-expressing human candidate cell lines

To improve expression level of human PrP^C expression in H4 and SHSY5Y (SH) cell lines, they were transfected with human PrP ORF and stable clones established. Cell lysates of wild-type cells and their human PrP^C-transfected clones were immunoblotted using anti-PrP antibody, biotinylated ICSM35. 25 µg protein from cell lysate and 50 µg protein from normal human brain homogenate (brain) was loaded per lane. Human PrP^C, which runs between 50-30 kDa, was significantly overexpressed compared to wild-type cells (wt) in 2 H4 clones (A and B) and slightly overexpressed in the SHSY5Y clone (A). The transfected human PrP^C in the H4 clones was of a slightly higher molecular weight than wild-type, possibly due to increased glycosylation.

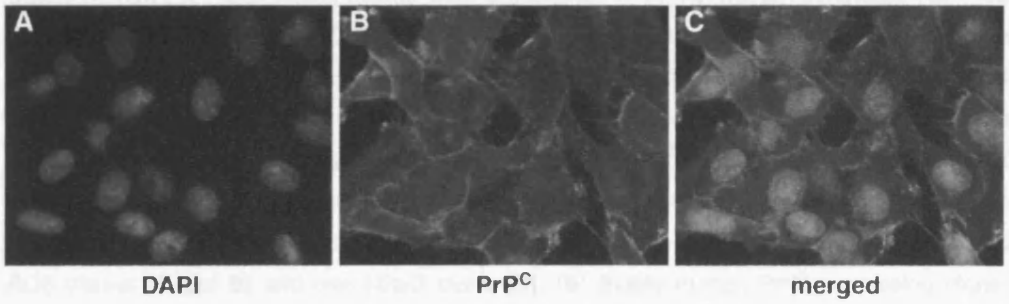

Figure 3.4 Representative image of PrP^C expression to confirm cell surface expression in candidate cell lines

SKN-SH human neuroblastoma cells were grown on poly-L-lysine coated glass coverslips and immunostained for PrP^C. (**A**) DAPI staining of nuclei (blue). (**B**) PrP^C staining with ICSM18 primary antibody and FITC-conjugated anti-mouse IgG secondary antibody (green). This was PrP^C-specific staining since secondary antibody only controls were blank (data not shown) Cells show PrP^C expression throughout the cell, particularly at the cell surface. (**C**) Merged image of A and B.

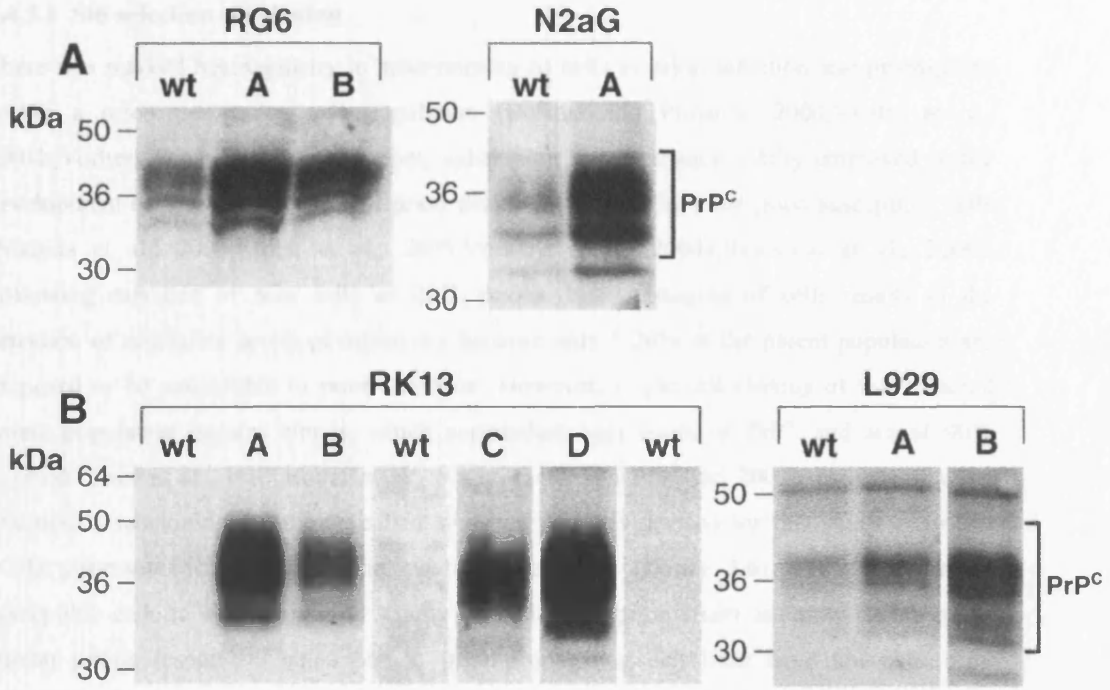

Figure 3.5 Heterologous human PrP^C expression in non-human candidate cell lines
Stable human PrP^C-expressing clones were established from non-human candidate cell lines: RG6, N2aG, RK13 and L929. Cell lysates of wild-type (wt) and human PrP^C-transfected clones were immunoblotted using anti-PrP antibody, biotinylated ICSM35. 25 µg protein from cell lysates was loaded per lane. Since ICSM35B detects rodent and human PrP, successful human PrP^C expression was indicated by an increased PrP^C band intensity (between 50-30 kDa) in human PrP^C-transfected clones compared to wild-type. (**A**) Stable human PrP^C-expressing clones established by plasmid transfection. Human PrP^C was highly expressed in 2 RG6 clones (A and B) and one N2aG clone (B). (**B**) Stable human PrP^C-expressing clones established by retroviral infection. Human PrP^C was highly expressed 3 RK13 clones (A, C and D) and in one L929 clone (B). One RK13 clone (B) and one L929 clone (A) showed intermediate expression levels of human PrP^C. Endogenous PrP^C expression was negligible in RK13 cells and very low in L929 cells. Appreciable levels of endogenous PrP^C were detected in RG6 and N2aG cells.

3.4.3 Optimisation of vCJD prion infection and screening methodology to isolate highly prion-susceptible cells

3.4.3.1 Sib-selection subcloning

There is a marked heterogeneity in susceptibility of cells to prion infection and propagation within a prion permissive cell population (Bosque and Prusiner, 2000;Vilette et al., 2001b;Vorberg et al., 2004b). Therefore, subcloning has been successfully employed in the development of some cell models of prion disease to isolate the most prion-susceptible cells (Nishida et al., 2000;Klohn et al., 2003;Vorberg et al., 2004a;Raymond et al., 2006). Following exposure of N2a cells to RML prions, bulk passaging of cells results in the detection of negligible levels of infectivity because only 1-20% of the parent population are proposed to be susceptible to prion infection. However, single cell cloning of this infected parent population isolates clones, which accumulate high levels of PrP^{Sc} and are 80-90% infected (Race et al., 1987;Butler et al., 1988;Bosque and Prusiner, 2000). In light of these findings, a subcloning technique, called sib-selection, was devised for this study to isolate vCJD prion-susceptible cells within candidate cell lines (**figure 3.6**). The proportion of susceptible cells in a population is strictly dependent on prion strain and may be lower for human prions (especially since human prion-propagating cell lines have not ever been identified). Therefore, we hypothesised (at least) 1 in 10,000 cells of a candidate population was susceptible to vCJD prions. According to the Poisson distribution (which models discrete random variables), in order to have a 95% chance of finding a vCJD prion-susceptible cell of this rarity, at least 30,000 cells needed to be screened, as explained by the equation below:

$P(0) = e^{-m}$. For $P \approx 0.05$, m (variance) = 3. Therefore 10,000 x 3 = 30,000.

To screen this number of clones in a time and cost-effective manner, rather than single cell cloning, the candidate lines were initially subcloned at 100 cells per 96-well following vCJD prion infection (**2.7.2.1**) and assayed for PrP^{Sc} by the high-throughput SCA (see **figure 3.6**). Because the SCA uses a 96-well format, only three plates needed to be assayed per cell line to determine vCJD prion susceptibility. If a candidate cell line consistently showed susceptibility to vCJD infection (indicated by highly PrP^{Sc} positive SCA wells), two strategies were planned for the isolation of vCJD prion-propagating line. First, clones from highly positive SCA wells could be re-infected with vCJD prions and single-cell cloned; any positive clone would be cured of vCJD prion infection with anti-PrP antibody treatment (Enari et al., 2001). Alternatively, the parent cell line could be single-cell cloned and each clone split to two wells (generating replica plates). One plate would be infected with vCJD prions and assayed for PrP^{Sc} by the SCA and the second plate would remain uninfected; highly susceptible uninfected clones could be traced back from highly positive SCA wells (Klohn et al., 2003).

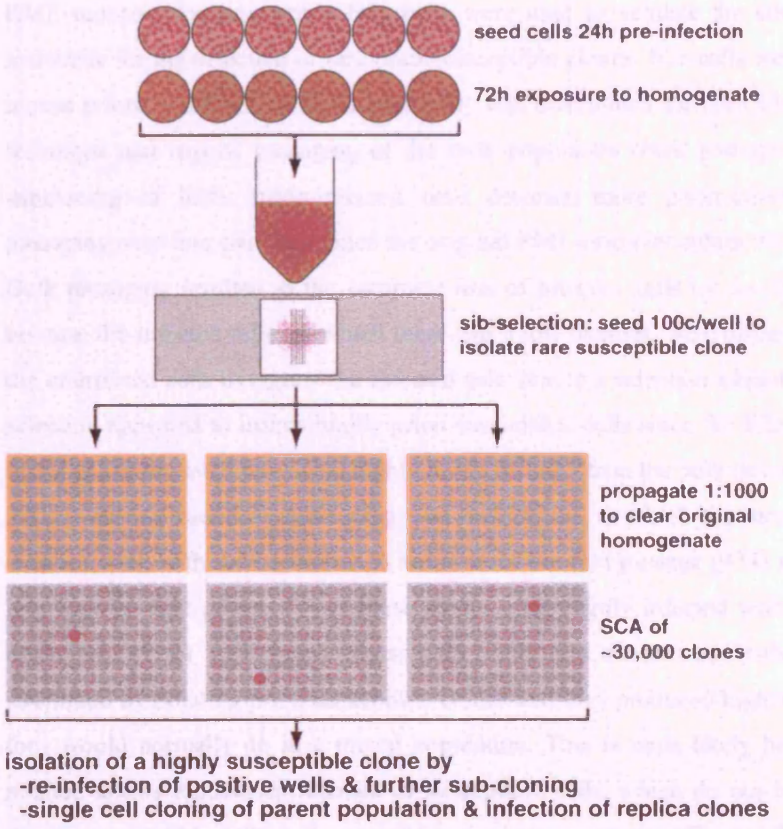

Figure 3.6 Sib-selection subcloning of candidate cell line for isolation of rare highly vCJD prion-susceptible clone

A candidate cell line was exposed to vCJD prion-infected brain homogenate for 72 hours. Viable cells were then counted (indicated by the haemocytometer) and seeded to yield 100 cells per well in three 96-well plates (yellow), thus allowing the screening of ~30,000 clones. Cells were grown to confluency and passaged normally. At each passage, 25,000 cells per well were seeded in Elispot plates (grey) to assay for the presence of PrP^{Sc} by SCA. Once the original vCJD inoculum had cleared from the cultures (indicated by negative SCA of the resistant particle monitor control cells; explained in **3.4.3.4**), positive SCA wells (solid pink wells) indicated prion-infected cells. In order to isolate a vCJD prion-propagating clone, these infected cells were either (1) re-infected with vCJD prions, single-cell cloned and cured of prion infection, or (2) the parent population was single-cell cloned, replica clones produced and one set re-infected with prions.

3.4.3.2 Validation of sib-selection subcloning strategy for the isolation of rare prion-susceptible clones

RML mouse prion-susceptible N2a cells were used to validate the sib-selection subcloning technique for the detection of rare prion-susceptible clones. N2a cells were infected with RML mouse prions and RML prion susceptibility was determined for both sib-selection subcloning technique and regular passaging of the bulk population (bulk passaging). The sib-selection subcloning of RML prion-infected cells detected more prion-infected wells than bulk passaging over four passages, once the original RML-prion inoculum was cleared (**figure 3.7**). Bulk passaging resulted in the complete loss of infected cells by the third passage, possibly because the infected cells, of which there was a low number, were discarded at passage and/or the uninfected cells overgrew the infected cells due to a selection advantage (**figure 3.7**). Sib-selection appeared to isolate highly prion-susceptible cells since the N2a subclones isolated in this way accumulated three-fold higher levels of PrP^{Sc} than the bulk passaged N2a cells (**figure 3.8**). A second round of subcloning was undertaken, in which the most highly RML prion-infected well, with the highest SCA value from the first passage (974) was single-cell cloned into four 96-well plates. 2% of these clones were highly infected with RML prions; with a mean (±SEM) of 1067 (±66). These data imply that sib-selection subcloning increased the likelihood of isolating prion-susceptible clones and they produced higher levels of prions than they would normally do in a mixed population. This is most likely because the subcloning method allows random enrichment of susceptible cells, which do not become overgrown by the non-susceptible cells as they would in the bulk population. Their isolation permits them to accumulate higher PrP^{Sc} levels than would otherwise be possible. Therefore, these findings validate the use of sib-selection subcloning for the detection of rare vCJD prion-susceptible cells in the candidate cell lines.

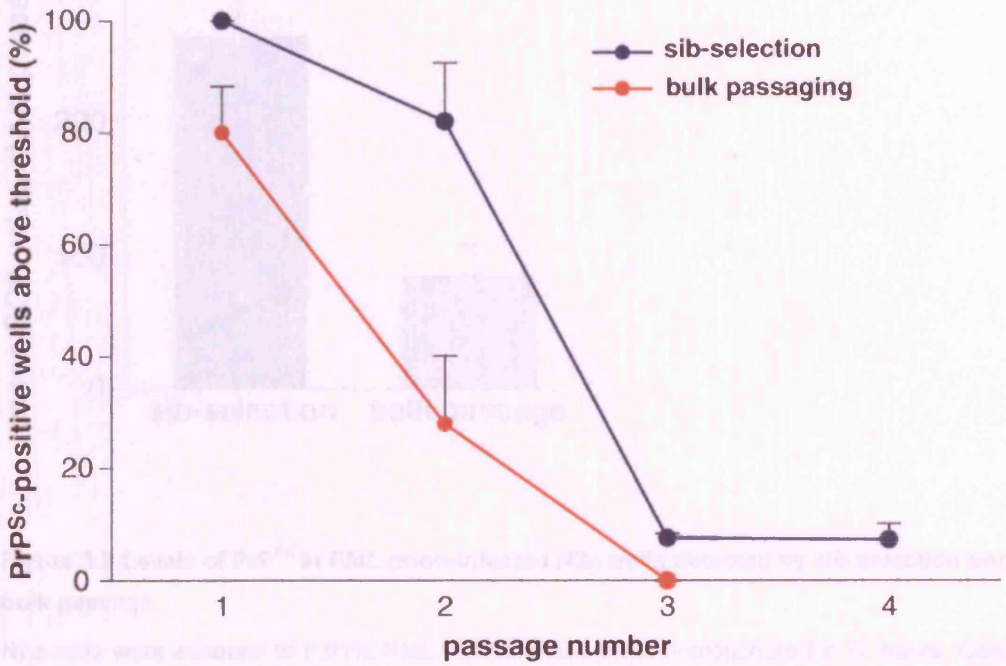

Figure 3.7 Detection of PrP^{Sc}-positive cells in an RML prion-infected N2a population by sib-selection subcloning and bulk passaging

N2a cells were exposed to 0.01% RML prion-infected brain homogenate for 72 hours. Cells were either passaged at 1:10 ratio 3 times *(bulk passaging)* in three 96-well plates, or cells were subcloned to yield 100 colonies per well in three 96-well plates(*sib-selected)*. When RML inoculum was clear (3x 1:10 passages for bulk passage and at the first passage for SCA), the presence of *de novo* PrP^{Sc} was assayed by SCA. Data are expressed as the percentage of PrP^{Sc}-positive wells per total number of wells screened (+ SEM). Sib-selection subcloning picks up significantly more RML prion-infected wells at the 1st, 2nd and 3rd passage than bulk passaging. RML prion-infected wells were detectable by sib-selection even up to the 3rd and 4th passage, whereas bulk passaging of N2a cells resulted in loss of infected cells by the 3rd passage. This may be due to the fact that infected cells were discarded at passage or that in the bulk cultures the uninfected clones grew faster and overgrew the infected cells.

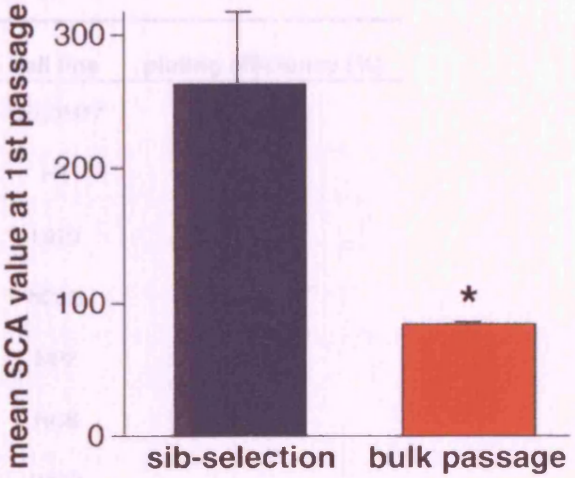

Figure 3.8 Levels of PrP^{Sc} in RML prion-infected N2a wells detected by sib-selection and bulk passage

N2a cells were exposed to 0.01% RML prion-infected brain homogenate for 72 hours. Cells were either passaged at 1:10 ratio 3 times *(bulk passage)*, or cells were subcloned to yield 100 colonies per well (*sib-selected)*. Both set of cells were grown to confluency and assayed for PrP^{Sc} by SCA. Data are presented as mean SCA value (PrP^{Sc}-positive cells) per well (+ SEM) of RML prion-infected wells at the 1st passage (at which the RML inoculum has been cleared from the cultures). The number of PrP^{Sc}-positive cells in RML prion-infected wells detected using sib-selection is significantly higher than when bulk passaging the cultures (*t*-test: *P<0.05).

3.4.3.3 Optimisation steps for each candidate cell line prior to screening

First, the plating efficiency for each candidate cell line was determined (**2.2.6**) in order to calculate the number of cells required for seeding to yield 100 colonies per well for sib-selection (**table 3.3**). Second, the concentration of vCJD prion-infected brain homogenate for infection of each cell line was optimised. Existing prion-propagating cell lines were developed by infecting cells with between 0.01% and 2.5% prion-infected brain homogenate (Archer et al., 2004;Cronier et al., 2004;Vorberg et al., 2004a;Vorberg et al., 2004b). Similar dilutions were used for this study; cells were infected with between 2% and 0.1% vCJD prion-infected brain homogenate. The highest concentration of vCJD prion-infected brain homogenate that each cell line could tolerate, without overtly affecting its normal proliferation rate and morphology, was selected. Third, the Proteinase K (PK) concentration used for SCA was

optimised for each cell line to ensure that all PrP^{C} was digested and thus only PrP^{Sc} detected. Each new batch of PK (Roche # 03115828001) required titration for each cell line. Dilutions used were between 1:15,000 and 1:20,000, which was equivalent to approximately 1 μg/ml.

cell line	plating efficiency (%)
BE(2)M17	40
H4	50
L929	50
N2aG	67
NP2	40
RG6	50
RK13	40
SHSY5Y	25
SKN-SH	25
U87	40

Table 3.3 Plating efficiency of candidate cell lines

Plating efficiency for each candidate cell line was determined (as described in **2.2.6**) in order to ascertain the number of cells to be seeded to yield 100 colonies per well for sib-selection. i.e., for BE(2)M17, 100/0.4 cells (250 cells) were seeded to give 100 colonies.

3.4.3.4 Summary of standard vCJD prion infection, "particle monitors" and PrP^{Sc} screening procedure of candidate cell lines

The standard infection and screening procedure involved 72 hour vCJD infection of candidate cell lines with between 0.1% and 2% vCJD prion-infected brain homogenate (I2811) diluted in culture medium. This was followed by subcloning of cells at 100 final clones per well in three 96-well plates. Cells were grown to confluency and simultaneously passaged normally and seeded (25,000 cells per well) into Elispot plates to be assayed for the presence of PrP^{Sc} by the SCA. In order to distinguish novel PrP^{Sc} production in the candidate cell lines from PrP^{Sc} in the vCJD inoculum, a vCJD prion-resistant cell line with a similar doubling time to each candidate line was infected with vCJD prions in parallel. In this way, the prion-resistant cell line was termed a "particle monitor" since it detected the presence of PrP^{Sc} particles from the vCJD inoculum. The rabbit RK13, mouse N2a and GT1 cells were all used for this purpose. Once the mean SCA value for these particle monitor cells was nearly the same as the mean of the

uninfected cells, the PrP^{Sc} signal could be attributed to *de novo* production of PrP^{Sc} in the candidate cells. Wells containing vCJD prion-infected cells were identified if they exceeded a threshold SCA spot number, which was calculated thus:

threshold SCA value to identify for vCJD prion-infected wells

= mean particle monitor SCA value + 5 x standard deviation

In this way, each cell line was given a measure of "vCJD prion susceptibility", based on the proportion of wells screened that was above this threshold SCA spot number. It was essential to calculate the threshold SCA value as described, rather than selecting an arbitrary SCA spot number, because SCA values can very considerably between assays. vCJD prion-infected wells were monitored over several passages. Consistently PrP^{Sc}-positive cell lines were single-cell cloned in one of two ways (summarised in **figure 3.6**) to isolate a highly vCJD prion-susceptible clone.

3.4.4 Screening of cell lines for susceptibility to vCJD prion infection

Taking into account the human PrP^{C}-expressing clones generated from candidate cell lines, 19 lines were screened in total. The standard infection and screening procedure (described in **3.4.3.4**) was used to assess the susceptibility of the majority of cell lines to vCJD prion infection. Some cell lines were screened by bulk passage and CBA because it was the most sensitive technique available at the start of the project. Promising cell lines indicated by CBA screens were subsequently assessed by the standard procedure.

3.4.4.1 Cell lines resistant to vCJD prion infection

Of the 19 cell lines screened, 13 showed no susceptibility to vCJD prion infection as demonstrated by negative CBA or SCA data (**table 3.4**). These included the neuroblastoma BE(2)M17, neuroglial H4, NP2 and U87 and epithelial HEK293 human cell lines. The L929 mouse fibroblast cell line, N2aG mouse neuroblastoma cell line and RG6 rat neuroglial cell line, all expressing human PrP^{C}, were also resistant.

3.4.4.2 Candidate cell lines susceptible to vCJD prion infection

6 cell lines, namely 4 human PrP^{C}-expressing RK13 clones, SKN-SH and SHSY5Y showed some susceptibility to vCJD prion infection

cell line	concentration vCJD prion-infected inoculum (%)	screening method	number of screens
BE(2)M17	2 & 0.2	CBA	2
BE(2)M17	1 & 0.1	SCA	3
H4	2 & 0.2	CBA	2
H4_A	0.1	SCA	1
H4_B	0.1	SCA	1
HEK 293	2	CBA	2
NP2	1 & 0.1	SCA	2
SHSY5Y	0.2	CBA	2
U87	0.1	SCA	2
L929_A	0.1	SCA	2
L929_B	0.1	SCA	2
N2aG_A	2 & 0.2	CBA	3
RG6_A	2 & 0.2	CBA	9
RG6_A	0.2	SCA	2
RG6_B	2 & 0.2	CBA	5

Table 3.4 Cell lines unable to propagate vCJD prions

Following vCJD prion infection (at the concentration indicated in column 2), cell lines were screened for the presence of PrP^{Sc} with cell blot assay (CBA; after bulk passaging) or by scrapie cell assay (SCA; after sib-selection). At least 300,000 cells were screened per CBA (3 coverslips) and ~28,800 clones per SCA (three 96-well plates). 13 of the 19 cell lines screened were not susceptible to vCJD prion infection are shown in the table. These included human neuroblastoma, neuroglial and epithelial, and non-human neuroglial and fibroblast cell lines.

3.4.4.2.1 Human PrP^C-expressing rabbit epithelial RK13 clones

Four RK13 human PrP^C-overexpressing clones, A-D, were screened by the standard protocol and showed susceptibility to vCJD prion infection (**figure 3.9** and **3.10**). RK13 clones B and D were initially highly susceptible with *de novo* PrP^{Sc} detected in about 40% and 50% of wells at the first passage, respectively. However, these clones lost prion infection rapidly and did not propagate prions for more than two passages. RK13 clones A and C were infected with *de novo* PrP^{Sc} at first passage since it was detected in approximately 20% and 30%, respectively. Although the proportion of prion-infected wells declined over time in these two clones, novel PrP^{Sc} was consistently produced over three passages. This suggested that there was short-term vCJD prion propagation in these clones (A and C) for approximately two weeks.

The most susceptible RK13 human PrP^C-overexpressing clone was RK13 clone C. First, it was susceptible to vCJD prion infection at a lower concentration of vCJD inoculum (0.1%) compared to the other RK13 clones (1%). Second, in one of the nine replicate infections, RK13 clone C showed the longest period of vCJD prion propagation of all the candidate cell lines. PrP^{Sc} was detected in RK13 clone C for six passages following infection with 0.1% vCJD, and for five passages following infection with 1% vCJD, which corresponded to a period of about three weeks (**figure 3.11**). For both inoculum concentrations *de novo* PrP^{Sc} was present in about 80% wells at first passage. The percentage of vCJD prion-infected wells decreased over time, particularly after the third passage. However, the increasing SCA value in the PrP^{Sc}-positive wells, suggested that there was accumulation of PrP^{Sc} in the infected clones over time, which further supported *de novo* PrP^{Sc} production in this clone (**figure 3.12**). The vCJD prion propagation observed over six passages in RK13 clone C could not be replicated more than once.

Attempts to subclone these highly vCJD prion-susceptible RK13 clone C wells failed. First, eight highly PrP^{Sc}-positive wells from the 0.1% vCJD prion infection (mean SCA value: 789 ± 136) were pooled after the second passage, single cell clones were generated and re-infected with 0.1% vCJD prion-infected brain homogenate. However, these clones were not prion-infected at the first SCA (after three 1:10 passages). Second, 864 single cell clones were derived from the uninfected RK13 clone C parent population, replica plates generated, and one set infected with vCJD prions. However, no PrP^{Sc} was present in these single cell clones by SCA.

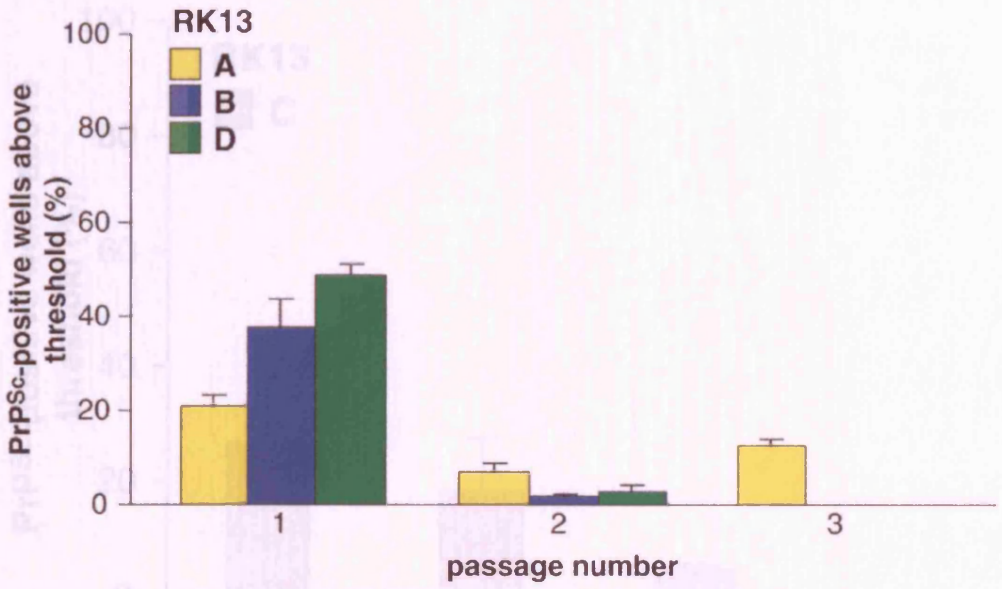

Figure 3.9 vCJD prion infection of human PrP^C-overexpressing RK13 clones A, B and D
RK13 clones A, B and D and RK13 wild-type particle monitor cells were infected with 1% vCJD prion-infected brain homogenate according to the standard procedure. Cells were assayed for the presence of PrP^{Sc} by SCA at passage 1-3. Data are expressed as the percentage of PrP^{Sc}-positive wells above threshold per total number of wells screened (+ SEM). Threshold for vCJD prion infection was calculated as *mean SCA value for vCJD prion-infected particle monitor plus 5 standard deviations*. Data presented are from three 96 well plates (28,800 clones). Although RK13 clones B and D were the most susceptible to vCJD prion infection at the 1st passage, with 40% and 50% wells prion-infected, this tailed off after the 2nd passage. 20% of wells from RK13 clone A were prion-infected at 1st passage and remained infected for three passages. The presence of PrP^{Sc} in RK13 clone A over 3 passages suggested there was short-term propagation of vCJD prions in this clone.

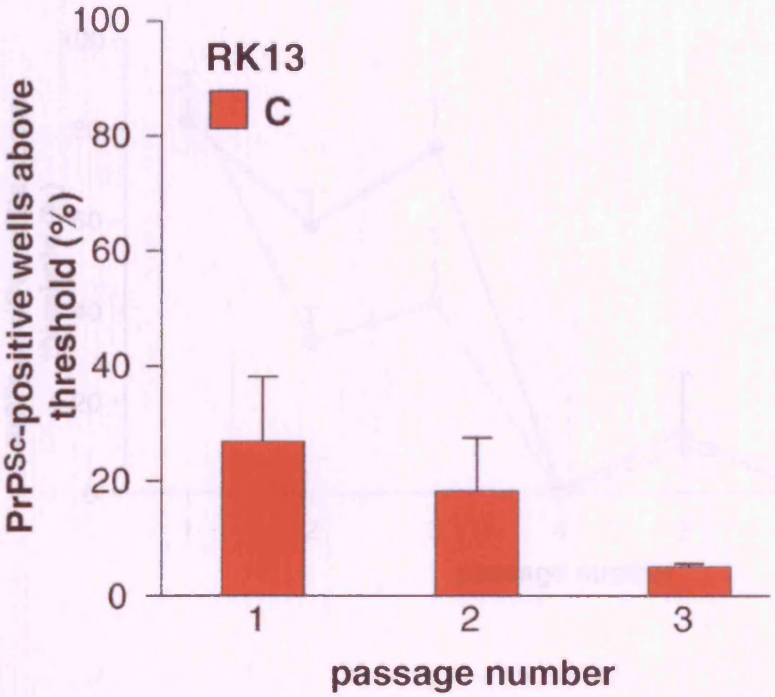

Figure 3.10 vCJD prion infection of human PrP^C-overexpressing RK13 clone C

RK13 clone C and RK13 wild-type particle monitor cells were infected with 0.1% vCJD prion-infected brain homogenate according to the standard procedure. Cells were sib-selected at 250 cells per well in three 96-well plates. Cells were assayed for the presence of PrP^{Sc} at each 1:10 passage. Data are expressed as the percentage of PrP^{Sc}-positive wells above threshold per total number of wells screened (+ SEM). Threshold for vCJD prion infection was calculated as *mean SCA value for vCJD prion-infected particle monitor plus 5 standard deviations*. Data presented are from 9 independent experiments. Approximately 20% of wells of RK13 clone C were prion-infected at 1st passage and the proportion of wells tailed off over 3 passages. The presence of PrP^{Sc} in RK13 clone C over three passages suggested there was short-term propagation of vCJD prions in this clone.

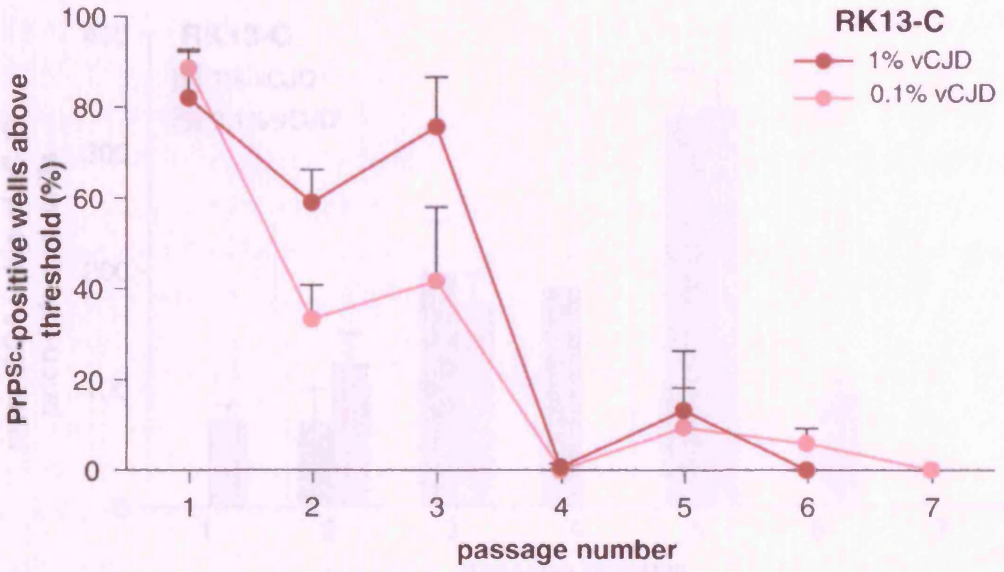

Figure 3.11 Short-term vCJD prion propagation in human PrP^C-overexpressing RK13 clone C

RK13 clone C cells and RK13 wild-type particle monitor cells were infected with 0.1% and 1% vCJD prion-infected brain homogenate according to the standard procedure. Cells were assayed for PrP^{Sc} by SCA at each 1:10 passage. Data are expressed as the percentage of PrP^{Sc}-positive wells above threshold per total number of wells screened (+ SEM). Threshold for vCJD prion infection was calculated as *mean SCA value for vCJD prion-infected particle monitor plus 5 standard deviations*. Data presented are from three 96- well plates (28,800 clones). The percentage of vCJD prion-infected clones was high (>30%) until the 3rd passage for both dilutions of inoculum, at which point it fell dramatically. A small percentage of wells remained infected up to the 5th passage for 1% infected cells (13%) and the 6th passage for the 0.1% infected cells (6%). This was the longest period of vCJD prion propagation observed in any of the candidate cell lines (~3 weeks).

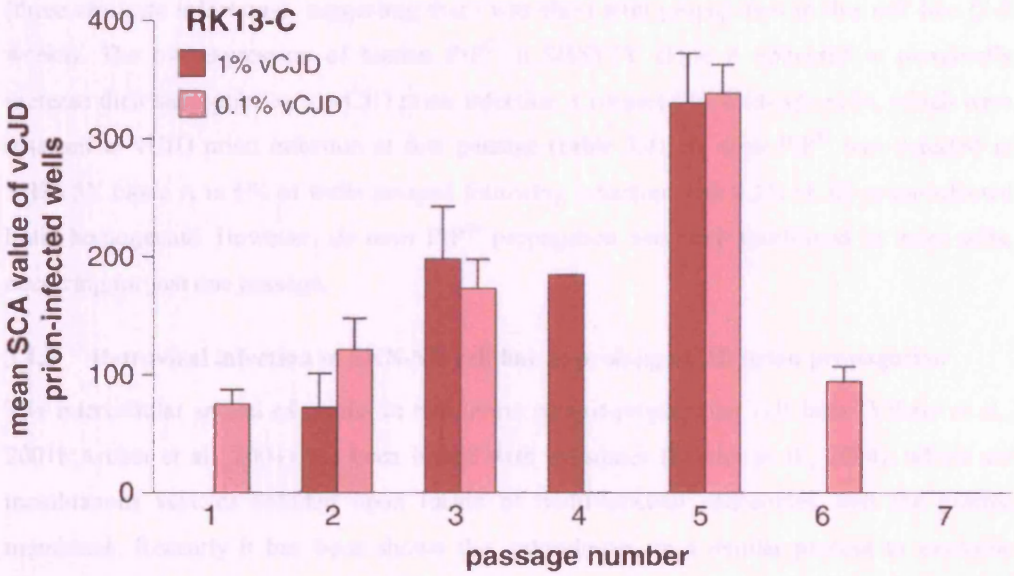

Figure 3.12 Time-course of PrP^{Sc}–positive levels in vCJD prion-infected human PrP^{C}-overexpressing RK13 clone C

RK13 clone C and RK13 wild-type particle monitor cells were infected with 0.1% and 1% vCJD prion-infected brain homogenate for 72 hours according to the standard procedure. Data presented are from three 96-well plates (28,800 clones). Data are presented as mean SCA value per well (+ SEM) for vCJD prion-infected wells. Mean SCA values increased over time from ~50 at passage 1 to ~350 at passage 5. This strongly suggested there was *de novo* production of PrP^{Sc} in the vCJD prion-infected cells of the RK13 clone C.

3.4.4.2.2 Human neuroblastoma cell lines: SKN-SH and SHSY5Y clone A

SKN-SH showed some susceptibility to vCJD prion infection with *de novo* PrP^{Sc} present in 18% of wells assayed the first passage, following infection with 0.1% vCJD prion-infected brain homogenate (**figure 3.13**). Prion infection was consistently present over two passages (three replicate infections), suggesting there was short-term propagation in this cell line (2-3 weeks). The overexpression of human PrP^{C} in SHSY5Y clone A appeared to marginally increase their susceptibility to vCJD prion infection. Compared to wild-type cells, which were resistant to vCJD prion infection at first passage (**table 3.4**), *de novo* PrP^{Sc} was detected in SHSY5Y clone A in 6% of wells assayed following infection with 0.1% vCJD prion-infected brain homogenate. However, *de novo* PrP^{Sc} propagation was very short-lived in these cells, occurring for just one passage.

3.4.5 Retroviral infection of SKN-SH cell line to prolong vCJD prion propagation

The intercellular spread of prions in two ovine scrapie-propagating cell lines (Vilette et al., 2001b;Archer et al., 2004) has been linked with exosomes (Fevrier et al., 2004), which are membranous vesicles secreted upon fusion of multivesicular endosomes with the plasma membrane. Recently it has been shown that retroviruses, in a similar process to exosome generation, exploit cellular multivesicular late endosomes for viral budding (Morita and Sundquist, 2004). Therefore, we hypothesised that co-infection of the SKN-SH human neuroblastoma cell line with vCJD prions and the retrovirus, murine leukaemia virus (MuLV), may initiate chronic prion infection in this weakly vCJD prion-susceptible cell line. It was proposed that infectious prions would be transmitted within the SKN-SH population by recruitment into viral particles, which would infect neighbouring cells.

Co-infection of SKN-SH cells with vCJD prions and replication-competent MuLV was done sequentially. Either MuLV infection was established in SKN-SH cells for ten days (**figure 3.14**), followed by infection with 0.1% and 0.01% vCJD prion-infected brain homogenate, or SKN-SH cells were first infected with vCJD prions followed by MuLV infection at the sib-selection stage. However, whichever co-infection regime was used, MuLV-infected SKN-SH cells were less susceptible to vCJD prion infection than uninfected cells. In three independent infections, MuLV-infected SKN-SH cells were completely clear of prion infection at the first SCA, whereas a small proportion of SKN-SH wild-type cells (mean 16% of wells) were prion-infected. Therefore, retroviral infection of SKN-SH cells did not enhance intercellular transmission of vCJD prions within the culture.

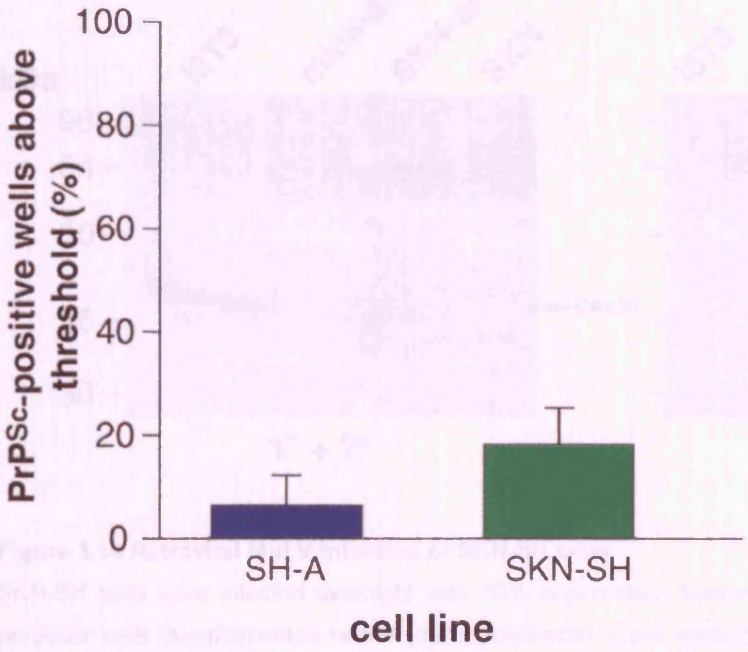

Figure 3.13 vCJD prion infection of human neuroblastoma cell lines SHSY5Y clone A and SKN-SH

SHSY5Y clone A, SKN-SH cells and BE(2)M17 particle monitor cells were infected with 0.1% vCJD prion-infected brain homogenate according to standard procedure. Data are expressed as the percentage of PrP^{Sc}-positive wells above threshold per total number of wells screened (+ SEM). Threshold for vCJD prion infection was calculated as *mean SCA value for vCJD prion-infected particle monitor plus 5 standard deviations*. Data are presented are from 3 independent experiments. Human PrP^{C}-overexpressing SHSY5Y clone A showed very low susceptibility to vCJD prion infection at the first passage, with 6.4% prion-infected wells. SKN-SH cells were more susceptible with PrP^{Sc} present in 18.2% wells.

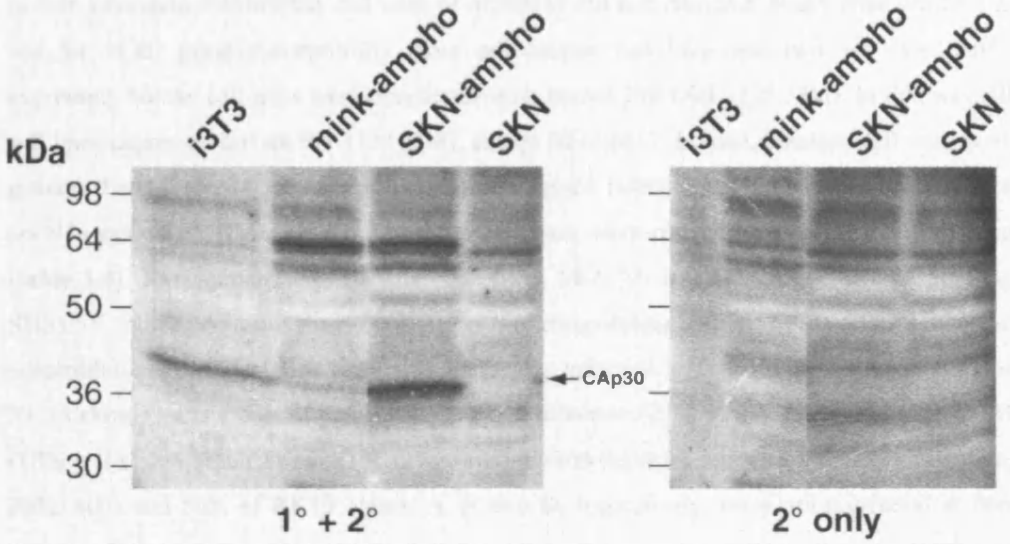

Figure 3.14 Retroviral MuLV infection of SKN-SH cells

SKN-SH cells were infected overnight with 33% supernatant from mink amphotropic MuLV producer cells (supplemented with 4 µg/ml polybrene). Cells were cultured for a further 10 days in the presence of 2 µg/ml polybrene to facilitate the spread of MuLV infection. Cell lysates were prepared from uninfected SKN-SH cells (SKN; 700,000 cells), amphotropic MuLV-infected SKN-SH cells (SKN-ampho; 700,000 cells), mink amphotropic MuLV producer cells (mink-ampho; 360,000 cells) and MuLV-infected 3T3 fibroblast cells (i3T3; gift from P.Klöhn). These cells were analysed for MuLV infection by immunoblotting with anti-Rauscher MuLV p30 primary (1°) goat polyclonal antibody and anti-goat-HRP secondary antibody (2°), which detects the viral capsid protein, CAp30. The CAp30 protein runs at ~36 kDa (left-hand blot) and was present in the positive controls, i3T3 and mink-ampho (although not as strongly, probably because less protein was loaded), in SKN-ampho but not in SKN-SH wild-type negative controls. The presence of the CAp30 band in SKN-ampho cells indicated they had been successfully infected with MuLV. A concurrent secondary antibody control blot (right-hand blot; 2° only) was run to distinguish the CAp30-specific bands from non-specific secondary antibody binding. Importantly there was no non-specific binding at 36 kDa.

3.4.6 Summary of results

Eleven candidate mammalian cell lines of neuronal and non-neuronal origin were selected to test for vCJD prion susceptibility. Four non-human cell lines and two very low PrP^{C}-expressing human cell lines were transfected with human PrP ORF (129 MM). In this way, all cell lines expressed human PrP (129 MM), except BE(2)M17. In total, nineteen cell lines were generated and screened for susceptibility to vCJD prion infection using methodology validated on N2a cells with RML prions. 13 of the cell lines were resistant to vCJD prion infection (**table 3.4**). Two human neuroblastoma cell lines, SKN-SH and human PrP^{C}-overexpressing SHSY5Y clone A, and four human PrP^{C}-overexpressing rabbit RK13 clones showed susceptibility to vCJD prion infection. Following infection with 0.1% vCJD inoculum, the RK13 clone C was the most susceptible to prion infection (27% wells), followed by SKN-SH (18% wells) and SHSY5Y clone A (2% wells). Following infection with 1% vCJD inoculum, 20%, 40% and 50% of RK13 clones A, B and D, respectively, were prion-infected at first passage. The prion infection observed in the cell lines was not persistent. *De novo* PrP^{Sc} was detected in SHSY5Y clone A for just one passage, in RK13 clones B and D and SKN-SH for two passages, and in RK13 clone A and C for three passages. In one infection of RK13 clone C, *de novo* PrP^{Sc} was detected over six passages (~3 weeks). Single cell subcloning of this highly susceptible RK13 clone C, in an infected and uninfected state, did not yield a stably vCJD-prion propagating cell line. SKN-SH cells were co-infected with MuLV retrovirus and vCJD prions in an attempt to prolong prion propagation in this line. However, the cells were made less susceptible to prion infection following MuLV retroviral infection.

3.5 Discussion

As described above, nineteen mammalian cell lines expressing human PrP^{C}, of neural and non-neural origin, were comprehensively screened for susceptibility to vCJD prion infection. This was not an exhaustive screen of cell lines due to pressure on time and resources. There are certainly a number of other human neuroblastoma, epithelial and fibroblast cell lines that could have been screened. Given the involvement of the lymphoreticular system in vCJD pathogenesis (Wadsworth et al., 2001), it would certainly have also been worth screening the follicular dendritic cell line, HK (Kim et al., 1994). Follicular dendritic cells reside in follicles and germinal centres of lymphoid tissue and are reported to highly express PrP^{C} (Brown et al., 1999), accumulate PrP^{Sc} *in vivo* (Kitamoto et al., 1991;van Keulen et al., 1996;Jeffrey et al., 2000) and play a key role in prion neuroinvasion and disease susceptibility (Montrasio et al., 2000;Mabbott et al., 2003;Mabbott and Bruce, 2003).

3.5.1 Dynamic susceptibility model of prion propagation

Despite efforts to ensure that genetic requirements for prion susceptibility were met in the cell lines by expression of human PrP^C with a similar sequence to PrP in the inoculum (codon 129 MM), this approach did not yield a stably vCJD prion-propagating cell line. Therefore, it is apparent that although PrP^C is indispensable for prion infection, other factors play a role in prion propagation in cells. The dynamic susceptibility model of prion propagation proposes that, whilst certain genetic factors must be present, prion propagation in a cell is determined by the relative rates of synthesis and degradation of PrP^{Sc} (see **figure 3.15;** Weissmann, 2004). For chronic prion infection to be established in a cell, a delicate balance between synthesis and degradation of infectivity must be struck; formation of infectivity should exceed degradation to avoid elimination of prion infection but not to the extent where infectivity reaches cytotoxic levels.

3.5.2 Possible reasons for lack of prion propagation in candidate cell lines

Taking into account the dynamic susceptibility model of prion propagation (**figure 3.15**), the cell lines screened in this study may have been resistant to vCJD prion infection for a number of epigenetic reasons. First, infectivity is not as stable as once thought, with less than a 24 hour half-life in N2a cells. It may be that PrP^{Sc}, from the vCJD inoculum and/or formed *de novo* within the cell, was degraded rapidly due to a high protease content in the candidate cell lines. For example, lysosomal cysteine proteases (but not aspartic and metalloproteases) have been proposed to degrade PrP^{Sc} in ScGT1 and CD11c+ dendritic cells *in vitro* (Luhr et al., 2004). Second, since infectivity is halved at each cell division, cell lines with a short doubling time, such as the RG6 cell line (which needed passaging three times a week), would lose infectivity if the rate of PrP^{Sc} synthesis could not compensate. However, selecting cell lines on the basis of long doubling times was not practical, since this would not have made a rapid diagnostic test. Attempts were made to culture the HCN-2 human cortical neuronal cell line but, even in the uninfected state, it did not withstand passaging at a one in three ratio every two weeks. Third, it may be that prion replication was very efficient in the cell lines and that PrP^{Sc} accumulated to lethal levels. This may certainly have been the case for the neuroblastoma cell lines since neurones are particularly susceptible to prion toxicity and there was evidence of some minimal cell death following vCJD prion infection (Muller et al., 1993;Cronier et al., 2004). Fourth, mechanical injury (scratch-wounding) to prion permissive cell lines reduces their susceptibility to prion infection, an effect proposed to be mediated by nucleotide release into the culture medium (Etessami et al., 2005). Therefore, poor tissue culture technique prior to prion infection, such as over-trypsinisation, over-trituration or brisk delivery of prion-infected brain homogenate to the wells may have rendered cells resistant to prion infection. This is unlikely to be the cause of the resistance of cells to vCJD prion infection

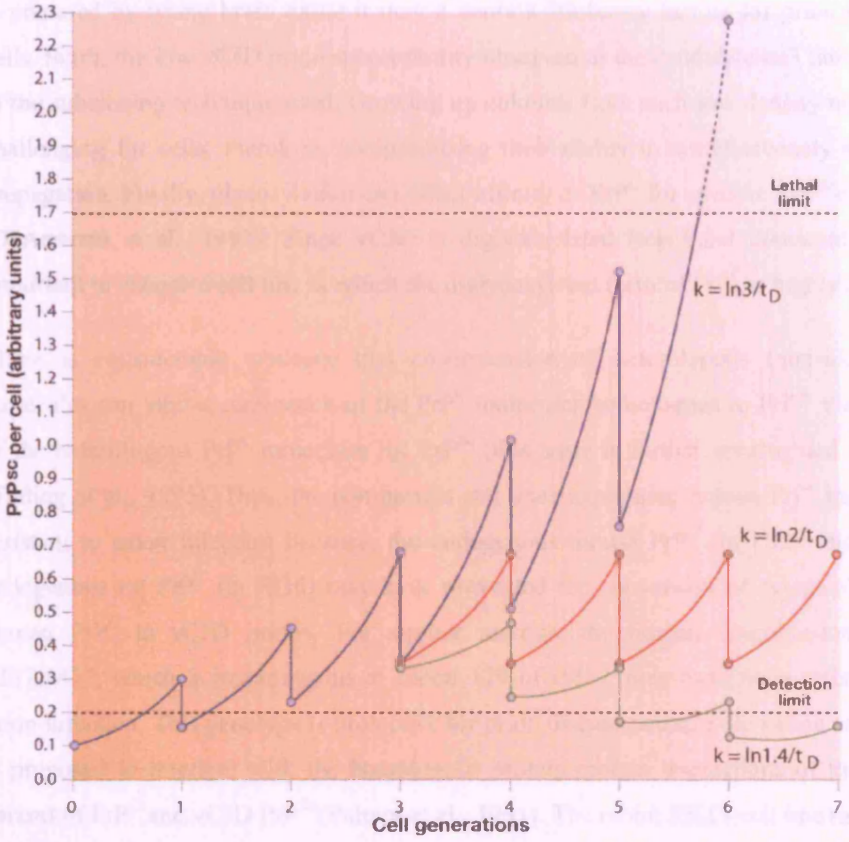

Figure 3.15 Dynamic susceptibility model of prion propagation in cells

The dynamic susceptibility model proposes that stable prion propagation in cells (with all the genetic and biochemical requisites for susceptibility present) is determined by the relative rate of prion synthesis and degradation, defined as K, and stable propagation can only occur within narrow limits of K. The amount of infectivity in a cell can be calculated as $P= P_{(0)}e^{ktD}$, where $P_{(0)}$ is the infectivity content of the cell at the start of the cell cycle and tD is the doubling time of the host cell. After each cell division, infectivity in each cell halves. In order to initiate infection in a cell, K must be equal to or larger than ln2/tD. If k>tD, there will be a steady accumulation of infectivity in the cell. If at the start and for the continuation of the experiment K=ln3/tD (blue line), infectivity will increase logarithmically until eventually the lethal limit is met and the cell will die. If K falls to ln2/tD (red line), there will be a stabilisation of infectivity levels over time and the cell will be chronically infected with prions. However, if K falls further to ln1.4/tD (green line), infectivity will fall to undetectable levels. An infected population contains a mixture of cells with different K values in dynamic equilibrium; chronic infection is maintained by cells with correct K values. In summary, accumulation of infectivity and stable propagation will only be observed if a cell population contains appropriate factors to favour formation at a certain rate over degradation.

Figure is modified from "The State of the Prion" (Weissmann, 2004).

in these experiments because we were aware of these data and, therefore, we took the utmost care to maintain cells in optimal condition. Fifth, since, vCJD prion-infected brain homogenate is prepared by lysing brain tissue it may it contain inhibitory factors for prion replication in cells. Sixth, the low vCJD prion susceptibility observed in the candidate cell lines may be due to the subcloning technique used. Growing up colonies from such low density may have been challenging for cells, therefore, compromising their ability to simultaneously support prion propagation. Finally, glycosylation can affect affinity of PrP^{C} for specific PrP^{Sc} conformations (DeArmond et al., 1997). Since vCJD is diglycosylated (top band dominant), it may be important to choose a cell line in which the diglycosylated form of PrP^{C} is highly expressed.

There is considerable evidence that co-expression of heterologous (non-identical) PrP^{C} molecules can inhibit conversion of the PrP^{C} molecules homologous to PrP^{Sc} via competition of the heterologous PrP^{C} molecules for PrP^{Sc} (this topic is further investigated in **chapter 4** (Telling et al., 1995). Thus, the non-human cell lines expressing human PrP^{C} may have been resistant to prion infection because, the endogenous mouse PrP^{C} (in L929 and N2aG) and endogenous rat PrP^{C} (in RG6) may have prevented the conversion of ectopically expressed human PrP^{C} to vCJD prions. For similar reasons, the human neuroblastoma cell line, BE(2)M17, which is heterozygous at codon 129 of *PRNP* may have been resistant to vCJD prion infection. This genotype is protective for prion disease because the valine variant of PrP^{C} is proposed to interfere with the homologous protein-protein interactions of the methionine variant of PrP^{C} and vCJD PrP^{Sc} (Palmer et al., 1991). The rabbit RK13 cell line may have been exempt from this inhibitory effect because rabbit PrP^{C} has a unique amino acid composition (Vorberg et al., 2003), which lacks sufficient sequence homology to human PrP^{C} to interfere with human vCJD prion replication.

3.5.3 Transient and chronic prion propagation are distinct

In this study, transient vCJD prion propagation was observed in three candidate lines. Typically, stable prion propagating cell lines remain infected for long periods, for example, RML prion infection was present in a PrP-overexpressing N2a cell line and mouse neurospheres for over 30 passages and for 70 days, respectively (Nishida et al., 2000;Giri et al., 2006). The most susceptible cell lines to vCJD prion infection found in this screening study, the human PrP^{C}-overexpressing RK13 clones A and C, propagated prions for three passages (two weeks). On one occasion, the RK13 clone C propagated prions for six passages (three weeks). The human neuroblastoma cell lines, SKNSH and human PrP^{C}-overexpressing SHSY5Y clone A, remained prion-infected for two passages (about two weeks) and for one passage (10 days), respectively. A study on mouse fibroblast and neuroblastoma cells found that following exposure to different prions, all cell lines could transiently generate PrP^{Sc} for up to 96 hours, possibly due to the interaction of the target cell PrP^{C} with the PrP^{Sc} in the

inoculum. However, only certain cell lines could establish chronic prion infection when the inoculum was cleared (Vorberg et al., 2004a). Due to a change observed in glycosylation of PrP^{Sc} in chronically prion-infected clones, it was inferred that chronic prion infection required the localisation of PrP^{Sc} formation to a specific cellular compartment under the direction of cell-specific and/or prion strain-specific factors. Endolysosomal organelles and the endoplasmic reticulum have been proposed as subcellular sites of prion replication. (Laszlo et al., 1992;Mayer et al., 1992;Taraboulos et al., 1992;Arnold et al., 1995;Harris, 2003). Lysosomes have been dubbed bioreactors for PrP^{Sc} because the acidic environment induces protein unfolding and may facilitate the conversion of PrP^{C} to PrP^{Sc} (Laszlo et al., 1992). It is unlikely that the transient vCJD prion propagation we observed in the experiments presented here was the result of contact with residual PrP^{Sc} in the vCJD inoculum because, not only did the particle monitor control cell lines indicate the inoculum had been cleared, but the time-frame of prion propagation here was much longer than in the Vorberg study. It is more likely that the transient nature of PrP^{Sc} formation we observed over a number of weeks is associated with the genetic instability of a tumour cell lines which leads to loss or change in factors required for prion propagation. Indeed, prolonged passaging of the highly RML prion-susceptible N2a clones has been reported to diminish their susceptibility to prions for this reason (Bosque and Prusiner, 2000;Klohn et al., 2003;Vorberg et al., 2004a).

3.5.4 Mechanisms of intercellular prion transfer

Rabbits are amongst the few species resistant to prion infection (CJD, kuru, and scrapie strains; Gibbs and Gajdusek, 1973), possibly because the unique amino acid composition of rabbit PrP^{C} prevents it folding into the disease-associated isoform (Vorberg et al., 2003). However, the rabbit epithelial kidney cell line, RK13, appears to be highly susceptible to prion infection when ectopically expressing the appropriate species of PrP^{C}; in this chapter it was shown to transiently propagate vCJD prions and it is also permissive to ovine scrapie (Rov) (Vilette et al., 2001a) and mouse-passaged CJD prions (A.Hill, Melbourne University, personal communication). The susceptibility of the RK13 cell line may be explained by its epithelial nature. The nervous system, which is highly susceptible to prion infection, is developmentally-derived from epithelium, thus it has been proposed these cell types may share prion susceptibility factors (Vilette et al., 2001b). However, the most likely reason for the exceptional prion permissive nature of the RK13 cell line is its ability to spread prions intercellularly via the secretion of exosomes containing PrP^{C} and PrP^{Sc} (Fevrier et al., 2004). Exosomes are membranous vesicles of 50-90 nm, which are secreted upon fusion of multivesicular endosomes with the plasma membrane. They are secreted by many cell types, particularly of the haematopoietic system, and are proposed to be involved in intercellular communication and eradication of undegraded proteins (reviewed in

Stoorvogel et al., 2002;Thery et al., 2002;van Niel et al., 2006). They have recently also been implicated in the transmission of retroviruses, including HIV (Nguyen et al., 2003). For the ovine scrapie-propagating RK13 cell line (Rov), both PrP^{C} and approximately 1% of cellular PrP^{Sc} are secreted in membrane vesicles, with the specific size, lipid and protein (Tsg101; flotillin) composition, and subcellular localisation characteristic of exosomes. Moreover, these exosomes were demonstrated to be infectious *in vitro* and *in vivo*. PrP^{Sc}-containing exosomes have also been detected in an ovine scrapie-propagating Schwann cell line (Fevrier et al., 2004) and there is evidence for their presence in other prion-propagating cell lines, whose culture supernatants contain infectivity (Schatzl et al., 1997;Cronier et al., 2004). Therefore, exosomes appear to represent an important mechanism of intercellular prion transfer and because they are secreted by many cell types, it is conceivable they are involved in transfer of prions *in vivo* from the periphery to the nervous system (Mabbott and MacPherson, 2006). Exosomes secreted from prion-infected cells may either fuse with the plasma membrane of uninfected cells or be internalised and then fuse with endosomal membranes; prion conversion of adjacent PrP molecules in a membrane occurs much more readily than when molecules are in facing membranes (Baron et al., 2002).

Intercellular prion transfer has been proposed to occur by other mechanisms. Direct cell-cell contact seems to be required for spread of infectious prions in some cell lines, such as the scrapie-infected mouse neuroblastoma SMB cell line (Kanu et al., 2002). Co-culture of scrapie-infected SMB cells and uninfected antibiotic-resistant SMB cells results in the transmission of prion infection to the uninfected cells (as shown by selective killing of the originally prion-infected cells with antibiotic). Moreover the culture supernatant from SMB cells is not infectious and neither is co-culture of both infected and uninfected cells separated by a porous membrane.

Given the involvement of exosomes in intercellular prion transfer in epithelial and Schwann cell lines (Fevrier et al., 2004) and that retroviral budding and prion release in exosomes are thought to share the same pathway (Pelchen-Matthews et al., 2004), we attempted to enhance the spread of vCJD prions within the SKN-SH cell line by infection with MuLV retrovirus. This approach has been taken in a mouse prion-infected 3T3 fibroblast cell line. MuLV infection of 3T3 cells stimulated release of prion infectivity in viral particles and cellular exosomes and increased infection of target cells (Leblanc et al., 2006). However, in our study, MuLV infection of the SKN-SH cell line reduced its susceptibility to prion infection, rather than prolonging the period of propagation. This may have been because the SKN-SH cells were rendered sick from viral infection and, therefore, had reduced capacity to replicate prions. However, it was most likely because the level of *de novo* PrP^{Sc} observed in the vCJD prion-

infected SKN-SH cells was too low to initiate prion infection in neighbouring cells in the first place.

Chapter 4

Humanisation of mouse prion-susceptible N2a-derived cell lines and their screening for susceptibility to human prion propagation

4.1 Introduction

This study set out to exploit the inherent cellular prion susceptibility of the N2a mouse neuroblastoma line (Race et al., 1987) and its highly RML prion-susceptible subclone, PK1 (Klohn et al., 2003b), for the propagation of human vCJD prions. Human PrP^{C} (129 MM) was expressed in these cells to eliminate the prion species barrier. However, it is known this is insufficient to render the cells susceptible to human vCJD prions (see human PrP-expressing N2aGary data, **chapter 3**) and considerable data suggests this is due to "dominant negative" inhibition of human prion propagation by endogenous murine PrP^{C} (Prusiner et al., 1990;Bueler et al., 1993;Priola et al., 1994;Telling et al., 1994;Telling et al., 1995;Collinge et al., 1995;Horiuchi et al., 2000;Perrier et al., 2002). The inhibition of PrP^{Sc} formation by non-homologous PrP^{C} molecules has been observed in transgenic mouse models, cell culture and cell-free conversion assays. Human PrP transgenic mice with endogenous murine *Prnp* expression are as resistant as wildtype mice to sCJD prions and require the ablation of *Prnp* to acquire susceptibility (Telling et al., 1994;Telling et al., 1995). Similarly, mice expressing both the hamster PrP transgene and endogenous murine *Prnp* exhibit longer disease incubation periods for hamster scrapie compared to those in which murine *Prnp* has been ablated (Bueler et al., 1993;Race et al., 2000) Furthermore, hamster PrP expression impairs mouse PrP^{Sc} formation in scrapie-infected mouse neuroblastoma cells (Priola et al., 1994). The basis for this inhibitory phenomenon of PrP^{Sc} formation is thought to be that non-homologous PrP^{C} molecules readily interact with PrP^{Sc} but cannot be converted (Horiuchi et al., 2000).

Therefore, in this study, to eliminate the inhibition of human prion propagation by endogenous murine PrP^{C} in human PrP^{C}-expressing N2a-derived cells, the murine *Prnp* gene was specifically silenced using RNA interference (RNAi). RNAi is a naturally-occurring, post-translational gene silencing mechanism that is highly conserved in eukaryotes. It refers to a pathway in which double-stranded RNAs trigger the degradation of homologous mRNA molecules. RNAi has been hailed as one of the most exciting biotechnology advances in recent decades by Science magazine (2002) and its discovery by Fire and Mello has since earned them the Nobel prize for medicine in 2006 (Fire et al., 1991;Fire et al., 1998). It is thought to have evolved to silence alleles in development and to protect the genome from invasion by mobile genetic elements, such as transposons and viruses (Jensen et al., 1999;Tabara et al., 1999).

The RNAi pathway (see **figure 4.1**) first involves the cleavage of precursor double-stranded RNA molecules (either endogenously expressed pre-microRNAs or exogenous double-

stranded RNAs) by a cytoplasmic ribonuclease III-like enzyme, called Dicer (Bernstein et al., 2001). Dicer cleavage results in short RNA duplexes of 21-22 nucleotides in length, with symmetric two nucleotide 3'-overhangs (Zamore et al., 2000;Elbashir et al., 2001b). These effector molecules of exogenous double-stranded RNA, called short interfering RNAs (siRNAs), become incorporated into a ribonucleoprotein complex called the RNA-inducing silencing protein complex (RISC) (Hammond et al., 2000;Hammond et al., 2001). The siRNA duplex is unwound by a helicase subunit of RISC and the anti-sense strand guides RISC to its homologous target mRNA (Martinez et al., 2002). Gene expression is inhibited by degradation of target mRNA molecules by an endonuclease component of RISC, Argonaute 2 (Liu et al., 2004;Meister et al., 2004). The microRNAs enter a distinct pathway to siRNAs and inhibit gene expression by repressing translation of target mRNA for which they are not perfectly complementary (Olsen and Ambros, 1999;Seggerson et al., 2002).

The use of RNAi technology as a tool to inhibit gene expression was originally limited to plants or *C.Elegans* since it proved cytotoxic in the mammals. This is because in mammalian cells double stranded RNA molecules of greater than 30 nucleotides in length activate an innate anti-viral response involving interferon production to non-specifically suppress gene expression (Williams, 1997;Clemens, 1997). Therefore, chemically synthesised siRNAs mimicking Dicer cleavage products were developed for use in the mammalian system (Elbashir et al., 2001a). Delivery of these exogenous siRNA molecules to cells with lipophilic agents allowed them to tap into the native RNAi pathway, incorporating into the cellular RISC and mediating the degradation of homologous mRNA. Stable long-term down-regulation ("knockdown") in gene expression by RNAi is now possible using DNA expression vectors containing RNA polymerase III promoters (Brummelkamp et al., 2002;Yu et al., 2002;Paddison et al., 2004). These vectors drive the expression of short hairpin RNAs (comprising an RNA duplex of 19-29 nucleotide stems, precisely complementary to the target sequence, linked by a 3-9 nucleotide loop), which are cleaved intracellularly by Dicer to produce functional siRNAs (see **figure 4.1**).

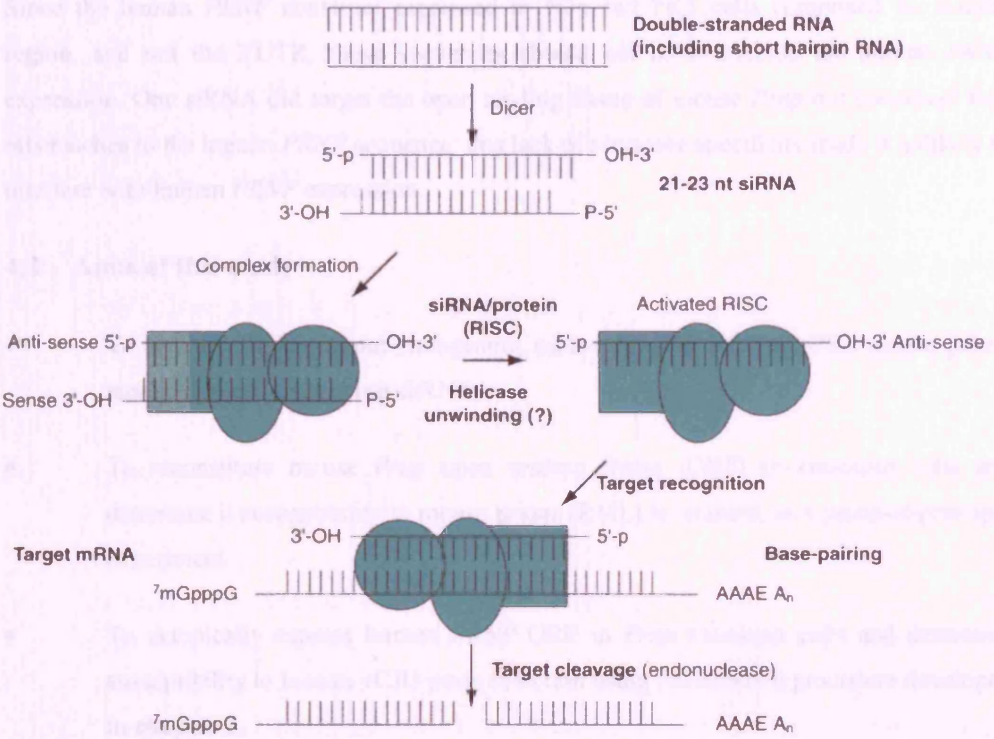

Figure 4.1 RNAi gene silencing pathway

Long double stranded RNA molecules and short hairpin (shRNA) precursor molecules are processed to siRNA duplexes of 21-23 nucleotides by the cytoplasmic ribonuclease III-like enzyme, Dicer. These siRNA molecules are assembled into effector complexes, RISC (RNA-induced silencing complex), and subsequently unwound by its helicase subunit. The sense strand is released and degraded, while the anti-sense strand guides RISC to its target mRNA. Sequence complementarity between siRNA and mRNA is required for specific degradation of target mRNA to take place. The endonuclease subunit (Argonaute 2) of activated RISC preferentially cleaves target mRNA between positions 10 and 11 relative to the 5' antisense strand to inhibit gene expression (Elbashir et al., 2001c). 7mG: 7-methylguanine, AAAA: polyadenosine tail, 5'p: 5'phosphate. *Figure modified from (Wall and Shi, 2003).*

For this project, eight siRNA sequences were designed to specifically target mouse *Prnp* gene but not the human *PRNP* gene (see **table 2.3**). Specificity against mouse *Prnp* was achieved by selecting siRNA sequences targeting the 3' untranslated region (3'UTR) of mouse *Prnp* gene. Since the human *PRNP* construct expressed in N2a and PK1 cells comprised the coding region, and not the 3'UTR, these sequences should not have affected the human *PRNP* expression. One siRNA did target the open reading frame of mouse *Prnp* but contained four mismatches to the human *PRNP* sequence; this lack of sequence specificity made it unlikely to interfere with human *PRNP* expression.

4.2 Aims of this study

- To specifically knock out endogenous mouse *Prnp* in N2a and PK1 mouse prion-susceptible cell lines using shRNAs.
- To reconstitute mouse *Prnp* open reading frame (ORF) in knockout cells and determine if susceptibility to mouse prions (RML) is retained, as a proof-of-principle experiment.
- To ectopically express human *PRNP* ORF in *Prnp* knockout cells and determine susceptibility to human vCJD prion infection using the standard procedure developed in **chapter 3**.

4.3 Methods

The data presented in this chapter were produced using methods described in chapter 2. *Prnp* sequences targeted by the eight siRNAs are shown in **table 2.3**. Their design, cloning as short hairpin RNAs into retroviral expression vectors and their expression in cells are described in section **2.5**. The effectiveness of *Prnp*-specific shRNAs was assessed by immunoblotting (**2.6.2**), immunofluorescence (**2.6.3**) and quantitative PCR (**2.5.6**). Human PrP^{C} expression in cells is described in **2.4** and was analysed by immunoblotting (**2.6.2**). High human PrP^{C}-expressing cells were isolated by subcloning (**2.4.2.1**) and FACS-sorting (**2.6.4**). vCJD prion infection of cells was done as described in section **2.7.2** and the presence of PrP^{Sc} assessed by the scrapie cell assay (SCA; **2.7.5.2**).

4.4 Results

4.4.1 Selection of siRNA target sequences in *Prnp* mRNA

4.4.1.1 Empirical rules of siRNA design

Not all siRNAs that are complementary to their target mRNA can efficiently silence their cognate target gene. At the start of this project (2003), the field of RNAi was in its infancy and little was known about what determined siRNA functionality. Empirical guidelines on siRNA design existed, which were based on the first successful siRNA sequences found by trial-and-error. These guidelines are briefly outlined below:

- Select siRNA from the mature mRNA target sequence (cDNA), preferably starting 50-100 nucleotides (nt) downstream of the start codon and avoiding the 3' and 5' UTRs to prevent interference from regulatory binding proteins of RISC binding to the mRNA (Elbashir et al., 2002).
- In the mRNA sequence, search for sequences 5'-AA(N19)UU, where N is any nt. SiRNA duplexes of 21 nt paired so as to have 2 nt 3'-overhangs were found to be the most efficient (Elbashir et al., 2001c). Selecting sequences to provide uridine in the two nucleotide overhangs of the siRNA duplexes is suggested because they offer protection from endonuclease degradation and 2'deoxythymidine can be used for RNA synthesis, which is cheaper and does not result in loss of activity (Elbashir et al., 2002).
- The siRNA duplexes should have ≤ 50% GC content. Too low a GC content is thought to destabilise the siRNA duplex and result in low affinity of the antisense strand for target mRNA, whilst a higher content may impede RISC loading and/or siRNA duplex unwinding (Elbashir et al., 2002;Holen et al., 2002).
- Avoid a run of 4 uridine or adenine residues because this is the termination signal for RNA polymerase (Geiduschek and Tocchini-Valentini, 1988).
- Avoid palindromic sequences that may form fold-back structures (Kirchner et al., 1998).
- Blast-search (www.ncbi.nlm.nih.gov/BLAST) the selected siRNA sequences against mRNA sequences of the respective organism to ensure only the desired gene is targeted (Elbashir et al., 2002).

These basic empirical guidelines were used to design the first set of four siRNA sequences targeting mouse *Prnp*, named siRNA#1-#4. SiRNA#1 targeted the coding region of *Prnp*. Despite the guidelines above, siRNAs#2-#4 were designed to target the 3'UTR of *Prnp* to allow the sequences to be mouse-specific. Moreover, there was growing evidence suggesting siRNAs targeting 3'UTRs could be effective (McManus et al., 2002).

4.4.1.2 *In silico* rational design of siRNA sequences

Improved understanding of the RNAi mechanism and the statistical analyses of siRNA libraries (with experimentally determined efficiencies) has lead to the development of computational tools to increase the probability of selecting effective siRNAs (Reynolds et al., 2004;Saetrom and Snove, Jr., 2004;Huesken et al., 2005). For this project, the second set of candidate siRNAs targeting *Prnp* was designed using SMART Selection™ technology (Dharmacon Inc., USA). Use of the Dharmacon algorithm has been estimated to increase the average probability of selecting an effective siRNA (which suppresses target gene expression by greater than 80%) 3.5-fold compared to random selection (Reynolds et al., 2004). This Dharmacon technology employs an algorithm integrating eight thermodynamic and sequence-related criteria outlined below. The thermodynamic criteria are proposed to affect the initial siRNA-RISC recognition and the sequence-related criteria are proposed to affect critical siRNA-protein interactions (Reynolds et al., 2004).

Thermodynamic criteria

- Absence of internal repeats to prevent inappropriate folding of siRNA.
- Low to moderate GC content (36-52%) promotes efficient unwinding of duplex.
- High internal stability of 5'-sense strand and low internal stability at 5'-antisense strand both promote antisense strand selection and incorporation into RISC.

Sequence-related criteria

- Sense strand base preferences at specific positions; 3, 10, 13 and 19. For example, the presence of U at position 10 and the absence of G at position 13.

A BLAST-search is conducted by default to ensure the siRNA sequences do not target other sequences in the genome. For our purposes, Dharmacon rationally designed a further four siRNA candidate sequences to target mouse *Prnp*, all of which targeted the 3'UTR of mouse *Prnp*.

4.4.2 Verification of *Prnp*-specific siRNA sequences

Following cloning into the pSuper.retro and pMSCV expression vectors, the sequence of siRNAs #1-#8 were checked and found to be correct by DNA sequencing using vector-specific primers.

4.4.3 Screening of candidate siRNA sequences for *Prnp* knockdown efficiency in N2a cells

The first set of mouse *Prnp* specific siRNAs #1-#4, designed by Professor Parmjit Jat using basic empirical rules, were cloned into the retroviral expression vector, pSuper.retro, and packaged into PhiNX-eco retroviral producer cell line. Ecotropic virus was harvested and used for the retroviral transduction of N2a cells with siRNAs #1-#4. Successfully transduced cells

were isolated by puromycin selection, and mixed clones stably expressing siRNA were established. Initial analysis by immunoblotting indicated that siRNA#2 and #4 were more effective than #1 and #3 at suppressing PrP^C protein expression in N2a cells and they produced about 75% PrP^C knockdown (**figure 4.3**). However, PrP^C knockdown was not complete and therefore insufficient for our purposes. As a result, a further four siRNA sequences (siRNA#5-#8) were designed using SMART Selection™ technology (Dharmacon Inc., USA; (Reynolds et al., 2004)) and cloned into pSuper.retro.

The efficiency of Dharmacon siRNAs to knockdown *Prnp* expression was first analysed by their transient expression in N2a cells followed by immunofluorescence for PrP^C expression (**figure 4.2**). SiRNA#8 produced the most significant and widespread PrP^C knockdown (**figure 4.2H**) compared to wildtype expression. There were variable levels of PrP^C knockdown in N2a siRNA#5 and N2a siRNA#7 mixed clones. They exhibited significant PrP^C knockdown in a small proportion of cells (**figure 4.2D** and **G**) but this was not widespread (**figure 4.2C** and **F**). Variability in knockdown observed following immunoflourescence may be explained by the fact puromycin selection was not complete (only 72 hours of gentle selection) and untransduced cells lacking the siRNA construct remained in the cultures. PrP^C knockdown was specifically due to siRNA expression since the negative control vector-only expressing cells had similar PrP^C expression levels to wildtype N2a cells (**figure 4.2B**).

Stable mixed clones of N2a cells expressing Dharmacon siRNA sequences were established so that a comparison of PrP^C knockdown efficiency could be made with the best empirically-designed siRNAs, #2 and #4 by immunoblotting (**figure 4.3**). SiRNA#8 exhibited the best PrP^C knockdown efficiency followed by #4, #2 (which was slightly underloaded as indicated by the endogenous biotin bands) and then #5. PrP^C knockout was not complete but expression was suppressed by between 50 and 80% in these clones. Interestingly, although siRNA#5 and #6 differed in sequence by just 2 nucleotides, siRNA#5 was more effective at suppressing PrP^C expression.

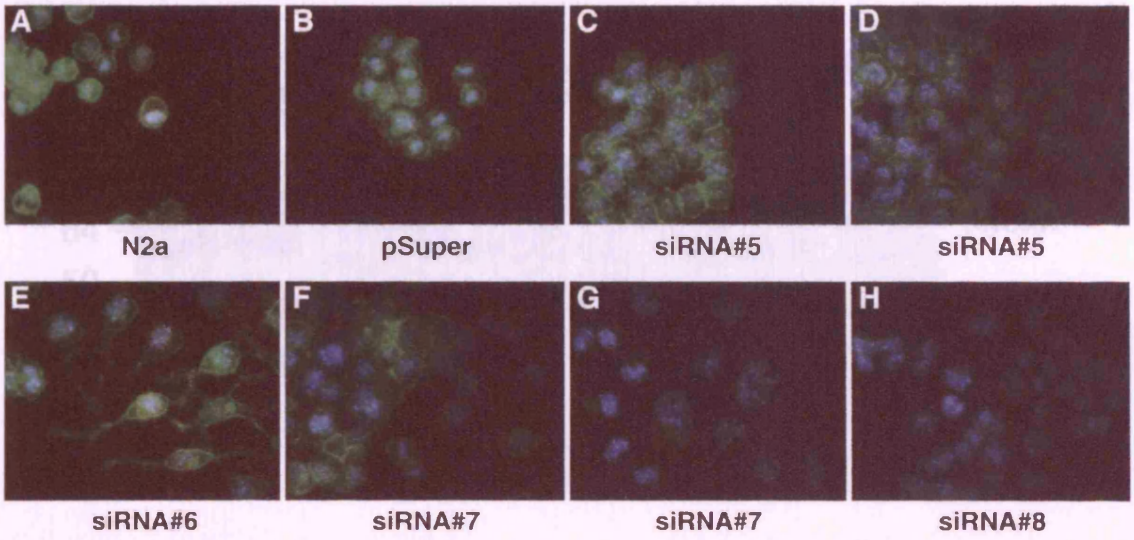

Figure 4.2 Transient expression of Dharmacon *Prnp*-specific siRNAs on PrP^C expression in N2a cells

N2a cells were grown on poly-L-lysine coated glass coverslips and retrovirally transduced at 50% confluency with Dharmacon siRNA sequences and pSuper vector-only negative control. 12 hours after transduction, gentle puromycin selection at 1.5 µg/ml was started. 72 hours after transduction, PrP^C expression was analysed by immunofluorescence. PrP^C is stained green with ICSM18 and FITC-conjugated anti-mouse IgG secondary antibody. Nuclei are stained blue with DAPI. Photographs A – H were acquired with fixed exposure times for DAPI and FITC (500 and 1500 ms, respectively) to accurately assess PrP^C levels. SiRNA#8 (H) produced the most significant and widespread suppression of PrP^C expression compared to wildtype N2a controls (A). PrP^C knockdown was not homogeneous within the mixed clones. For example, siRNA#5 and siRNA#7 clones had regions of almost complete PrP^C knockdown (D and G), whilst others retained wildtype expression levels (C and F). SiRNA#6 was least effective at knocking down PrP^C expression (E).

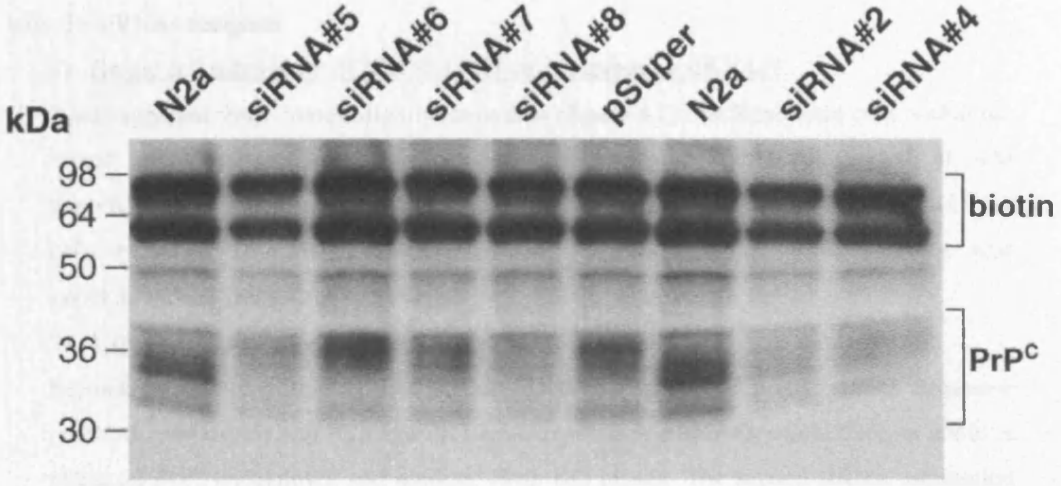

Figure 4.3 Comparison of the PrP^C knockdown efficiency of empirically and Dharmacon designed *Prnp*-specific siRNAs in N2a cells

Cell lysates from stable puromycin-resistant mixed clones of N2a cells expressing siRNA#2, #4 and #5 - #8 were immunoblotted using anti-PrP antibody, biotinylated ICSM35. 25 µg protein from cell lysates was loaded per lane. Endogenous biotin bands (two bands between ~100 and 60 kDa detected by avidin-biotin-AP secondary complex) are included to indicate differences in protein loading. The most effective suppression of PrP^C expression compared to wildtype N2a cells was produced by siRNA sequences #8, #4, #2 (underloaded) and #5, in that order. PrP^C knockdown was between 50 and 80% in these clones.

4.4.4 Achieving maximal mouse *Prnp* knockdown in N2a and PK1 cells

As mentioned above, in order to prevent interference of endogenous *Prnp* expression with human prion propagation in N2a and PK1 cells, it was essential to achieve as close to complete *Prnp* knockout as possible. Two strategies were adopted to achieve maximal *Prnp* knockdown with the siRNAs designed.

1) Single cell subcloning of N2a and PK1 cells expressing siRNA#8

It was apparent from immunofluorescence data (**figure 4.2**) that there were cells within the mixed siRNA-expressing populations that expressed negligible PrP^C. First, it was hypothesised that single cell cloning of the stable mixed population of both N2a and PK1 cells expressing the most effective siRNA, #8, would isolate cells with the best knockdown and yield *Prnp* KO clones.

2) Expression of 2 anti-*Prnp* siRNA sequences

Second, it was hypothesised that the introduction of a second potent siRNA sequence (siRNA#2, #4 or #5) into N2a and PK1 cells expressing siRNA#8 would have an additive effect on PrP^C knockdown and produce *Prnp* KO clones. The second siRNA expression cassette was moved from pSuper into a different retroviral vector, pMSCV, with a hygromycin B selectable marker and subsequently introduced into siRNA#8 mixed clones by retroviral transduction.

4.4.4.1 Improving *Prnp* knockdown in N2a and PK1 siRNA#8 expressing cells by single cell subcloning

4.4.4.1.1 N2a siRNA#8 clones

Forty-two single cell clones were isolated by limiting dilution subcloning (see **2.4.2.1**) from N2a mixed clones stably expressing siRNA#8 (N8). PrP^C knockdown was first screened by immunofluorescence, promising clones were expanded and PrP^C knockdown was assessed by immunoblotting. Approximately 50% PrP^C knockdown was observed in most clones but four clones exhibited approximately 80 and 90% PrP^C knockdown compared to N2a wildtype cells (**figure 4.4**). The best PrP^C knockdown was observed in a clone named N8a, in which protein expression was reduced by approximately 90%. PrP^C was deglycosylated so that it ran as a single unglycosylated band, which allowed more accurate estimation of PrP^C knockdown (**figure 4.7**). Following deglycosylation, unglycosylated PrP^C was undetectable in N8a by immunoblotting. Quantitative PCR demonstrated that the reduction of PrP^C expression in clone N8a was associated with a concomitant 90% reduction in *Prnp* mRNA transcript levels compared to N2a wildtype (**figure 4.8A**), confirming that the observed reduction in PrP^C protein expression was due to siRNA-mediated mRNA degradation and not inhibition of protein synthesis.

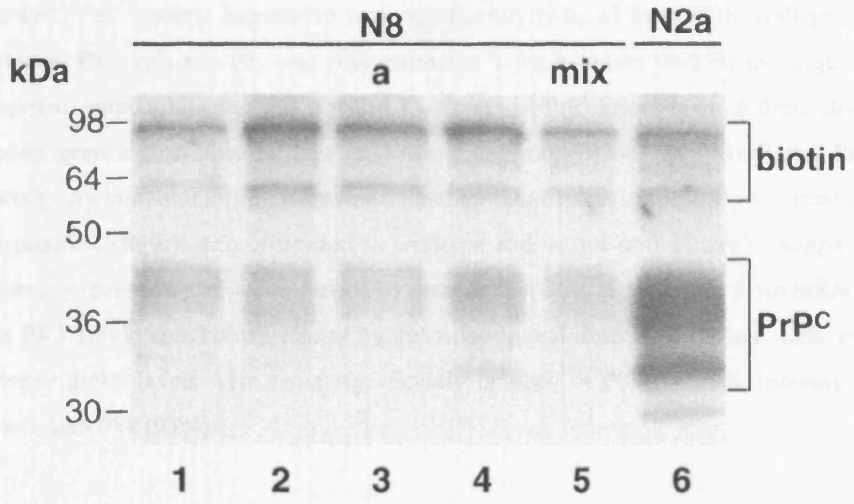

Figure 4.4 PrP^C knockdown in N2a clones expressing siRNA#8

Cell lysates from single cell clones isolated from N2a mixed clones stably expressing siRNA#8 (N8), N2a siRNA#8 mixed clone (N8mix) and N2a wildtype were immunoblotted using anti-PrP antibody, biotinylated ICSM35. 25 µg protein from cell lysates was loaded per lane. PrP^C expression in four single cell clones of N8 was reduced by an estimated 80-90% (lanes 1-4). Compared to N2a wildtype expression (lane 6), only N8a (lane 3) showed greater PrP^C knockdown than N8 mixed clones (lane 5). The band running just above 30 kDa in N2a lane is a degradation product of PrP^C.

4.4.4.1.2 PK1 siRNA#8 clones

PK1 cells were retrovirally transduced with siRNA#8 and when puromycin selection was complete, single cell clones were picked (by P.Arora; **2.4.2.1**). PrP^C knockdown in clones was initially assessed by immunofluorescence (**figure 4.5**) and then confirmed by immunoblotting (**figure 4.6**). PrP^C protein expression was significantly reduced from PK1 wildtype levels in three clones, P8a, P8b and P8c and was estimated to be between 80-85% using quantitative densitometric immunoblot analysis (**table 4.1**). However, PrP^C knockdown in these clones may have been greater than this because following deglycosylation, unglycosylated PrP^C was undetectable by immunoblotting (**figure 4.7**) and immunofluorescence analysis failed to detect PrP^C expression (**figure 4.5**) compared to wildtype and vector-only controls. Suppression of PrP^C protein expression was accompanied by greater than 90% reduction in *Prnp* mRNA levels in these PK1 single knockdown clones by quantitative real-time PCR (**figure 4.8B** and **table 4.1**). *Prnp* mRNA levels were most significantly reduced in P8b by 99%, followed by P8c (97%) and then P8a (93%).

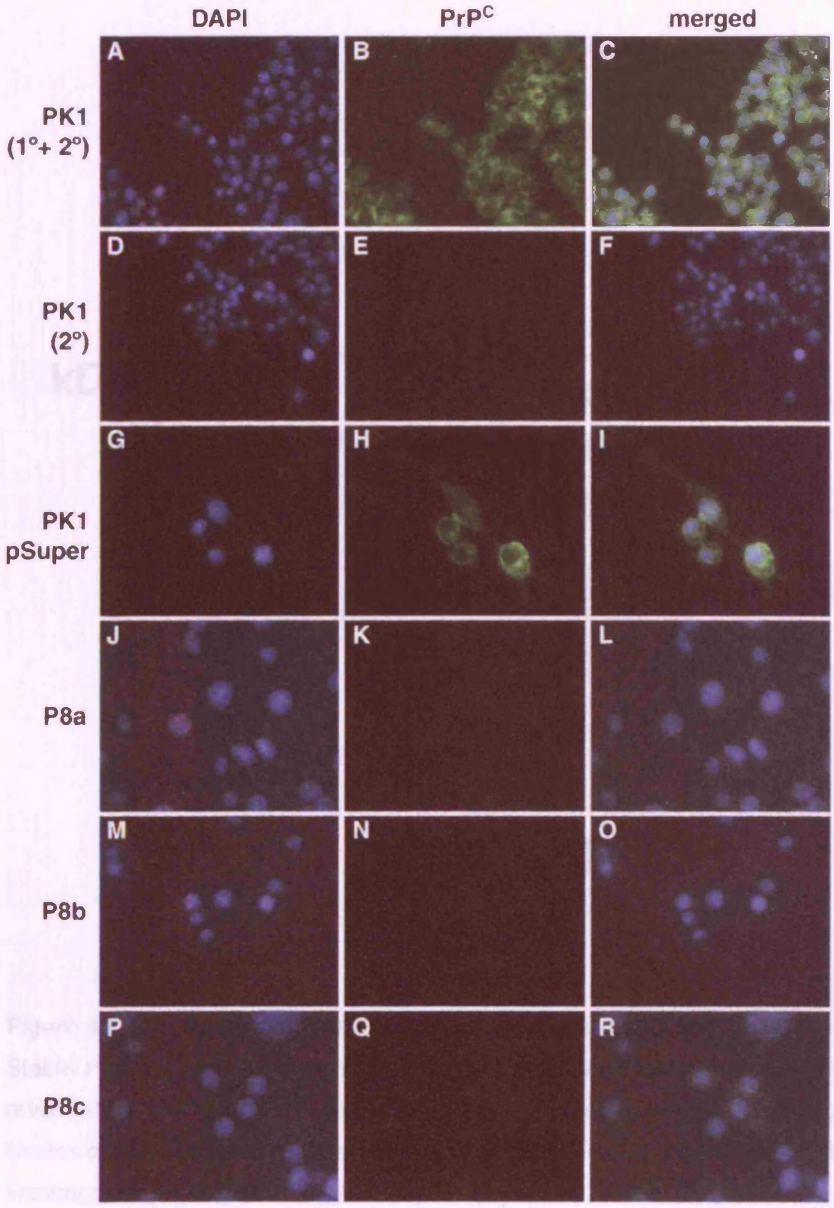

Figure 4.5 Immunofluorescence analysis of PrP^C knockdown in PK1 clones expressing siRNA#8

Stable PK1 siRNA#8-expressing single cell clones were isolated by retroviral transduction of PK1 cells with siRNA#8, followed by 4 µg/ml puromycin selection and clone picking of surviving clones. Clones were grown on poly-L-lysine coated glass coverslips. Middle column shows immunostaining for PrP^C (green) with ICSM18 primary (1^o) antibody and FITC-conjugated anti-mouse IgG secondary (2^o) antibody. Left-hand column shows cells by nuclear DAPI staining (blue). Right-hand column shows merged images. Images A-I were acquired with fixed exposure times for DAPI and FITC (500 and 1500 ms, respectively). PrP^C expression was knocked out in three PK1 siRNA#8 single cell clones, P8a, P8b, and P8c (**L**,**O**,**R**) compared to wildtype (**C**) and vector-only controls (**I**). *These data were produced by P.Arora.*

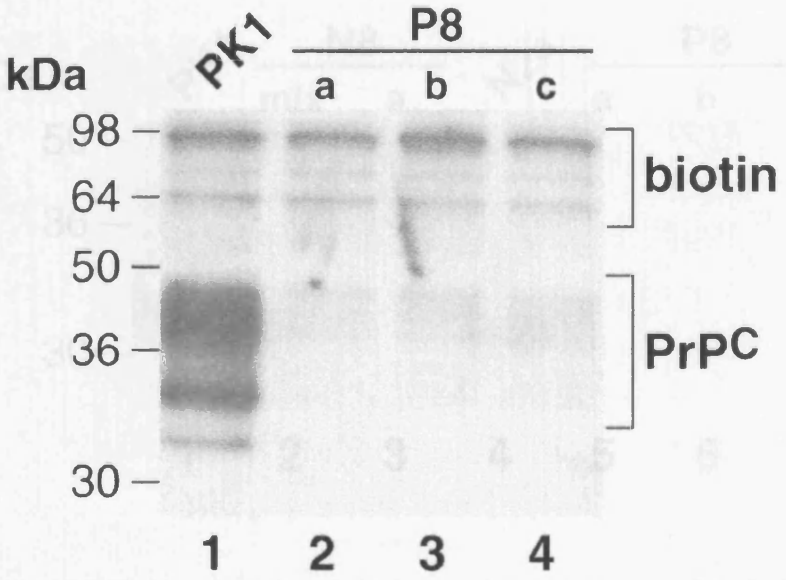

Figure 4.6 PrP^C knockdown in PK1 clones expressing siRNA#8

Stable PK1 single cell clones expressing siRNA#8 were isolated by clone picking following retroviral transduction of PK1 with siRNA#8 and subsequent 4 µg/ml puromycin selection. Cell lysates of PK1 single cell clones expressing siRNA#8 clones, P8a, P8b and P8c and PK1 were immunoblotted using anti-PrP antibody, biotinylated ICSM35. 25 µg protein from cell lysates was loaded per lane. PrP^C expression in three clones, P8a (lane 2), P8b (lane 3) and P8c (lane 4) was significantly reduced compared to wildtype PK1 cells (lane 1).

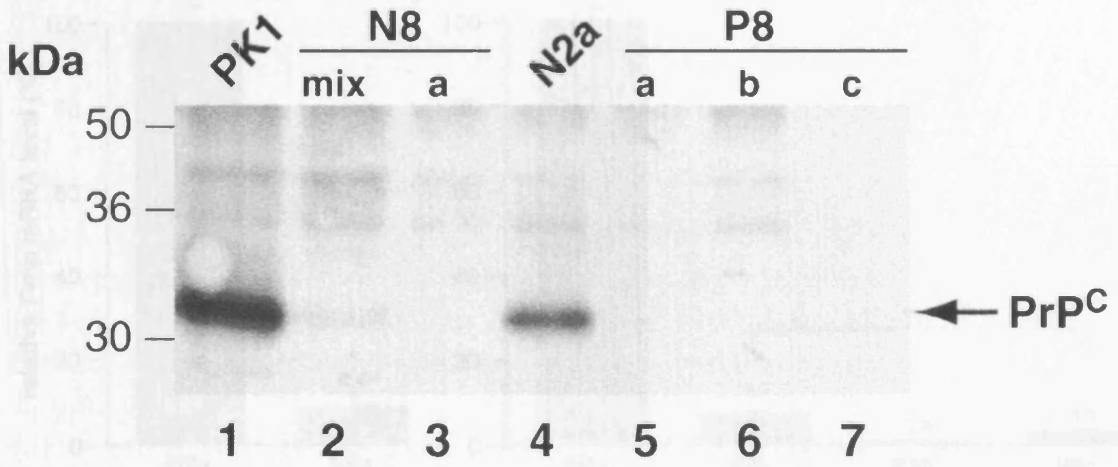

Figure 4.7 PrP^C deglycosylation in PK1 and N2a clones expressing siRNA#8

Cell lysates were deglycosylated with 30U/ml N-glycosidase-F and immunoblotted using anti-PrP antibody, biotinylated ICSM35. 30 µg protein was loaded per lane. Unglycosylated PrP^C was visualised as a single band at ~30 kDa. No PrP^C expression was observed in P8a (lane 5), P8b (lane 6), P8c (lane 7) compared to PK1 wildtype (lane 1) or N8a (lane 3) clones compared to N2a wildtype (lane 4). Very low PrP^C expression was detected in N8 mixed clones (lane 2) compared with N2a wildtype expression.

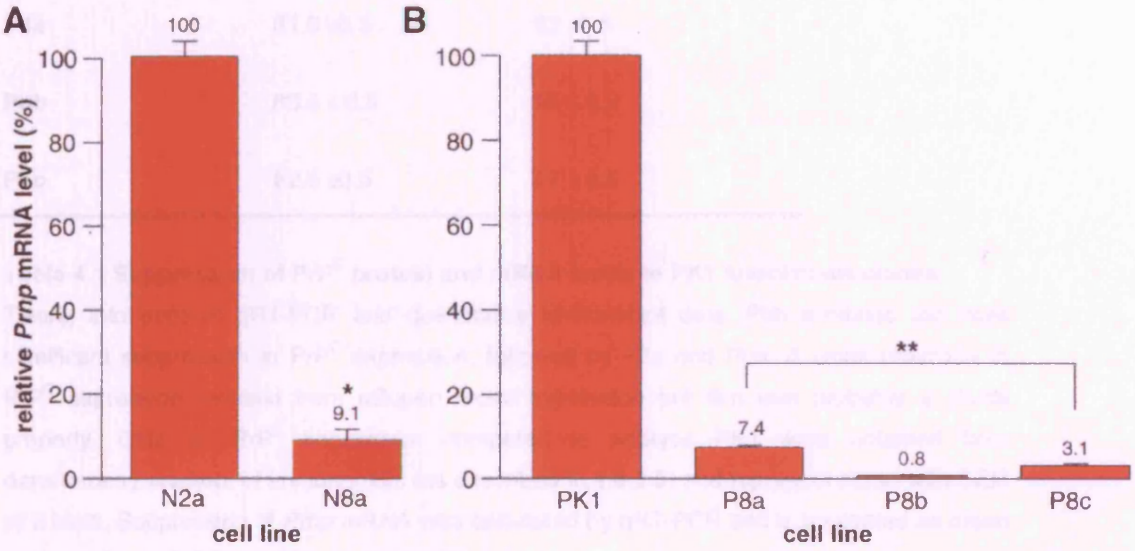

Figure 4.8 Quantitation of *Prnp* mRNA knockdown in PK1 and N2a clones expressing siRNA#8 by quantitative real-time PCR (qRT-PCR)

Relative *Prnp* gene expression compared to wildtype (N2a or PK1) cells was determined for single siRNA knockdown clones using qRT-PCR and the comparative threshold method (described in **2.5.6.4**), for which GAPDH house-keeping gene was used to normalise the data. Validation experiments were performed and it was determined that GAPDH and *Prnp* probe amplification efficiencies were equal because the difference of *Prnp* and GAPDH slopes was 0.12. Data are presented as mean relative *Prnp* mRNA and represent means of triplicate samples (+ SEM). *Prnp* mRNA levels were significantly reduced in N8a to 10% N2a wildtype level. *Prnp* mRNA levels were further reduced in PK1 single KO clones, P8a, P8b, P8c, to 7.4%, 0.8% and 3.1% of PK1 wildtype, respectively. 2-tailed *t*-tests were performed * = $P<0.05$ and ** = $P<0.005$. *J.Podesta performed the experiments and I performed the data analysis.*

P8 clone	PrP^C knockdown (%±SEM)	mean *Prnp* mRNA suppression (%±SEM)
PK1 pSuper	18	not done
P8a	81.5 ±0.5	93 ±0.5
P8b	83.5 ± 0.5	99 ± 0.2
P8c	82.5 ±0.5	97 ± 0.5

Table 4.1 Suppression of PrP^C protein and mRNA levels in PK1 knockdown clones
Taking into account qRT-PCR and quantitative immunoblot data, P8b exhibited the most significant suppression in PrP^C expression, followed by P8c and P8a. A small reduction in PrP^C expression resulted from pSuper vector expression but this was probably a clonal property. Data for PrP^C knockdown compared to wildtype PK1 were obtained from densitometry analysis of immunoblots (as described in **2.6.3.5**) and represent mean with SEM of 2 blots. Suppression of *Prnp* mRNA was calculated by qRT-PCR and is presented as mean suppression (+ SEM) relative to wildtype PK1.

4.4.4.2 *Prnp* knockdown in N2a and PK1 cells by double siRNA expression

4.4.4.2.1 N2a double siRNA PrP^C knockdown clones

A second siRNA construct #2, 4 or 5 (cloned into pMSCV.hyg) was sequentially introduced into the N8 stable mixed clone by retroviral transduction. Following hygromycin selection, which typically took 10-14 days, mixed double siRNA clones were established. Fifty-four single cell clones were subsequently isolated by limiting dilution subcloning (**2.4.2.1**). Twenty-four clones of both N8 siRNA#2 and N8 siRNA#4 were isolated however the N2a siRNA#5 clones were less viable and only six survived. The clones were screened for PrP^C knockdown compared to wildtype N2a cells by immunofluorescence, for which eighteen clones appeared promising with areas of significant knockdown. PrP^C knockdown was assessed in these clones by immunoblotting. The best PrP^C knockdown achieved was about 80% in two N8 siRNA#4 single cell clones (e and f) (**figure 4.9**). 75% and 60% PrP^C knockdown was observed in three other N8 siRNA#4 single cell clones, 40 and 50% in most N8 siRNA#2 clones but no significant PrP^C knockdown was observed in the N8 siRNA#5 clones. The PrP^C knockdown observed by immunofluorescence in the double siRNA clones was very heterogeneous. In one

N8 siRNA#2 clone, in which the total PrP^C knockdown was 50%, there were regions of complete PrP^C knockout (**figure 4.10**). Although these lines were supposed to be clonal, during proliferation from a single cell it is inevitable there are some changes, particularly if PrP^C knockdown were conferring a growth disadvantage. In summary, PrP^C knockdown in N2a double siRNA clones was not as good as seen in single siRNA clone, N8a (approximately 90% PrP^C knockdown).

4.4.4.2.2 PK1 double siRNA PrP^C knockdown clones

The best PK1 single siRNA PrP^C knockdown clone, P8b, was chosen and a second siRNA construct #2, 4 or 5 was sequentially introduced by retroviral transduction. Following hygromycin selection, single cell clones were picked (**2.2.4.1**) and fifty clones were assessed for PrP^C knockdown by immunofluorescence and verified by immunoblotting (P.Arora). Three PK1 clones expressing double siRNA exhibited improved PrP^C knockdown compared to P8b (**figure 4.11**). One of the clones expressed siRNA#8 and siRNA#2 and was named P8b2a, the other two clones expressed siRNA#8 and #4 and were named P8b4a and P8b4b. Since PrP^C was almost undetectable by immunoblotting and immunofluorescence, PrP^C knockdown was estimated to be between 95 and 99% in these three clones.

4.4.4.3 Summary of maximal PrP^C knockdown in PK1 and N2a cells

In the PrP^C RNAi study, the maximal PrP^C knockout achieved in PK1 and N2a cells with a single siRNA was 90% in P8b and N8a clones. Expression of two siRNA constructs did not improve PrP^C knockdown in N2a cells. However, PrP^C knockdown was improved in PK1 double siRNA clones, P8b2a, P8b4a and P8b4b, and was estimated to be between 95 and 99%. These maximally PrP^C suppressed clones were used to ectopically express human PrP^C in order to develop a human vCJD prion-propagating cell line.

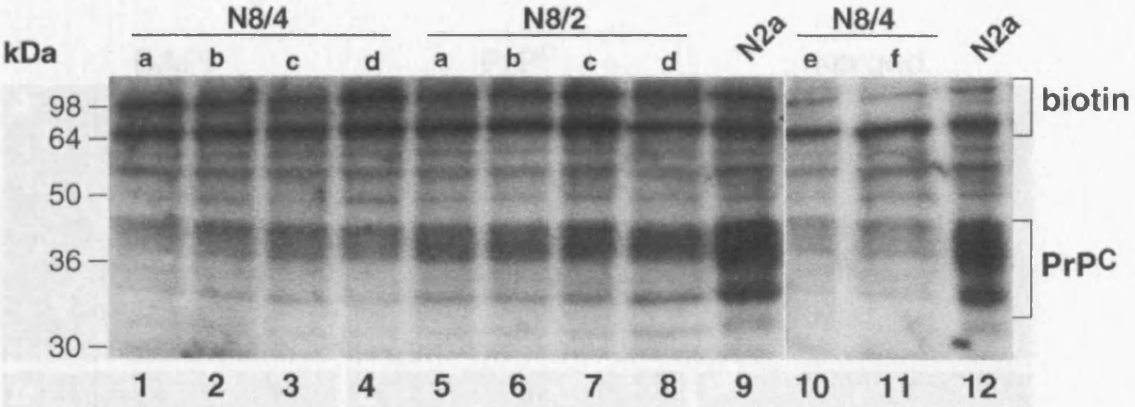

Figure 4.9 PrP^C knockdown in N2a clones expressing double siRNA sequences

N2a double siRNA single cell clones were generated by introduction of siRNA#2 or #4 into N8 mixed clone followed by limiting dilution subcloning. Cell lysates of four N8 siRNA#2 clones (N8/2) and six N8 siRNA#4 clones (N8/2) and N2a were immunoblotted using anti-PrP antibody, biotinylated ICSM35. 25 µg protein from cell lysates was loaded per lane. PrP^C expression was most significantly reduced in the N8 siRNA#4 clones; two clones exhibited an estimated 80% PrP^C suppression (lanes 10 and 11), one clone exhibited 75% PrP^C suppression (lane 1) and three clones exhibited 60% PrP^C suppression (lanes 2-4) compared to wildtype N2a (lanes 9 and 12). PrP^C expression was suppressed by an estimated 40-50% in N8 siRNA#2 clones (lanes 5-8).

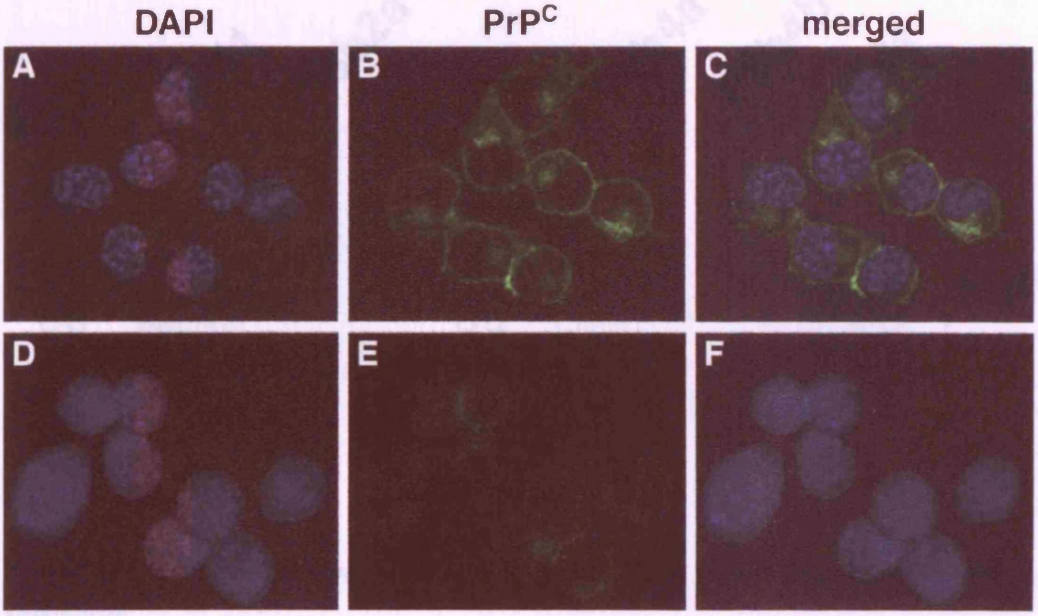

Figure 4.10 Confocal analysis of PrP^C knockout in N8 siRNA#2 double siRNA knockout clone, N8/2b

N8/2b clone and N2a wildtype cells were grown on poly-L-lysine coated glass coverslips and immunostained for PrP^C (green) with ICSM18 and FITC-conjugated anti-mouse IgG secondary antibody and nuclei were stained blue with DAPI. (**A-C**) represents N2a controls and (**D-F**) represent N8/2b. (**B**) PrP^C expression was predominantly seen at the plasma membrane in wildtype N2a cells. (**E**) N8/2b (double siRNA knockdown clone expressing both siRNA#8 and #2) exhibited almost total PrP^C knockout in some regions (**E**), though expression was maintained to a low level at points of cell-cell contact.

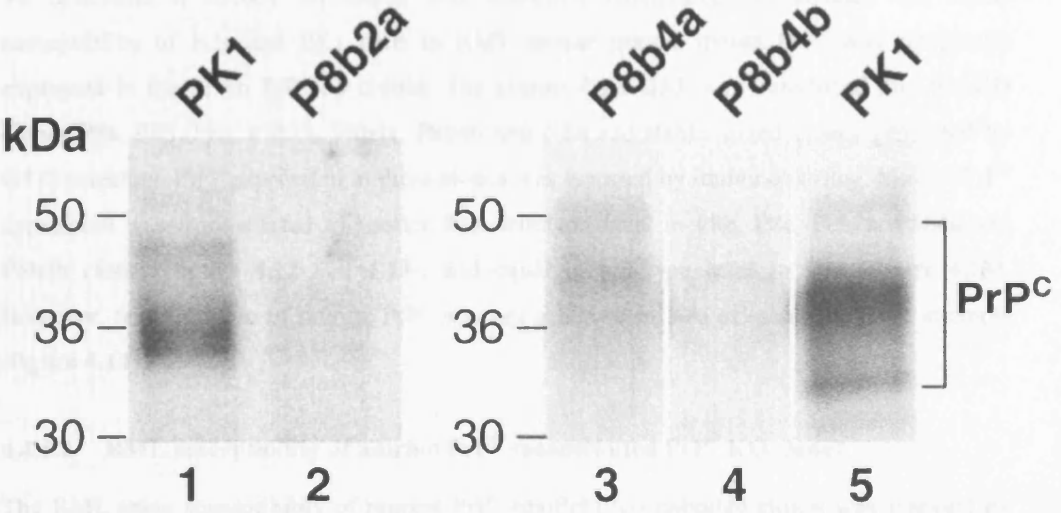

Figure 4.11 PrP^C knockdown in PK1 single cell clone expressing double siRNA sequences

PK1 double siRNA PrP^C knockdown clones were generated by the introduction of siRNA#2 or siRNA#4 into the P8b clone. Cell lysates of one P8b siRNA#2 clone, two P8b siRNA#4 clones and PK1 were immunoblotted using anti-PrP antibody, biotinylated ICSM35. 25 µg protein from cell lysates was loaded per lane. Compared to wildtype PK1 cells (lanes 1 and 5), PrP^C expression was suppressed to >90% in three clones (lanes 2-4) The clone in lane 2 expressed siRNA#8 and #2 and was named P8b2a. The clones in lanes 3 and 4 expressed siRNA#8 and #4 and were named P8b4a and P8b4b, respectively.

4.4.5 Reconstitution of PrP^C KO cells with ectopically expressed murine PrP^C restores susceptibility to RML prions

4.4.5.1 Ectopic expression of murine PrP^C in PrP^C KO N2a and PK1 cells

To determine if siRNA expression and extensive subcloning had affected the innate susceptibility of N2a and PK1 cells to RML mouse prions, mouse PrP^C was ectopically expressed in the seven PrP KO clones. The mouse *Prnp* ORF was transduced into the KO clones P8a, P8b, P8c, P8b2a, P8b4a, P8b4b and N8a and stable mixed clones generated by G418 selection. PrP^C expression in these clones was assessed by immunoblotting. Murine PrP^C expression was reconstituted to greater than wildtype level in P8b, P8c, P8b2a, P8b4a and P8b4b clones (**figure 4.12** and **4.13**), and equal to wildtype level in P8a (**figure 4.13**). However, reconstitution of murine PrP^C was not achieved in N8a cells despite three attempts (**figure 4.14**).

4.4.5.2 RML susceptibility of murine PrP^C reconstituted PrP^C KO clones

The RML prion susceptibility of murine PrP^C (moPrP) reconstituted clones was assessed by the scrapie cell assay (SCA). P8b moPrP and P8c moPrP, which overexpressed PrP^C, showed very similar RML prion susceptibility to PK1 cells (**figure 4.15**). P8b4a and P8b4b, which also overexpressed murine PrP^C, exhibited about 80% susceptibility of PK1 to RML prion infection (at 3 x 10^{-5} dilution of RML-infected brain homogenate; **figure 4.17**). However, P8b2a moPrP, which overexpressed PrP^C, showed about 50% susceptibility of PK1 to RML prion infection (**figure 4.16**) and P8a moPrP, which expressed wildtype levels of PrP^C, showed only 30% PK1 susceptibility to RML prions (**figure 4.15**).

4.4.5.3 Summary of RML prion susceptibility of PK1 PrP^C KO clones

In summary, reconstitution of murine PrP^C in PrP^C KO PK1 clones restored susceptibility to RML prions. RML prion susceptibility did not correlate with murine PrP^C expression levels. These were P8b moPrP and P8c moPrP, in which susceptibility was fully restored, followed by P8b4a and P8b4b, in which susceptibility was partially restored. All murine PrP^C-reconstituted clones showed susceptibility at very low RML prion-infected brain homogenate concentrations (from 1 x 10^{-6} dilution). These data demonstrate that following siRNA expression and extensive subcloning, overexpression of PrP^C is required to restore cellular prion susceptibility. This was an important proof-of-principle experiment validating the strategy of ectopically expressing human PrP^C in PK1 and N2a KO clones for the generation of vCJD prion-propagating cell line.

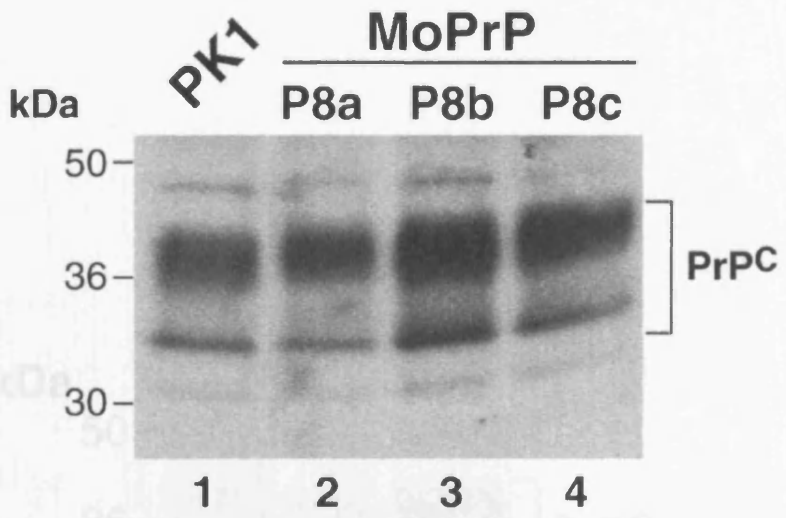

Figure 4.12 Reconstitution of murine PrP^C in PK1 single siRNA PrP^C KO clones
Stable mixed clones expressing murine PrP ORF (moPrP) were established in PK1 single siRNA KO clones, P8a, P8b and P8c. Cell lysates of murine PrP^C reconstituted clones and PK1 wildtype were immunoblotted using anti-PrP antibody, biotinylated ICSM35. 25 µg protein from cell lysates was loaded per lane. Murine PrP^C expression was reconstituted to wildtype PK1 level (lane 1) in P8a clone (lane 2) and to above wildtype level in P8b and P8c clones (lanes 3 and 4, respectively). *These data were produced by P.Arora.*

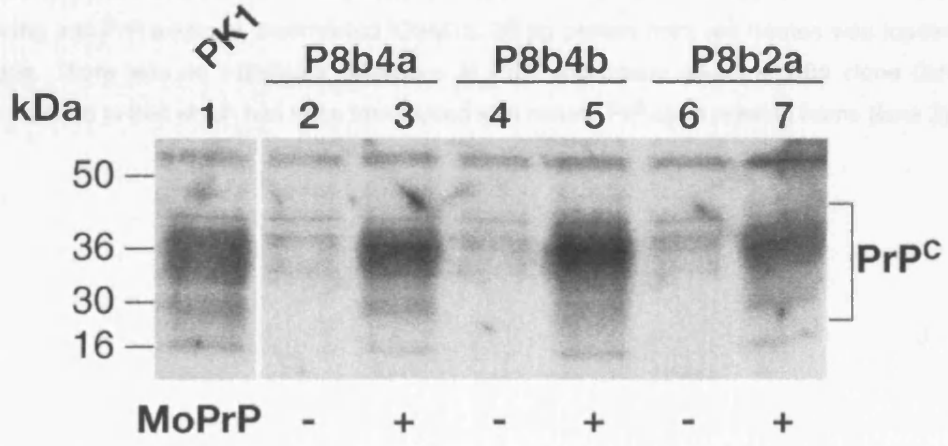

Figure 4.13 Reconstitution of murine PrP^C in PK1 double siRNA PrP^C KO clones
Stable mixed clones expressing murine PrP open reading frame (moPrP) were established in PK1 double siRNA KO clones, P8b2a, P8b4a and P8b4b. Cell lysates of KO clones and their corresponding murine PrP^C-reconstituted clones and PK1 wildtype were immunoblotted using anti-PrP antibody, biotinylated ICSM35. 25 µg protein from cell lysates was loaded per lane. Murine PrP^C expression was reconstituted to greater than PK1 wildtype level (lane 1) in P8b2a (lane 7), P8b4a and P8b4b (lanes 3 and 5, respectively). *These data were produced by P.Arora.*

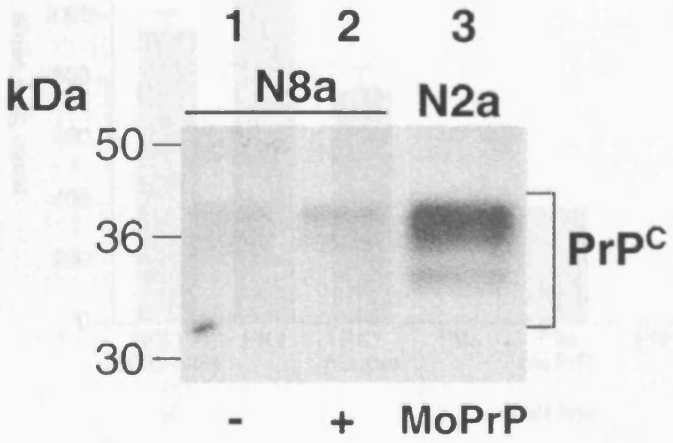

Figure 4.14 Failure to reconstitute murine PrP^C in N8a single siRNA PrP^C KO clone
Stable G418-resistant mixed clones of N8a transduced with murine PrP open reading frame (moPrP) were established. Cell lysates of N8a, N8a mo PrP^C and N2a were immunoblotted using anti-PrP antibody, biotinylated ICSM35. 25 µg protein from cell lysates was loaded per lane. There was no significant difference in PrP^C expression levels in N8a clone (lane 1) compared to that which had been transduced with mouse PrP open reading frame (lane 2).

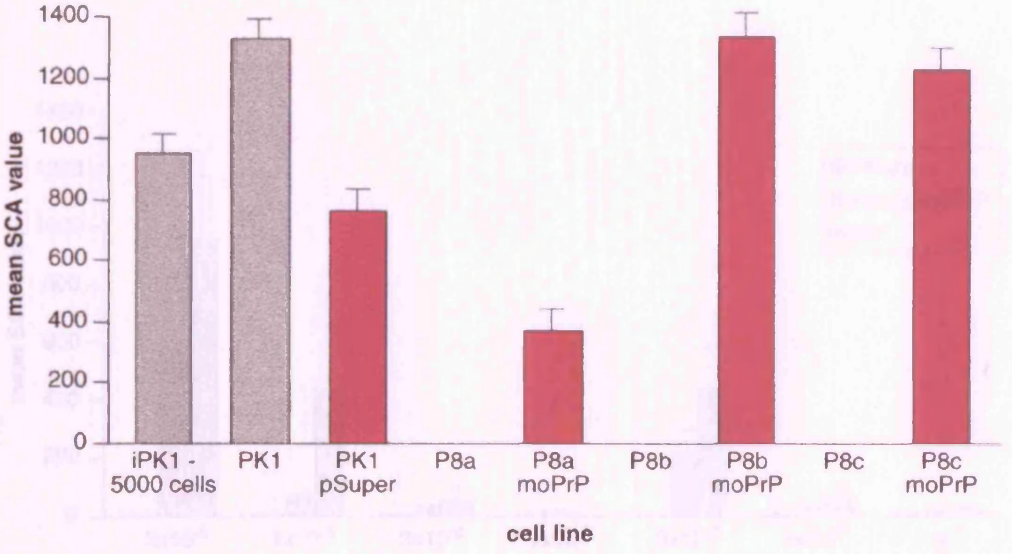

Figure 4.15 RML prion infection of PK1 single siRNA PrP^C KO clones following reconstitution with murine PrP^C

PK1 PrP^C KO clones (P8a, P8b and P8c), corresponding murine PrP^C-reconstituted clones and PK1 (positive control) cells were infected with 0.01% RML prion infected brain homogenate (I3165) and negative controls were not infected. After the third passage at 1:8 ratio (when the original inoculum had been cleared), cells were assayed for presence of PrP^{Sc} by the scrapie cell assay (SCA; see **2.7.5.2**). The graph shows RML infection data only. Each bar represents *mean SCA value per well* (+ SEM) of 12 replicates – this value is the number of PrP^{Sc} positive spots in a well and is an indicator of RML prion susceptibility. The experiment controls are shown in grey and the samples in pink. PK1 cells are highly susceptible to RML prions and represent the positive control for the prion infection; a SCA value of ~1300 spots indicates that the infection was successful. The iPK1 cells are chronically RML prion-infected PK1 cells and were used as a positive control for the SCA; a SCA value of nearly 1000 (938) indicates that the SCA assay was also successful. The pSuper vector only clone showed reduced susceptibility to RML compared to PK1 cells (~40% reduction) but this may have been due to the 18% reduction in PrP^C expression level observed (**table 4.1**). The PrP^C KO clones were all resistant to RML infection. P8a moPrP, which expressed PrP^C to wildtype level, exhibited ~70% reduction in susceptibility to RML prions compared to PK1 wildtype. P8b moPrP and P8c moPrP clones, which overexpressed PrP^C, exhibited similar susceptibility to RML prions compared to PK1 cells.

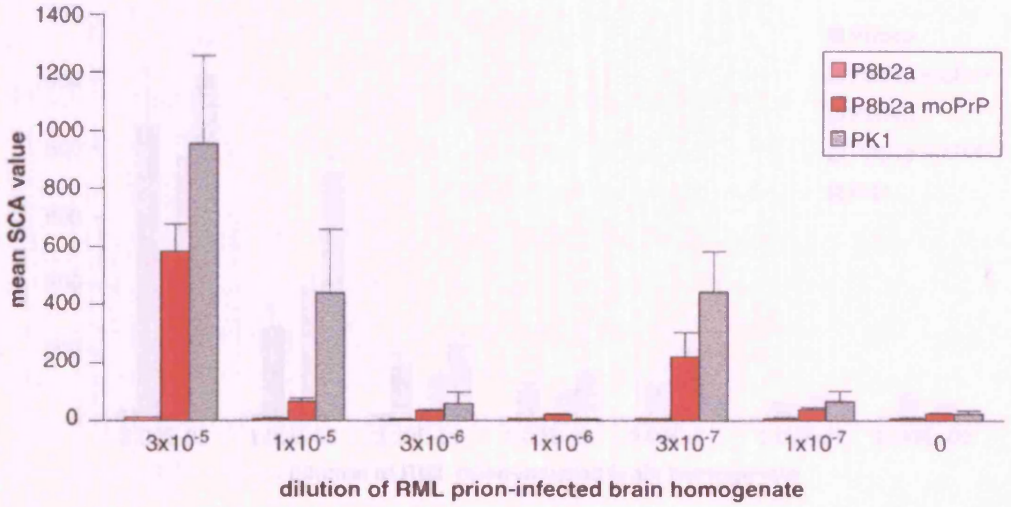

Figure 4.16 RML prion infection of PK1 double siRNA PrP^C KO clone, P8b2a, following reconstitution with murine PrP^C

P8b2a and P8b2a murine PrP^C reconstituted cells and PK1 (positive control) cells were infected with seven dilutions of RML prion-infected brain homogenate (0 - $3x10^{-5}$). After the 3rd passage at 1:8 ratio (when the original inoculum had been cleared), cells were assayed for PrP^{Sc} by SCA. Mean SCA value per well (+ SEM) of 12 replicates are presented. Murine PrP^C reconstitution of P8b2a to over wildtype expression level improves RML susceptibility (compared to the PrP^C KO clone, which is resistant). However, on average only 50% susceptibility is restored compared to PK1 cells over all RML prion dilutions. *These data were produced by P.Arora.*

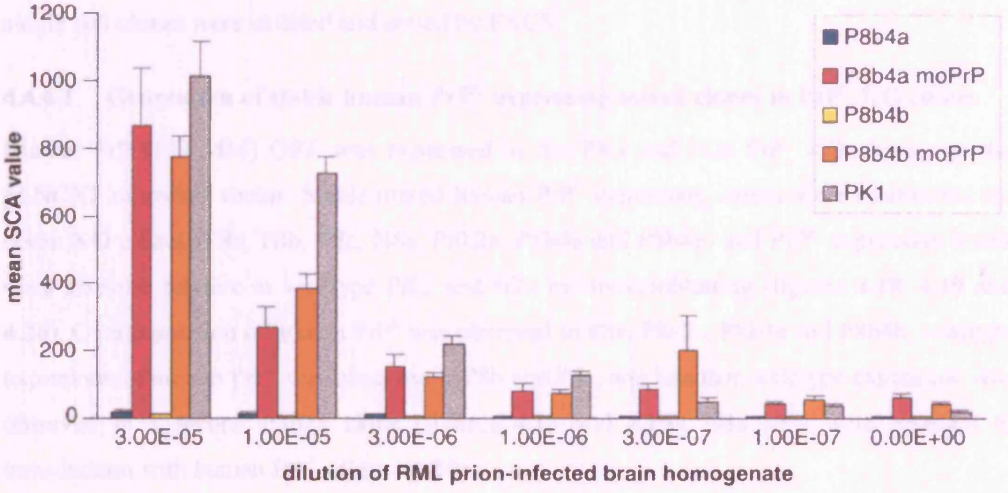

Figure 4.17 RML prion infection of PK1 double siRNA PrP^C KO clones, P8b4a and P8b4b, following reconstitution with murine PrP^C

P8b4a and P8b4b PrP^C KO, corresponding moPrP^C reconstituted cells and PK1 (positive control) cells were infected with seven dilutions of RML homogenate (0 - $1x10^{-7}$). After the 2nd 1:10 passage, cells were assayed for PrP^{Sc} by SCA. Mean SCA value per well (+ SEM) of 12 replicates are presented. Murine PrP^C reconstitution of clones P8b4a and P8b4b to over wildtype level restores their susceptibility to RML prions. RML prion susceptibility is not fully restored to PK1 wildtype level but is not significantly different; approximately an 80% reduction in susceptibility at 3 x 10^{-5} dilution of brain homogenate was observed. *These data were produced by P.Arora.*

4.4.6 Ectopic expression of human PrP^C in PrP knockdown lines

In order to eliminate the species barrier for vCJD prion propagation in the N2a and PK1 mouse cells, human PrP^C (codon 129 MM) was expressed in PrP^C KO clones. Initially, mixed human PrP^C-expressing clones were established. In order to achieve higher PrP^C expression levels, single cell clones were isolated and sorted by FACS.

4.4.6.1 Generation of stable human PrP^C expressing mixed clones in PrP^C KO clones

Human PrP (129 MM) ORF was expressed in the PK1 and N2a PrP^C KO clones via the pLNCX2 retroviral vector. Stable mixed human PrP^C-expressing clones were established for seven KO clones (P8a, P8b, P8c, N8a, P8b2a, P8b4a and P8b4b) and PrP^C expression levels were assessed relative to wildtype PK1 and N2a by immunoblotting (figures **4.18**, **4.19** and **4.20**). Overexpression of human PrP^C was observed in P8a, P8b2a, P8b4a and P8b4b, wildtype expression of human PrP^C was observed in P8b and P8c, and less than wildtype expression was observed in a second P8b2a clone (figures **4.18** and **4.19**). N8a cells were resistant to transduction with human PrP^C (**figure 4.20**).

4.4.6.2 Achieving maximal human PrP^C expression in P8b PrP^C KO line

PrP^C overexpression has been found to increase susceptibility of some cell lines to prion infection (Nishida et al., 2000;Giri et al., 2006). The murine PrP^C reconstitution of PrP^C KO cells presented here corroborates this since overexpression of murine PrP^C increased susceptibility to RML prion infection. It was hypothesised that human PrP^C overexpression would enhance susceptibility of KO clones to vCJD prions due to increased availability of human PrP^C template for conversion to human PrP^{Sc}. The P8b line was used for this study because at the time of experiments it was the clone with the best PrP^C KO clone available and had also showed the most susceptibility to RML prions (**figure 4.15**). Two strategies were adopted for the isolation of clones maximally overexpressing human PrP^C, (1) single cell cloning of P8b human PrP^C mixed clone and (2) isolation of P8b human PrP^C cells highly expressing PrP^C by FACS sorting.

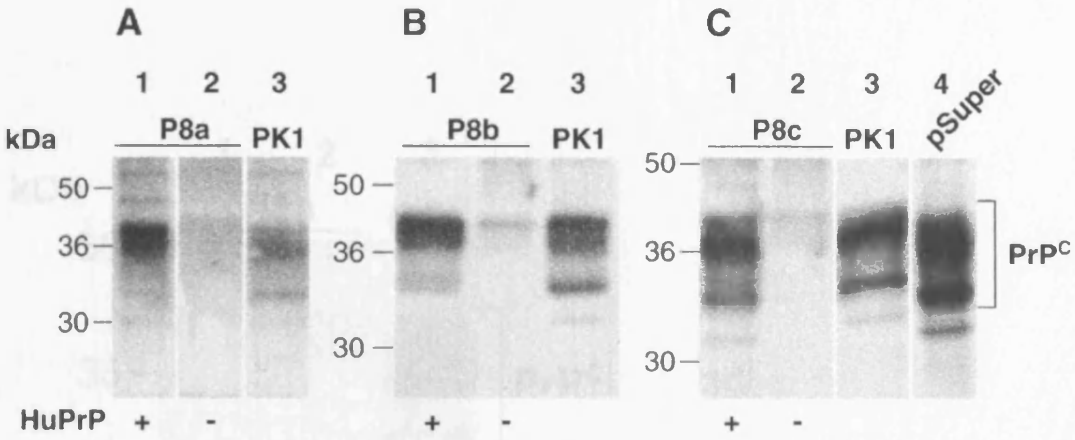

Figure 4.18 Ectopic expression of human PrP^C in PK1 single siRNA PrP^C KO clones

PK1 single siRNA clones (P8a, P8b and P8c) were retrovirally transduced with human PrP ORF (129 MM) and G418-resistant stable mixed clones established. Cell lysates of stable mixed human PrP^C clones (HuPrP+) and corresponding PK1 PrP^C KO clones (HuPrP-), PK1 pSuper and PK1 positive control were immunoblotted using anti-PrP antibody, biotinylated ICSM35. 25 µg protein from cell lysates was loaded per lane. Human PrP^C was expressed to at least PK1 wildtype level (lane 3 A-C) in all PK1 single siRNA PrP^C KO clones, P8a, P8b and P8c (lane 1 A-C respectively) compared to KO clones (lane 2 A-C). P8aH (lane A1) overexpressed human PrP^C.

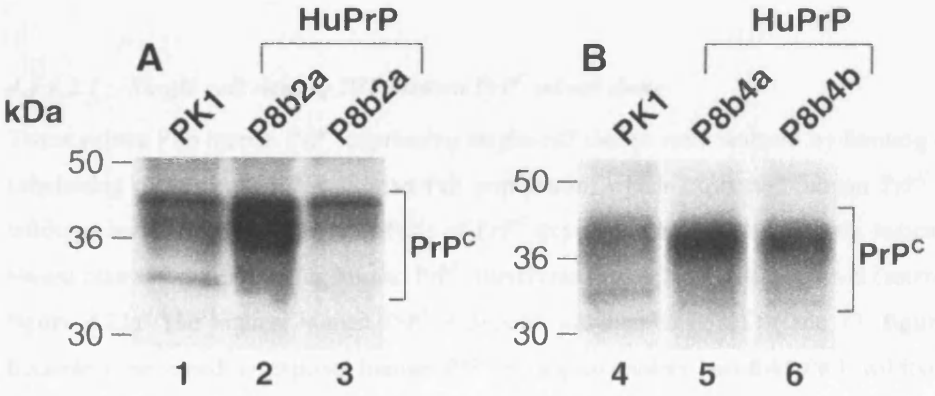

Figure 4.19 Ectopic expression of human PrP^C in PK1 double siRNA PrP^C KO clones

PK1 double siRNA clones, P8b2a, P8b4a and P8b4b, were retrovirally transduced with human PrP ORF (129 MM) and G418-resistant stable mixed clones established. Cell lysates of stable mixed human PrP^C clones and PK1 positive control were immunoblotted using anti-PrP antibody, biotinylated ICSM35. 25 µg protein from cell lysates was loaded per lane. Compared to PK1 wildtype (lanes 1 and 4), human PrP^C was overexpressed in P8b2a (lane 2), P8b4a (lane 5) and P8b4b (lane 6). In an independent transduction, human PrP^C was expressed to below wildtype level in P8b2a (lane 3).

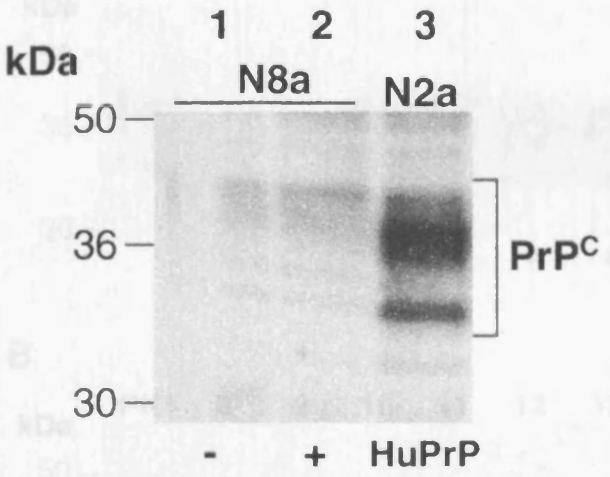

Figure 4.20 Failure to generate human PrP^C –expressing N8a cells

Cell lysates of G418-resistant mixed human PrP-transduced N8a cells (lane 1), N8a KO clone (lane 2) and N2a (positive control; lane 3) were immunoblotted using anti-PrP antibody, biotinylated ICSM35. 25 µg protein from cell lysates was loaded per lane. No human PrP^C expression was observed following transduction of N8 with human PrP^C.

4.4.6.2.1 Single cell cloning P8b human PrP^C mixed clone

Twenty-three P8b human PrP^C-expressing single cell clones were isolated by limiting dilution subcloning of the mixed P8b human PrP population, which expressed human PrP^C to PK1 wildtype level (**figure 4.18B**). Analysis of PrP^C expression by immunoblotting indicated that eleven clones were expressing human PrP^C significantly over PK1 wildtype level (asterisked in **figure 4.21**). The highest human PrP^C expressor was named P8bH2 (lane 17, **figure 4.21**) because it appeared to express human PrP^C to approximately two-fold PK1 wildtype level (**figure 4.22**).

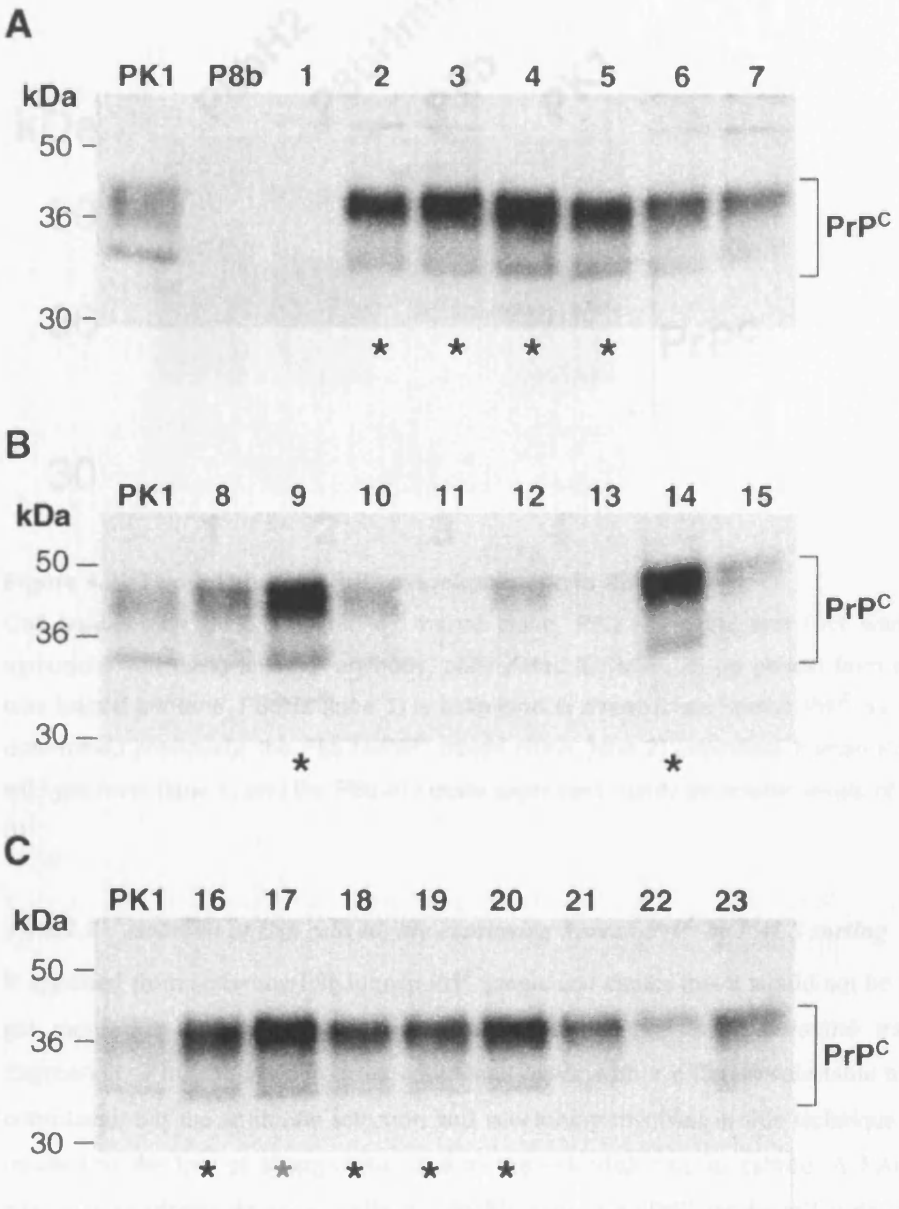

Figure 4.21 Screening for human PrP^C overexpression in P8b clones

23 P8b human PrP^C-expressing single cell clones (labelled 1 -23) were isolated by limiting dilution subcloning of P8b human PrP mixed population. Cell lysates of clones and PK1 wildtype were immunoblotted using anti-PrP antibody, biotinylated ICSM35. 25 µg protein from cell lysates was loaded per lane. Eleven clones overexpressing human PrP^C clones above PK1 wildtype level are indicated by an asterisk (*). Compared to PK1 wildtype, the highest human PrP^C overexpressor was clone 17, named P8bH2 (red asterisk).

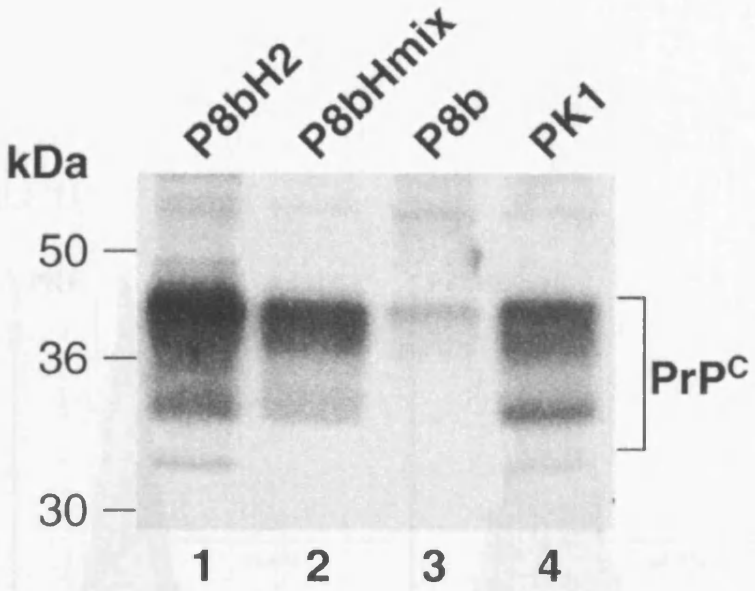

Figure 4.22 Two-fold human PrP^C overexpression in P8bH2

Cell lysates of P8bH2, P8b $huPrP^C$ mixed clone, P8b KO clone and PK1 wildtype were immunoblotted using anti-PrP antibody, biotinylated ICSM35. 25 µg protein from cell lysates was loaded per lane. P8bH2 (lane 1) is estimated to overexpress human PrP^C by >2-fold. As determined previously, the P8b $huPrP^C$ mixed clone (lane 2) expresses human PrP^C to PK1 wildtype level (lane 4) and the P8b KO clone expresses barely detectable levels of PrP^C (lane 3).

4.4.6.2.2 Isolation of P8b cells highly expressing human PrP^C by FACS sorting

It appeared from screening P8b human PrP^C single cell clones that it would not be possible to get more than 2-fold wildtype expression of human PrP^C with retroviral transduction. Expression of human PrP^C from an additional vector with a different selectable marker was considered, but the antibiotic selection and subcloning involved in this technique may have resulted in the loss of susceptibility due to the extended time in culture. A FACS sorting strategy was adopted to isolate cells very highly expressing PrP^C (at the cell surface) from the two-fold overexpressing P8bH2 clone. The P8bH2 clone underwent a further three overnight retroviral transductions with human PrP^C viral supernatant and forty-eight hours later the highest overexpressors were isolated by FACS sorting (**figure 4.23**). 7% of P8bH2 population had significantly higher PrP^C expression compared to PK1 wildtype expression. The relative prion-FITC brightness of this FACS-isolated clone, expressed as mean fluorescent intensity (MFI), was 5-fold greater than that of PK1 wild-type. Densitometric analysis of immunoblot demonstrated that this FACS-sorted clone overexpressed human PrP^C to four times wildtype level and was thus named P8bH4 (**figure 4.24**).

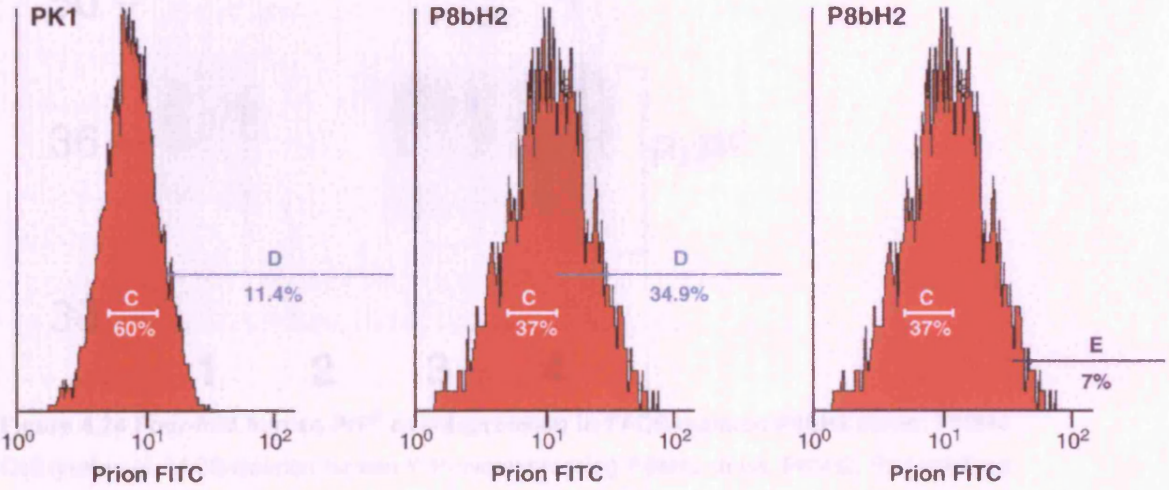

Figure 4.23 Isolation of highly expressing human PrP^C cells from P8bH2 clone by FACS sorting

48 hours following human PrP transduction, P8bH2 cells were stained for PrP^C with ICSM35 and FITC-conjugated anti-mouse IgG Fab and then sorted on Beckman Coulter Epics Altra sorter for human PrP^C overexpression. PK1 cells were assayed to determine wildtype level PrP^C expression (gate **C**). Gate **D** was set at approximately top 10% brightness of wildtype PK1 population to allow isolation of cells expressing greater than wild-type PrP^C levels. 34.9% P8bH2 cells were overexpressing human PrP^C (gate **D**). Another gate was set to isolate the very highest human PrP^C expressors (gate **E**). 7% of the P8bH2 population was isolated for significantly higher human PrP^C expression by FACS. *FACS data were generated with the help of J.Buddle, Institute of Child Health, London*

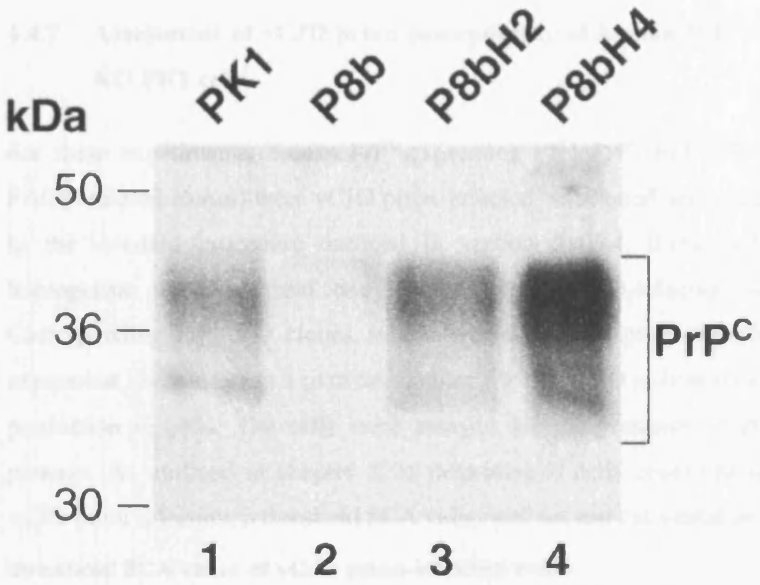

Figure 4.24 Four-fold human PrP^C overexpression in FACS-isolated P8bH2 clone: P8bH4
Cell lysates of FACS-isolated human PrP-overexpressing P8bH2 clone, P8bH2, PK1 wildtype and P8b PrP^C KO clone were immunoblotted using anti-PrP antibody, biotinylated ICSM35 to assess PrP^C levels. 25 µg protein from cell lysates was loaded per lane. FACS sorting of P8bH2 (lane 3) isolated a population of cells overexpressing human PrP^C to four-fold PK1 wildtype level (determined by densitometric analysis of the immunoblot; lane4), which was named P8bH4.

4.4.6.3 Summary of human PrP^C-expressing murine PrP^C KO cells

Human PrP^C was expressed in the six PK1 PrP^C (single and double siRNA) KO clones. Four of the mixed clones expressed PrP^C to just over PK1 wildtype level (P8a, P8b2a, P8b4a P8b4b), and two expressed PrP^C equal to wildtype level (P8b and P8c). No N2a KO cells expressing human PrP^C were isolated. Single cell subcloning of P8b human PrP mixed clone generated eleven clones overexpressing human PrP^C, P8bH2 being the highest expressor that exhibited about 2-fold wildtype PK1 PrP^C expression levels. Further retroviral transduction of P8bH2 with human PrP^C and sorting of the highest human PrP^C expressing population by FACS isolated a 4-fold human PrP^C overexpressing clone: P8bH4.

4.4.7 Assessment of vCJD prion susceptibility of human PrP^C-expressing mouse PrP^C KO PK1 cells

For these experiments, human PrP^C-expressing PK1 PrP^C KO cells (mixed, single cell and FACS-isolated clones) were vCJD prion-infected, subcloned and screened for PrP^{Sc} according to the standard procedure outlined in section **3.4.3.4**. 0.1% vCJD prion-infected brain homogenate was used and one 96-well plate of sib-selection subclones was assayed. Corresponding PrP^C KO clones, which are resistant to prion infection due to lack of PrP^C expression, were used as a particle monitor for the vCJD infections to identify *de novo* PrP^{Sc} production in cells. The cells were assayed for the presence of PrP^{Sc} by SCA after each passage. As outlined in chapter 3, to determine if cells contained *de novo* PrP^{Sc} following vCJD prion infection, a threshold SCA value was set and calculated as follows:

threshold SCA value of vCJD prion-infected wells

> mean particle monitor SCA value + 5 x standard deviations

4.4.7.1 vCJD prion susceptibility of human PrP^C-expressing mixed clones of PK1 PrP^C KO clones

Of the six mixed human PrP^C-expressing PK1 PrP^C KO clones, only two showed any susceptibility to vCJD prion infection but this was very low. PrP^{Sc} was detected in 8% of P8a huPrP wells and 3% of P8b huPrP^C wells by SCA (**figure 4.25**). P8b huPrP^C, P8b2a huPrP^C, P8b4a huPrP^C and P8b4b huPrP^C were all resistant to vCJD prion infection since no positive wells were detected. Levels of PrP^C did not correlate with susceptibility; P8c huPrP^C expressed wildtype levels of human PrP^C but was more susceptible than the overexpressing P8b2a huPrP^C, P8b4a huPrP^C and P8b4b huPrP^C.

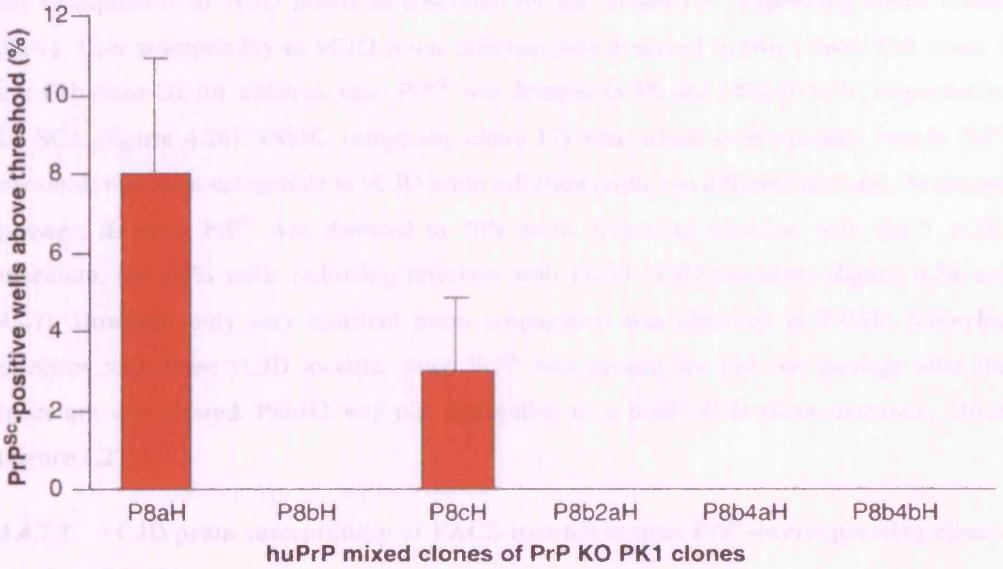

Figure 4.25 vCJD prion infection of mixed human PrP^C expressing PK1 PrP^C KO clones
Mixed human PrP^C, clones were infected with 0.1% vCJD prion-infected brain homogenate (I2811) and the standard infection, subcloning and PrP^{Sc} assay procedures were followed. vCJD prion infection of the mixed human PrP^C clones cells was evident if SCA values per well (PrP^{Sc}-positive spots) were above a certain threshold value, calculated as "mean SCA value for vCJD prion-infected particle monitor plus 5x standard deviations". SCA data from three experiments at 2nd 1:8 passage (when particle monitor indicated the inoculum was cleared) are presented as mean percentage wells (+ SEM) above this threshold SCA value. (24 wells of each PK1 KO clone and 96 wells $huPrP^C$ mixed clones were assayed per experiment). *De novo* PrP^{Sc} was detected in a low proportion of P8a $huPrP^C$ and P8c $huPrP^C$ wells, 8% and 3%, respectively. No PrP^{Sc} was detected in the other mixed clones, P8b $huPrP^C$, P8b2a $huPrP^C$, P8b4a $huPrP^C$, P8b4b $huPrP^C$.

4.4.7.2 vCJD prion susceptibility of human PrP^C over-expressing P8b single cell clones

Eleven P8b clones over-expressing human PrP^C (asterisked in **figure 4.21**) were investigated for susceptibility to vCJD prions as described for the human PrP^C-expressing mixed clones above. Low susceptibility to vCJD prion infection was observed in two clones, P8b clone 4 and P8b clone 20, for which *de novo* PrP^{Sc} was detected in 3% and 14% of wells, respectively, by SCA (**figure 4.26**). P8bH2 (originally clone 17) was, which overexpresses human PrP^C two-fold, was most susceptible to vCJD prion infection (with two different inocula). At second passage, *de novo* PrP^{Sc} was detected in 70% wells following infection with I2811 vCJD inoculum, and 60% wells following infection with I3139 vCJD inoculum (**figure 4.26** and **4.27**). However, only very transient prion propagation was observed in P8bH2 following infection with these vCJD inocula, since PrP^{Sc} was present for just one passage after the inoculum was cleared. P8bH2 was not susceptible to a third vCJD prion inoculum, I4618 (**figure 4.27**).

4.4.7.3 vCJD prion susceptibility of FACS-isolated human PrP^C-overexpressing clone - P8bH4

It was hypothesised that to achieve more persistent vCJD prion propagation in P8bH2, which overexpressed human PrP^C two-fold, higher PrP^C expression was required. A four-fold human PrP^C overexpressing clone was isolated from P8bH2 by FACS sorting, P8bH4 (see **figure 4.24**). The vCJD prion susceptibility of P8bH4 was assessed, as described above. PrP^{Sc} was detected in 6% of P8bH4 wells compared to 42% of P8bH2 wells, showing that FACS sorting to increase the PrP^C expression actually reduced susceptibility to vCJD prion infection 7-fold (**figure 4.28**). A number of reasons may explain this reduction in vCJD prion susceptibility. First the combined human PrP^C retroviral transductions and FACS procedure was stressful for the cells because at the time of the FACS sort, only 22% P8bH2 were viable compared to 55% of PK1 controls. It is known that if PK1 cells are not kept in optimal conditions, they lose their susceptibility RML prions (Dr P. Klohn, personal communication). Second, by selecting for high human PrP^C expression, currently unknown prion susceptibility factors may have been lost.

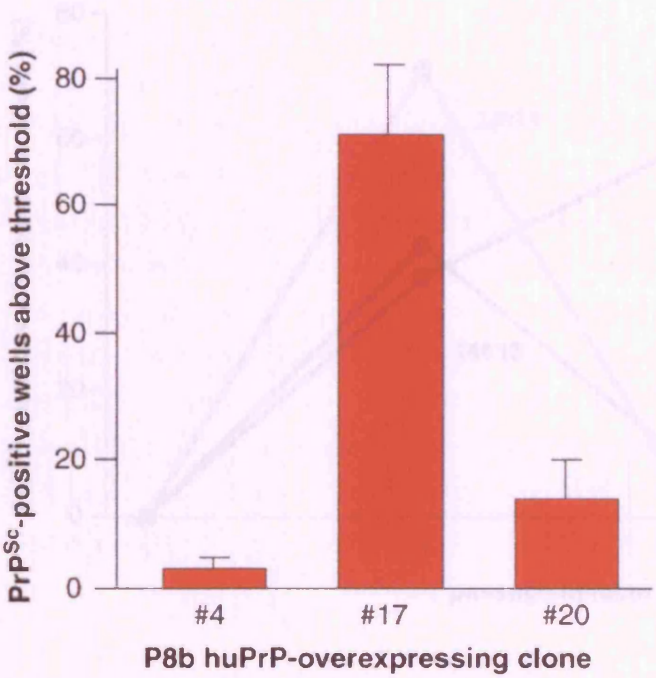

Figure 4.26 vCJD prion infection of human PrP^C-overexpressing P8b clones

Human PrP^C-overexpressing P8b clones (4, 17, 20) were infected with with 0.1% vCJD prion-infected brain homogenate (I2811) and the standard infection, subcloning and PrP^{Sc} assay procedures were followed. vCJD prion infection of the human PrP^C–expressing P8b clones was evident if SCA values per well (PrP^{Sc} –positive spots) were above a certain threshold value, calculated as "mean SCA value for vCJD prion-infected particle monitor plus 5x standard deviations". Data from three experiments at 2nd 1:8 passage (when particle monitor indicated inoculum was cleared) are presented as mean percentage wells (+ SEM) above this threshold SCA value. (24 wells of each PK1 KO clone and 96 wells $huPrP^C$ P8b clones were assayed per experiment). P8bH clone 4, and 20 showed only low susceptibility to vCJD prion infection, with the presence of *de novo* PrP^{Sc} detected in 3% and 14% wells, respectively. P8bH2 (originally clone 17) appeared highly susceptible to vCJD prions at this passage number with *de novo* PrP^{Sc} being detected in 70% wells.

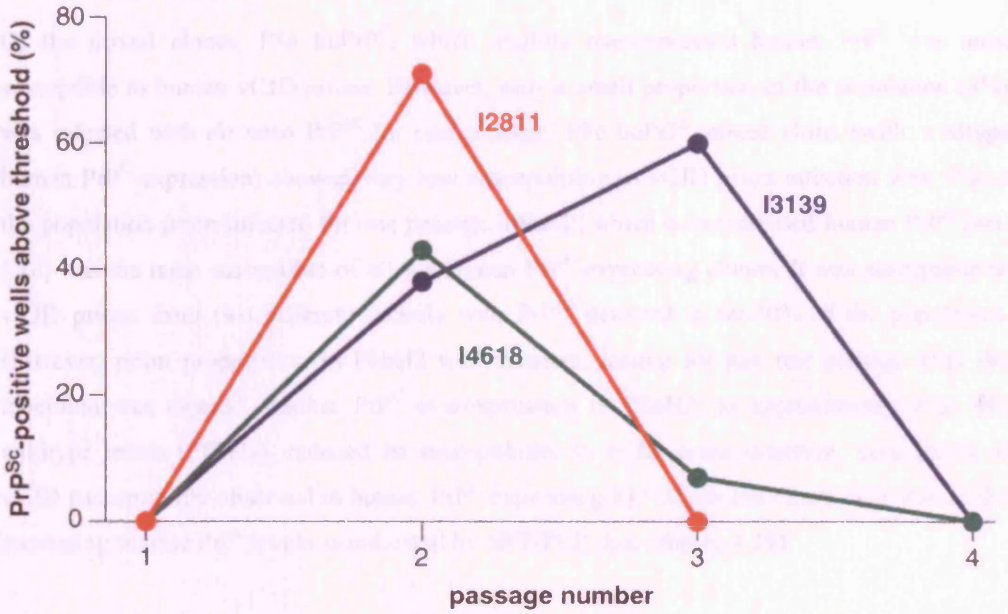

Figure 4.27 Prion infection of P8bH2 with 3 different vCJD inocula

P8bH2 was exposed to three different vCJD prion inocula, I2811, I3139 and I4618 at 0.1% dilution and the standard infection, subcloning and PrP^{Sc} assay procedures were followed. vCJD prion infection in P8bH2 was determined if SCA values per well (PrP^{Sc}-positive spots) were above a certain threshold value, calculated as "mean SCA value for vCJD prion-infected particle monitor plus 5x standard deviations". Data from one experiment are presented as mean percentage of P8bH2 wells (+ SEM) above this threshold SCA value over 4 passages. I2811 vCJD inoculum has the lowest PrP^{Sc} titre because the particle monitor cleared earlier (at the 2nd passage) than the other inocula (at 3rd passage). There is no *de novo* PrP^{Sc} production in P8bH2 at first passage following vCJD infection. *De novo* PrP^{Sc} accumulates in P8bH2 up to the second passage, following infection with I2811 and I4618, and up to the 3rd passage, following infection with I3139. The longer prion infection observed in I3139-infected cells compared to I2811-infected cells is probably be due to prion conversion induced by PrP^{Sc} from the residual inoculum in the I3139 cultures instead of genuine *de novo* prion propagation. Prion conversion as a result of contact with PrP^{Sc} in the residual inoculum is probably also responsible for the accumulation of vCJD prions in cells infected with I4618 between passage 1 and 2. P8bH2 is most susceptible to I2811 at 2nd passage, when PrP^{Sc} is present in 70% wells, compared to about 40% for I3139 and I4618. In summary, in response to infection by 2 of the 3 vCJD inocula (I2811 and I3139) there is transient prion propagation for one passage after the inocula are cleared from the cultures.

4.4.7.4 Summary of vCJD prion susceptibility of human PrP^C expressing PrP^C KO PK1 clones

Of the mixed clones, P8a huPrP^C, which slightly overexpressed human PrP^C was most susceptible to human vCJD prions. However, only a small proportion of the population (8%) was infected with *de novo* PrP^{Sc} for one passage. P8c huPrP^C mixed clone (with wildtype human PrP^C expression) showed very low susceptibility to vCJD prion infection with 3% of the population prion-infected for one passage. P8bH2, which overexpressed human PrP^C two-fold, was the most susceptible of all the human PrP^C-expressing clones. It was susceptible to vCJD prions from two different inocula with PrP^{Sc} detected in 60-70% of the population. However, prion propagation in P8bH2 was transient, lasting for just one passage after the inoculum was cleared. Further PrP^C overexpression in P8bH2, to approximately four-fold wildtype levels (P8bH4), reduced its susceptibility to vCJD prion infection. Low levels of vCJD susceptibility observed in human PrP^C-expressing KO clones may have been due to the increasing murine PrP^C levels as indicated by qRT-PCR data (**figure 4.29**).

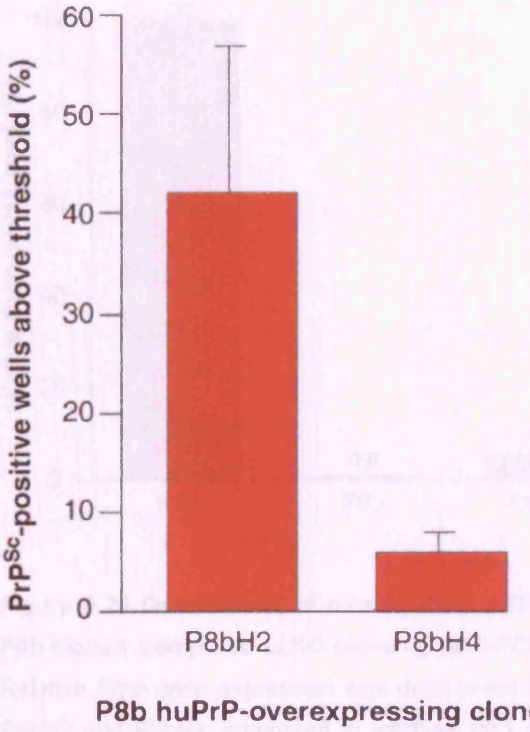

Figure 4.28 vCJD prion susceptibility of human PrP^C-overexpressing P8bH4 clone isolated by FACS

P8bH4 clone overexpresses human PrP^C four-fold and was isolated by FACS from P8bH2, which overexpresses human PrP^C two-fold. Both P8bH2 and P8bH4, were infected with 0.1% vCJD prion-infected brain homogenate (I2811) and the standard infection, subcloning and PrP^{Sc} assay procedures were followed. vCJD prion infection of cells was determined if SCA values per well (PrP^{Sc}-positive spots) were above a certain threshold value, calculated as "mean SCA value for vCJD prion-infected particle monitor plus 5x standard deviations". SCA data from 2nd 1:8 passage (when particle monitor indicated the inoculum was cleared) are presented as mean percentage wells (+ SEM) above this threshold SCA value. (24 wells of P8b KO clone and 96 wells of P8bH4 and P8bH2 were assayed). The P8bH4 clone was 7-fold less susceptible to vCJD prion infection than its parent population, P8bH2 since PrP^{Sc} was detected in 6% wells by SCA compared to 42% wells for P8bH2. Thus, further overexpression of human PrP^C in P8bH2 clone did not improve susceptibility to vCJD prion infection.

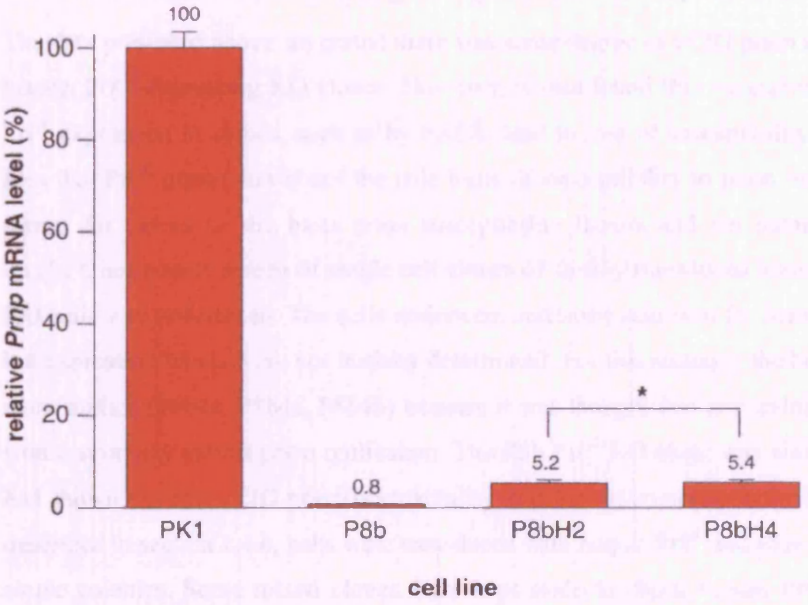

Figure 4.29 Quantitation of murine *Prnp* mRNA levels in human PrP^C-overexpressing P8b clones compared to KO clone by qRT-PCR

Relative *Prnp* gene expression was determined for human PrP^C-overexpressing P8b clones, P8bH2 and P8bH4, compared to wildtype PK1 cells and P8b KO clone by the comparative threshold method (described in **2.5.7.4**), using GAPDH to normalise the data. Validation experiments were performed to determine that GAPDH and *Prnp* probe amplification efficiencies were equal because the slope of log input amount vs ΔC_T plot was 0.12. Data are presented as relative *Prnp* mRNA levels and represent means of triplicate samples (+ SEM). 2-tailed *t*-tests were performed to determine if there was a difference in *Prnp* expression in human PrP^C-expressing clones compared to the control P8b KO clone. *Prnp* mRNA levels in the human PrP^C-expressing clones, P8bH2 and P8bH4, had significantly (*$P<0.05$) increased by 7-fold compared to the P8b KO. *J.Podesta performed the experiments and I performed the data analysis.*

4.4.7.5 Screening human PrP^C expressing clones for susceptibility to vCJD prion infection without selecting for high human PrP^C expression levels

The data presented above suggested there was some degree of vCJD prion susceptibility in the human PrP^C–expressing KO clones. However, it was found that excessive selection for high PrP^C expression in clones, such as by FACS, lead to loss of susceptibility. This supports the idea that PrP^C expression is not the sole basis of susceptibility to prion infection. In order to screen for clones on the basis prion susceptibility factors and not human PrP^C expression levels, a large-scale screen of single cell clones of freshly transduced human PrP^C–expressing KO cells was undertaken. The cells underwent antibiotic selection for human PrP^C expression but expression levels were not initially determined. For this strategy, the best PrP^C KO clones were studied (P8b2a, P8b4a, P8b4b) because it was thought that any endogenous mouse PrP^C would seriously inhibit prion replication. The P8b PrP^C KO clone was also studied because it had shown the best vCJD prion susceptibility in prior experiments, in the form of P8bH2. As described in section **2.4.6**, cells were transduced with human PrP^C and then clones picked from single colonies. Some mixed clones were kept aside to check human PrP^C expression. The single clones were grown to confluency in 96-well plates and split to two replica plates. One plate was infected with vCJD prions and the other was stored at –80°C, to be thawed when a positive clone was identified. Prion-infected plates underwent three 1:8 passages to clear the inoculum and were then assayed for the presence of PrP^{Sc} by SCA. Results are summarised in **table 4.2**. The human PrP^C–expressing P8b4a and P8b4b subclones (300 of each) were not at all susceptible to vCJD prions demonstrating that improved PrP^C knockdown did not increase susceptibility. Human PrP^C–expressing P8b and P8b2a subclones (referred to as P8bH and P8b2aH) appeared more susceptible to vCJD prion infection with 12% and 10%, respectively, of clones containing PrP^{Sc} (**figure 4.30**). However, the level of PrP^{Sc} accumulation in the clones indicated by the SCA values was very low; 39 being the highest SCA value for one P8b2aH subclone. This method detected lower susceptibility of human PrP^C–expressing P8b to vCJD prions than studying clones isolated on the basis of high PrP^C expression levels. This could have been because the human PrP^C expression levels of the freshly transduced clones were too low; mixed clones were lower than wildtype. It was apparent in the murine PrP^C reconstitution experiments expression needed to be wildtype or above to regain susceptibility to RML prions.

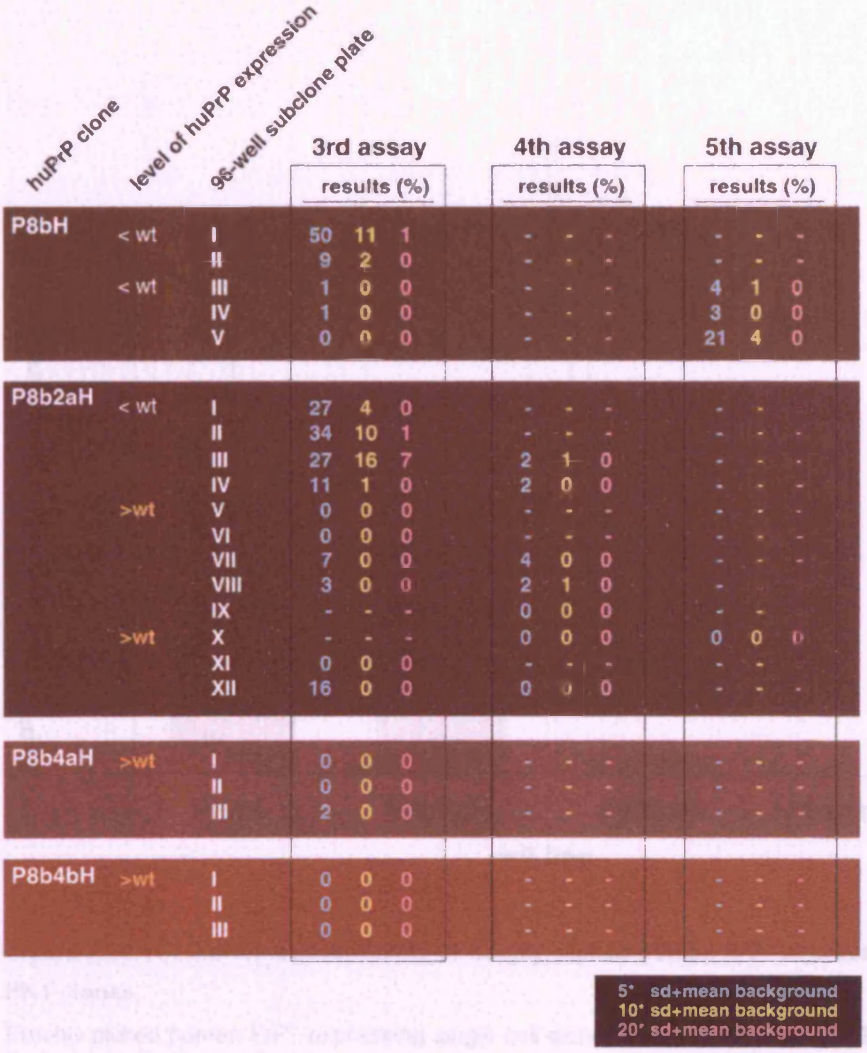

Table 4.2 Summary of vCJD prion susceptibility of freshly picked human PrP^C-expressing PrP^C KO PK1 clones

PrP^C KO clones P8b (brown panel), P8b2a (purple panel), P8b4a (pink panel), P8b4b (red panel) were retrovirally transduced with human *PRNP* ORF. G418-resistant single colonies were picked and transferred to 96-well plates and split to two sister plates when confluent. One plate was stored at -80°C, the other infected with 0.1% vCJD inoculum. The appropriate PrP^C KO clone was infected in parallel as a particle monitor. SCA was performed after the 3rd, 4th and 5th passage for the presence of *de novo* PrP^{Sc}. vCJD prion susceptibility data are expressed as mean percentage human PrP^C-expressing clones above threshold SCA value (calculated as "mean SCA value for vCJD prion-infected particle monitor plus 5x standard deviations"). (-) indicates SCA was not performed. The human PrP^C expression level of mixed clones is shown in 2nd column and the number of clones screened in the 3rd column. There was essentially negligible susceptibility to vCJD prion infection. Any indication that there was vCJD prion susceptibility, for example in P8bH subclone plate I and in P8b2aH subclone plate I-IV, was due to the fact that the threshold level was very low because the particle monitor was virtually zero. The highest SCA value observed was 39.

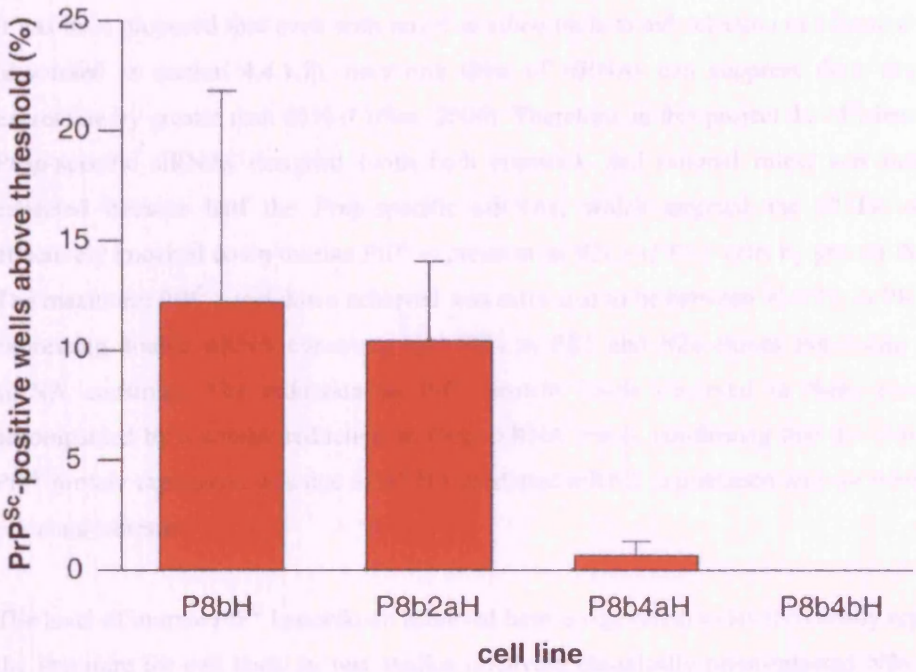

Figure 4.30 vCJD prion susceptibility of freshly picked human PrP^C-expressing PrP^C KO PK1 clones

Freshly picked human PrP^C-expressing single cell clones from KO clones, P8b, P8b2a, P8b4a and P8b4b were infected with 0.1% dilution of vCJD prion-infected brain homogenate (I2811) without analysis for PrP^C expression levels. The appropriate PrP^C KO clone was infected in parallel as a particle monitor. These clones were assayed for the presence of PrP^{Sc} by SCA after three 1:8 passages (to clear the inoculum). SCA data after the 3rd 1:8 passage are presented as mean percentage wells above SCA threshold value (those with PrP^{Sc} SCA value greater than mean vCJD prion-infected particle monitor plus 5 standard deviations) indicating which wells are prion-infected. The P8bH and P8b2aH subclones were most susceptible to vCJD prion infection but at a relatively low level, with with PrP^{Sc} detected in 12 and 10% wells, respectively. P8b4aH and P8b4bH were not at all susceptible to vCJD prion infection.

4.5 Discussion

4.5.1 Knockdown of PrP^C expression by RNAi

It has been proposed that even with novel *in silico* tools to aid selection of effective siRNAs (discussed in section **4.4.1.2**), only one third of siRNAs can suppress their target gene expression by greater than 80% (Cullen, 2006). Therefore, in this project the efficiency of the *Prnp*-specific siRNAs designed (with both empirical and rational rules) was better than expected because half the *Prnp*-specific siRNAs, which targeted the 3'UTR of *Prnp*, effectively knocked down murine PrP^C expression in N2a and PK1 cells by greater than 80%. The maximum PrP^C knockdown achieved was estimated to be between 95-99% in PK1 clones expressing double siRNA constructs and 90% in PK1 and N2a clones expressing a single siRNA construct. The reduction in PrP^C protein levels observed in these clones was accompanied by a similar reduction in *Prnp* mRNA levels, confirming that the reduction in PrP^C protein expression was due to siRNA-mediated mRNA degradation and not inhibition of protein synthesis.

The level of murine PrP^C knockdown achieved here is equivalent to levels recently reported in the literature for cell lines. In two studies involving chronically prion-infected N2a cells, in which the siRNAs targeted different sequences of the *Prnp* coding region, endogenous PrP^C expression was suppressed by 97% using lentiviral-delivered shRNA (Pfeifer et al., 2006), and by approximately 95% using transiently transfected siRNA duplexes (Daude et al., 2003). In both cases depletion of PrP^C in these cells abrogated PrP^{Sc} accumulation. The lentiviral-delivered anti-PrP shRNA was also expressed in chimeric mice from embryonic stages and was found to prolong the life-span of RML-prion infected mice. In another study, 96% reduction in expression of murine PrP^C in rabbit epithelial kidney cells was achieved by stable plasmid-based expression of shRNA targeting the coding region of *Prnp* (Tilly et al., 2003).

The level of *Prnp* knockdown achieved in the N2a-derived lines did not meet the original aim of completely knocking-out murine PrP^C expression. Complete *Prnp* knockout (KO) was required because murine PrP^C is proposed to inhibit human prion formation in human transgenic mice by a dominant negative inhibition, whereby non-homologous host murine PrP^C inhibits conversion of human PrP^C to PrP^{Sc} (Telling et al., 1995;Collinge et al., 1995;Perrier et al., 2002). As already outlined, complete *Prnp* KO in cell lines by RNAi has not been achieved by any groups, and there are several reasons which may explain why this is such a challenging task. First, N2a cells possess 5-7 copies of the *Prnp* gene (Dr Solstadt, personal communication). RNAi may not be the ideal technique to completely knockout *Prnp*

expression in N2a cells due to the potential abundance of target *Prnp* mRNA. Either the expression level of *Prnp*-specific siRNA may be insufficient to target the degradation of the large quantity of *Prnp* mRNA or the capacity of the cellular RNAi machinery may be inadequate.

Second, complete *Prnp* knockout may be lethal to cells because PrP^C has been proposed to play a role in cell survival (Chiarini et al., 2002;Zanata et al., 2002;Chen et al., 2003;Lopes et al., 2005;Zhang et al., 2006). For example, decreasing endogenous PrP^C expression in human neurones with antisense PrP cDNA renders them more susceptible to Bax-mediated cell death, whilst co-expression of PrP^C with Bax prevents cell death (Bounhar et al., 2001). In addition, PrP-deficient primary cerebellar and cortical neurones are more susceptible to oxidative stress *in vitro* (Brown et al., 1997). PrP^C is proposed to exert its neuroprotective effect by interaction with apoptotic pathways to prevent permeability of the mitochondrial membrane (Roucou and LeBlanc, 2005). Therefore, the lower viability observed in the N2a and PK1 double siRNA *Prnp* KO clones with both siRNA#5 and siRNA#8 may be due to the fact that this combination of siRNAs resulted in complete PrP^C KO. However, in general the proliferation rate of the *Prnp* KO clones compared to vector-only clones was similar. In accordance with this observation, *Prnp* KO in mice is not lethal and they show no overt phenotype (Bueler et al., 1992). Moreover, neither does depletion of neuronal PrP^C in *Prnp* conditional KO mice (with the Cre-lox system) produce an overtly deleterious phenotype in adulthood (Mallucci et al., 2002).

Third, siRNA-induced knockdown of gene expression may not be stable, therefore it may not be possible to sustain 100% PrP^C knockdown even if it were achieved. The RNAi technique is relatively new so the duration of gene suppression by shRNA has not been well documented. In order to attain stable *Prnp* knockdown in our experiments, a polymerase III H1 promoter driven retroviral expression vector was used to deliver shRNA to the cells. With this system, the shRNA integrates into the host cell genome and produces persistent knockdown compared to chemically synthesised siRNAs, which are delivered directly to the cytoplasm and only provide transient knockdown (Jia et al., 2006). This retroviral-based shRNA delivery system also overcomes the problem of knocking down expression of proteins with long half-lives because siRNA is persistently transcribed to degrade target mRNA; fortunately the half-life of PrP^C is short at five hour (Daude et al., 2003). To further ensure stable *Prnp* shRNA expression, cells were constantly maintained in selection antibiotics. However, despite taking these steps the qRT-PCR data on the human PrP^C-expressing *Prnp* KO clones (**figure 4.29**) suggested *Prnp* mRNA levels had slightly increased after the *Prnp* KO clones had been in culture for three months. Stability of *Prnp* knockdown observed here is consistent with duration of stable knockdown reported in the literature; shRNA-induced GFP knockdown by a

U6-driven lentiviral vector is stable for three months *in vitro* (Makinen et al., 2006)

4.5.2 Reconstitution of murine PrP^C restores susceptibility to RML prions

Reconstitution of murine PrP^C to wildtype expression levels restored susceptibility of *Prnp* KO PK1 clones to RML prion infection confirming that PrP^C is crucial for prion infection (Bueler et al., 1993;Fischer et al., 1996). However, susceptibility to RML prions was fully restored to PK1 wildtype levels only in two clones (P8a and P8b), despite all clones having similar PrP^C expression levels (all were overexpressing except P8a, which expressed to wildtype level). This finding that the level of PrP^C expression is not related to susceptibility to prion infection corroborates previous work (Montrasio et al., 2001;Enari et al., 2001) and confirms that additional factors contribute to cellular prion susceptibility (discussed below). Since it was expression of the ORF of the murine *Prnp* gene that restored susceptibility to RML prions, the non-coding sequences of the *Prnp* gene do not seem critical determinants of prion susceptibility. This may be a prion strain-specific observation since in a genetic study of the *PRNP* locus, one polymorphism identified upstream of exon 1 was associated with susceptibility to sCJD (Mead et al., 2001;Vollmert et al., 2006). The identification of genetic susceptibility factors to human prion disease, outside of the *PRNP* locus, has been seriously hampered by small sample sizes, due to the rarity of prion disease and the lack of technology for a true genome-wide study (although this technology has recently become available). A putative association of vCJD and the HLA-DQB7 serogroup (Jackson et al., 2001) has not been replicated in a larger study (Pepys et al., 2003).

The murine PrP^C reconstitution study presented here was a crucial proof-of-principle experiment, which suggested that the ectopic expression of the PrP ORF in *Prnp* KO PK1 cells may confer susceptibility to prions. Thus, in much the same way as for PrP KO mice (Weissmann and Flechsig, 2003), expression of different species of PrP ORF in *Prnp* KO PK1 cells may provide a permissive cell system for the propagation different prion strains, such as sCJD, inherited CJD, BSE and hamster prions. These PrP ORF reconstitution experiments in *Prnp* KO PK1 cells are currently being pursued in the department and would provide a much more rapid way of studying prion propagation. Overexpression of a truncated murine PrP construct (residues 89-231) in *Prnp* KO PK1 cells has been shown to restore their susceptibility to RML mouse prions (Jat, unpublished data), supporting similar work in PrP KO mice implying that the N-terminus of PrP^C is not critical for prion propagation (Shmerling et al., 1998;Flechsig et al., 2000).

4.5.3 Human PrP^C expression does not render *Prnp* KO cells susceptible to vCJD prions

To eliminate the transmission barrier for vCJD prion propagation in PK1 *Prnp* KO cells, human *PRNP* (129 MM) ORF was ectopically expressed in *Prnp* KO clones so that donor and recipient PrP sequence were identical. A high degree of sequence homology between the infecting PrP^{Sc} and resident host PrP^C is often, but not always, crucial for efficient prion replication (Prusiner et al., 1990;Priola and Chesebro, 1995). A single siRNA *Prnp* KO clone overexpressing human PrP^C to twice wildtype level (P8bH2) was isolated. FACS sorting of this clone resulted in the isolation of a four-fold overexpressing human PrP^C clone (P8bH4). Indeed, this approach in transgenic mice, in which the human *PRNP* 129 MM transgene is overexpressed to 2 and 4-fold wildtype level on a murine *Prnp* KO background, has successfully generated mice that are susceptible to vCJD prions (Tg35 and Tg45 strains; (Asante et al., 2002). 100% of these mice become infected with vCJD prions, indicated by the detection of type 4 PrP^{Sc} distributed as florid plaques in the brain. However, they do not exhibit clinical signs of prion disease in their normal lifespan (Asante et al., 2002); a recently recognised phenomenon referred to as subclinical infection which may result from the lack of PrP^L (the lethal intermediate of PrP; (Hill et al., 2000). In this chapter, the two-fold human PrP^C overexpressing line (P8bH2) proved the most susceptible to vCJD prion infection with two different inocula. There appeared to be short-term *de novo* production of vCJD prions for one passage. Four-fold overexpression of human PrP^C in this clone did not enhance susceptibility to vCJD prions; instead it reduced susceptibility. The double siRNA *Prnp* KO clones overexpressing human PrP^C were not susceptible to vCJD prion infection. In summary, the strategy of generating a human transgenic N2a-derived cell line, by knocking out endogenous murine PrP^C and ectopically expressing human PrP^C, failed to produce a susceptible cell line that *stably* propagated vCJD prions. There are a number of reasons why this might have occurred.

First, the fact that PK1 *Prnp* KO cells do not propagate human prions once the transmission barrier has been eliminated raises important issues with regard to cellular susceptibility factors and prion strains. The data presented here support several lines of evidence (including the fact that full length PrP^C alone has been refractory to infectious prion conversion in cell-free reactions), which strongly suggest PrP^C is insufficient to allow prion replication and that other factors may be involved. It was Stanley Prusiner who first conjectured the existence of a molecular chaperone for prion conversion and named it protein X (Telling et al., 1995). Its identity is still unknown but a number of candidate molecules have since been proposed. Recently polyanionic polymers, such as nucleic acids and sulphated glycosaminoglycans, have gained favour. Host-derived small RNA molecules have been shown to stimulate PrP^{Sc}

formation *in vitro* and RNAase enzymes abolish this effect (Deleault et al., 2003). This finding supports Weissmann's "unified prion theory" (Weissmann, 1991), which represents an alternative to the "protein-only hypothesis" and postulates a small host-encoded nucleic acid, named a co-prion, is associated with PrP^{Sc}. Sulphated glycosaminoglycans (GAGs), particularly those involving heparan sulphate (HSPG), can also stimulate *in vitro* prion conversion (Wong et al., 2001) and have been implicated in PrP^{Sc} biosynthesis and PrP^{Sc} uptake in cell lines (Ben Zaken et al., 2003;Hijazi et al., 2005;Horonchik et al., 2005). The demonstration that the LDL-related receptor protein (LRP1) internalises scrapie-associated fibrils and is also a key interactive partner for PrP^{C} endocytic trafficking (Taylor and Hooper, 2006) has led to the suggestion that this transmembrane receptor may be the scaffold that brings both PrP^{C} and PrP^{Sc} together for conversion on neurons (C.Parkyn, Kings College London, personal communication). Due to the different sites identified for interacting molecules on PrP^{C}, it has been hypothesised that multi-component protein complexes may be involved in PrP^{C} conversion (Caughey and Baron, 2006). One such complex may include the 37 kDa/67 kDa laminin receptor and its precursor (LRP/LR), which can both bind PrP^{C} and take part in PrP^{Sc} formation in scrapie-infected lines (Morel et al., 2005;Vana and Weiss, 2006). This complex may also include the above-mentioned HSPG, which can bind LRP/LR (Hundt et al., 2001) and copper, which participates in HSPG binding to PrP^{C} (Gonzalez-Iglesias et al., 2002) and hence may bring PrP^{C} and PrP^{Sc} together to mediate prion conversion. However, definitive evidence for this is still lacking. Therefore, it may be that these *Prnp* KO cells may, for some reason, lack critical factors for human prion conversion. However, because the PK1 cell line is a highly murine prion-susceptible line, permissive to RML (Klohn et al., 2003a) and 22L mouse prions (Professor C.Weissmann, unpublished data), one may assume that they do, in fact, possess the critical conversion factors for mouse prion propagation, but not human prion conversion.

Therefore, the second reason that the human PrP^{C}-expressing *Prnp* KO cells may be resistant to human prion propagation is that these conversion factors were "knocked out" in the *Prnp* KO clones due to off-target effects of *Prnp*-specific siRNA. Off-target effects are a commonly reported problem with the RNAi technique. These occur when the siRNA targets unrelated genes with only partial sequence complementarity. The technologies available for the selection of effective siRNA attempt to minimise off-target effects, for example by performing a Blast-search on the sequence, but these steps still do not completely eliminate off-target effects (Pei and Tuschl, 2006). Since off-target effects are more likely with two siRNA molecules, this may explain why the double siRNA *Prnp* KO clones were more resistant than single siRNA *Prnp* KO clones to both RML and vCJD prions; the conversion factors are more likely to have been silenced. However, this is doubtful because susceptibility is mostly restored by murine PrP ORF reconstitution whilst the siRNA knockout system is operating.

Third, these prion conversion factors may be prion strain-specific. At the start of this project it was initially hypothesised that N2a and PK1 cells possess "prion-propagating cellular machinery" and that human PrP^C would be able to hijack this machinery for the formation of vCJD prions. However, human PrP^C may not bind murine prion conversion factors with sufficient affinity to achieve efficient human PrP^{Sc} formation; particularly because human PrP^C differs from murine PrP^C at the putative protein X binding site at the C-terminus by five amino acids (Telling et al., 1995). Therefore, the affinity of PrP^C for protein X, or cofactors for prion conversion, may also underlie the prion transmission barrier. However, because human prions can be efficiently propagated in human transgenic mice (*Prnp-/-, PRNP* 129 MM +/+), this is unlikely to account for the absence of stable vCJD prion propagation observed in these cells.

Fourth, the fact this strategy (*Prnp* KO and human PrP 129 MM expression) allows vCJD prion propagation in human transgenic mice but not cells, strongly suggests that one of the principal reasons for the inability of PK1 cells to propagate vCJD prions is the nature of the cell system. The dynamic susceptibility model (outlined in **chapter 3**) would predict that these PK1 *Prnp* KO cells are resistant to prion infection simply because the degradation rate of PrP^{Sc} exceeds the formation rate (Weissmann, 2004). It may be that vCJD prions are more sensitive than RML prions to murine proteases, which would speed up vCJD prion degradation. Indeed, different prion strains have distinct susceptibility to proteinase K digestion (Kuczius et al., 1998). Alternatively, vCJD prion synthesis may be slower because conversion is less efficient with murine cell factors, as mentioned above. These two possibilities are not mutually exclusive.

Fifth, the importance of eliminating murine PrP^C expression to prevent dominant negative inhibition of human prion propagation has already been highlighted. However, the maximal murine PrP^C KO achieved in the cells screened for susceptibility to vCJD prions was between 90-99%, meaning there was between 1-10% murine PrP^C remaining. There is also suggestion from the qRT-PCR data presented here that murine PrP^C expression may have increased to more than this level in the human PrP^C-expressing KO clones. Thus, this residual murine PrP^C may well have been sufficient to inhibit vCJD prion propagation and seems like another very likely reason for the lack of vCJD prion susceptibility observed; particularly because in transgenic mice even 5-10% expression of endogenous murine PrP^C compared to human PrP^C (V129) expression can inhibit human PrP^{Sc} formation (sCJD) (Telling et al., 1995).

Chapter 5

Development of a vCJD prion-propagating cell line from a human foetal neural stem cell line

5.1 Introduction

Stem cells, by definition, possess twin properties; the capacity for extended self-renewal in an undifferentiated state and the capacity to differentiate into specialised cell types, a property known as potency. Embryonic stem (ES) cells, which are derived from the inner cell mass of a blastocyst stage embryo (4-5 days old in humans), are pluripotent. They can develop into any cell type generated from the three primary embryonic germ layers (ectoderm, mesoderm and endoderm); that is, any cell in the body except the placenta. As ES cells develop they become more restricted in their potential, generating only a defined set of cell types. Neural stem cells (NSC) are multipotent primary progenitors, found in the embryonic, foetal and adult mammalian brain, which give rise solely to cells of neural lineage: neurones, astrocytes and oligodendrocytes (Davis and Temple, 1994;Gritti et al., 1996;Weiss et al., 1996;Vescovi et al., 1999;Johansson et al., 1999;Nunes et al., 2003). It is possible to propagate NSC *ex vivo* and this has proved critical in improving the understanding of mechanisms controlling developmental decisions in NSC (reviewed in McKay, 1997;Gage, 2000;Nunes et al., 2003;Galli et al., 2003), the development of cell replacement therapies for neurological diseases (Lindvall et al., 2004) and the development of disease models (De Filippis et al., 2006). NSC lines are a versatile *in vitro* model system. Using chemically defined media containing mitogens, they can be cultured as undifferentiated self-renewing stem cells, either as an adherent monolayer or as neurospheres (non-adherent spherical aggregates of neural precursor cells; (Uchida et al., 2000). Alternatively, reflecting their stem cell nature, they can be differentiated into a mixture of neurones and glia by mitogen withdrawal or exposure to extrinsic factors. Factors for directed differentiation towards a specific neural cell lineage have also been established, for example, ciliary neurotrophic factor (CNTF) induces astrocyte differentiation of NSC (Weiss et al., 1996;Johe et al., 1996;van der and Weiss, 2000).

This chapter details the investigation of the 197 human foetal neural stem cell line (ReNcell 197VM; ReNeuron Ltd., UK) for susceptibility to human vCJD prion infection. These human NSC terminally differentiate into cells resembling primary neurones and glia. Therefore it was hypothesised they may be permissive to vCJD prions because they recapitulate the human brain much better than any CNS tumour cell line, potentially providing the necessary factors for prion propagation. Furthermore, chronic propagation of several mouse prion strains has recently been reported in CNS stem cell-derived cultures, including differentiated mouse foetal and adult NSC (Milhavet et al., 2006) and mouse embryonic neurospheres (Giri et al., 2006).

5.2 Aims of this study

- To determine the suitability of the ReNcell 197VM human foetal neural stem cell line (referred to throughout as 197 cells) for infection with vCJD prions by characterising *PRNP* codon 129 genotype and PrP^{C} expression levels.
- To optimise conditions for the vCJD prion infection of 197 cells in both their undifferentiated and differentiated states.
- To investigate the susceptibility of the 197 cell line to vCJD prion infection in both undifferentiated and differentiated states.

5.3 Methods

197 NSC and PrP^{C}-null mouse embryonic neurospheres were cultured and differentiated as described in **2.2.4** and **2.2.5**, respectively. The *PRNP* genotype of the 197 cell line was determined using DNA sequence analysis (**2.3.7**) and PrP^{C} expression levels were assessed by immunoblotting (**2.6.2**). Undifferentiated 197 cells were infected with vCJD prions using the standard infection procedure (**2.7.2**), whilst differentiating 197 cells were infected with semi-purified vCJD brain homogenate, as described in section **2.7.3**. The presence of PrP^{Sc} in cells was detected using either the SCA (**2.7.5.2**) or immunoblotting of PK-digested material (**2.6.2**).

5.4 Results

5.4.1 197 characterisation

197 cells are immortalised human foetal neural stem cell line derived from the ventral mesencephalon of an electively aborted 10-week human foetus (ReNeuron Ltd., UK; detailed in Hoffrogge et al., 2006). They were immortalised by overexpression of the v-myc oncogene and are karyotypically stable for more than forty-five passages (Dr. E.Miljan, ReNeuron Ltd., unpublished data). As proliferating 197 multipotent undifferentiated cells they appear morphologically as small polygonal cells with few processes (**figure 5.1A**). They were identified phenotypically as neural stem cells by positive staining for nestin (**figure 5.1C**), a member of the intermediate filament family present in undifferentiated cells of neuroepithelial origin (Lendahl et al., 1990). 197 NSC were reliably differentiated by removal of two growth factors; epidermal growth factor (EGF) and basic fibroblast growth factor (bFGF). Upon differentiation, cells adopted a predominantly neuronal phenotype; with shrunken cell bodies and extended neuritic processes, that lead to the formation of a complex dendritic lattice by day 14 (**figure 5.1B** and **D**). By immunofluorescence, the cultures were determined to comprise 80-90% βIII-tubulin-positive neurones (of which 10% were dopaminergic), with the remainder being predominantly astroglial (Dr. E.Miljan, ReNeuron Ltd.). Following 7-14 days

of differentiation, cells displayed a neuronal physiology with 25% of cells exhibiting voltage-gated sodium currents (**figure 5.2**) and firing action potentials (Dr R.Donato, in press BMC Neuroscience). Transmission electron microscopy indicated that differentiated 197 cells form synapses *in vitro*, with evidence of axonal transport of synaptic vesicles (Dr A.Wood-Kaczmar, unpublished data; **figure 5.3**).

5.4.2 Determining suitability of 197 cell line for vCJD prion infection

Since PrP^C is absolutely required for prion infection (Bueler et al., 1993), the 197 cell line was also analysed for PrP^C expression by immunoblotting, which showed substantial PrP^C expression in the 197 cell line that appeared to marginally increase following differentiation (**figure 5.4**). DNA sequence analysis of the *PRNP* locus demonstrated that the 197 NSC line was methionine homozygous at *PRNP* codon 129; this is the most susceptible genotype for vCJD *in vivo* (Collinge, 2005).

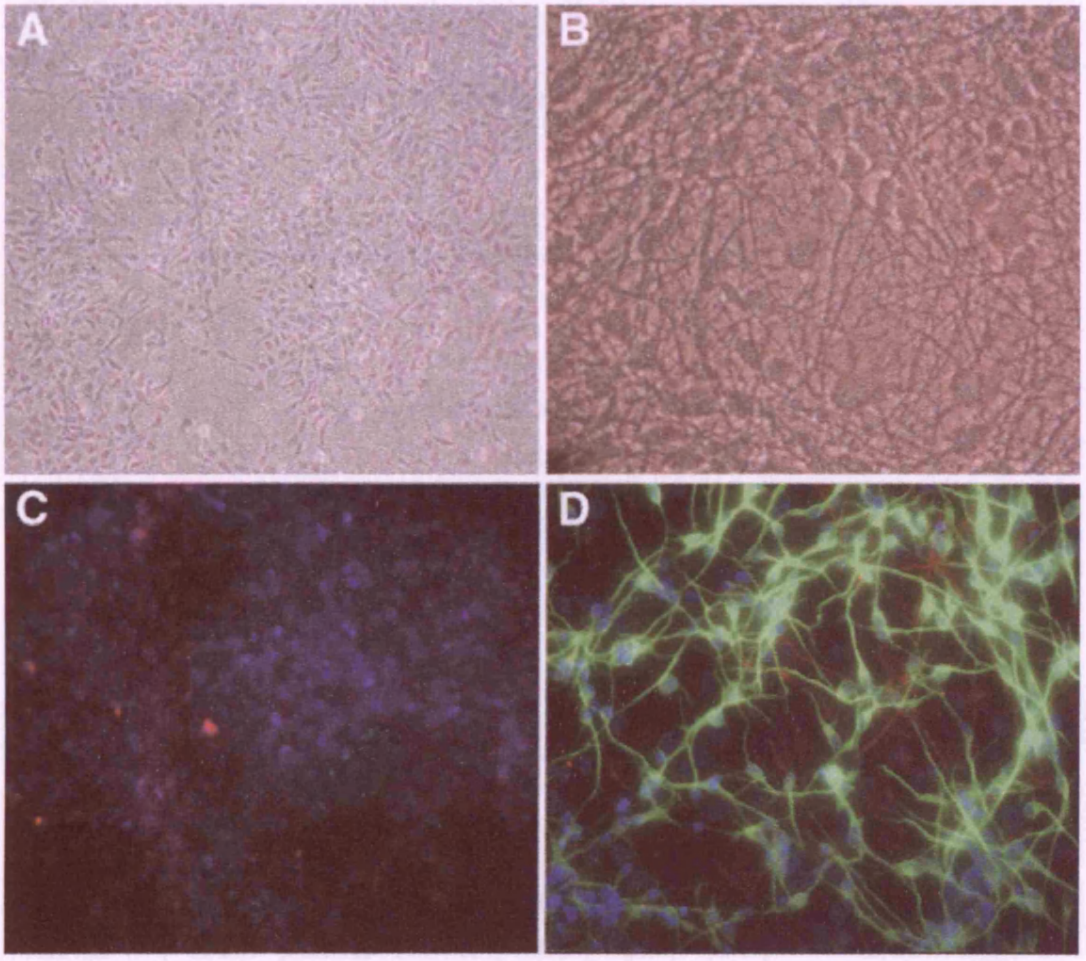

Figure 5.1 Morphology and phenotype of undifferentiated and differentiated 197 cells

(**A**) By light microscopy, undifferentiated 197 cells displayed paving stone morphology and (**C**) by immunofluorescence stained positive for the CNS stem cell marker nestin (blue). Rare spontaneous differentiation of NSC into GFAP-positive astrocytes (red) appeared in the undifferentiated population. (**B**) 197 NSC were differentiated by removal of growth factors (EGF and bFGF) from the culture medium. After 14 days, cells had adopted a neuronal phenotype, in which neuritic processes extended from the rounded, shrunken cell bodies to form a complex dendritic lattice. (**D**) Immunofluorescence staining at day 14 differentiation showed a predominance of βIII-tubulin-positive neurones (green); a small number of GFAP-positive astrocytes (red) were also present. Nuclei were visualised with Hoechst (blue). *Images C and D were produced by Dr. E. Miljan, ReNeuron Ltd., UK.*

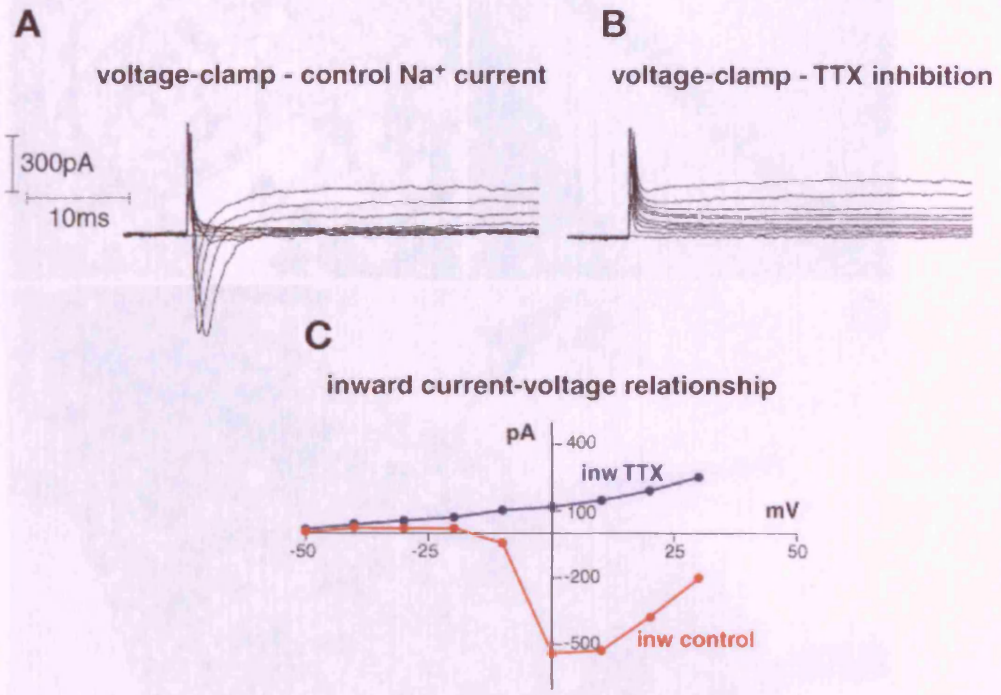

Figure 5.2 Neuronal physiology of differentiated 197 cells

(**A**) Incremental voltage steps of 10mV (between -20mV and +20mV) activated a fast inward current in 7 to 14-day differentiated 197 cells. (**B**) This inward current was abolished in the presence of a voltage-gated sodium (Na^+) channel blocker (0.6 µM tetrodotoxin, TTX), indicating it was mediated by the type of Na^+ channels that underlie the generation of action potentials. (**C**) Inward current-voltage relationship in control differentiated 197 cells with and without exposure to TTX. *Data produced by Dr R. Donato, UCL.*

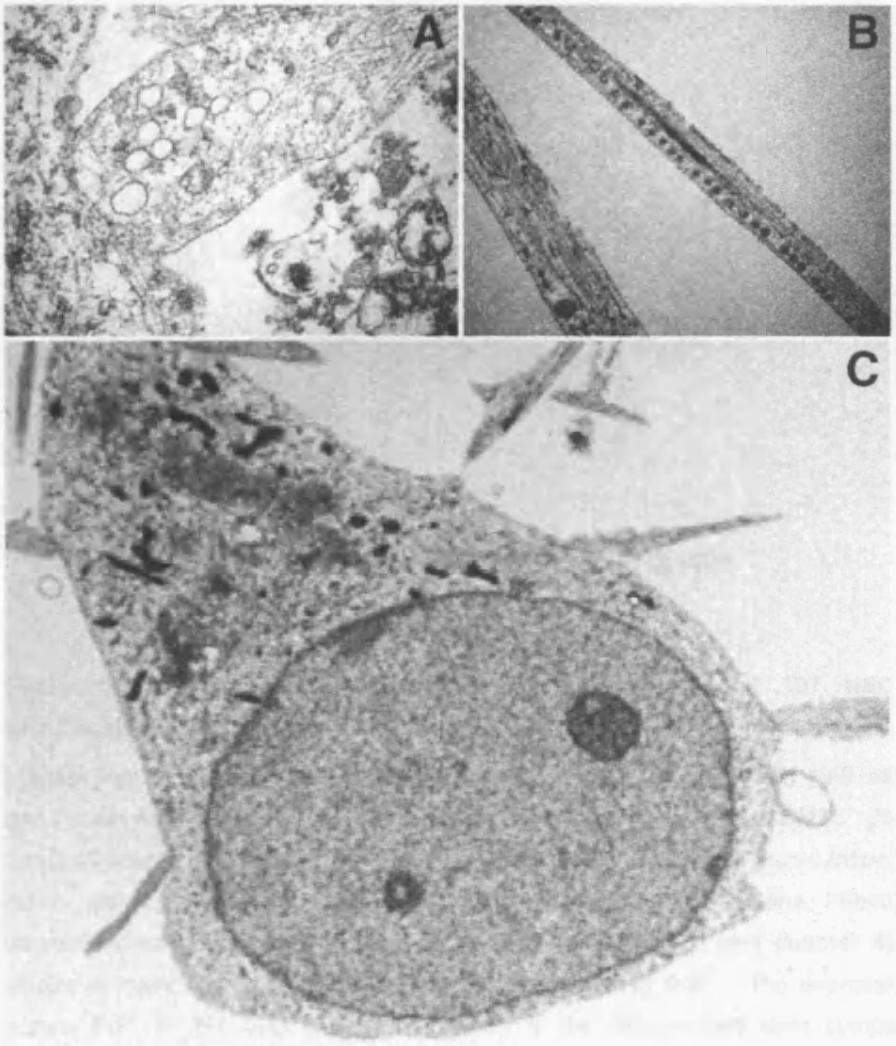

Figure 5.3 Ultrastructure of 197 neurones

Transmission electron microscopy shows (**A**) that 197 neurones can form synapses *in vitro*, as demonstrated by the accumulation of vesicles in the pre-synaptic terminal, parallel membranes and post-synaptic densities; (**B**) axonal transport of vesicles; (**C**) higher magnification cross-section through an axon transporting vesicles. *Data produced by Dr A. Wood-Kaczmar, Institute of Neurology, UCL*

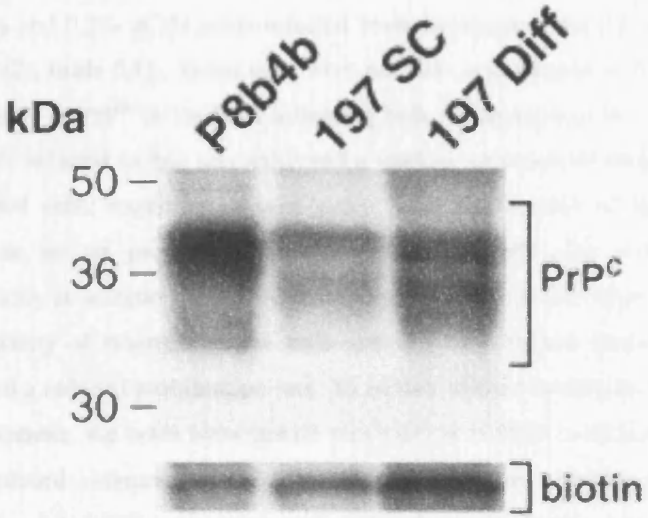

Figure 5.4 Endogenous PrP^C expression in human foetal 197 NSC in both undifferentiated and differentiated states

Lysates from undifferentiated 197 cells (197 SC), differentiated (day 14) 197 cells (197 diff) and P8b4b were immunoblotted using anti-PrP antibody, biotinylated ICSM35. 25 µg protein from cell lysates was loaded. PrP^C ran between ~50-30 kDa in its 3 glycosylation states (di-, mono- and un-glycosylated). Compared to the positive control cell line, P8b4b, a mouse neuroblastoma cell line that highly overexpresses human PrP^C (see **chapter 4**), 197 cells displayed lower, but still substantial expression of human PrP^C. The expression level of human PrP^C in 197 cells was slightly higher in the differentiated state compared to the undifferentiated state even taking into account the fact that the differentiated lane was overloaded, as indicated by the non-specific biotin band.

5.4.3 vCJD prion infection of human undifferentiated 197 cells

Undifferentiated 197 cells were initially infected according to the standard protocol (see **2.7.2**) with 2% and 0.2% vCJD prion-infected brain homogenate for 72 hours (infection conditions (1) and (2), **table 5.1**). These cells were not able to propagate vCJD prions as determined by the absence of PrP^{Sc} in the SCA following bulk passaging (see low SCA values in **table 5.1**). The cells infected in this way exhibited a marked reduction in proliferation rate compared to uninfected cells; requiring passage every 7-10 days instead of the usual every other day. Moreover, on six previous attampts, cells died shortly after vCJD prion infection. The cytotoxicity at infection appeared to be due to factors in the brain homogenate itself, rather than toxicity of prions, because cells infected with normal human brain homogenate also exhibited a reduced proliferation rate. To reduce soluble toxicity by factors, such as cytokines and glutamate, the brain homogenate was washed in PBS (as described in section **2.7.3.2.1**), and reduced concentrations were used (infection conditions (3)-(5), **table 5.1**). Undifferentiated 197 cells grew well under these conditions, but still did not demonstrate vCJD prion propagation as determined by the absence of PrP^{Sc} in the SCA. To further purify the vCJD inoculum, it was treated with lysis buffer in a process termed "semi-purification" (described in **2.7.3.2.2**) and cells were infected at 0.01% brain homogenate (infection condition (6), **table 5.1**). However, although cells remained mostly healthy under these conditions, they were not susceptible to vCJD prion infection. In summary, undifferentiated 197 cells were unequivocally unable to propagate vCJD prions.

Infection condition	vCJD inoculum preparation	vCJD inoculum concentration (%)	Passage # (and ratio) post-vCJD infection	Mean SCA value (+ SEM)	Comments on cell viability
(1)	crude	2	5^{th} (1:3)	3.4 (+1.4)	Significantly slowed cell proliferation; duration of experiment was 50 days post-infection
(2)	crude	0.2	5^{th} (1:3)	1.9 (+5.1)	Slowed proliferation; as above
(3)	washed-crude	0.1	4^{th} (1:3)	0.1 (+0.7)	Normal proliferation
(4)	washed-crude	0.01	4^{th} (1:3)	1.6 (+1.6)	Normal proliferation
(5)	washed-crude	0.001	4^{th} (1:3)	0.0 (+0.8)	Normal proliferation
(6)	semi-purified	0.1	3^{rd} (1:4)	0.3 (+1.2)	Normal proliferation; duration of experiment was 5 days post-infection

Table 5.1 vCJD prion infection of undifferentiated 197 cells

Summary of scrapie cell assay (SCA) data for vCJD prion infection of undifferentiated 197 cells. "Crude" indicates the brain homogenate was prepared in PBS (see **2.7.1**), "washed-crude" represents a rinse in PBS (see **2.7.3.2.1**) and "semi-purified" involved a detergent incubation step (see **2.7.3.2.2**). Passage number (#) post-vCJD prion infection at the time of the SCA is given as well as the passage ratio, indicating the inoculum is likely to have been diluted out. SCA values (minus mean uninfected 197 NSC background value) are given plus standard error of mean (SEM). SCA values were extremely low, indicating an absence of PrP^{Sc} in the 197 cells and that they were unable to propagate vCJD prions.

5.4.4 vCJD prion infection of human differentiated 197 cells

Previous published data shows that whilst mouse undifferentiated NSC are resistant to mouse prion infection, differentiation of the cultures renders them more susceptible such that they are able to chronically propagate three strains of mouse prions (Milhavet et al., 2006). Based on this work and the close resemblance of differentiated 197 cells to cells in the human brain *in vivo*, the susceptibility of differentiated human NSC to vCJD prion infection was investigated.

5.4.4.1 Optimisation of vCJD prion infection and PrP^{Sc} screening for differentiated 197 cells

Optimisation of vCJD prion-infected brain homogenate preparation

Since differentiated NSC cultures are post-mitotic, the vCJD prion-infected inoculum could not be cleared from the differentiated cultures merely by passaging. Therefore, a partial purification step termed "semi-purification" (modified from Milhavet et al., 2006) involving incubation with a lysis buffer was employed to clarify the vCJD prion-infected brain homogenate (see **2.7.3.2.2**). This step lysed the cells and disaggregated the brain homogenate, to minimise it sticking to the cultures and to increase the number of infectious seeds, but critically not to reduce infectivity (since PrP^{Sc} is partially detergent resistant). Cells were exposed to semi-purified vCJD brain homogenate for 96 hours at differentiation day 0-4 and assayed for PrP^{Sc} approximately every 5-10 days by SCA or immunoblotting.

Optimisation of vCJD prion particle monitor control

In order to distinguish PrP^{Sc} in the inoculum from active cellular prion replication, a particle monitor control stem cell line was used. Initially, PrP^{C}-null FVB mouse embryonic neurospheres were differentiated on laminin (these are described in **2.2.5**) and used as the particle monitor cell line. Due to their lack of PrP^{C} expression they are resistant to any form of prion infection (Milhavet et al., 2006). However, this cell line has disadvantages. It was derived from a different species (mouse) to the human 197 cell line and most likely has a different cellular composition as neurospheres are reported to differentiate more readily into astrocytes than neurones *in vitro* (Morshead et al., 2002), whereas the differentiated 197 cells were predominantly neuronal. Therefore, following the preliminary experiments, a more relevant particle monitor was devised. This involved the use of an anti-PrP antibody to treat the vCJD prion infected differentiated 197 cells. Anti-PrP antibody treatment inhibits prion replication in cells by sequestering cell surface PrP^{C} and preventing its conversion to PrP^{Sc} (Enari et al., 2001). This particle monitor strategy was validated by the demonstration that

ICSM18 anti-PrP antibody treatment for five days cured chronically RML prion-infected PK1 cells (iPK1), but did not clear residual brain homogenate from prion-resistant PrP^{C}-null differentiated mouse NSCs exposed to vCJD prions (**figure 5.5**).

Optimisation of Proteinase K (PK) concentration for digestion of PrP^{C} in differentiated 197 cell lysates for immunoblotting

Lysates prepared from uninfected, differentiated (day 14) 197 cells were incubated with PK (for 37°C, 30 minutes) at 2.5 and 5 µg/mg protein. 2.5 µg/mg PK almost completely digested PrP^{C} bands in uninfected 197 differentiated cultures, but 5 µg/mg PK fully digested the host PrP^{C} (**figure 5.6**). To be confident that PrP^{C} was completely digested in the differentiated 197 cells, 5 µg/mg PK concentration was selected for subsequent experiments.

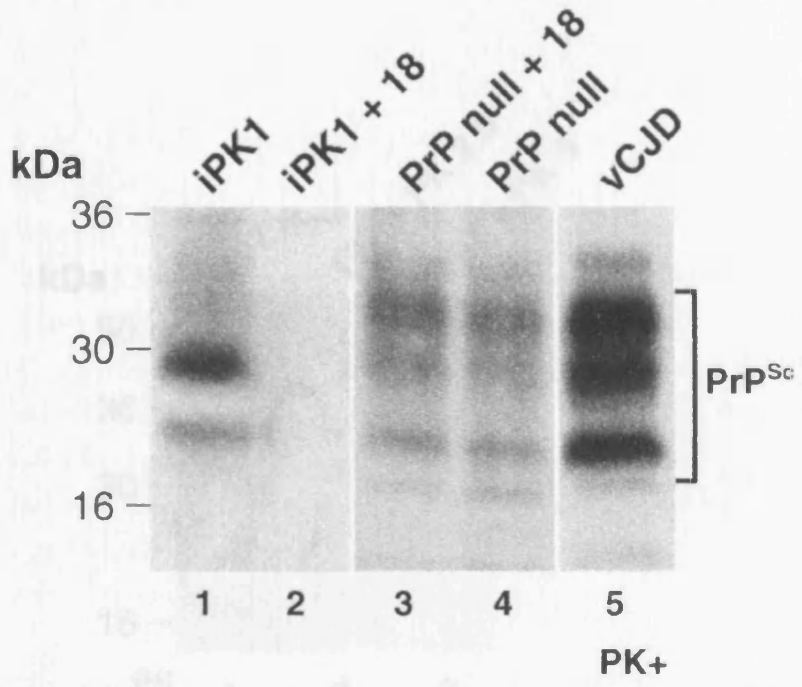

Figure 5.5 Validation of anti-PrP antibody curing of prion-propagating cells as a particle monitor for vCJD prion infections of differentiated 197 cells

Chronically RML prion-infected PK1 (iPK1) cells and 0.1% vCJD prion-exposed PrP^{C}-null differentiated NSC (PrP null; 29 days post-infection) were treated with 5 µg/ml ICSM18 anti-PrP antibody (18) for 5 days. Cell lysates were prepared, PK digested (5 µg/mg protein) and immunoblotted (25 µg protein) for PrP^{Sc} using anti-PrP antibody, biotinylated ICSM35. PK digested (10 µg/mg) vCJD prion-infected brain homogenate (25 µg protein) was run alongside as an immunoblotting positive control for PrP^{Sc} (lane 5). Three bands representing the three glycosylation states of PrP^{Sc} (di-, mono-, and unglycosylated) were observed between 33-16 kDa. iPK1 cells propagate mouse RML prions, comprising mainly monoglycosylated PrP^{Sc} (middle band ~27 kDa), whereas vCJD prions are mainly diglycosylated (top band ~32 kDa). iPK1 cells were cured of prion infection after ICSM18 treatment (lane 2) compared to untreated cells (lane 1). PrP^{Sc} levels in prion-resistant PrP^{C}-null cells exposed to vCJD prion-infected brain homogenate (lane 4) were unaffected by ICSM18 treatment (lane 3), demonstrating that the antibody treatment specifically cures prion-propagating cells, but does not induce a clearing of brain homogenate from the cultures.

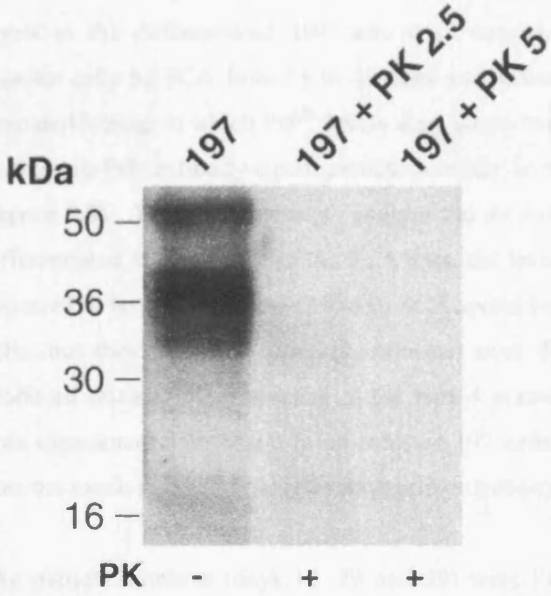

Figure 5.6 Determination of optimal PK concentration to digest PrP^C in differentiated 197 cells

Cell lysates of differentiated (day 14) 197 cells were digested with PK at 0, 2.5 and 5 µg/mg protein. 50 µg protein was loaded per lane and samples were immunoblotted for PrP^C using anti-PrP antibody, biotinylated ICSM35. PrP^C remained in the PK-untreated sample (197) and ran characteristically between ~50-30 kDa. Very faint bands remained in the differentiated 197 sample digested with 2.5 µg/mg PK (197 + PK 2.5) but 5 µg/mg PK protein appeared to completely digest PrP^C (197 + PK 5).

5.4.4.2 Chronic vCJD prion infection in differentiated 197 cultures

Exposure of differentiating 197 cells to 0.1% semi-purified vCJD inoculum resulted in chronic and stable vCJD prion infection of the cells as determined by SCA and immunoblot. PrP^{Sc} levels in the differentiated 197 cells were consistently higher than the PrP^{C}-null particle monitor cells by SCA from 15 to 49 days post-infection (**figure 5.7**). This was replicated by immunoblotting, in which PrP^{Sc} levels were consistently higher in differentiated 197 cells than in the anti-PrP antibody-cured particle monitor controls from 12 to 39 days post-infection (**figure 5.8**). These data strongly suggest the *de novo* production and replication of PrP^{Sc} in differentiated 197 cells. From the SCA data, the levels of *de novo* PrP^{Sc} produced in the cells appeared to be relatively low (250-550 SCA spots) compared to mouse prion-propagating PK1 cells, but they remained relatively constant over the course of the experiment. The PrP^{Sc} produced retained the properties of the type 4 prions characterised by vCJD (**figure 5.9**). In both experiments, the vCJD prion-infected 197 cells died earlier (40-50 days post-infection) than the mock-infected cells (80+ days post-infection).

The particle monitors (days 12, 29 and 39) were PrP^{Sc}-positive throughout the immunoblot experiment, indicating that some PrP^{Sc} from the original inoculum remained in the cultures. The SCA experiment indicates about one third of the inoculum (about 400 spots) appeared to be cleared by media changes over the course of the 49-day experiment.

Across the data, it appears that there was variation in the amount of PrP^{Sc} delivered to the wells at the time of infection. This is exemplified by the particle monitor in the immunoblot experiment; at day 20 it was clear, but PrP^{Sc} was then detected at day 29 (**figure 5.8**). This may be explained by the total amount of protein loaded in each experiment. However, equal amounts of protein from antibody-treated and untreated samples were loaded at each time-point, verified by Coomassie staining of the polyacrylamide gels (see section **2.6.3.4**). It was not possible to show equal protein loading by stripping the blots and reprobing for β-actin because the samples had been PK-digested. The "reappearance" of the particle monitor was unlikely to result from lack of antibody-curing efficacy, since each antibody batch was tested on iPK1 cells and freeze-thawing was avoided. Optimising the homogeneity of the inoculum preparation required further work.

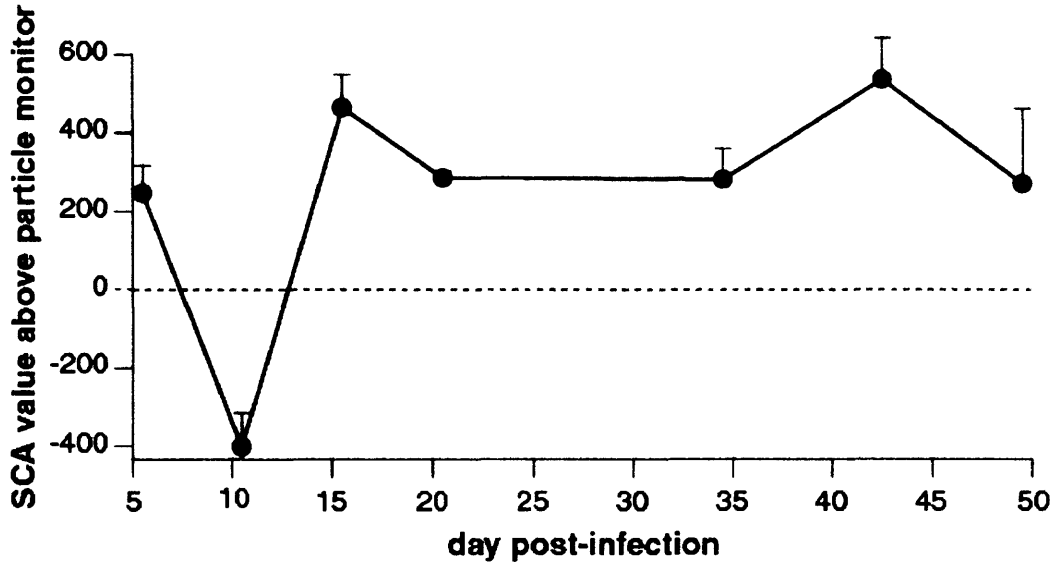

Figure 5.7 *De novo* production of PrP^{Sc} in vCJD prion-infected differentiated 197 cultures

197 NSC, at 60% confluency, on differentiation day 0, were prion infected with 0.1% semi-purified vCJD inoculum (I2811) for 96 hours. Mouse PrP^{C}-null differentiated NSC were infected in parallel as the particle monitor. Data are presented as mean SCA value (PrP^{Sc}-positive spots) for vCJD prion-infected 197 cultures minus mean particle monitor (+ SEM, n=8). Values above zero represent *de novo* PrP^{Sc} production in 197 cells. 197 cells appeared to clear more vCJD inoculum than the particle monitor cells at approximately day 10 post-infection, at which point the 197 cells started to actively replicate and accumulate *de novo* PrP^{Sc}. PrP^{Sc} remained at a steady level between day 15 and day 49 post-infection when the cells died, about 30 days earlier than mock-infected 197 cells. One-way analysis of variance (ANOVA) showed a significant difference in PrP^{Sc} levels in 197 cells and the particle monitor cells over the 7 time time points ($P<0.001$).

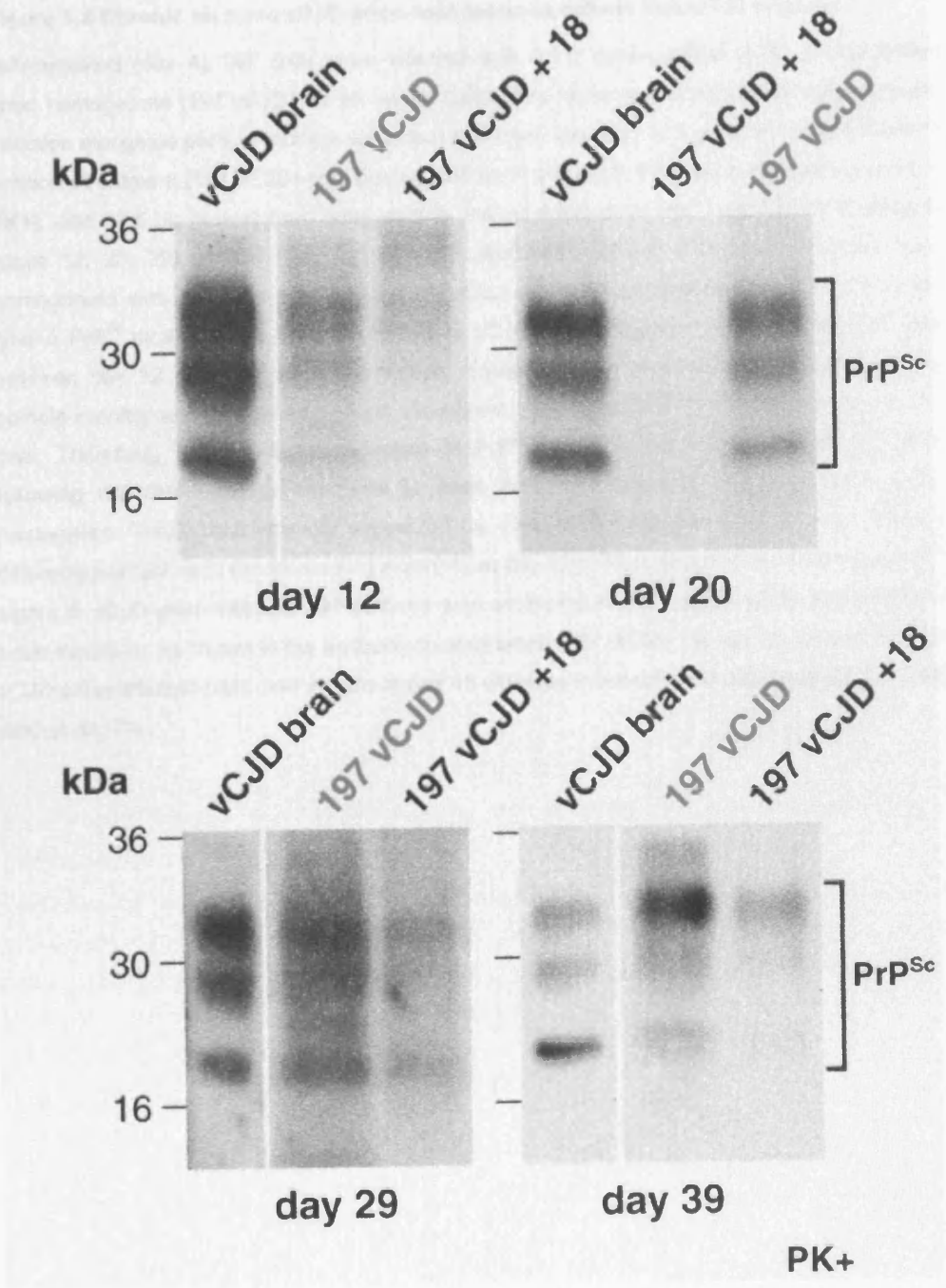
kDa
vCJD brain
197 vCJD
197 vCJD + 18
vCJD brain
197 vCJD + 18
197 vCJD
36
30
16
PrPSc
day 12
day 20
kDa
vCJD brain
197 vCJD
197 vCJD +18
vCJD brain
197 vCJD
197 vCJD +18
36
30
16
PrPSc
day 29
day 39
PK+

Figure 5.8 Chronic *de novo* vCJD prion replication in differentiated 197 cultures

Differentiated (day 4) 197 cells were infected with 0.1% semi-purified vCJD prion-infected brain homogenate (197 vCJD) for 96 hours. Cells were harvested at regular time-points post-infection alongside particle monitor wells that had been exposed to 5 days of 5 µg/ml ICSM18 antibody treatment (197 vCJD+18). Cell lysates were prepared, PK digested (5 µg/mg protein; PK+), and 37.5 µg protein from each sample immunoblotted for PrP^{Sc} with either ICSM35 B (days 12, 20, 29) or 3F4 (day 39) anti-PrP antibodies. 25 µg vCJD prion-infected brain homogenate was run as a positive control (vCJD brain) for each time-point. Diglycosylated type 4 PrP^{Sc} strain (which is characteristic of vCJD) was present in differentiated 197 cells between day 12 and day 39 post-infection. Equal amounts of protein were loaded in the particle monitor and 197 lanes at each time-point, determined by Coomassie staining of the gels. Therefore, the significant reduction in PrP^{Sc} levels in the vCJD-infected 197 cells following ICSM18 antibody treatment at each time-point indicates curing of active prion propagation. These data strongly suggested *de novo* prion synthesis in vCJD prion-infected differentiated 197 cells (lanes marked in red) from day 12 to 39 post-infection. Part of the PrP^{Sc} signal in vCJD prion-infected 197 cultures was attributed to the original vCJD prion-infected brain inoculum, as shown in the antibody-treated lanes (197 vCJD+18) day 12, 29 and 39. The vCJD prion-infected cells died *in vitro* at day 45 whereas mock-infected differentiated 197 cells died at day 80.

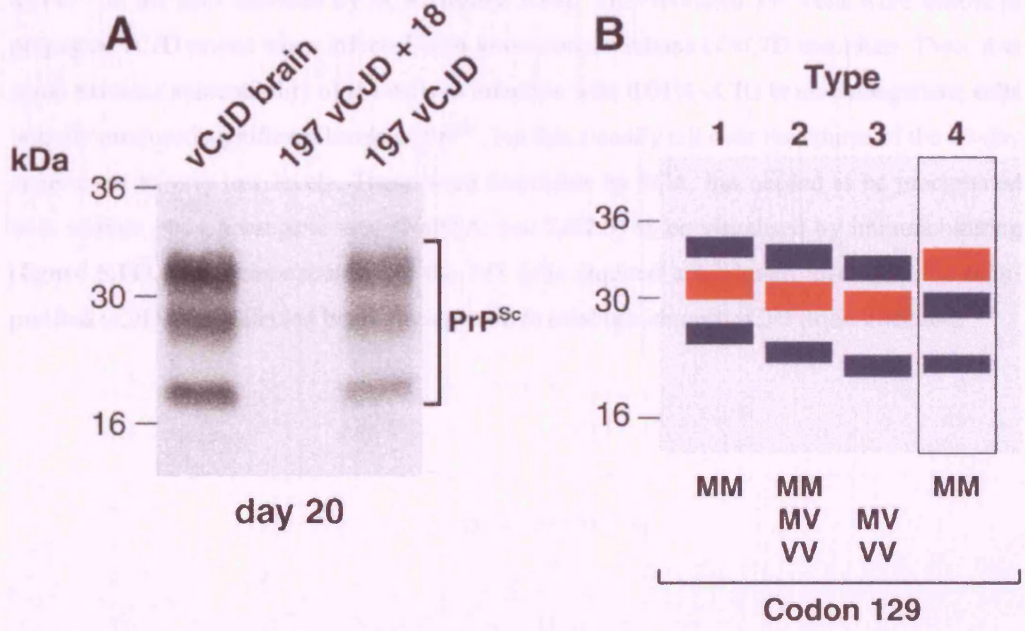

Figure 5.9 Following vCJD prion infection differentiated 197 cells propagate type 4 human prions

(**A**) Following infection with vCJD prions, differentiated 197 cells produce PrP^{Sc} characteristic of the type 4 strain type associated with vCJD prions. (**B**) Type 4 prions are predominantly diglycosylated (top band dominant) according to Hill's human prion strain classification system (Hill et al., 2003). This observation indicates that there is no cellular modification of the vCJD prion strain by 197 cells.

5.4.4.3 Determining susceptibility of differentiated 197 cells to vCJD prions

Differentiated 197 cells were exposed to a range of concentrations of semi-purified vCJD inoculum (0.01, 0.001 and 0.0001%) to assess their susceptibility to infection. Cultures were infected with vCJD prions according to the standard protocol (section **2.7.3**) and the presence of PrP^{Sc} in the cells assessed by SCA (**figure 5.10**). Differentiated 197 cells were unable to propagate vCJD prions when infected with lower concentrations of vCJD inoculum. There was some transient susceptibility of the cells to infection with 0.01% vCJD brain homogenate; cells initially produced significant levels of PrP^{Sc}, but this steadily fell over the course of the 23-day experiment to very low levels. These were detectable by SCA, but needed to be precipitated with sodium phosphotungstic acid (NaPTA; see **2.6.2.5**) to be visualised by immunoblotting (**figure 5.11**). This demonstrates that the 197 cells required a minimum level of 0.1% semi-purified vCJD prion infected brain homogenate to establish chronic vCJD prion infection.

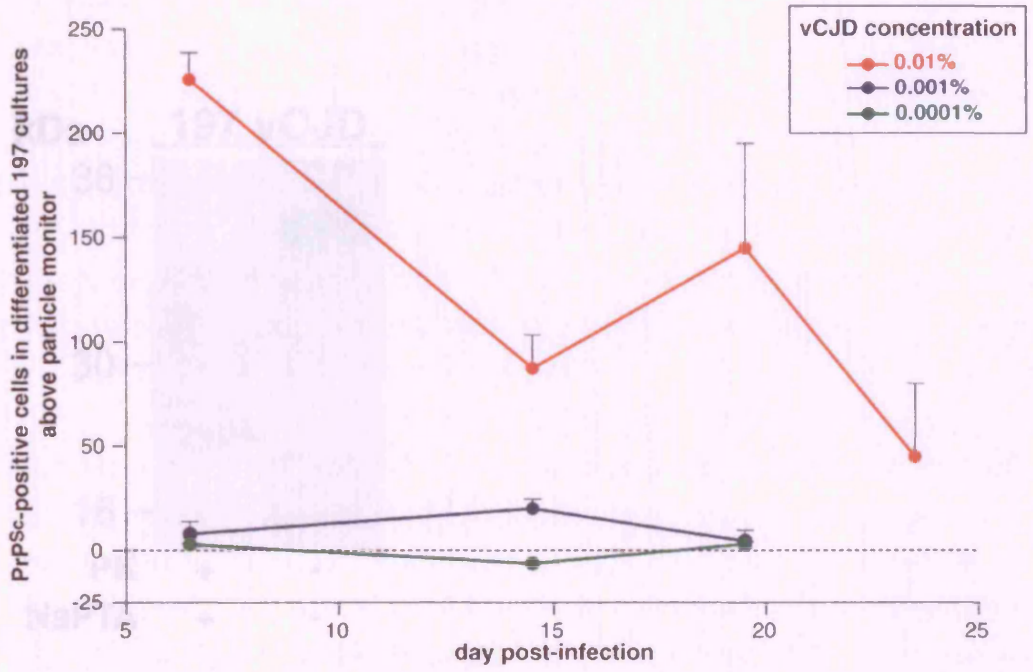

Figure 5.10 Susceptibility of human differentiated 197 cells to vCJD prion infection at lower inoculum concentrations

197 NSC, at 60% confluency, on differentiation day 0, were prion infected with 0.1, 0.001 and 0.0001% semi-purified vCJD inoculum (I2811) for 96 hours. Mouse PrP^{C}-null differentiated NSC were infected in parallel as the particle monitor. Data are presented as mean SCA value (PrP^{Sc}-positive spots) for vCJD prion-infected differentiated 197 cells minus mean particle monitor (+ SEM, n=8). Following infection with 0.001 and 0.0001% vCJD, PrP^{Sc} was barely detectable by SCA over 18 days post-infection. Following infection with 0.01% vCJD, there was more PrP^{Sc} in 197 cells at 6 days post-infection, but the level fell rapidly to insignificant levels over the course of the 23-day infection.

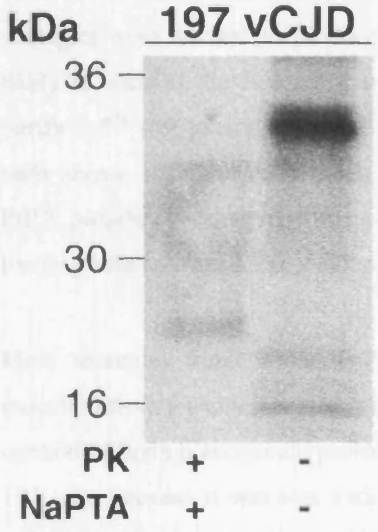

Figure 5.11 Detection of vCJD prions in differentiated 197 cells following infection with 0.01% vCJD prion-infected brain homogenate

Cell lysates were prepared from differentiated 197 cells infected with 0.01% vCJD prion-infected brain homogenate at 23 days post-infection. A single sample (60 µg) was run without PK digestion (right-hand lane). PrP^{Sc} was precipitated from the other sample (200 µg) using NaPTA precipitation followed by PK digestion (5 µg/mg protein; left-hand lane). Samples were immunoblotted for PrP using anti-PrP antibody, biotinylated ICSM35. PrP^{Sc} was only just detectable in the 197 cultures 23 days post-infection, following NaPTA precipitation (left-hand lane). The PrP band shift following PK digestion is indicative of PrP^{Sc}; cleavage of ~70 amino acids from the N-terminus of PrP^{Sc} caused it to migrate faster on the gel (~35 and 16 kDa) than the PK-undigested sample (which is composed of both PrP^{C} and full-length PrP^{Sc}).

5.4.4.4 Attempts to accelerate clearance of inoculum from differentiated 197 cells

It is evident from the experiments presented above that despite semi-purification of vCJD brain homogenate, washing the cells post-infection and 50% media changes every week, a low level of vCJD inoculum remained in the cultures when the cells died (day 39 and day 49). Simple strategies were devised to produce a clarified suspension of brain homogenate that was less likely to stick to the cultures, but also retain infectivity. It is important not to excessively purify PrP^{Sc} (for example by NaPTA precipitation), because membrane-associated PrP^{Sc} has been shown to infect cells much more efficiently than membrane-free detergent extracted PrP^{Sc}, possibly because membrane-associated PrP^{Sc} may more readily gain access to cells via binding with cell-surface receptors (Baron et al., 2006).

Most strategies tested reduced PrP^{Sc} levels, but none improved clearance of the vCJD inoculum from the cultures (see **table 5.2** for details). Therefore, the original semi-purification method of brain homogenate probably remains the best method for infecting the differentiated 197 cells because it was less toxic compared to crude brain homogenate and retained most infectivity. The low level residual inoculum in the vCJD prion-propagating cultures does not pose a problem for further experiments on the cell line since it should not affect most methods used to study cell biology.

5.4.5 Summary of results

The 197 human NSC line proved a suitable candidate for testing susceptibility to vCJD prion infection; it was methionine homozygous at codon 129 of *PRNP*, and expression levels of PrP^{C} in both undifferentiated and differentiated states were good. Crude human brain homogenate *per se* was toxic to undifferentiated 197 cells, but it was determined that they could tolerate lower concentrations of a "semi-purified" preparation of vCJD prion-infected brain homogenate. However, undifferentiated 197 cells did not propagate vCJD prions. Conversely, differentiated 197 cells that were predominantly neuronal were susceptible to infection with 0.1% dilution of vCJD semi-purified brain homogenate. They produced *de novo* PrP^{Sc} over approximately 50 days post-infection as demonstrated by both SCA and immunoblotting. Differentiated 197 cells appeared to undergo prion-induced cell death because vCJD prion-infected cells died about 30 days earlier than mock-infected cells. The fact that these differentiated neurones chronically and stably propagate vCJD prions will enable the study of the cellular pathophysiology of human prion disease.

vCJD inoculum preparation	Effect on PrP^{Sc} clearance from cultures
sonication (section **2.7.3.2.3**)	37% reduction in PrP^{Sc} at time of infection (SCA) and not cleared from culture at 29 days post-infection
filtration (through 5µm PVDF membrane)	40% reduction in PrP^{Sc} at time of infection (SCA) but not cleared from culture by 20 days post-infection
0.01% triton wash (at every media change)	no effect

Table 5.2 Strategies to clear vCJD inoculum from differentiated 197 cultures

A number of different strategies were attempted to clear residual vCJD inoculum from the cultures: semi-purified vCJD brain homogenate was sonicated to disaggregate clumps; crude homogenate was filtered through a 5 µm PVDF membrane; cells were washed with a very low concentration of triton detergent at each media change. Most strategies reduced PrP^{Sc} in the inoculum, but none improved clearance from the cultures compared to the regular semi-purified vCJD inoculum.

5.5 Discussion

5.5.1 A novel human differentiated NSC model of vCJD

In this chapter, I demonstrated that a differentiated human neuronal culture derived from a human immortalised foetal neural stem cell line (ReNcell 197VM) was able to chronically propagate vCJD prions. Following infection with a semi-purified preparation of vCJD prion-infected brain homogenate, the cultures consistently produced low steady-state levels of type 4 PrP^{Sc} for up to 50 days post-infection and subsequently died about 30 days earlier than mock-infected cultures (**figures 5.7** and **5.8**). This is the first description of an *in vitro* cellular system for replicating human prions. This is a highly relevant model system for several reasons. First, it closely mimics the human brain since it is a predominantly neuronal culture derived from the differentiation of human foetal midbrain NSC. Furthermore, these neurones can form synapses and appear to be electrically active. Second, the vCJD prion-propagating cell line only produces low levels of PrP^{Sc}, a feature consistent with vCJD patient brains, in which low prion titres are found (Dr J.Wadsworth, personal communication). Third, the cell line undergoes a delayed vCJD prion-induced cell death as occurs in disease. Fourth, the v-myc gene used for immortalisation (by enhancing tert and telomerase expression), confers genetic stability on the undifferentiated NSC over many passages making it a highly reproducible model (Dang et al., 1999;Villa et al., 2004;Kim, 2004). This is in contrast to genetically unstable tumour cell line-derived prion models, including many of the non-human prion disease cell models (Klohn et al., 2003). Finally, the stem cell nature of the model means there is an unlimited resource to study, unlike other primary neuronal culture models of prion disease (Cronier et al., 2004).

5.5.2 Differentiated phenotype influences cellular susceptibility to vCJD prion infection

Undifferentiated 197 cells were unable to propagate vCJD prions. This is consistent with a previous report in which mouse NSC were resistant to mouse prion infection (Milhavet et al., 2006). The fact that differentiation renders both mouse and human NSC susceptible to prion infection suggests that a terminally differentiated cell phenotype is a key determinant of prion susceptibility. This hypothesis is supported by the fact that mouse embryonic neurospheres are susceptible to mouse prions. Though mouse NSC do not propagate mouse prions, the prion permissive nature of the neurospheres was attributed to the fact they are comprised of neural progenitor cells at different stages of maturation, with few stem cells; that is, the more differentiated cells were proposed to propagate prions (Garcion et al., 2004;Giri et al., 2006). There may be several reasons why a differentiated cellular phenotype confers susceptibility to prion infection. First, as the dynamic susceptibility model of cellular prion infection predicts,

it may simply be that because the cultures are non-dividing, therefore, they have the opportunity to synthesise and accumulate *de novo* PrP^{Sc}, rather than the prion load of the cell being reduced at each cell division (Weissmann, 2004). Second, differentiation of NSC has been shown to result in a dramatic increase in PrP^{C} expression (Steele et al., 2006;Milhavet et al., 2006), a factor that has been proposed to underlie enhanced susceptibility to prion infection. However, this does not explain the lack of susceptibility of undifferentiated 197 cells, because a marked difference in PrP^{C} expression levels between the undifferentiated and differentiation states was not observed; a relatively high PrP^{C} expression was observed in both. Third, a recent study of the proteome of undifferentiated and differentiated 197 cells may explain the increased susceptibility of differentiated 197 cultures to vCJD prion infection (Hoffrogge et al., 2006). Changes in expression of proteins involved in protein metabolism were most common. Therefore, one could speculate this influenced PrP^{Sc} production and/or accumulation. For example, there was down-regulation of a lid subunit of the proteasome, S3/Rpn3, in the differentiated 197 cells. Since the proteasome, is a structure responsible for the non-lysosomal degradation of misfolded proteins in eukaryotic cells (Hershko and Ciechanover, 1998), this may have contributed to the accumulation of PrP^{Sc} in the cells. A down-regulation in heat shock proteins (Hsp) 70, 90, and 7C, was also observed. The constitutive form of Hsp70, a molecular chaperone, is expressed in neurones and has been implicated in the transport of misfolded proteins to the lysosome for degradation (Chang et al., 1989). Therefore, Hsp70 down-regulation in differentiated 197 cells may have reduced the degradation of PrP^{Sc} and led to its further cellular accumulation.

5.5.3 Neuronal phenotype influences cellular susceptibility to vCJD prion infection

Differentiation of the human 197 NSC line by withdrawal of mitogens from the culture medium resulted in a culture made up of between 80-90% neurones and about 10-20% astroglia. This is a very high proportion of neurones compared to glia, particularly given that a recently developed human (8-9 week) foetal cortical NSC line generated a culture of only 11% βIII-tubulin-positive neurones following differentiation (Cacci et al., 2007). The high proportion of neurones in the differentiated 197 cultures could be explained by the high PrP^{C} expression observed in the undifferentiated state (**figure 5.4**). PrP^{C} has been proposed to play a role in guiding multipotent neural precursor cells to differentiate into mature neurones, because PrP^{C} expression in mouse neural precursor cells positively correlated with the number of neurones generated *in vitro* (Steele et al., 2006). Alternatively, the v-myc gene may have integrated into the 197 genome and disrupted a gene involved in the regulation of neuronal differentiation or the culture conditions used may have favoured neuronal differentiation. Basic FGF is known to induce neurone formation from NSC cultures (Carpenter et al., 1999).

Moreover, the 197 cell line was not allowed to become overconfluent or maintained in culture for prolonged periods, since both these practices reduce its neuronal differentiation potential (Dr. E.Miljan, personal communication). However, it cannot be discounted that the high neuronal component of the 197 cultures was due to chance, perhaps related to the original donor tissue from which it was derived being of particularly high quality.

The high proportion of neurones in the differentiated 197 cultures may explain their susceptibility to vCJD prion infection. This would add to a growing body of evidence suggesting that a neuronal phenotype confers susceptibility to prion infection. First, directing mouse prion-susceptible NSC cultures towards a neuronal fate (with factors such as retinoic acid and nerve growth factor) results in the increased production of PrP^{Sc} compared to a mixed differentiated NSC population or those NSC directed to a glial fate (with CNTF), an effect which is independent of PrP^{C} expression level (Milhavet et al., 2006). Second, prion-resistant N2a-derived clones were switched to a RML prion-susceptible phenotype with retinoic acid-induced neuronal differentiation (Dr P.Klohn, unpublished data). Third, a microarray study of highly RML prion-susceptible PK1 clones and RML prion-resistant sister clones indicated that the prion-susceptible cells differentially expressed genes that promoted neuronal differentiation (Dr. P.Klohn, unpublished data). These included the upregulation of Sharp2, a transcription factor involved in the regulation of neuronal differentiation, marking the neurones that have reached their desired position (Rossner et al., 1997) and the down regulation of Id4, a negative regulator of differentiation in development (Bedford et al., 2005).

5.5.4 Clearance of brain homogenate from non-dividing neuronal cultures

The particle monitors used (differentiated PrP^{C}-null mouse NSC and anti-PrP antibody-treated differentiated 197 cells) indicate that residual vCJD prion-infected brain homogenate remained in the cultures at a low level throughout the course of the experiments. Other groups have managed to achieve early clearance of prion-infected brain homogenate from differentiated PrP^{C}-null post-mitotic cultures at 7 and 2 days post-infection (Cronier et al., 2004;Milhavet et al., 2006). However, the data produced by Milhavet *et al.* has been unreproducible in our hands; when their PrP^{Sc} purification process of brain homogenate was applied to our vCJD brain homogenate it removed all the infectivity. However, Cronier *et al.* used a low dose of sonicated crude mouse-adapted scrapie brain homogenate to facilitate clearance from primary cerebellar granular neuronal cultures in seven days post-infection. The same dose of semi-purified vCJD prion-infected brain homogenate was used in these experiments, but did not clear from the 197 cultures in seven days. One possible reason for faster clearance of inoculum from the cerebellar cultures was the presence of 1% microglial cells, which were proposed to degrade the inoculum by virtue of their phagocytic properties. There is also suggestion that

microglia are important for neuronal and glial survival in prion disease *in vivo* as they have been found near PrP^{Sc} aggregates in the brain (Marella and Chabry, 2004). Since NSC do not have the capacity to develop into microglia, this mechanism of inoculum clearance was not available in the 197 cultures. Another possibility is that vCJD prion-infected human brain homogenate is physically different to brain homogenate (mainly mouse) used in the development of other prion-propagating cell lines; it was much stickier and more aggregated. This may be due to the fact the vCJD-affected human brain is much older than scrapie-infected mouse brains, or because there is a longer post-mortem delay before freezing of human brain. However, the presence of low levels of vCJD inoculum in the cultures should not affect the use of the vCJD prion-propagating differentiated 197 cells in the study of pathophysiology of human prion disease.

5.5.5 Summary

The evidence presented in this chapter strongly suggests that differentiated 197 human foetal NSC stably propagate vCJD prions. The predominantly neuronal cultures appear to mimic *in vivo* disease by undergoing a delayed prion-induced cell death. Therefore, the 197 cell model represents a physiologically relevant system on which to study the biology of human prions at the cellular level (see **chapter 6** for future experiments).

Chapter 6

Conclusions and Future Work

6.1 Conclusions

This thesis aimed to develop a cell line that stably propagated human vCJD prions. This cellular model is of critical importance to the future of human prion disease research but is currently lacking, despite over forty years of investigation. To-date, research into human prion disease has been undertaken in transgenic mouse models but these possess inherent limitations, such as long disease incubation times. A cellular model is needed to provide a cheaper, faster assay system for human prions without the ethical constraints associated with animal experiments, and to provide a more easily manipulated model for the study of disease pathophysiology at the cellular and molecular levels.

In this thesis, mammalian cell lines were investigated for their ability to chronically propagate human vCJD prions. Because numerous cell models of prion disease are derived from tumour cell lines, in chapter 3 a panel of rodent and human tumour cell lines, derived from tissues capable of propagating prions *in vivo* and *in vitro*, were screened for susceptibility to human vCJD prion infection. It became apparent that expression of human PrP^{C}, which was methionine homozygous at codon 129 (to match the PrP^{Sc} sequence in the vCJD brain homogenate), was insufficient to establish vCJD prion infection in these cell lines. Therefore, it can be concluded that cellular susceptibility to human prions is determined by multiple, as yet unidentified, factors (discussed in **chapter 4**). The transient propagation of human vCJD prions observed in one cell line, the rabbit RK13 line expressing human PrP^{C}, was most likely due to its ability to transmit prions intercellularly via exosomes (Fevrier et al., 2004). The RK13 cell line highlighted that tumour cell lines are not ideal cellular models due to their genetic instability, which may indeed have caused the loss of their vCJD prion susceptible phenotype.

In chapter 4, the mouse PK1 cell line was hypothesised to possess factors required for cellular prion propagation because it is permissive to RML and 22L mouse prions (Professor C.Weissmann, unpublished data and Klohn et al., 2003). Cellular equivalents of the vCJD prion-susceptible transgenic mouse lines were generated. The inhibitory endogenous murine PrP^{C} was knocked out and human PrP^{C} overexpressed in PK1 cells. Nonetheless these cells were unable to propagate vCJD prions. This and the fact that the PK1 cell line is not permissive to mouse ME7 or hamster prions (Dr P.Klohn, unpublished data), suggested that cellular prion propagation factors may be prion strain-specific. Alternatively, human prion conversion in cell lines may be less efficient than mouse prion conversion to RML and 22L, requiring additional cellular factors.

Given that vCJD is readily transmitted to both wild-type and human PrP^C transgenic mice (Asante et al., 2002) but vCJD prion propagation was not achieved in either the human PrP^C-overexpressing PK1 mouse PrP^C knockout lines or the mammalian tumour cell lines, it can be concluded that transmission of vCJD prion infection to cell lines is much more difficult than to mice. Indeed, prion strains behave differently in cells than in animals. This is evidenced by the fact prion disease incubation times in mice do not influence cellular prion susceptibility; that is, short incubation time prion strains do not infect cells more easily than long incubation time strains (Vorberg et al., 2004). Therefore the whole organism appears to provide mechanisms to facilitate cellular prion uptake and/or propagation that may not be available in the reductionist approach of cell lines. Such mechanisms may include, first, cleavage of PrP^{Sc} by digestive enzymes. The protease-resistant PrP^{Sc} fragments resulting from enzymatic digestion of PrP^{Sc} are thought to form complexes with ferritin which results in their endocytosis into epithelial cells thus mediating their transport from gut to lymphoid tissue (Mishra et al., 2004). Second, complement component, C1q, has been reported to bind PrP^{Sc} and therefore may facilitate its uptake into complement receptor-expressing cells, such as follicular dendritic cells (Blanquet-Grossard et al., 2005). Third, the long incubation times associated with prion disease (a clinically silent phase prior to symptom onset) are critical for prion accumulation in non-dividing cells, such as follicular dendritic cells and neurones. This time period is not available in rapidly dividing cell cultures and therefore could be the reason why they cannot achieve high enough prion levels to establish infection.

The experiments described in chapter 5 led to the establishment of chronic, stable vCJD prion propagation in a primary human neuronal culture, derived from a foetal neural stem cell line (ReNcell 197VM). This is the first known description of cellular human prion propagation *in vitro*. The fact that the NSC line, 197, was only susceptible to vCJD prion infection in its differentiated neuronal state, strongly suggests a neuronal phenotype is a key determinant of cellular prion susceptibility. This work demonstrates that it is essential to recapitulate PrP^{Sc} processing *in vivo* most faithfully in order to achieve human prion propagation *in vitro*. The development of a vCJD prion propagating cell line opens up many avenues of investigation to further our knowledge of human prion neurobiology.

6.2 Future Work

6.2.1 Further development of the vCJD prion-propagating differentiated 197 cell line

6.2.1.1 Confirmation of infectivity in vCJD prion-infected 197 differentiated cultures

The chronic presence of protease-resistant PrP (the surrogate marker for prion infection) in the differentiated 197 cultures was shown in chapter 5. However, as is standard for prion-propagating cell lines, it would be important to demonstrate that the vCJD prion-infected 197 cells are producing infectious prions by transmission of infectivity *in vitro* and *in vivo*. This could be done by inoculating cell homogenate prepared from vCJD prion-infected differentiated 197 cultures into (1) uninfected differentiated 197 cultures and (2) vCJD prion-susceptible mice; Tg45 (which overexpress human PrP 129M four-fold) and SJL (wild-type) strains (Asante et al., 2002). PrP^{Sc} would be detected in the cell cultures by the SCA or immunoblotting (Milhavet et al., 2006;Cronier et al., 2004). Since vCJD prion-inoculated mice do not always develop clinical signs of disease (Asante et al., 2002), prion transmission from 197 cultures to mice would be assessed by histopathological examination of brain tissue for PrP^{Sc} and immunoblotting of brain tissue for type 4 PrP^{Sc}. It would be important to include particle monitor cell homogenate in these experiments to control for infectivity from the residual inoculum. In some cases, infectivity from prion-propagating cell lines has been demonstrated using cell culture supernatant (Schatzl et al., 1997;Fevrier et al., 2004;Cronier et al., 2004). This method may also demonstrate the presence of infectious prions in the vCJD prion-infected 197 cultures and additionally show if PrP^{Sc} is being released into the culture medium (perhaps in exosomes). In order to quantify infectivity in the differentiated 197 model, vCJD prion-infected cell homogenate from the cultures would need to be titrated against dilutions of vCJD brain homogenate in either the cellular system or the mouse bioassay.

6.2.1.2 Confirmation of *de novo* production of PrP^{Sc} in the vCJD prion-infected 197 differentiated cultures

Further evidence of *de novo* PrP^{Sc} production in differentiated 197 cultures could be achieved by metabolic radiolabelling of cellular proteins (using methods similar to those described in Schatzl et al., 1997;Follet et al., 2002). After vCJD prion infection of the differentiated 197 cultures, cells would be incubated for several hours with methionine-free medium supplemented with L-[^{35}S] methionine to allow incorporation of radiolabelled methionine into newly synthesised proteins. This would be followed by protein extraction from the cells and PK digestion of the material (as described in section **2.6.2**) and analysis by SDS-PAGE. Newly converted PrP^{Sc} in the differentiated 197 cultures would be radiolabelled and visualised by autoradiography, clearly distinguishing it from the unlabelled PrP^{Sc} in the residual vCJD

inoculum. Assaying 197 cultures at different time-points post-infection would indicate the rate of cellular PrP^{Sc} production during the lifespan of the cultures.

6.2.1.3 Investigation of susceptibility of differentiated 197 cultures to other human prion strains

Since vCJD differs in its clinicopathological phenotype to sporadic CJD, it would also be useful for basic and therapeutic research to have a cellular model of sCJD. Therefore, it would be important to test if the differentiated 197 cells could propagate type 1 and type 2 sCJD prions (derived from *PRNP* codon 129 methionine homozygotes), using the methods described in chapter 5.

6.2.2 Human PrP^{Sc} cell biology

Since the differentiated 197 cells appear to undergo delayed prion-induced cell death, they may closely model the effect of human prions on neurones during *in vivo* disease, in which progressive neuronal dysfunction precedes cell death.

6.2.2.1 Subcellular localisation of human PrP^{Sc}

It would be important to determine where PrP^{Sc} accumulates in the vCJD prion-infected 197 cells over time so this could be correlated with changes in biological parameters studied. Subcellular localisation of PrP^{Sc} is difficult to assess (Taraboulos et al., 1990;Archer et al., 2004) because the lack of a PrP^{Sc}-specific antibody means pre-treatment of cells with denaturants (formic acid, guanidinium thiocyanate or thermolysin) is required to remove PrP^{C} and reveal PrP^{Sc} epitopes, but this pre-treatment results in poor immunoreactivity. Previous work has suggested that PrP^{Sc} is localised at the plasma membrane (Caughey and Raymond, 1991), in the endolysosomal compartment (Arnold et al., 1995) and in the cytosol (in perinuclear structures responsible for clearance of cytoplasmic misfolded protein aggregates called aggresomes; Kristiansen et al., 2005). Immunofluorescence staining of the vCJD prion-infected differentiated 197 cells may allow the subcellular localisation of human PrP^{Sc} accumulation to be determined and may provide clues to some fundamental unanswered questions in the prion field, such as the site of PrP^{Sc} conversion and intra-cellular trafficking of human PrP^{Sc}. Confocal analysis of PrP^{Sc}-stained cells would determine localisation at the cell membrane. It would also demonstrate the proportion of the cells in the culture that become infected with vCJD prions. Determining the presence of PrP^{Sc} in the endolysosomal compartment and in the cytosol could be achieved by dual label immunostaining demonstrating co-localisation of PrP^{Sc} with the endolysosomal marker (LAMP-1) and cytosolic marker (Hsc70), respectively. The presence of PrP^{Sc} aggresomes could be established by demonstrating colocalisation of PrP^{Sc} with vimentin, Hsc70, ubiquitin and 20S proteasome subunits.

6.2.2.2 Study of apoptosis in differentiated 197 cultures

Apoptosis is regarded as the principal mechanism of cell death in prion disease as determined by *in vivo* and *in vitro* studies (Schatzl et al., 1997;Jamieson et al., 2001;Siso et al., 2002;Hetz and Soto, 2003;Hetz et al., 2003;Cronier et al., 2004;Kristiansen et al., 2005). The work presented in chapter 5 shows that vCJD prion infection of differentiated 197 cultures resulted in a delayed cell death, suggestive of apoptosis. To confirm this mechanism of cell death, the simultaneous presence of several apoptotic markers would need to be assessed in vCJD prion-infected differentiated 197 cultures at late stage infection (possibly day 45). Apoptotic cells exhibit fragmented nuclei (Oberhammer et al., 1993), the presence of which could be determined in the vCJD prion infected 197 cultures by nuclear DNA staining with DAPI (4',6-diamidino-2-phenylindole) and subsequent analysis by fluorescence microscopy. Poly (ADP-ribose) polymerase (PARP), a nuclear enzyme involved in DNA repair, is cleaved late in the apoptotic cascade by caspase 3. The presence of PARP cleavage products could be assessed in the vCJD prion infected 197 cultures by immunoblotting with a specific antibody. Apoptosis can be initiated through a number of different pathways (Thornberry and Lazebnik, 1998) and both *in vitro* and *in vivo* studies of prion disease suggest that caspases 3, 8 and 12 are activated (Jamieson et al., 2001;Siso et al., 2002;Kristiansen et al., 2005;Hetz et al., 2007). Caspase 8 mediates cell surface death receptor (Fas-L)-induced pathway of apoptosis, caspase 12 mediates ER-stress induced pathway and caspase 3 is a common downstream effector of apoptosis. Therefore, the vCJD prion-infected differentiated 197 cultures could be analysed for the presence of these activated caspases using *in vitro* assays specific for each caspase (Oncogene) or immunoblotting with specific antibodies.

6.2.2.3 Evaluating ubiquitin-proteasome system dysfunction in differentiated 197 cells

Until recently the cause of prion-mediated neurodegeneration was not known. As for other neurodegenerative diseases, evidence is now emerging to suggest the involvement of ubiquitin-proteasome system (UPS) dysfunction in prion-induced cell death (Ciechanover and Brundin, 2003). The UPS is a cellular protein quality control system responsible for the non-lysosomal degradation of short-lived, mutant and misfolded protein and is involved in many cellular functions, including transcriptional regulation, cell cycle control and control of apoptosis. Evidence for proteasome impairment in prion-infected neurones is observed in mouse prion-propagating cell lines. Mild proteasome inhibition of mouse prion-infected neuroblastoma cells results in PrP^{Sc} aggresome formation, which triggers caspase-dependent cell death (Ciechanover and Brundin, 2003). More recently an intracellular neurotoxic mechanism of prions has been proposed, in which oligomers of misfolded prion protein impair proteasome function by specifically inhibiting catalytic β-subunits of the 26S proteasome (Kristiansen et al., 2007). The vCJD prion-propagating differentiated 197 line will be useful in

establishing whether proteasome impairment is also a feature of human prion disease pathogenesis and specifically whether the vCJD prions inhibit catalytic β-subunits of the 26S proteasome. Proteasome function could be assessed (as described in Kristiansen et al., 2007) using fluorogenic peptide enzyme assays, a proteasome β-subunit activity probe (Berkers et al., 2005) and a ubiquitinated-GFP-tagged live cell proteasome reporter. Assessment of proteasome function over time will allow better understanding of the relationship between proteasome dysfunction and neuronal dysfunction following prion infection.

ER stress (caused by accumulation of protein aggregates or excessive protein traffic in the ER) has also been implicated in neuronal death in prion disease (Yoo et al., 2002;Hetz et al., 2003;Hetz et al., 2005;Hetz et al., 2007). ER stress results in the unfolded protein response (UPR) involving three signalling pathways that serve to increase folding capacity of the ER and reduce protein load. UPR induced chaperones are found in the cortex of sCJD and vCJD patients and in mouse prion-infected neuroblastoma cells (Yoo et al., 2002;Hetz et al., 2003). Whether the involvement of the ER-stress in prion disease pathogenesis is primary or secondary to UPS dysfunction is unclear at present. Inhibition of the UPS by prions (as described in Kristiansen et al., 2007) may contribute to ER stress because the proteasome is essential for normal ER-associated degradation (ERAD) of protein. Therefore, misfolded proteins destined for degradation by ERAD may remain in the ER. Alternatively, prion infection may directly result in ER stress, the latter of which is thought to inhibit proteasome dysfunction (Menendez-Benito et al., 2005). ER stress can be assessed (as described in Hetz et al., 2007) by the detection of upregulated genes involved in UPR, UPR chaperones and markers of ER stress-induced cell death, such as the transcription factor GADD153/CHOP and activated caspase-12. A time-course experiment measuring both proteasome function and ER stress markers in the vCJD prion-infected 197 cells would clarify the relationship between these two cellular pathways and their contribution to neuronal pathogenesis in human prion disease.

6.2.2.4 The effect of vCJD prion infection on synaptic function

Electroencephalogram (EEG) abnormalities are a common feature of human prion diseases and synaptic dysfunction is believed to be an early pathological event during prion infection (Cathala and Baron, 1987). Since uninfected 197 neurones have the capacity to generate action potentials (Dr Roberta Donato, UCL, unpublished work), these cells represent a unique system on which to study human neurophysiological changes in response to human prion infection, prior to neuronal death. Electrophysiology data from hippocampal and cortical neurones from scrapie-infected animals, suggest that prion infection increases neuronal membrane excitability as a result of reduced potassium conductances (Jefferys et al., 1994;Johnston et al., 1997;Johnston et al., 1998). Changes in membrane excitability in the vCJD prion-infected 197

neurones could be determined by measuring resting membrane potential, action potential threshold and amplitude. The use of the non-specific potassium channel antagonist, tetraethylammonium (TEA) would determine if membrane potential changes were due to potassium conductances (as described in Johnston et al., 1998)). Both prion-infected and PrP^{C} knock-out mice exhibit significantly reduced long slow afterhyperpolarisation potentials (AHP) (Colling et al., 1996;Johnston et al., 1998;Barrow et al., 1999;Mallucci et al., 2002), which are responsible for preventing repetitive action potential firing and are mediated by TEA-insensitive calcium-activated potassium channels. Therefore, loss of the long slow AHP could be demonstrated in vCJD prion-infected 197 neurones by repetitive firing of calcium spikes in response to a long depolarising current pulse, which would not be inhibited by TEA. The levels of synaptic proteins, including syntaxin 1A, SNAP-25, synaptobrevin, synapsin and synaptophysin, could also be studied by quantitative immunoblotting of infected and uninfected cells to assess prion-induced changes in synaptic function.

Prion infection causes a number of changes in neuronal morphology. Prior to neuronal loss, synaptic loss and axonal degeneration are observed in scrapie-infected mouse models (Jeffrey et al., 2000). Furthermore, increased branching of basal dendrites has been detected in hippocampal CA1 pyramidal cells (Barrow et al., 1999). Therefore, it would be interesting to study the ultrastructure of vCJD prion-infected 197 neurones using transmission electron microscopy (described in **2.9**). Alterations in neurite morphology (neurite length and branches), number of synapses formed, vesicle trafficking and evidence of axonal degeneration and neuronal vacuolation could all be assessed. The Cellomics™ Arrayscan robotic fluorescence microscope may also be useful for these experiments because it can directly quantify cell body morphology, neurite length and branching using their neurite outgrowth assay.

6.2.3 Screening potential therapeutics for human prion disease

Prion diseases remain incurable and the screening of potential therapeutics for prion disease has been performed on *in vivo* and *in vitro* experimental models of non-human prions. Therefore, the results of these studies may not be relevant for the treatment of human prion disease. The human vCJD prion-propagating neuronal 197 line represents a physiologically more relevant model on which to specifically assay compounds for potential therapeutic effect in vCJD. The vCJD prion-infected cell line would need to be developed for use in a high-throughput screening assay. The MRC Prion Unit has a collaboration with GlaxoSmithKline to screen the GSK compound library for anti-prion activity. It is anticipated that the human cell line will form part of a tertiary screen to assess 100 potential vCJD therapies.

Reference List

1. Archer F, Bachelin C, Andreoletti O, Besnard N, Perrot G, Langevin C, Le Dur A, Vilette D, Baron-Van Evercooren A, Vilotte JL, Laude H (2004) Cultured peripheral neuroglial cells are highly permissive to sheep prion infection. J Virol 78: 482-490.

2. Arnold JE, Tipler C, Laszlo L, Hope J, Landon M, Mayer RJ (1995) The abnormal isoform of the prion protein accumulates in late-endosome-like organelles in scrapie-infected mouse brain. J Pathol 176: 403-411.

3. Asante EA, Linehan JM, Desbruslais M, Joiner S, Gowland I, Wood A, Welch J, Hill AF, Lloyd SE, Wadsworth JDF, Collinge J (2002) BSE prions propagate as either variant CJD-like or sporadic CJD-like prion strains in transgenic mice expressing human prion protein. EMBO J 21 (23): 6358-6366.

4. Barrow PA, Holmgren CD, Tapper AJ, Jeffreys JGR (1999) Intrinsic physiological and morphological properties of principal cells of the hippocampus and neocortex in hamsters infected with scrapie. Neurobiology of Disease 6: 406-423.

5. Berkers CR, Verdoes M, Lichtman E, Fiebiger E, Kessler BM, Anderson KC, Ploegh HL, Ovaa H, Galardy PJ (2005) Activity probe for in vivo profiling of the specificity of proteasome inhibitor bortezomib. Nat Methods 2: 357-362.

6. Blanquet-Grossard F, Thielens NM, Vendrely C, Jamin M, Arlaud GJ (2005) Complement Protein C1q Recognizes a Conformationally Modified Form of the Prion Protein. Biochemistry 44: 4349-4356.

7. Cathala F, Baron H (1987) Clinical Aspects of Creutzfeldt-Jakob Disease. In: Prions: Novel infectious pathogens causing scrapie and Creutzfeldt-Jakob disease. (Prusiner SB, McKinley MP, eds), pp 467-509. San Diego: Academic Press.

8. Caughey B, Raymond GJ (1991) The scrapie-associated form of PrP is made from a cell surface precursor that is both protease- and phospholipase-sensitive. J Biol Chem 266 No 27: 18217-18223.

9. Ciechanover A, Brundin P (2003) The ubiquitin proteasome system in neurodegenerative diseases. Sometimes the chicken, sometimes the egg. Neuron 40: 427-446.

10. Colling SB, Collinge J, Jefferys JGR (1996) Hippocampal slices from prion protein null mice: Disrupted Ca^{2+}-activated K^+ currents. Neurosci Lett 209: 49-52.

11. Cronier S, Laude H, Peyrin JM (2004) Prions can infect primary cultured neurons and astrocytes and promote neuronal cell death. Proc Natl Acad Sci USA 101: 12271-12276.

12. Fevrier B, Vilette D, Archer F, Loew D, Faigle W, Vidal M, Laude H, Raposo G (2004) Cells release prions in association with exosomes. Proc Natl Acad Sci U S A.

13. Follet J, Lemaire-Vieille C, Blanquet-Grossard F, Podevin-Dimster V, Lehmann S, Chauvin JP, Decavel JP, Varea R, Grassi J, Fontes M, Cesbron JY (2002) PrP expression and replication by Schwann cells: implications in prion spreading
407. J Virol 76: 2434-2439.

14. Hetz C, Castilla J, Soto C (2007) Perturbation of endoplasmic reticulum homeostasis facilitates prion replication. J Biol Chem.

15. Hetz C, Russelakis-Carneiro M, Maundrell K, Castilla J, Soto C (2003) Caspase-12 and endoplasmic reticulum stress mediate neurotoxicity of pathological prion protein. EMBO J 22: 5435-5445.

16. Hetz C, Russelakis-Carneiro M, Walchli S, Carboni S, Vial-Knecht E, Maundrell K, Castilla J, Soto C (2005) The disulfide isomerase Grp58 is a protective factor against prion neurotoxicity. J Neurosci 25: 2793-2802.

17. Hetz C, Soto C (2003) Protein misfolding and disease: the case of prion disorders. Cell Mol Life Sci 60: 133-143.

18. Jamieson E, Jeffrey M, Ironside JW, Fraser JR (2001) Activation of Fas and caspase 3 precedes PrP accumulation in 87V scrapie. Neuroreport 12: 3567-3572.

19. Jefferys JGR, Empson RM, Whittington MA, Prusiner SB (1994) Scrapie infection of transgenic mice leads to network and intrinsic dysfunction of cortical and hippocampal neurons. Neurobiology of Disease 1: 3-15.

20. Jeffrey M, Halliday WG, Bell J, Johnston AR, Macleod NK, Ingham C, Sayers AR, Brown DA, Fraser JR (2000) Synapse loss associated with abnormal PrP precedes neuronal degeneration in the scrapie-infected murine hippocampus. Neuropathol Appl Neurobiol 26: 41-54.

21. Johnston AR, Black C, Fraser J, MacLeod N (1997) Scrapie infection alters the membrane and synaptic properties of mouse hippocampal CA1 pyramidal neurones. J Physiol 500: 1-15.

22. Johnston AR, Fraser JR, Jeffrey M, MacLeod N (1998) Alterations in potassium currents may trigger neurodegeneration in murine scrapie. Exp Neurol 151: 326-333.

23. Klohn PC, Stoltze L, Flechsig E, Enari M, Weissmann C (2003) A quantitative, highly sensitive cell-based infectivity assay for mouse scrapie prions. Proc Natl Acad Sci U S A 100: 11666-11671.

24. Kristiansen M, Deriziotis P, Dimcheff DE, Jackson GS, Ovaa H, Naumann H, Clarke AR, van Leeuwen FW, Menendez-Benito V, Dantuma NP, Portis JL, Collinge J, Tabrizi SJ (2007) Disease-Associated Prion Protein Oligomers Inhibit the 26S Proteasome. Mol Cell 26: 175-188.

25. Kristiansen M, Messenger MJ, Klohn PC, Brandner S, Wadsworth JD, Collinge J, Tabrizi SJ (2005) Disease-related prion protein forms aggresomes in neuronal cells leading to caspase-activation and apoptosis. J Biol Chem 280: 38851-38861.

26. Mallucci GR, Ratté S, Asante EA, Linehan J, Gowland I, Jefferys JGR, Collinge J (2002) Post-natal knockout of prion protein alters hippocampal CA1 properties, but does not result in neurodegeneration. EMBO J 21: 202-210.

27. Menendez-Benito V, Verhoef LG, Masucci MG, Dantuma NP (2005) Endoplasmic reticulum stress compromises the ubiquitin-proteasome system. Hum Mol Genet 14: 2787-2799.

28. Milhavet O, Casanova D, Chevallier N, McKay RD, Lehmann S (2006) Neural stem cell model for prion propagation. Stem Cells.

29. Mishra RS, Basu S, Gu Y, Luo X, Zou WQ, Mishra R, Li R, Chen SG, Gambetti P, Fujioka H, Singh N (2004) Protease-resistant human prion protein and ferritin are cotransported across Caco-2 epithelial cells: implications for species barrier in prion uptake from the intestine
19. J Neurosci 24: 11280-11290.

30. Oberhammer F, Wilson JW, Dive C, Morris ID, Hickman JA, Wakeling AE, Walker PR, Sikorska M (1993) Apoptotic death in epithelial cells: cleavage of DNA to 300 and/or 50 kb fragments prior to or in the absence of internucleosomal fragmentation. EMBO J 12: 3679-3684.

31. Schatzl HM, Laszlo L, Holtzman DM, Tatzelt J, DeArmond SJ, Weiner RI, Mobley WC, Prusiner SB (1997) A hypothalamic neuronal cell line persistently infected with scrapie prions exhibits apoptosis. J Virol 71: 8821-8831.

32. Siso S, Puig B, Varea R, Vidal E, Acin C, Prinz M, Montrasio F, Badiola J, Aguzzi A, Pumarola M, Ferrer I (2002) Abnormal synaptic protein expression and cell death in murine scrapie. Acta Neuropathol (Berl) 103: 615-626.

33. Taraboulos A, Serban D, Prusiner SB (1990) Scrapie prion proteins accumulate in the cytoplasm of persistently infected cultured cells. J Cell Biol 110: 2117-2132.

34. Thornberry NA, Lazebnik Y (1998) Caspases: enemies within. Science 281: 1312-1316.

35. Vorberg I, Raines A, Priola SA (2004) Acute formation of protease-resistant prion protein does not always lead to persistent scrapie infection in vitro. J Biol Chem 279: 29218-29225.

36. Yoo BC, Krapfenbauer K, Cairns N, Belay G, Bajo M, Lubec G (2002) Overexpressed protein disulfide isomerase in brains of patients with sporadic Creutzfeldt-Jakob disease. Neurosci Lett 334: 196-200.

Chapter 6

Conclusions and Future Work

6.1 Conclusions

This thesis aimed to develop a cell line that stably propagated human vCJD prions. This cellular model is of critical importance to the future of human prion disease research but is currently lacking, despite over forty years of investigation. To-date, research into human prion disease has been undertaken in transgenic mouse models but these possess inherent limitations, such as long disease incubation times. A cellular model is needed to provide a cheaper, faster assay system for human prions without the ethical constraints associated with animal experiments, and to provide a more easily manipulated model for the study of disease pathophysiology at the cellular and molecular levels.

In this thesis, mammalian cell lines were investigated for their ability to chronically propagate human vCJD prions. Because numerous cell models of prion disease are derived from tumour cell lines, in chapter 3 a panel of rodent and human tumour cell lines, derived from tissues capable of propagating prions *in vivo* and *in vitro*, were screened for susceptibility to human vCJD prion infection. It became apparent that expression of human PrP^{C}, which was methionine homozygous at codon 129 (to match the PrP^{Sc} sequence in the vCJD brain homogenate), was insufficient to establish vCJD prion infection in these cell lines. Therefore, it can be concluded that cellular susceptibility to human prions is determined by multiple, as yet unidentified, factors (discussed in **chapter 4**). The transient propagation of human vCJD prions observed in one cell line, the rabbit RK13 line expressing human PrP^{C}, was most likely due to its ability to transmit prions intercellularly via exosomes (Fevrier et al., 2004). The RK13 cell line highlighted that tumour cell lines are not ideal cellular models due to their genetic instability, which may indeed have caused the loss of their vCJD prion susceptible phenotype.

In chapter 4, the mouse PK1 cell line was hypothesised to possess factors required for cellular prion propagation because it is permissive to RML and 22L mouse prions (Professor C.Weissmann, unpublished data and Klohn et al., 2003). Cellular equivalents of the vCJD prion-susceptible transgenic mouse lines were generated. The inhibitory endogenous murine PrP^{C} was knocked out and human PrP^{C} overexpressed in PK1 cells. Nonetheless these cells were unable to propagate vCJD prions. This and the fact that the PK1 cell line is not permissive to mouse ME7 or hamster prions (Dr P.Klohn, unpublished data), suggested that cellular prion propagation factors may be prion strain-specific. Alternatively, human prion conversion in cell lines may be less efficient than mouse prion conversion to RML and 22L, requiring additional cellular factors.

Given that vCJD is readily transmitted to both wild-type and human PrP^C transgenic mice (Asante et al., 2002) but vCJD prion propagation was not achieved in either the human PrP^C-overexpressing PK1 mouse PrP^C knockout lines or the mammalian tumour cell lines, it can be concluded that transmission of vCJD prion infection to cell lines is much more difficult than to mice. Indeed, prion strains behave differently in cells than in animals. This is evidenced by the fact prion disease incubation times in mice do not influence cellular prion susceptibility; that is, short incubation time prion strains do not infect cells more easily than long incubation time strains (Vorberg et al., 2004). Therefore the whole organism appears to provide mechanisms to facilitate cellular prion uptake and/or propagation that may not be available in the reductionist approach of cell lines. Such mechanisms may include, first, cleavage of PrP^{Sc} by digestive enzymes. The protease-resistant PrP^{Sc} fragments resulting from enzymatic digestion of PrP^{Sc} are thought to form complexes with ferritin which results in their endocytosis into epithelial cells thus mediating their transport from gut to lymphoid tissue (Mishra et al., 2004). Second, complement component, C1q, has been reported to bind PrP^{Sc} and therefore may facilitate its uptake into complement receptor-expressing cells, such as follicular dendritic cells (Blanquet-Grossard et al., 2005). Third, the long incubation times associated with prion disease (a clinically silent phase prior to symptom onset) are critical for prion accumulation in non-dividing cells, such as follicular dendritic cells and neurones. This time period is not available in rapidly dividing cell cultures and therefore could be the reason why they cannot achieve high enough prion levels to establish infection.

The experiments described in chapter 5 led to the establishment of chronic, stable vCJD prion propagation in a primary human neuronal culture, derived from a foetal neural stem cell line (ReNcell 197VM). This is the first known description of cellular human prion propagation *in vitro*. The fact that the NSC line, 197, was only susceptible to vCJD prion infection in its differentiated neuronal state, strongly suggests a neuronal phenotype is a key determinant of cellular prion susceptibility. This work demonstrates that it is essential to recapitulate PrP^{Sc} processing *in vivo* most faithfully in order to achieve human prion propagation *in vitro*. The development of a vCJD prion propagating cell line opens up many avenues of investigation to further our knowledge of human prion neurobiology.

6.2 Future Work

6.2.1 Further development of the vCJD prion-propagating differentiated 197 cell line

6.2.1.1 Confirmation of infectivity in vCJD prion-infected 197 differentiated cultures

The chronic presence of protease-resistant PrP (the surrogate marker for prion infection) in the differentiated 197 cultures was shown in chapter 5. However, as is standard for prion-propagating cell lines, it would be important to demonstrate that the vCJD prion-infected 197 cells are producing infectious prions by transmission of infectivity *in vitro* and *in vivo*. This could be done by inoculating cell homogenate prepared from vCJD prion-infected differentiated 197 cultures into (1) uninfected differentiated 197 cultures and (2) vCJD prion-susceptible mice; Tg45 (which overexpress human PrP 129M four-fold) and SJL (wild-type) strains (Asante et al., 2002). PrP^{Sc} would be detected in the cell cultures by the SCA or immunoblotting (Milhavet et al., 2006;Cronier et al., 2004). Since vCJD prion-inoculated mice do not always develop clinical signs of disease (Asante et al., 2002), prion transmission from 197 cultures to mice would be assessed by histopathological examination of brain tissue for PrP^{Sc} and immunoblotting of brain tissue for type 4 PrP^{Sc}. It would be important to include particle monitor cell homogenate in these experiments to control for infectivity from the residual inoculum. In some cases, infectivity from prion-propagating cell lines has been demonstrated using cell culture supernatant (Schatzl et al., 1997;Fevrier et al., 2004;Cronier et al., 2004). This method may also demonstrate the presence of infectious prions in the vCJD prion-infected 197 cultures and additionally show if PrP^{Sc} is being released into the culture medium (perhaps in exosomes). In order to quantify infectivity in the differentiated 197 model, vCJD prion-infected cell homogenate from the cultures would need to be titrated against dilutions of vCJD brain homogenate in either the cellular system or the mouse bioassay.

6.2.1.2 Confirmation of *de novo* production of PrP^{Sc} in the vCJD prion-infected 197 differentiated cultures

Further evidence of *de novo* PrP^{Sc} production in differentiated 197 cultures could be achieved by metabolic radiolabelling of cellular proteins (using methods similar to those described in Schatzl et al., 1997;Follet et al., 2002). After vCJD prion infection of the differentiated 197 cultures, cells would be incubated for several hours with methionine-free medium supplemented with L-[^{35}S] methionine to allow incorporation of radiolabelled methionine into newly synthesised proteins. This would be followed by protein extraction from the cells and PK digestion of the material (as described in section **2.6.2**) and analysis by SDS-PAGE. Newly converted PrP^{Sc} in the differentiated 197 cultures would be radiolabelled and visualised by autoradiography, clearly distinguishing it from the unlabelled PrP^{Sc} in the residual vCJD

inoculum. Assaying 197 cultures at different time-points post-infection would indicate the rate of cellular PrP^{Sc} production during the lifespan of the cultures.

6.2.1.3 Investigation of susceptibility of differentiated 197 cultures to other human prion strains

Since vCJD differs in its clinicopathological phenotype to sporadic CJD, it would also be useful for basic and therapeutic research to have a cellular model of sCJD. Therefore, it would be important to test if the differentiated 197 cells could propagate type 1 and type 2 sCJD prions (derived from *PRNP* codon 129 methionine homozygotes), using the methods described in chapter 5.

6.2.2 Human PrP^{Sc} cell biology

Since the differentiated 197 cells appear to undergo delayed prion-induced cell death, they may closely model the effect of human prions on neurones during *in vivo* disease, in which progressive neuronal dysfunction precedes cell death.

6.2.2.1 Subcellular localisation of human PrP^{Sc}

It would be important to determine where PrP^{Sc} accumulates in the vCJD prion-infected 197 cells over time so this could be correlated with changes in biological parameters studied. Subcellular localisation of PrP^{Sc} is difficult to assess (Taraboulos et al., 1990;Archer et al., 2004) because the lack of a PrP^{Sc}-specific antibody means pre-treatment of cells with denaturants (formic acid, guanidinium thiocyanate or thermolysin) is required to remove PrP^{C} and reveal PrP^{Sc} epitopes, but this pre-treatment results in poor immunoreactivity. Previous work has suggested that PrP^{Sc} is localised at the plasma membrane (Caughey and Raymond, 1991), in the endolysosomal compartment (Arnold et al., 1995) and in the cytosol (in perinuclear structures responsible for clearance of cytoplasmic misfolded protein aggregates called aggresomes; Kristiansen et al., 2005). Immunofluorescence staining of the vCJD prion-infected differentiated 197 cells may allow the subcellular localisation of human PrP^{Sc} accumulation to be determined and may provide clues to some fundamental unanswered questions in the prion field, such as the site of PrP^{Sc} conversion and intra-cellular trafficking of human PrP^{Sc}. Confocal analysis of PrP^{Sc}-stained cells would determine localisation at the cell membrane. It would also demonstrate the proportion of the cells in the culture that become infected with vCJD prions. Determining the presence of PrP^{Sc} in the endolysosomal compartment and in the cytosol could be achieved by dual label immunostaining demonstrating co-localisation of PrP^{Sc} with the endolysosomal marker (LAMP-1) and cytosolic marker (Hsc70), respectively. The presence of PrP^{Sc} aggresomes could be established by demonstrating colocalisation of PrP^{Sc} with vimentin, Hsc70, ubiquitin and 20S proteasome subunits.

6.2.2.2 Study of apoptosis in differentiated 197 cultures

Apoptosis is regarded as the principal mechanism of cell death in prion disease as determined by *in vivo* and *in vitro* studies (Schatzl et al., 1997;Jamieson et al., 2001;Siso et al., 2002;Hetz and Soto, 2003;Hetz et al., 2003;Cronier et al., 2004;Kristiansen et al., 2005). The work presented in chapter 5 shows that vCJD prion infection of differentiated 197 cultures resulted in a delayed cell death, suggestive of apoptosis. To confirm this mechanism of cell death, the simultaneous presence of several apoptotic markers would need to be assessed in vCJD prion-infected differentiated 197 cultures at late stage infection (possibly day 45). Apoptotic cells exhibit fragmented nuclei (Oberhammer et al., 1993), the presence of which could be determined in the vCJD prion infected 197 cultures by nuclear DNA staining with DAPI (4',6-diamidino-2-phenylindole) and subsequent analysis by fluorescence microscopy. Poly (ADP-ribose) polymerase (PARP), a nuclear enzyme involved in DNA repair, is cleaved late in the apoptotic cascade by caspase 3. The presence of PARP cleavage products could be assessed in the vCJD prion infected 197 cultures by immunoblotting with a specific antibody. Apoptosis can be initiated through a number of different pathways (Thornberry and Lazebnik, 1998) and both *in vitro* and *in vivo* studies of prion disease suggest that caspases 3, 8 and 12 are activated (Jamieson et al., 2001;Siso et al., 2002;Kristiansen et al., 2005;Hetz et al., 2007). Caspase 8 mediates cell surface death receptor (Fas-L)-induced pathway of apoptosis, caspase 12 mediates ER-stress induced pathway and caspase 3 is a common downstream effector of apoptosis. Therefore, the vCJD prion-infected differentiated 197 cultures could be analysed for the presence of these activated caspases using *in vitro* assays specific for each caspase (Oncogene) or immunoblotting with specific antibodies.

6.2.2.3 Evaluating ubiquitin-proteasome system dysfunction in differentiated 197 cells

Until recently the cause of prion-mediated neurodegeneration was not known. As for other neurodegenerative diseases, evidence is now emerging to suggest the involvement of ubiquitin-proteasome system (UPS) dysfunction in prion-induced cell death (Ciechanover and Brundin, 2003). The UPS is a cellular protein quality control system responsible for the non-lysosomal degradation of short-lived, mutant and misfolded protein and is involved in many cellular functions, including transcriptional regulation, cell cycle control and control of apoptosis. Evidence for proteasome impairment in prion-infected neurones is observed in mouse prion-propagating cell lines. Mild proteasome inhibition of mouse prion-infected neuroblastoma cells results in PrP^{Sc} aggresome formation, which triggers caspase-dependent cell death (Ciechanover and Brundin, 2003). More recently an intracellular neurotoxic mechanism of prions has been proposed, in which oligomers of misfolded prion protein impair proteasome function by specifically inhibiting catalytic β-subunits of the 26S proteasome (Kristiansen et al., 2007). The vCJD prion-propagating differentiated 197 line will be useful in

establishing whether proteasome impairment is also a feature of human prion disease pathogenesis and specifically whether the vCJD prions inhibit catalytic β-subunits of the 26S proteasome. Proteasome function could be assessed (as described in Kristiansen et al., 2007) using fluorogenic peptide enzyme assays, a proteasome β-subunit activity probe (Berkers et al., 2005) and a ubiquitinated-GFP-tagged live cell proteasome reporter. Assessment of proteasome function over time will allow better understanding of the relationship between proteasome dysfunction and neuronal dysfunction following prion infection.

ER stress (caused by accumulation of protein aggregates or excessive protein traffic in the ER) has also been implicated in neuronal death in prion disease (Yoo et al., 2002;Hetz et al., 2003;Hetz et al., 2005;Hetz et al., 2007). ER stress results in the unfolded protein response (UPR) involving three signalling pathways that serve to increase folding capacity of the ER and reduce protein load. UPR induced chaperones are found in the cortex of sCJD and vCJD patients and in mouse prion-infected neuroblastoma cells (Yoo et al., 2002;Hetz et al., 2003). Whether the involvement of the ER-stress in prion disease pathogenesis is primary or secondary to UPS dysfunction is unclear at present. Inhibition of the UPS by prions (as described in Kristiansen et al., 2007) may contribute to ER stress because the proteasome is essential for normal ER-associated degradation (ERAD) of protein. Therefore, misfolded proteins destined for degradation by ERAD may remain in the ER. Alternatively, prion infection may directly result in ER stress, the latter of which is thought to inhibit proteasome dysfunction (Menendez-Benito et al., 2005). ER stress can be assessed (as described in Hetz et al., 2007) by the detection of upregulated genes involved in UPR, UPR chaperones and markers of ER stress-induced cell death, such as the transcription factor GADD153/CHOP and activated caspase-12. A time-course experiment measuring both proteasome function and ER stress markers in the vCJD prion-infected 197 cells would clarify the relationship between these two cellular pathways and their contribution to neuronal pathogenesis in human prion disease.

6.2.2.4 The effect of vCJD prion infection on synaptic function

Electroencephalogram (EEG) abnormalities are a common feature of human prion diseases and synaptic dysfunction is believed to be an early pathological event during prion infection (Cathala and Baron, 1987). Since uninfected 197 neurones have the capacity to generate action potentials (Dr Roberta Donato, UCL, unpublished work), these cells represent a unique system on which to study human neurophysiological changes in response to human prion infection, prior to neuronal death. Electrophysiology data from hippocampal and cortical neurones from scrapie-infected animals, suggest that prion infection increases neuronal membrane excitability as a result of reduced potassium conductances (Jefferys et al., 1994;Johnston et al., 1997;Johnston et al., 1998). Changes in membrane excitability in the vCJD prion-infected 197

neurones could be determined by measuring resting membrane potential, action potential threshold and amplitude. The use of the non-specific potassium channel antagonist, tetraethylammonium (TEA) would determine if membrane potential changes were due to potassium conductances (as described in Johnston et al., 1998)). Both prion-infected and PrP^{C} knock-out mice exhibit significantly reduced long slow afterhyperpolarisation potentials (AHP) (Colling et al., 1996;Johnston et al., 1998;Barrow et al., 1999;Mallucci et al., 2002), which are responsible for preventing repetitive action potential firing and are mediated by TEA-insensitive calcium-activated potassium channels. Therefore, loss of the long slow AHP could be demonstrated in vCJD prion-infected 197 neurones by repetitive firing of calcium spikes in response to a long depolarising current pulse, which would not be inhibited by TEA. The levels of synaptic proteins, including syntaxin 1A, SNAP-25, synaptobrevin, synapsin and synaptophysin, could also be studied by quantitative immunoblotting of infected and uninfected cells to assess prion-induced changes in synaptic function.

Prion infection causes a number of changes in neuronal morphology. Prior to neuronal loss, synaptic loss and axonal degeneration are observed in scrapie-infected mouse models (Jeffrey et al., 2000). Furthermore, increased branching of basal dendrites has been detected in hippocampal CA1 pyramidal cells (Barrow et al., 1999). Therefore, it would be interesting to study the ultrastructure of vCJD prion-infected 197 neurones using transmission electron microscopy (described in **2.9**). Alterations in neurite morphology (neurite length and branches), number of synapses formed, vesicle trafficking and evidence of axonal degeneration and neuronal vacuolation could all be assessed. The Cellomics™ Arrayscan robotic fluorescence microscope may also be useful for these experiments because it can directly quantify cell body morphology, neurite length and branching using their neurite outgrowth assay.

6.2.3 Screening potential therapeutics for human prion disease

Prion diseases remain incurable and the screening of potential therapeutics for prion disease has been performed on *in vivo* and *in vitro* experimental models of non-human prions. Therefore, the results of these studies may not be relevant for the treatment of human prion disease. The human vCJD prion-propagating neuronal 197 line represents a physiologically more relevant model on which to specifically assay compounds for potential therapeutic effect in vCJD. The vCJD prion-infected cell line would need to be developed for use in a high-throughput screening assay. The MRC Prion Unit has a collaboration with GlaxoSmithKline to screen the GSK compound library for anti-prion activity. It is anticipated that the human cell line will form part of a tertiary screen to assess 100 potential vCJD therapies.

References

Reference List

Aguzzi A, Glatzel M, Montrasio F, Prinz M, Heppner FL (2001) Interventional strategies against prion diseases. Nat Rev Neurosci 2: 745-749.

Alpers MP (1987) Epidemiology and Clinical Aspects of Kuru. In: Prions: Novel infectious pathogens causing scrapie and Creutzfeldt-Jakob disease. (Prusiner SB, McKinley MP, eds), pp 451-465. San Diego: Academic Press.

Anderson RM, Donnelly CA, Ferguson NM, Woolhouse MEJ, Watt CJ, Udy HJ, MaWhinney S, Dunstan SP, Southwood TRE, Wilesmith JW, Ryan JBM, Hoinville LJ, Hillerton JE, Austin AR, Wells GAH (1996) Transmission dynamics and epidemiology of BSE in British cattle. Nature 382: 779-788.

Archer F, Bachelin C, Andreoletti O, Besnard N, Perrot G, Langevin C, Le Dur A, Vilette D, Baron-Van Evercooren A, Vilotte JL, Laude H (2004) Cultured peripheral neuroglial cells are highly permissive to sheep prion infection. J Virol 78: 482-490.

Arnold JE, Tipler C, Laszlo L, Hope J, Landon M, Mayer RJ (1995) The abnormal isoform of the prion protein accumulates in late-endosome-like organelles in scrapie-infected mouse brain. J Pathol 176: 403-411.

Asante EA, Linehan JM, Desbruslais M, Joiner S, Gowland I, Wood A, Welch J, Hill AF, Lloyd SE, Wadsworth JDF, Collinge J (2002) BSE prions propagate as either variant CJD-like or sporadic CJD-like prion strains in transgenic mice expressing human prion protein. EMBO J 21 (23): 6358-6366.

Baron GS, Magalhaes AC, Prado MA, Caughey B (2006) Mouse-Adapted Scrapie Infection of SN56 Cells: Greater Efficiency with Microsome-Associated versus Purified PrP-res. J Virol 80: 2106-2117.

Baron GS, Wehrly K, Dorward DW, Chesebro B, Caughey B (2002) Conversion of raft associated prion protein to the protease-resistant state requires insertion of PrP-res (PrPSc) into contiguous membranes.328. EMBO J 21: 1031-1040.

Barrow PA, Holmgren CD, Tapper AJ, Jeffreys JGR (1999) Intrinsic physiological and morphological properties of principal cells of the hippocampus and neocortex in hamsters infected with scrapie. Neurobiology of Disease 6: 406-423.

Baskakov IV, Legname G, Gryczynski Z, Prusiner SB (2004) The peculiar nature of unfolding of the human prion protein. Protein Sci.

Bedford L, Walker R, Kondo T, van C, I, King ER, Sablitzky F (2005) Id4 is required for the correct timing of neural differentiation. Dev Biol 280: 386-395.

Ben Zaken O, Tzaban S, Tal Y, Horonchik L, Esko JD, Vlodavsky I, Taraboulos A (2003) Cellular heparan sulfate participates in the metabolism of prions. J Biol Chem 278: 40041-40049.

Beranger F, Mange A, Solassol J, Lehmann S (2001) Cell culture models of transmissible spongiform encephalopathies. Biochem Biophys Res Commun 289: 311-316.

Berkers CR, Verdoes M, Lichtman E, Fiebiger E, Kessler BM, Anderson KC, Ploegh HL, Ovaa H, Galardy PJ (2005) Activity probe for in vivo profiling of the specificity of proteasome inhibitor bortezomib. Nat Methods 2: 357-362.

Bernstein E, Caudy AA, Hammond SM, Hannon GJ (2001) Role for a bidentate ribonuclease in the initiation step of RNA interference. Nature 409: 363-366.

Bertoni JM, Brown P, Goldfarb LG, Rubenstein R, Gajdusek DC (1992) Familial Creutzfeldt-Jakob disease (codon 200 mutation) with supranuclear palsy. JAMA 268: 2413-2415.

Bishop MT, Hart P, Aitchison L, Baybutt HN, Plinston C, Thomson V, Tuzi NL, Head MW, Ironside JW, Will RG, Manson JC (2006) Predicting susceptibility and incubation time of human-to-human transmission of vCJD. Lancet Neurol 5: 393-398.

Blanquet-Grossard F, Thielens NM, Vendrely C, Jamin M, Arlaud GJ (2005) Complement Protein C1q Recognizes a Conformationally Modified Form of the Prion Protein. Biochemistry 44: 4349-4356.

Blanton JR, Jr., Bidwell CA, Sanders DA, Sharkey CM, McFarland DC, Gerrard DE, Grant AL (2000) Plasmid transfection and retroviral transduction of porcine muscle cells for cell-mediated gene transfer. J Anim Sci 78: 909-918.

Bolton DC, McKinley MP, Prusiner SB (1982) Identification of a protein that purifies with the scrapie prion. Science 218: 1309-1311.

Bosque PJ, Prusiner SB (2000) Cultured cell sublines highly susceptible to prion infection. Journal of Virology 74: 4377-4386.

Bounhar Y, Zhang Y, Goodyer CG, LeBlanc A (2001) Prion protein protects human neurons against Bax-mediated apoptosis. Journal of Biological Chemistry 276: 39145-39149.

Brown DR (1999) Prion protein expression aids cellular uptake and veratridine-induced release of copper. J Neurosci Res 58: 717-725.

Brown DR, Qin K, Herms JW, Madlung A, Manson J, Strome R, Fraser PE, Kruck T, von Bohlen A, Schulz-Schaeffer W, Giese A, Westaway D, Kretzschmar H (1997a) The cellular prion protein binds copper in vivo. Nature 390: 684-687.

Brown DR, Schulz-Schaeffer WJ, Schmidt B, Kretzschmar HA (1997b) Prion protein-deficient cells show altered response to oxidative stress due to decreased SOD-1 activity. Exp Neurol 146: 104-112.

Brown DR, Wong BS, Hafiz F, Clive C, Haswell SJ, Jones IM (1999a) Normal prion protein has an activity like that of superoxide dismutase. Biochemical Journal 344: 1-5.

Brown KL, Stewart K, Ritchie DL, Mabbott NA, Williams A, Fraser H, Morrison WI, Bruce ME (1999b) Scrapie replication in lymphoid tissues depends on prion protein-expressing follicular dendritic cells. Nat Med 5: 1308-1312.

Brown P, Gibbs CJJr, Rodgers Johnson P, Asher DM, Sulima MP, Bacote A, Goldfarb LG, Gajdusek DC (1994) Human spongiform encephalopathy: the National Institutes of Health series of 300 cases of experimentally transmitted disease. Ann Neurol 35: 513-529.

Brown P, Preece M, Brandel JP, Sato T, McShane L, Zerr I, Fletcher A, Will RG, Pocchiari M, Cashman NR, D'Aignaux JH, Cervenáková L, Fradkin J, Schonberger LB, Collins SJ (2000) Iatrogenic Creutzfeldt-Jakob disease at the millennium. Neurology 55: 1075-1081.

Brown P, Preece MA, Will RG (1992) "Friendly fire" in medicine: hormones, homografts, and Creutzfeldt-Jakob disease. Lancet 340: 24-27.

Bruce M, Chree A, McConnell I, Foster J, Pearson G, Fraser H (1994) Transmission of bovine spongiform encephalopathy and scrapie to mice: Strain variation and the species barrier. Philos Trans R Soc Lond [Biol] 343: 405-411.

Bruce ME, Will RG, Ironside JW, McConnell I, Drummond D, Suttie A, McCardle L, Chree A, Hope J, Birkett C, Cousens S, Fraser H, Bostock CJ (1997) Transmissions to mice indicate that 'new variant' CJD is caused by the BSE agent. Nature 389: 498-501.

Brummelkamp TR, Bernards R, Agami R (2002) A system for stable expression of short interfering RNAs in mammalian cells. Science 296: 550-553.

Bucciantini M, Giannoni E, Chiti F, Baroni F, Formigli L, Zurdo J, Taddei N, Ramponi G, Dobson CM, Stefani M (2002) Inherent toxicity of aggregates implies a common mechanism for protein misfolding diseases. Nature 416: 507-511.

Bueler H, Aguzzi A, Sailer A, Greiner RA, Autenried P, Aguet M, Weissmann C (1993a) Mice devoid of PrP are resistant to scrapie. Cell 73: 1339-1347.

Bueler H, Fischer M, Lang Y, Bluethmann H, Lipp H-P, DeArmond SJ, Prusiner SB, Aguet M, Weissmann C (1992) Normal development and behaviour of mice lacking the neuronal cell-surface PrP protein. Nature 356: 577-582.

Bueler H, Fischer M, Lang Y, Bluthmann H, Lipp H-P, DeArmond SJ, Prusiner SB, Aguet M, Weissmann C (1993b) PrP protein is not essential for normal development and behavior of the mouse. Nature.

Butler DA, Scott MR, Bockman JM, Borchelt DR, Taraboulos A, Hsiao KK, Kingsbury DT, Prusiner SB (1988) Scrapie-infected murine neuroblastoma cells produce protease- resistant prion proteins. J Virol 62: 1558-1564.

Cacci E, Villa A, Parmar M, Cavallaro M, Mandahl N, Lindvall O, Martinez-Serrano A, Kokaia Z (2007) Generation of human cortical neurons from a new immortal fetal neural stem cell line. Exp Cell Res 313: 588-601.

Calzolai L, Lysek DA, Perez DR, Guntert P, Wuthrich K (2005) Prion protein NMR structures of chickens, turtles, and frogs. Proc Natl Acad Sci U S A 102: 651-655.

Carimalo J, Cronier S, Petit G, Peyrin JM, Boukhtouche F, Arbez N, Lemaigre-Dubreuil Y, Brugg B, Miquel MC (2005) Activation of the JNK-c-Jun pathway during the early phase of neuronal apoptosis induced by PrP106-126 and prion infection. Eur J Neurosci 21: 2311-2319.

Carlson GA, Ebeling C, Yang S-L, Telling G, Torchia M, Groth D, Westaway D, DeArmond SJ, Prusiner SB (1994) Prion isolate specified allotypic interactions between the cellular and scrapie prion proteins in congenic and transgenic mice. Proc Natl Acad Sci USA 91: 5690-5694.

Carp RI, Merz PA, Kascsak RJ, Merz GS, Wisniewski HM (1985) Nature of the scrapie agent: current status of facts and hypotheses. J Gen Virol 66 (Pt 7): 1357-1368.

Carpenter MK, Cui X, Hu ZY, Jackson J, Sherman S, Seiger A, Wahlberg LU (1999) In vitro expansion of a multipotent population of human neural progenitor cells. Exp Neurol 158: 265-278.

Cashman NR, Loertscher R, Nalbantoglu J, Shaw I, Kascsak RJ, Bolton DC, Bendheim PE (1990) Cellular isoform of the scrapie agent protein participates in lymphocyte activation. Cell 61: 185-192.

Castilla J, Saa P, Soto C (2005) Detection of prions in blood. Nat Med 11: 982-985.

Cathala F, Baron H (1987) Clinical Aspects of Creutzfeldt-Jakob Disease. In: Prions: Novel infectious pathogens causing scrapie and Creutzfeldt-Jakob disease. (Prusiner SB, McKinley MP, eds), pp 467-509. San Diego: Academic Press.

Caughey B, Baron GS (2006) Prions and their partners in crime. Nature 443: 803-810.

Caughey B, Lansbury PT, Jr. (2003) Protofibrils, Pores, Fibrils, and Neurodegeneration: Separating the Responsible Protein Aggregates from the Innocent Bystanders. Annu Rev Neurosci.

Caughey B, Raymond GJ (1991) The scrapie-associated form of PrP is made from a cell surface precursor that is both protease- and phospholipase-sensitive. J Biol Chem 266 No 27: 18217-18223.

Caughey B, Raymond GJ (1993) Sulfated polyanion inhibition of scrapie-associated PrP accumulation in cultured cells. J Virol 67: 643-650.

Cervenakova L, Goldfarb L, Garruto R, Lee HS, Gajdusek CD, Brown P (1999) Phenotype-genotype studies in kuru: Implications for new variant Creutzfeldt-Jakob disease. Proc Natl Acad Sci USA 95: 13239-13241.

Chandler RL (1961) Encephalopathy in mice produced by inoculation with scrapie brain material. Lancet 1378-1379.

Chang MP, Baldwin RL, Bruce C, Wisnieski BJ (1989) Second cytotoxic pathway of diphtheria toxin suggested by nuclease activity. Science 246: 1165-1168.

Chen S, Mange A, Dong L, Lehmann S, Schachner M (2003) Prion protein as trans-interacting partner for neurons is involved in neurite outgrowth and neuronal survival. Mol Cell Neurosci 22: 227-233.

Chiarini LB, Freitas AR, Zanata SM, Brentani RR, Martins VR, Linden R (2002) Cellular prion protein transduces neuroprotective signals.26. EMBO J 21: 3317-3326.

Chiesa R, Harris DA (2001) Prion diseases: what is the neurotoxic molecule? Neurobiol Dis 8: 743-763.

Ciechanover A, Brundin P (2003) The ubiquitin proteasome system in neurodegenerative diseases. Sometimes the chicken, sometimes the egg. Neuron 40: 427-446.

Clarke MC, Haig DA (1970a) Evidence for the multiplication of scrapie agent in cell culture. Nature 225: 100-101.

Clarke MC, Haig DA (1970b) Multiplication of scrapie agent in cell culture. Res Vet Sci 11: 500-501.

Clemens MJ (1997) PKR--a protein kinase regulated by double-stranded RNA. Int J Biochem Cell Biol 29: 945-949.

Coitinho AS, Freitas AR, Lopes MH, Hajj GN, Roesler R, Walz R, Rossato JI, Cammarota M, Izquierdo I, Martins VR, Brentani RR (2006) The interaction between prion protein and laminin modulates memory consolidation. Eur J Neurosci 24: 3255-3264.

Coitinho AS, Lopes MH, Hajj GN, Rossato JI, Freitas AR, Castro CC, Cammarota M, Brentani RR, Izquierdo I, Martins VR (2007) Short-term memory formation and long-term memory consolidation are enhanced by cellular prion association to stress-inducible protein 1. Neurobiol Dis.

Colling SB, Collinge J, Jefferys JGR (1996) Hippocampal slices from prion protein null mice: Disrupted Ca^{2+}-activated K^{+} currents. Neurosci Lett 209: 49-52.

Collinge J (1999) Variant Creutzfeldt-Jakob disease. Lancet 354: 317-323.

Collinge J (2001) Prion diseases of humans and animals: their causes and molecular basis1. Annu Rev Neurosci 24: 519-550.

Collinge J (2005) Molecular neurology of prion disease. J Neurol Neurosurg Psychiatry 76: 906-919.

Collinge J, Palmer MS, Dryden AJ (1991) Genetic predisposition to iatrogenic Creutzfeldt-Jakob disease. Lancet 337: 1441-1442.

Collinge, J., Palmer, M. S., Gowland, I., Sidle, K. C. L., Hill, A. F., and Meads, J. Transmission of human prion disease to transgenic mice expressing human prion protein. QJM - Monthly Journal of the Association of Physicians . 1995a. Ref Type: In Press

Collinge J, Palmer MS, Sidle KCL, Gowland I, Medori R, Ironside J, Lantos PL (1995b) Transmission of fatal familial insomnia to laboratory animals. Lancet 346: 569-570.

Collinge J, Palmer MS, Sidle KCL, Hill AF, Gowland I, Meads J, Asante E, Bradley R, Doey LJ, Lantos PL (1995c) Unaltered susceptibility to BSE in transgenic mice expressing human prion protein. Nature 378: 779-783.

Collinge J, Rossor M (1996) A new variant of prion disease. Lancet 347: 916-917.

Collinge J, Sidle KCL, Meads J, Ironside J, Hill AF (1996) Molecular analysis of prion strain variation and the aetiology of 'new variant' CJD. Nature 383: 685-690.

Collinge J, Whitfield J, McKintosh E, Beck J, Mead S, Thomas DJ, Alpers MP (2006) Kuru in the 21st century--an acquired human prion disease with very long incubation periods. Lancet 367: 2068-2074.75. Collinge J, Whittington MA, Sidle KCL, Smith CJ, Palmer MS, Clarke AR, Jefferys JGR (1994) Prion protein is necessary for normal synaptic function. Nature 370: 295-297.

Collins S, Law MG, Fletcher A, Boyd A, Kaldor J, Masters CL (1999) Surgical treatment and risk of sporadic Creutzfeldt-jakob disease: a case-control study. Lancet 353: 693-697.

Cordeiro Y, Machado F, Juliano L, Juliano MA, Brentani RR, Foguel D, Silva JL (2001) DNA converts cellular prion protein into the beta-sheet conformation and inhibits prion peptide aggregation. J Biol Chem 276: 49400-49409.

Cotto E, Andre M, Forgue J, Fleury HJ, Babin PJ (2005) Molecular characterization, phylogenetic relationships, and developmental expression patterns of prion genes in zebrafish (Danio rerio). FEBS J 272: 500-513.

Cronier S, Laude H, Peyrin JM (2004) Prions can infect primary cultured neurons and astrocytes and promote neuronal cell death. Proc Natl Acad Sci USA 101: 12271-12276.

Cuillé J, Chelle PL (1936) La maladie dite tremblante du mouton est-elle inocuable? C R Acad Sci 203: 1552-1554.

Cullen BR (2006) Induction of stable RNA interference in mammalian cells. Gene Ther 13: 503-508.

Dang CV, Resar LM, Emison E, Kim S, Li Q, Prescott JE, Wonsey D, Zeller K (1999) Function of the c-Myc oncogenic transcription factor. Exp Cell Res 253: 63-77.

Daude N, Marella M, Chabry J (2003) Specific inhibition of pathological prion protein accumulation by small interfering RNAs. J Cell Sci 116: 2775-2779.

Davidson BL, Paulson HL (2004) Molecular medicine for the brain: silencing of disease genes with RNA interference. Lancet Neurol 3: 145-149.

Davis AA, Temple S (1994) A self-renewing multipotential stem cell in embryonic rat cerebral cortex. Nature 372: 263-266.

De Almeida CJ, Chiarini LB, da Silva JP, PM ES, Martins MA, Linden R (2005) The cellular prion protein modulates phagocytosis and inflammatory response. J Leukoc Biol 77: 238-246.

De Filippis L, Foglieni C, Silva S, Vescovi AL, Lusso P, Malnati MS (2006) Differentiated human neural stem cells: a new ex vivo model to study HHV-6 infection of the central nervous system. J Clin Virol 37 Suppl 1: S27-S32.

DeArmond SJ, Sanchez H, Yehiely F, Qiu Y, Ninchak-Casey A, Daggett V, Camerino AP, Cayetano J, Rogers M, Groth D, Torchia M, Tremblay P, Scott MR, Cohen FE, Prusiner SB (1997) Selective neuronal targeting in prion disease. Neuron 19: 1337-1348.

Deleault NR, Lucassen RW, Supattapone S (2003) RNA molecules stimulate prion protein conversion. Nature 425: 717-720.

Demaimay R, Adjou KT, Beringue V, Demart S, Lasmézas CI, Deslys JP, Seman M, Dormont D (1997) Late treatment with polyene antibiotics can prolong the survival time of scrapie-infected animals. J Virol 71: 9685-9689.

Dodelet VC, Cashman NR (1998b) Prion protein expression in human leukocyte differentiation. Blood 91: 1556-1561.

Dodelet VC, Cashman NR (1998a) Prion protein expression in human leukocyte differentiation. Blood 91: 1556-1561.

Doh-ura K, Ishikawa K, Murakami-Kubo I, Sasaki K, Mohri S, Race R, Iwaki T (2004) Treatment of Transmissible Spongiform Encephalopathy by Intraventricular Drug Infusion in Animal Models. J Virol 78: 4999-5006.

Doh-ura K, Iwaki T, Caughey B (2000) Lysosomotropic agents and cysteine protease inhibitors inhibit scrapie-associated prion protein accumulation. J Virol 74: 4894-4897.

Edenhofer F, Rieger R, Famulok M, Wendler W, Weiss S, Winnacker EL (1996) Prion protein PrP^c interacts with molecular chaperones of the Hsp60 family. J Virol 70: 4724-4728.

Elbashir SM, Harborth J, Lendeckel W, Yalcin A, Weber K, Tuschl T (2001a) Duplexes of 21-nucleotide RNAs mediate RNA interference in cultured mammalian cells. Nature 411: 494-498.

Elbashir SM, Harborth J, Weber K, Tuschl T (2002) Analysis of gene function in somatic mammalian cells using small interfering RNAs. Methods 26: 199-213.

Elbashir SM, Lendeckel W, Tuschl T (2001b) RNA interference is mediated by 21- and 22-nucleotide RNAs. Genes Dev 15: 188-200.

Elbashir SM, Martinez J, Patkaniowska A, Lendeckel W, Tuschl T (2001c) Functional anatomy of siRNAs for mediating efficient RNAi in Drosophila melanogaster embryo lysate. EMBO J 20: 6877-6888.

Elleman CJ (1984) Attempts to establish the scrapie agent in cell lines. Vet Res Commun 8: 309-316.

Enari M, Flechsig E, Weissmann C (2001) Scrapie prion protein accumulation by scrapie-infected neuroblastoma cells abrogated by exposure to a prion protein antibody. Proc Natl Acad Sci USA 98: 9295-9299.

Etessami R, Chaumontet C, Laude H, Vilette D (2005) Scratch-wounding renders cultivated cells less permissive to prion infection. Biochem Biophys Res Commun 330: 5-10.

Fevrier B, Vilette D, Archer F, Loew D, Faigle W, Vidal M, Laude H, Raposo G (2004) Cells release prions in association with exosomes. Proc Natl Acad Sci U S A.

Fire A, Albertson D, Harrison SW, Moerman DG (1991) Production of antisense RNA leads to effective and specific inhibition of gene expression in C. elegans muscle. Development 113: 503-514.

Fire A, Xu S, Montgomery MK, Kostas SA, Driver SE, Mello CC (1998) Potent and specific genetic interference by double-stranded RNA in Caenorhabditis elegans. Nature 391: 806-811.

Fischer M, Rulicke T, Raeber A, Sailer A, Moser M, Oesch B, Brandner S, Aguzzi A, Weissmann C (1996) Prion protein (PrP) with amino-proximal deletions restoring susceptibility of PrP knockout mice to scrapie. EMBO J 15: 1255-1264.

Flechsig E, Shmerling D, Hegyi I, Raeber AJ, Fischer M, Cozzio A, von Mering C, Aguzzi A, Weissmann C (2000) Prion protein devoid of the octapeptide repeat region restores susceptibility to scrapie in PrP knockout mice. Neuron 27: 399-408.

Follet J, Lemaire-Vieille C, Blanquet-Grossard F, Podevin-Dimster V, Lehmann S, Chauvin JP, Decavel JP, Varea R, Grassi J, Fontes M, Cesbron JY (2002) PrP expression and replication by Schwann cells: implications in prion spreading.407. J Virol 76: 2434-2439.

Forloni G, Angeretti N, Chiesa R, Monzani E, Salmona M, Bugiani O, Tagliavini F (1993) Neurotoxicity of a prion protein fragment. Nature 362: 543-546.

Gabus C, Auxilien S, Péchoux C, Dormont D, Swietnicki W, Morillas M, Surewicz W, Nandi P, Darlix JL (2001a) The prion protein has DNA strand transfer properties similar to retroviral nucleocapsid protein. Journal of Molecular Biology 307: 1011-1021.

Gabus C, Derrington E, Leblanc P, Chnaiderman J, Dormont D, Swietnicki W, Morillas M, Surewicz WK, Marc D, Nandi P, Darlix JL (2001b) The prion protein has RNA binding and chaperoning properties characteristic of nucleocapsid protein NCp7 of HIV-1. Journal of Biological Chemistry 276: 19301-19309.

Gage FH (2000) Mammalian neural stem cells. Science 287: 1433-1438.

Gajdusek DC, Gibbs CJJr, Alpers MP (1966) Experimental transmission of a kuru-like syndrome to chimpanzees. Nature 209: 794-796.

Gajdusek DC, Gibbs CJJr, Rogers NG, Basnight M, Hooks J (1972) Persistence of viruses of kuru and Creutzfeldt-Jakob disease in tissue cultures of brain cells. Nature 235: 104-105.

Galli R, Gritti A, Bonfanti L, Vescovi AL (2003) Neural stem cells: an overview. Circ Res 92: 598-608.

Gambetti P, Kong Q, Zou W, Parchi P, Chen SG (2003) Sporadic and familial CJD: classification and characterisation. Br Med Bull 66: 213-239.

Garcion E, Halilagic A, Faissner A, ffrench-Constant C (2004) Generation of an environmental niche for neural stem cell development by the extracellular matrix molecule tenascin C. Development 131: 3423-3432.

Gauczynski S, Peyrin JM, Haïk S, Leucht C, Hundt C, Rieger R, Krasemann S, Deslys JP, Dormont D, Lasmézas CI, Weiss S (2001) The 37-kDa/67-kDa laminin receptor acts as the cell-surface receptor for the cellular prion protein. EMBO J 20: 5863-5875.

Geiduschek EP, Tocchini-Valentini GP (1988) Transcription by RNA polymerase III. Annu Rev Biochem 57: 873-914.

Ghani AC, Donnelly CA, Ferguson NM, Anderson RM (2003) Updated projections of future vCJD deaths in the UK. BMC Infect Dis 3: 4.

Gibbs CJ, Jr., Gajdusek DC, Asher DM, Alpers MP, Beck E, Daniel PM, Matthews WB (1968) Creutzfeldt-Jakob disease (spongiform encephalopathy): transmission to the chimpanzee. Proc-Natl-Acad-Sci-U-S-A 161: 388-389.

Gibbs CJJr, Gajdusek DC (1973) Experimental subacute spongiform virus encephalopathies in primates and other laboratory animals. Science 182: 67-68.

Gilch S, Wopfner F, Renner-Muller I, Kremmer E, Bauer C, Wolf E, Brem G, Groschup MH, Schatzl HM (2003) Polyclonal anti-PrP auto-antibodies induced with dimeric PrP interfere efficiently with PrPSc propagation in prion-infected cells. J Biol Chem 278: 18524-18531.

Giri RK, Young R, Pitstick R, DeArmond SJ, Prusiner SB, Carlson GA (2006) Prion infection of mouse neurospheres. Proc Natl Acad Sci U S A.

Goldberg AL (2003) Protein degradation and protection against misfolded or damaged proteins. Nature 426: 895-899.

Goldfarb LG, Brown P, Mitrova E, Cervenakova L, Goldin L, Korczyn AD, Chapman J, Galvez S, Cartier L, Rubenstein R, et al (1991) Creutzfeldt-Jacob disease associated with the PRNP codon 200Lys mutation: an analysis of 45 families. Eur J Epidemiol 7: 477-486.

Goldfarb LG, Korczyn AD, Brown P, Chapman J, Gajdusek DC (1990) Mutation in codon 200 of scrapie amyloid precursor gene linked to Creutzfeldt-Jakob disease in Sephardic Jews of Libyan and non- Libyan origin. Lancet 336: 637-638.

Gonzalez-Iglesias R, Pajares MA, Ocal C, Carlos EJ, Oesch B, Gasset M (2002) Prion Protein Interaction with Glycosaminoglycan Occurs with the Formation of Oligomeric Complexes Stabilized by Cu(II) Bridges. J Mol Biol 319: 527-540.

Gossert AD, Bonjour S, Lysek DA, Fiorito F, Wuthrich K (2005) Prion protein NMR structures of elk and of mouse/elk hybrids. Proc Natl Acad Sci U S A 102: 646-650.

Graner E, Mercadante AF, Zanata SM, Forlenza OV, Cabral ALB, Veiga SS, Juliano MA, Roesler R, Walz R, Minetti A, Izquierdo I, Martins VR, Brentani RR (2000a) Cellular prion protein binds laminin and mediates neuritogenesis. Mol Brain Res 76: 85-92.

Graner E, Mercadante AF, Zanata SM, Martins VR, Jay DG, Brentani RR (2000b) Laminin-induced PC-12 cell differentiation is inhibited following laser inactivation of cellular prion protein. FEBS Letters 482: 257-260.

Gritti A, Parati EA, Cova L, Frolichsthal P, Galli R, Wanke E, Faravelli L, Morassutti DJ, Roisen F, Nickel DD, Vescovi AL (1996) Multipotential stem cells from the adult mouse brain proliferate and self-renew in response to basic fibroblast growth factor. J Neurosci 16: 1091-1100.

Hammond SM, Bernstein E, Beach D, Hannon GJ (2000) An RNA-directed nuclease mediates post-transcriptional gene silencing in Drosophila cells. Nature 404: 293-296.

Hammond SM, Boettcher S, Caudy AA, Kobayashi R, Hannon GJ (2001) Argonaute2, a link between genetic and biochemical analyses of RNAi. Science 293: 1146-1150.

Harris DA (2003) Trafficking, turnover and membrane topology of PrP. Br Med Bull 66: 71-85.

Heid CA, Stevens J, Livak KJ, Williams PM (1996) Real time quantitative PCR. Genome Res 6: 986-994.

Hershko A, Ciechanover A (1998) The ubiquitin system. Annu Rev Biochem 67: 425-479.

Hetz C, Castilla J, Soto C (2007) Perturbation of endoplasmic reticulum homeostasis facilitates prion replication. J Biol Chem.

Hetz C, Russelakis-Carneiro M, Maundrell K, Castilla J, Soto C (2003) Caspase-12 and endoplasmic reticulum stress mediate neurotoxicity of pathological prion protein. EMBO J 22: 5435-5445.

Hetz C, Russelakis-Carneiro M, Walchli S, Carboni S, Vial-Knecht E, Maundrell K, Castilla J, Soto C (2005) The disulfide isomerase Grp58 is a protective factor against prion neurotoxicity. J Neurosci 25: 2793-2802.

Hetz C, Soto C (2003) Protein misfolding and disease: the case of prion disorders. Cell Mol Life Sci 60: 133-143.

Hijazi N, Kariv-Inbal Z, Gasset M, Gabizon R (2005) PrPSc incorporation to cells requires endogenous GAGs expression. J Biol chem.

Hill AF, Butterworth RJ, Joiner S, Jackson G, Rossor MN, Thomas DJ, Frosh A, Tolley N, Bell JE, Spencer M, King A, Al-Sarraj S, Ironside JW, Lantos PL, Collinge J (1999) Investigation of variant Creutzfeldt-Jakob disease and other human prion diseases with tonsil biopsy samples. Lancet 353: 183-189.

Hill AF, Collinge J (2003a) Subclinical prion infection. Trends Microbiol 11: 578-584.

Hill AF, Collinge J (2003b) Subclinical prion infection in humans and animals. Br Med Bull 66: 161-170.

Hill AF, Desbruslais M, Joiner S, Sidle KCL, Gowland I, Collinge J (1997a) The same prion strain causes vCJD and BSE. Nature 389: 448-450.

Hill AF, Joiner S, Linehan J, Desbruslais M, Lantos PL, Collinge J (2000) Species barrier independent prion replication in apparently resistant species. Proc Natl Acad Sci U S A 97: 10248-10253.

Hill AF, Joiner S, Wadsworth JD, Sidle KC, Bell JE, Budka H, Ironside JW, Collinge J (2003) Molecular classification of sporadic Creutzfeldt-Jakob disease. Brain 126: 1333-1346.

Hill AF, Zeidler M, Ironside J, Collinge J (1997b) Diagnosis of new variant Creutzfeldt-Jakob disease by tonsil biopsy. Lancet 349: 99-100.

Hilton DA, Ghani AC, Conyers L, Edwards P, McCardle L, Ritchie D, Penney M, Hegazy D, Ironside JW (2004) Prevalence of lymphoreticular prion protein accumulation in UK tissue samples. J Pathol 203: 733-739.

Hoffrogge R, Mikkat S, Scharf C, Beyer S, Christoph H, Pahnke J, Mix E, Berth M, Uhrmacher A, Zubrzycki IZ, Miljan E, Volker U, Rolfs A (2006) 2-DE proteome analysis of a proliferating and differentiating human neuronal stem cell line (ReNcell VM). Proteomics 6: 1833-1847.

Holen T, Amarzguioui M, Wiiger MT, Babaie E, Prydz H (2002) Positional effects of short interfering RNAs targeting the human coagulation trigger Tissue Factor. Nucleic Acids Res 30: 1757-1766.

Hooper NM (2003) Could inhibition of the proteasome cause mad cow disease? Trends Biotechnol 21: 144-145.

Horiuchi M, Priola SA, Chabry J, Caughey B (2000) Interactions between heterologous forms of prion protein: Binding, inhibition of conversion, and species barriers. Proc Natl Acad Sci USA 97: 5836-5841.

Horonchik L, Tzaban S, Ben Zaken O, Yedidia Y, Rouvinski A, Papy-Garcia D, Barritault D, Vlodavsky I, Taraboulos A (2005) Heparan sulfate is a cellular receptor for purified infectious prions. J Biol Chem 280: 17062-17067.

Hosszu LLP, Baxter NJ, Jackson GS, Power A, Clarke AR, Waltho JP, Craven CJ, Collinge J (1999) Structural mobility of the human prion protein probed by backbone hydrogen exchange. Nature Struct Biol 6: 740-743.

Huesken D, Lange J, Mickanin C, Weiler J, Asselbergs F, Warner J, Meloon B, Engel S, Rosenberg A, Cohen D, Labow M, Reinhardt M, Natt F, Hall J (2005) Design of a genome-wide siRNA library using an artificial neural network. Nat Biotechnol 23: 995-1001.

Huillard d'Aignaux J, Costagliola D, Maccario J, Billette de Villemeur T, Brandel JP, Deslys JP, Hauw JJ, Chaussain JL, Agid Y, Dormont D, Alperovitch A (1999) Incubation period of Creutzfeldt-Jakob disease in human growth hormone recipients in France. Neurology 53: 1197-1201.

Hundt C, Peyrin JM, Haïk S, Gauczynski S, Leucht C, Rieger R, Riley ML, Deslys JP, Dormont D, Lasmézas CI, Weiss S (2001) Identification of interaction domains of the prion protein with its 37-kDa/67-kDa laminin receptor. EMBO J 20: 5876-5886.

Hwang L, Gilboa E (1984) Expression of Genes Introduced into cells by retroviral infection is more efficient than that of genes introduced into cells by DNA transfection. J. Virol 50(2); 417-24

Iwamaru Y, Takenouchi T, Ogihara K, Hoshino M, Takata M, Imamura M, Tagawa Y, Hayashi-Kato H, Ushiki-Kaku Y, Shimizu Y, Okada H, Shinagawa M, Kitani H, Yokoyama T (2007) Microglial cell line established from prion protein-overexpressing mice is susceptible to various murine prion strains. J Virol 81: 1524-1527.

Jackson GS, Beck JA, Navarrete C, Brown J, Sutton PM, Contreras M, Collinge J (2001a) HLA-DQ7 antigen and resistance to variant CJD. Nature 414: 269-270.

Jackson GS, Murray I, Hosszu LLP, Gibbs N, Waltho JP, Clarke AR, Collinge J (2001b) Location and properties of metal-binding sites on the human prion protein. Proc Natl Acad Sci U S A 98: 8531-8535.

James TL, Liu H, Ulyanov NB, Farr-Jones S, Zhang H, Donne DG, Kaneko K, Groth D, Mehlhorn I, Prusiner SB, Cohen FE (1997) Solution structure of a 142-residue recombinant prion protein corresponding to the infectious fragment of the scrapie isoform. Proc Natl Acad Sci USA 94: 10086-10091.

Jamieson E, Jeffrey M, Ironside JW, Fraser JR (2001) Activation of Fas and caspase 3 precedes PrP accumulation in 87V scrapie. Neuroreport 12: 3567-3572.

Jefferys JGR, Empson RM, Whittington MA, Prusiner SB (1994) Scrapie infection of transgenic mice leads to network and intrinsic dysfunction of cortical and hippocampal neurons. Neurobiology of Disease 1: 3-15.

Jeffrey M, Halliday WG, Bell J, Johnston AR, Macleod NK, Ingham C, Sayers AR, Brown DA, Fraser JR (2000a) Synapse loss associated with abnormal PrP precedes neuronal degeneration in the scrapie-infected murine hippocampus. Neuropathol Appl Neurobiol 26: 41-54.

Jeffrey M, Martin S, Gonzalez L (2003) Cell-associated variants of disease-specific prion protein immunolabelling are found in different sources of sheep transmissible spongiform encephalopathy. J Gen Virol 84: 1033-1046.

Jeffrey M, McGovern G, Goodsir CM, Brown KL, Bruce ME (2000b) Sites of prion protein accumulation in scrapie-infected mouse spleen revealed by immuno-electron microscopy. J Pathol 191: 323-332.

Jensen S, Gassama MP, Heidmann T (1999) Taming of transposable elements by homology-dependent gene silencing. Nat Genet 21: 209-212.

Jia P, Shi T, Cai Y, Li Y (2006) Demonstration of two novel methods for predicting functional siRNA efficiency. BMC Bioinformatics 7: 271.

Johansson CB, Svensson M, Wallstedt L, Janson AM, Frisen J (1999) Neural stem cells in the adult human brain. Exp Cell Res 253: 733-736.

Johe KK, Hazel TG, Muller T, Dugich-Djordjevic MM, McKay RD (1996) Single factors direct the differentiation of stem cells from the fetal and adult central nervous system. Genes Dev 10: 3129-3140.

Johnston AR, Black C, Fraser J, MacLeod N (1997) Scrapie infection alters the membrane and synaptic properties of mouse hippocampal CA1 pyramidal neurones. J Physiol 500: 1-15.

Johnston AR, Fraser JR, Jeffrey M, MacLeod N (1998) Alterations in potassium currents may trigger neurodegeneration in murine scrapie. Exp Neurol 151: 326-333.

Kahana E, Alter M, Braham J, Sofer D (1974) Creutzfeldt-jakob disease: focus among Libyan Jews in Israel. Science 183: 90-91.

Kahana E, Zilber N (1991) Do Creutzfeldt-Jakob disease patients of Jewish Libyan origin have unique clinical features? Neurology 41: 1390-1392.

Kanaani J, Prusiner SB, Diacovo J, Baekkeskov S, Legname G (2005) Recombinant prion protein induces rapid polarization and development of synapses in embryonic rat hippocampal neurons in vitro. J Neurochem 95: 1373-1386.

Kaneko K, Zulianello L, Scott M, Cooper CM, Wallace AC, James TL, Cohen FE, Prusiner SB (1997) Evidence for protein X binding to a discontinuous epitope on the cellular prion protein during scrapie prion propagation. Proc Natl Acad Sci USA 94: 10069-10074.

Kanu N, Imokawa Y, Drechsel DN, Williamson RA, Birkett CR, Bostock CJ, Brockes JP (2002) Transfer of scrapie prion infectivity by cell contact in culture.246. Curr Biol 12: 523-530.

Kayed R, Head E, Thompson JL, McIntire TM, Milton SC, Cotman CW, Glabe CG (2003) Common structure of soluble amyloid oligomers implies common mechanism of pathogenesis1. Science 300: 486-489.

Kikuchi Y, Kakeya T, Sakai A, Takatori K, Nakamura N, Matsuda H, Yamazaki T, Tanamoto K, Sawada J (2004) Propagation of a protease-resistant form of prion protein in long-term cultured human glioblastoma cell line T98G. J Gen Virol 85: 3449-3457.

Kim HS, Zhang X, Choi YS (1994) Activation and proliferation of follicular dendritic cell-like cells by activated T lymphocytes. J Immunol 153: 2951-2961.

Kim SU (2004) Human neural stem cells genetically modified for brain repair in neurological disorders. Neuropathology 24: 159-171.

King A, Doey L, Rossor M, Mead S, Collinge J, Lantos P (2003) Phenotypic variability in the brains of a family with a prion disease characterized by a 144-base pair insertion in the prion protein gene. Neuropathol Appl Neurobiol 29: 98-105.

Kirchner R, Vogtherr M, Limmer S, Sprinzl M (1998) Secondary structure dimorphism and interconversion between hairpin and duplex form of oligoribonucleotides. Antisense Nucleic Acid Drug Dev 8: 507-516.

Kitamoto T, Muramoto T, Mohri S, Doh-Ura K, Tateishi J (1991) Abnormal isoform of prion protein accumulates in follicular dendritic cells in mice with Creutzfeldt-Jakob disease. J Virol 65: 6292-6295.

Klohn PC, Stoltze L, Flechsig E, Enari M, Weissmann C (2003a) A quantitative, highly sensitive cell-based infectivity assay for mouse scrapie prions. Proc Natl Acad Sci U S A 100: 11666-11671.

Klohn PC, Stoltze L, Flechsig E, Enari M, Weissmann C (2003b) A quantitative, highly sensitive cell-based infectivity assay for mouse scrapie prions. Proc Natl Acad Sci U S A 100: 11666-11671.

Kocisko DA, Come JH, Priola SA, Chesebro B, Raymond GJ, Lansbury PT, Caughey B (1994) Cell-free formation of protease-resistant prion protein. Nature 370: 471-474.

Kopacek J, Sakaguchi S, Shigematsu K, Nishida N, Atarashi R, Nakaoke R, Moriuchi R, Niwa M, Katamine S (2000) Upregulation of the genes encoding lysosomal hydrolases, a perforin-like protein, and peroxidases in the brains of mice affected with an experimental prion disease. Journal of Virology 74: 411-417.

Korth C, Kaneko K, Groth D, Heye N, Telling G, Mastrianni J, Parchi P, Gambetti P, Will R, Ironside J, Heinrich C, Tremblay P, DeArmond SJ, Prusiner SB (2003) Abbreviated incubation times for human prions in mice expressing a chimeric mouse-human prion protein transgene. Proc Natl Acad Sci U S A.

Kretzschmar HA, Tings T, Madlung A, Giese A, Herms J (2000) Function of PrP(C) as a copper-binding protein at the synapse. Arch Virol Suppl 239-249.

Kristiansen M, Deriziotis P, Dimcheff DE, Jackson GS, Ovaa H, Naumann H, Clarke AR, van Leeuwen FW, Menendez-Benito V, Dantuma NP, Portis JL, Collinge J, Tabrizi SJ (2007) Disease-Associated Prion Protein Oligomers Inhibit the 26S Proteasome. Mol Cell 26: 175-188.

Kristiansen M, Messenger MJ, Klohn PC, Brandner S, Wadsworth JD, Collinge J, Tabrizi SJ (2005) Disease-related prion protein forms aggresomes in neuronal cells leading to caspase-activation and apoptosis. J Biol Chem 280: 38851-38861.

Kuczius T, Haist I, Groschup MH (1998) Molecular analysis of bovine spongiform encephalopathy and scrapie strain variation. J Infect Dis 178: 693-699.

Kurschner C, Morgan JI (1995) The cellular prion protein (PrP) selectively binds to Bcl-2 in the yeast two-hybrid system. Brain Res Mol Brain Res 30: 165-168.

Ladogana A, Liu Q, Xi YG, Pocchiari M (1995) Proteinase-resistant protein in human neuroblastoma cells infected with brain material from Creutzfeldt-Jakob patient. Lancet 345: 594-595.

Lassle M, Blatch GL, Kundra V, Takatori T, Zetter BR (1997) Stress-inducible, murine protein mSTI1. Characterization of binding domains for heat shock proteins and in vitro phosphorylation by different kinases. J Biol chem 272: 1876-1884.

Laszlo L, Lowe J, Self T, Kenward N, Landon M, McBride T, Farquhar C, McConnell I, Brown J, Hope J, Mayer RJ (1992) Lysosomes as key organelles in the pathogenesis of prion encephalopathies. J Pathol 166: 333-341.

Leblanc P, Alais S, Porto-Carreiro I, Lehmann S, Grassi J, Raposo G, Darlix JL (2006) Retrovirus infection strongly enhances scrapie infectivity release in cell culture. EMBO J.

Lee KS, Linden R, Prado MA, Brentani RR, Martins VR (2003) Towards cellular receptors for prions. Rev Med Virol 13: 399-408.

Lehmann S, Harris DA (1995) A mutant prion protein displays an aberrant membrane association when expressed in cultured cells. J Biol Chem 270: 24589-24597.

Lehmann S, Harris DA (1997) Blockade of glycosylation promotes acquisition of scrapie- like properties by the prion protein in cultured cells. J Biol Chem 272: 21479-21487.

Lendahl U, Zimmerman LB, McKay RD (1990) CNS stem cells express a new class of intermediate filament protein. Cell 60: 585-595.

Liberski PP, Sikorska B, Bratosiewicz-Wasik J, Carleton GD, Brown P (2004) Neuronal cell death in transmissible spongiform encephalopathies (prion diseases) revisited: from apoptosis to autophagy. Int J Biochem Cell Biol 36: 2473-2490.

Lindenbaum S (1979) Kuru Sorcery: Disease and Danger in the New Guinea Highlands. Palo Alto: Mayfield.

Lindvall O, Kokaia Z, Martinez-Serrano A (2004) Stem cell therapy for human neurodegenerative disorders-how to make it work. Nat Med 10 Suppl: S42-S50.

Liu J, Carmell MA, Rivas FV, Marsden CG, Thomson JM, Song JJ, Hammond SM, Joshua-Tor L, Hannon GJ (2004) Argonaute2 is the catalytic engine of mammalian RNAi. Science 305: 1437-1441.

Llewelyn CA, Hewitt PE, Knight RSG, Amar K, Cousens S, Mackenzie J, Will RG (2004) Possible transmission of variant Creutzfeldt-Jakob disease by blood transfusion. Lancet 363: 417-421.

Lloyd SE, Onwuazor ON, Beck JA, Mallinson G, Farrall M, Targonski P, Collinge J, Fisher EMC (2001) Identification of multiple quantitative trait loci linked to prion disease incubation period in mice. Proc Natl Acad Sci USA 98: 6279-6283.

Lloyd SE, Uphill JB, Targonski PV, Fisher EM, Collinge J (2002) Identification of genetic loci affecting mouse-adapted bovine spongiform encephalopathy incubation time in mice. Neurogenetics 4: 77-81.

Lopes MH, Hajj GN, Muras AG, Mancini GL, Castro RM, Ribeiro KC, Brentani RR, Linden R, Martins VR (2005) Interaction of cellular prion and stress-inducible protein 1 promotes neuritogenesis and neuroprotection by distinct signaling pathways. J Neurosci 25: 11330-11339.

Lucassen R, Nishina K, Supattapone S (2003) In vitro amplification of protease-resistant prion protein requires free sulfhydryl groups. Biochemistry 42: 4127-4135.

Luhr KM, Nordstrom EK, Low P, Ljunggren HG, Taraboulos A, Kristensson K (2004) Scrapie Protein Degradation by Cysteine Proteases in CD11c(+) Dendritic Cells and GT1-1 Neuronal Cells. J Virol 78: 4776-4782.

Lysek DA, Schorn C, Nivon LG, Esteve-Moya V, Christen B, Calzolai L, Von Schroetter C, Fiorito F, Herrmann T, Guntert P, Wuthrich K (2005) Prion protein NMR structures of cats, dogs, pigs, and sheep. Proc Natl Acad Sci U S A 102: 640-645.

Ma J, Lindquist S (2002) Conversion of PrP to a Self-Perpetuating PrPSc-like Conformation in the Cytosol. Science.

Mabbott NA, Bruce ME (2003) Prion disease: bridging the spleen-nerve gap. Nat Med 9: 1463-1464.

Mabbott NA, MacPherson GG (2006) Prions and their lethal journey to the brain. Nat Rev Microbiol.

Mabbott NA, Young J, McConnell I, Bruce ME (2003) Follicular dendritic cell dedifferentiation by treatment with an inhibitor of the lymphotoxin pathway dramatically reduces scrapie susceptibility. J Virol 77: 6845-6854.

Makinen PI, Koponen JK, Karkkainen AM, Malm TM, Pulkkinen KH, Koistinaho J, Turunen MP, Yla-Herttuala S (2006) Stable RNA interference: comparison of U6 and H1 promoters in endothelial cells and in mouse brain. J Gene Med 8: 433-441.

Mallucci G, Dickinson A, Linehan J, Klohn PC, Brandner S, Collinge J (2003) Depleting neuronal PrP in prion infection prevents disease and reverses spongiosis. Science 302: 871-874.

Mallucci GR, Ratté S, Asante EA, Linehan J, Gowland I, Jefferys JGR, Collinge J (2002) Post-natal knockout of prion protein alters hippocampal CA1 properties, but does not result in neurodegeneration. EMBO J 21: 202-210.

Mangé A, Nishida N, Milhavet O, McMahon HEM, Casanova D, Lehmann S (2000) Amphotericin B inhibits the generation of the scrapie isoform of the prion protein in infected cultures. J Virol 74: 3135-3140.

Marella M, Chabry J (2004) Neurons and astrocytes respond to prion infection by inducing microglia recruitment. J Neurosci 24: 620-627.

Markovits P, Dautheville C, Dormont D, Dianoux L, Latarjet R (1983) In vitro propagation of the scrapie agent. I. Transformation of mouse glia and neuroblastoma cells after infection with the mouse- adapted scrapie strain c-506. Acta Neuropathol (Berl) 60: 75-80.

Marsh RF, Bessen RA, Lehmann S, Hartsough GR (1991) Epidemiological and experimental studies on a new incident of transmissible mink encephalopathy. J Gen Virol 72: 589-594.

Martinez J, Patkaniowska A, Urlaub H, Luhrmann R, Tuschl T (2002) Single-stranded antisense siRNAs guide target RNA cleavage in RNAi. Cell 110: 563-574.

Mathiason CK, Powers JG, Dahmes SJ, Osborn DA, Miller KV, Warren RJ, Mason GL, Hays SA, Hayes-Klug J, Seelig DM, Wild MA, Wolfe LL, Spraker TR, Miller MW, Sigurdson CJ, Telling GC, Hoover EA (2006) Infectious prions in the saliva and blood of deer with chronic wasting disease. Science 314: 133-136.

Mayer RJ, Landon M, Laszlo L, Lennox G, Lowe J (1992) Protein processing in lysosomes: the new therapeutic target in neurodegenerative disease. Lancet 340: 156-159.

McKay R (1997) Stem cells in the central nervous system. Science 276: 66-71.

McManus MT, Haines BB, Dillon CP, Whitehurst CE, van Parijs L, Chen J, Sharp PA (2002) Small interfering RNA-mediated gene silencing in T lymphocytes. J Immunol 169: 5754-576

Mead S (2006) Prion disease genetics. Eur J Hum Genet.

Mead S, Mahal SP, Beck J, Campbell T, Farrall M, Fisher E, Collinge J (2001) Sporadic - but not variant - Creutzfeldt-Jakob disease is associated with polymorphisms upstream of *PRNP* Exon 1. Am J Hum Genet 69: 1225-1235.

Mead S, Stumpf MP, Whitfield J, Beck JA, Poulter M, Campbell T, Uphill J, Goldstein D, Alpers M, Fisher EM, Collinge J (2003) Balancing Selection at the Prion Protein Gene Consistent with Prehistoric Kurulike Epidemics. Science 2003: 640-643.

Medori R, Tritschler HJ, LeBlanc A, Villare F, Manetto V, Chen HY, Xue R, Leal S, Montagna P, Cortelli P, Tinuper P, Avoni P, Mochi M, Baruzzi Q, Hauw JJ, Ott J, Lugaresi E, Autilio-Gambetti L, Gambetti P (1992) Fatal familial insomnia, a prion disease with a mutation at codon 178 of the prion protein gene [see comments]. N Engl J Med 326: 444-449.

Meiner Z, Halimi M, Polikiewicz RD, Prusiner SB, Gabizon R (1992) Presence of prion protein in peripheral tissues of Libyan Jews with Creutzfeldt-Jakob disease. Neurology 42: 1355-1360.

Meister G, Landthaler M, Patkaniowska A, Dorsett Y, Teng G, Tuschl T (2004) Human Argonaute2 mediates RNA cleavage targeted by miRNAs and siRNAs. Mol Cell 15: 185-197.

Menendez-Benito V, Verhoef LG, Masucci MG, Dantuma NP (2005) Endoplasmic reticulum stress compromises the ubiquitin-proteasome system. Hum Mol Genet 14: 2787-2799.

Milhavet O, Casanova D, Chevallier N, McKay RD, Lehmann S (2006) Neural stem cell model for prion propagation. Stem Cells.

Milhavet O, McMahon HEM, Rachidi W, Nishida N, Katamine S, Mangé A, Arlotto M, Casanova D, Riondel J, Favier A, Lehmann S (2000) Prion infection impairs the cellular response to oxidative stress. Proc Natl Acad Sci USA 97: 13937-13942.

Miller MW, Williams ES (2003) Prion disease: horizontal prion transmission in mule deer. Nature 425: 35-36.

Mishra RS, Basu S, Gu Y, Luo X, Zou WQ, Mishra R, Li R, Chen SG, Gambetti P, Fujioka H, Singh N (2004) Protease-resistant human prion protein and ferritin are cotransported across Caco-2 epithelial cells: implications for species barrier in prion uptake from the intestine.19. J Neurosci 24: 11280-11290.

Montrasio F, Cozzio A, Flechsig E, Rossi D, Klein MA, Rülicke T, Raeber AJ, Vosshenrich CAJ, Proft J, Aguzzi A, Weissmann C (2001) B lymphocyte-restricted expression of prion protein does not enable prion replication in prion protein knockout mice. Proc Natl Acad Sci USA 98: 4034-4037.

Montrasio F, Frigg R, Glatzel M, Klein MA, Mackay F, Aguzzi A, Weissmann C (2000) Impaired prion replication in spleens of mice lacking functional follicular dendritic cells. Science 288: 1257-1259.

Morel E, Andrieu T, Casagrande F, Gauczynski S, Weiss S, Grassi J, Rousset M, Dormont D, Chambaz J (2005) Bovine Prion Is Endocytosed by Human Enterocytes via the 37 kDa/67 kDa Laminin Receptor. Am J Pathol 167: 1033-1042.

Morita E, Sundquist WI (2004) Retrovirus budding. Annu Rev Cell Dev Biol 20: 395-425.

Morshead CM, Benveniste P, Iscove NN, van der KD (2002) Hematopoietic competence is a rare property of neural stem cells that may depend on genetic and epigenetic alterations. Nat Med 8: 268-273.

Moscardini M, Pistello M, Bendinelli M, Ficheux D, Miller JT, Gabus C, Le Grice SFJ, Surewicz WK, Darlix JL (2002) Functional interactions of nucleocapsid protein of feline immunodeficiency virus and cellular prion protein with the viral RNA. J Mol Biol 318: 149-159.

Muller WE, Ushijima H, Schroder HC, Forrest JM, Schatton WF, Rytik PG, Heffner-Lauc M (1993) Cytoprotective effect of NMDA receptor antagonists on prion protein ($Prion^{Sc}$)-induced toxicity in rat cortical cell cultures. Eur J Pharmacol 246: 261-267.

Nandi PK, Leclerc E, Nicole JC, Takahashi M (2002) DNA-induced partial unfolding of prion protein leads to its polymerisation to amyloid. J Mol Biol 322: 153-161.

Naslavsky N, Stein R, Yanai A, Friedlander G, Taraboulos A (1997) Characterization of detergent-insoluble complexes containing the cellular prion protein and its scrapie isoform. J Biol Chem 272: 6324-6331.

Nguyen DG, Booth A, Gould SJ, Hildreth JE (2003) Evidence that HIV budding in primary macrophages occurs through the exosome release pathway. J Biol Chem 278: 52347-52354.

Nishida N, Harris DA, Vilette D, Laude H, Frobert Y, Grassi J, Casanova D, Milhavet O, Lehmann S (2000) Successful transmission of three mouse-adapted scrapie strains to murine neuroblastoma cell lines overexpressing wild-type mouse prion protein. J Virol 74: 320-325.

Nunes MC, Roy NS, Keyoung HM, Goodman RR, McKhann G, Jiang L, Kang J, Nedergaard M, Goldman SA (2003) Identification and isolation of multipotential neural progenitor cells from the subcortical white matter of the adult human brain. Nat Med 9: 439-447.

Oberhammer F, Wilson JW, Dive C, Morris ID, Hickman JA, Wakeling AE, Walker PR, Sikorska M (1993) Apoptotic death in epithelial cells: cleavage of DNA to 300 and/or 50 kb fragments prior to or in the absence of internucleosomal fragmentation. EMBO J 12: 3679-3684.

Oesch B, Westaway D, Walchli M, McKinley MP, Kent SB, Aebersold R, Barry RA, Tempst P, Teplow DB, Hood LE, Raeber AJ (1985) A cellular gene encodes scrapie PrP 27-30 protein. Cell 40: 735-746.

Olsen PH, Ambros V (1999) The lin-4 regulatory RNA controls developmental timing in Caenorhabditis elegans by blocking LIN-14 protein synthesis after the initiation of translation. Dev Biol 216: 671-680.

Owen F, Poulter M, Collinge J, Crow TJ (1990) Codon 129 changes in the prion protein gene in Caucasians. Am J Hum Genet 46: 1215-1216.

Paddison PJ, Caudy AA, Sachidanandam R, Hannon GJ (2004) Short hairpin activated gene silencing in mammalian cells. Methods Mol Biol 265: 85-100.

Palmer MS, Dryden AJ, Hughes JT, Collinge J (1991) Homozygous prion protein genotype predisposes to sporadic Creutzfeldt-Jakob disease. Nature 352: 340-342.

Pan K-M, Baldwin MA, Nguyen J, Gasset M, Serban A, Groth D, Mehlhorn I, Huang Z, Fletterick RJ, Cohen FE, Prusiner SB (1993) Conversion of α-helices into β-sheets features in the formation of the scrapie prion proteins. Proc Natl Acad Sci USA 90: 10962-10966.

Pan T, Wong BS, Liu T, Li R, Petersen RB, Sy MS (2002) Cell surface prion protein interacts with glycosaminoglycans. Biochem J Pt.

Parry HB (1979) Elimination of natural scrapie in sheep by sire genotype selection. Nature 277: 127-129.

Pauly PC, Harris DA (1998) Copper stimulates endocytosis of the prion protein. Journal of Biological Chemistry 273: 33107-33110.

Pear WS, Nolan GP, Scott ML, Baltimore D (1993) Production of high-titer helper-free retroviruses by transient transfection. Proc Natl Acad Sci U S A 90: 8392-8396.

Peden AH, Head MW, Ritchie DL, Bell JE, Ironside JW (2004) Preclinical vCJD after blood transfusion in a PRNP codon 129 heterozygous patient. Lancet 364: 527-529.

Peden AH, Ritchie DL, Head MW, Ironside JW (2006) Detection and Localization of PrPSc in the Skeletal Muscle of Patients with Variant, Iatrogenic, and Sporadic Forms of Creutzfeldt-Jakob Disease. Am J Pathol 168: 927-935.

Pei Y, Tuschl T (2006) On the art of identifying effective and specific siRNAs. Nat Methods 3: 670-676.

Pelchen-Matthews A, Raposo G, Marsh M (2004) Endosomes, exosomes and Trojan viruses. Trends Microbiol 12: 310-316.

Pepys MB, Bybee A, Booth DR, Bishop MT, Will RG, Little AM, Prokupek B, Madrigal JA (2003) MHC typing in variant Creutzfeldt-Jakob disease. Lancet 361: 487-489.

Peretz D, Williamson RA, Kaneko K, Vergara J, Leclerc E, Schmitt-Ulms G, Mehlhorn IR, Legname G, Wormald MR, Rudd PM, Dwek RA, Burton DR, Prusiner SB (2001) Antibodies inhibit prion propagation and clear cell cultures of prion infectivity. Nature 412: 739-743.

Perrier V, Kaneko K, Safar J, Vergara J, Tremblay P, DeArmond SJ, Cohen FE, Prusiner SB, Wallace AC (2002) Dominant-negative inhibition of prion replication in transgenic mice. Proc Natl Acad Sci U S A 99: 13079-13084.

Petersen RB, Parchi P, Richardson SL, Urig CB, Gambetti P (1996) Effect of the D178N mutation and the codon 129 polymorphism on the metabolism of the prion protein. J Biol Chem 271: 12661-12668.

Pfeifer A, Eigenbrod S, Al Khadra S, Hofmann A, Mitteregger G, Moser M, Bertsch U, Kretzschmar H (2006) Lentivector-mediated RNAi efficiently suppresses prion protein and prolongs survival of scrapie-infected mice. J Clin Invest 116: 3204-3210.

Poulter M, Baker HF, Frith CD, Leach M, Lofthouse R, Ridley RM, Shah T, Owen F, Collinge J, Brown J, Hardy J, Mullan M, Harding AE, Bennett C, Doshi B, Crow TJ (1992) Inherited prion disease with 144 base pair gene insertion: I: Genealogical and molecular studies. Brain 115: 675-685.

Priola SA, Caughey B, Race RE, Chesebro B (1994) Heterologous PrP molecules interfere with accumulation of protease-resistant PrP in scrapie-infected murine neuroblastoma cells. J Virol 68: 4873-4878.

Priola SA, Chesebro B (1995) A single hamster PrP amino acid blocks conversion to protease-resistant PrP in scrapie-infected mouse neuroblastoma cells. J Virol 69: 7754-7758.

Priola SA, Chesebro B (1998) Abnormal properties of prion protein with insertional mutations in different cell types. J Biol Chem 273: 11980-11985.

Prusiner SB, Scott M, Foster D, Pan KM, Groth D, Mirenda C, Torchia M, Yang SL, Serban D, Carlson GA, Raeber AJ (1990) Transgenetic studies implicate interactions between homologous PrP isoforms in scrapie prion replication. Cell 63: 673-686.

Race R (1991) The scrapie agent in vitro. Curr Top Microbiol Immunol 172: 181-193.

Race R, Oldstone M, Chesebro B (2000) Entry versus blockade of brain infection following oral or intraperitoneal scrapie administration: Role of prion protein expression in peripheral nerves and spleen. Journal of Virology 74: 828-833.

Race RE, Fadness LH, Chesebro B (1987) Characterization of scrapie infection in mouse neuroblastoma cells. J Gen Virol 68: 1391-1399.

Race RE, Priola SA, Bessen RA, Ernst D, Dockter J, Rall GF, Mucke L, Chesebro B, Oldstone MBA (1995) Neuron-specific expression of a hamster prion protein minigene in transgenic mice induces susceptibility to hamster scrapie agent. Neuron 15: 1183-1191.

Raeber AJ, Brandner S, Klein MA, Benninger Y, Musahl C, Frigg R, Roeckl C, Fischer MB, Weissmann C, Aguzzi A (1998) Transgenic and knockout mice in research on prion diseases. Brain pathol 8: 715-733.

Raymond GJ, Olsen EA, Lee KS, Raymond LD, Bryant PK, III, Baron GS, Caughey WS, Kocisko DA, McHolland LE, Favara C, Langeveld JP, van Zijderveld FG, Mayer RT, Miller MW, Williams ES, Caughey B (2006) Inhibition of protease-resistant prion protein formation in a transformed deer cell line infected with chronic wasting disease. J Virol 80: 596-604.

Reynolds A, Leake D, Boese Q, Scaringe S, Marshall WS, Khvorova A (2004) Rational siRNA design for RNA interference. Nat Biotechnol 22: 326-330.

Reynolds BA, Tetzlaff W, Weiss S (1992) A multipotent EGF-responsive striatal embryonic progenitor cell produces neurons and astrocytes. J Neurosci 12: 4565-4574.

Reynolds BA, Weiss S (1992) Generation of neurons and astrocytes from isolated cells of the adult mammalian central nervous system. Science 255: 1707-1710.

Riek R, Hornemann S, Wider G, Billeter M, Glockshuber R, Wuthrich K (1996) NMR structure of the mouse prion protein domain PrP (121-231). Nature 382: 180-182.

Roikhel VM, Fokina GI, Lisak VM, Kondakova LI, Korolev MB, Pogodina VV (1987) Persistence of the scrapie agent in glial cells from rat Gasserian ganglion. Acta Virol Praha 31: 36-42.

Rossner MJ, Dorr J, Gass P, Schwab MH, Nave KA (1997) SHARPs: mammalian enhancer-of-split- and hairy-related proteins coupled to neuronal stimulation. Mol Cell Neurosci 9: 460-475.

Roucou X, LeBlanc AC (2005) Cellular prion protein neuroprotective function: implications in prion diseases. J Mol Med 83: 3-11.

Rubenstein R, Carp RI, Callahan SM (1984) In vitro replication of scrapie agent in a neuronal model: infection of PC12 cells. J Gen Virol 65: 2191-2198.

Ryder S, Dexter G, Bellworthy S, Tongue S (2004) Demonstration of lateral transmission of scrapie between sheep kept under natural conditions using lymphoid tissue biopsy. Res Vet Sci 76: 211-217.

Saborio GP, Permanne B, Soto C (2001) Sensitive detection of pathological prion protein by cyclic amplification of protein misfolding. Nature 411: 810-813.

Saetrom P, Snove O, Jr. (2004) A comparison of siRNA efficacy predictors. Biochem Biophys Res Commun 321: 247-253.

Safar J, Wille H, Itri V, Groth D, Serban H, Torchia M, Cohen FE, Prusiner SB (1998) Eight prion strains PrP^{Sc} molecules with different conformations. Nat Med 4: 1157-1165.

Sanchez-Valle R, Saiz A, Graus F (2002) 14-3-3 Protein isoforms and atypical patterns of the 14-3-3 assay in the diagnosis of Creutzfeldt-Jakob disease.368. Neurosci Lett 320: 69-72.

Santuccione A, Sytnyk V, Leshchyns'ka I, Schachner M (2005) Prion protein recruits its neuronal receptor NCAM to lipid rafts to activate p59fyn and to enhance neurite outgrowth. J Cell Biol 169: 341-354.

Schatzl HM, Laszlo L, Holtzman DM, Tatzelt J, DeArmond SJ, Weiner RI, Mobley WC, Prusiner SB (1997) A hypothalamic neuronal cell line persistently infected with scrapie prions exhibits apoptosis. J Virol 71: 8821-8831.

Schmitt-Ulms G, Legname G, Baldwin MA, Ball HL, Bradon N, Bosque PJ, Crossin KL, Edelman GM, DeArmond SJ, Cohen FE, Prusiner SB (2001) Binding of neural cell adhesion molecules (N-CAMs) to the cellular prion protein. Journal of Molecular Biology 314: 1209-1225.

Scott MR, Groth D, Tatzelt J, Torchia M, Tremblay P, DeArmond SJ, Prusiner SB (1997) Propagation of prion strains through specific conformers of the prion protein. J Virol 71: 9032-9044.

Seggerson K, Tang L, Moss EG (2002) Two genetic circuits repress the Caenorhabditis elegans heterochronic gene lin-28 after translation initiation. Dev Biol 243: 215-225.

Shmerling D, Hegyi I, Fischer M, Blättler T, Brandner S, Götz J, Rülicke T, Flechsig E, Cozzio A, von Mering C, Hangartner C, Aguzzi A, Weissmann C (1998) Expression of amino-terminally truncated PrP in the mouse leading to ataxia and specific cerebellar lesions. Cell 93: 203-214.

Shyng S-L, Heuser JE, Harris DA (1994) A glycolipid-anchored prion protein is endocytosed via clathrin- coated pits. J Cell Biol 125: 1239-1250.

Sigurdsson EM, Brown DR, Daniels M, Kascsak RJ, Kascsak R, Carp R, Meeker HC, Frangione B, Wisniewski T (2002) Immunization delays the onset of prion disease in mice. Am J Pathol 161: 13-17.

Silveira JR, Raymond GJ, Hughson AG, Race RE, Sim VL, Hayes SF, Caughey B (2005) The most infectious prion protein particles. Nature 437: 257-261.

Siso S, Puig B, Varea R, Vidal E, Acin C, Prinz M, Montrasio F, Badiola J, Aguzzi A, Pumarola M, Ferrer I (2002) Abnormal synaptic protein expression and cell death in murine scrapie. Acta Neuropathol (Berl) 103: 615-626.

Solassol J, Crozet C, Lehmann S (2003) Prion propagation in cultured cells. Br Med Bull 66: 87-97.

Solforosi L, Criado JR, McGavern DB, Wirz S, Sanchez-Alavez M, Sugama S, DeGiorgio LA, Volpe BT, Wiseman E, Abalos G, Masliah E, Gilden D, Oldstone MB, Conti B, Williamson RA (2004) Cross-Linking Cellular Prion Protein Triggers Neuronal Apoptosis in Vivo. Science.

Spielhaupter C, Schatzl HM (2001) PrPC directly interacts with proteins involved in signaling pathways. J Biol Chem 276: 44604-44612.

Stahl N, Borchelt DR, Prusiner SB (1990) Differential release of cellular and scrapie prion proteins from cellular membranes by phosphatidylinositol-specific phospholipase. Biochemistry 29: 5405-5412.

Steele AD, Emsley JG, Ozdinler PH, Lindquist S, Macklis JD (2006) Prion protein (PrPc) positively regulates neural precursor proliferation during developmental and adult mammalian neurogenesis. Proc Natl Acad Sci U S A.

Stephenson DA, Chiotti K, Ebeling C, Groth D, DeArmond SJ, Prusiner SB, Carlson GA (2000) Quantitative trait loci affecting prion incubation time in mice. Genomics 69: 47-53.

Stockel J, Hartl FU (2001) Chaperonin-mediated de novo generation of prion protein aggregates. J Mol Biol 313: 861-872.

Stoorvogel W, Kleijmeer MJ, Geuze HJ, Raposo G (2002) The biogenesis and functions of exosomes. Traffic 3: 321-330.

Tabara H, Sarkissian M, Kelly WG, Fleenor J, Grishok A, Timmons L, Fire A, Mello CC (1999) The rde-1 gene, RNA interference, and transposon silencing in C. elegans. Cell 99: 123-132.

Tahiri-Alaoui A, Gill AC, Disterer P, James W (2004) Methionine 129 variant of human prion protein oligomerizes more rapidly than the valine 129 variant: Implications for disease susceptibility to CJD. J Biol Chem.

Taraboulos A, Raeber A, Borchelt DR, Serban D, Prusiner SB (1992) Synthesis and trafficking of prion proteins in cultured cells. Mol Biol of the Cell 3: 851-863.

Taraboulos A, Serban D, Prusiner SB (1990) Scrapie prion proteins accumulate in the cytoplasm of persistently infected cultured cells. J Cell Biol 110: 2117-2132.

Taylor DR, Hooper NM (2006) The low-density lipoprotein receptor-related protein 1 (LRP1) mediates the endocytosis of the cellular prion protein. Biochem J.

Telling GC, Scott M, Hsiao KK, Foster D, Yang S-L, Torchia M, Sidle KCL, Collinge J, DeArmond SJ, Prusiner SB (1994) Transmission of Creutzfeldt-Jakob disease from humans to transgenic mice expressing chimeric human-mouse prion protein. Proc Natl Acad Sci USA 91: 9936-9940.

Telling GC, Scott M, Mastrianni J, Gabizon R, Torchia M, Cohen FE, DeArmond SJ, Prusiner SB (1995) Prion propagation in mice expressing human and chimeric PrP transgenes implicates the interaction of cellular PrP with another protein. Cell 83: 79-90.

Thery C, Zitvogel L, Amigorena S (2002) Exosomes: composition, biogenesis and function. Nat Rev Immunol 2: 569-579.

Thornberry NA, Lazebnik Y (1998) Caspases: enemies within. Science 281: 1312-1316.

Tilly G, Chapuis J, Vilette D, Laude H, Vilotte JL (2003) Efficient and specific down-regulation of prion protein expression by RNAi. Biochem Biophys Res Commun 305: 548-551.

Trevitt CR, Collinge J (2006) A systematic review of prion therapeutics in experimental models. Brain.

Uchida N, Buck DW, He D, Reitsma MJ, Masek M, Phan TV, Tsukamoto AS, Gage FH, Weissman IL (2000) Direct isolation of human central nervous system stem cells. Proc Natl Acad Sci U S A 97: 14720-14725.

Van der KD, Weiss S (2000) Why stem cells? Science 287: 1439-1441.

Van Keulen LJ, Schreuder BE, Meloen RH, Mooij-Harkes G, Vromans ME, Langeveld JP (1996) Immunohistochemical detection of prion protein in lymphoid tissues of sheep with natural scrapie. J Clin Microbiol 34: 1228-1231.

Van Niel G, Porto-Carreiro I, Simoes S, Raposo G (2006) Exosomes: a common pathway for a specialized function. J Biochem (Tokyo) 140: 13-21.

Vana K, Weiss S (2006) A Trans-dominant Negative 37kDa/67kDa Laminin Receptor Mutant Impairs PrP(Sc) Propagation in Scrapie-infected Neuronal Cells. J Mol Biol.

Vassallo N, Herms J (2003) Cellular prion protein function in copper homeostasis and redox signalling at the synapse. J Neurochem 86: 538-544.

Vescovi AL, Parati EA, Gritti A, Poulin P, Ferrario M, Wanke E, Frolichsthal-Schoeller P, Cova L, Arcellana-Panlilio M, Colombo A, Galli R (1999) Isolation and cloning of multipotential stem cells from the embryonic human CNS and establishment of transplantable human neural stem cell lines by epigenetic stimulation. Exp Neurol 156: 71-83.

Vey M, Pilkuhn S, Wille H, Nixon R, DeArmond SJ, Smart EJ, Anderson RGW, Taraboulos A, Prusiner SB (1996) Subcellular colocalization of the cellular and scrapie prion proteins in caveolae-like membranous domains. Proc Natl Acad Sci USA 93: 14945-14949.

Vilette D, Andreoletti O, Archer F, Madelaine MF, Vilotte JL, Lehmann S, Laude H (2001b) *Ex vivo* propagation of infectious sheep scrapie agent in heterologous epithelial cells expressing ovine prion protein. Proc Natl Acad Sci USA 98: 4055-4059.

Vilette D, Andreoletti O, Archer F, Madelaine MF, Vilotte JL, Lehmann S, Laude H (2001a) Ex vivo propagation of infectious sheep scrapie agent in heterologous epithelial cells expressing ovine prion protein. Proceedings of the National Academy of Sciences of the United States of America 98: 4055-4059.

Villa A, Navarro-Galve B, Bueno C, Franco S, Blasco MA, Martinez-Serrano A (2004) Long-term molecular and cellular stability of human neural stem cell lines. Exp Cell Res 294: 559-570.

Vollmert C, Windl O, Xiang W, Rosenberger A, Zerr I, Wichmann HE, Bickeboller H, Illig T, Kretzschmar HA (2006) Significant association of a M129V independent polymorphism in the 5' UTR of the PRNP gene with sporadic Creutzfeldt-Jakob disease in a large German case-control study. J Med Genet 43: e53.

Vorberg I, Groschup MH, Pfaff E, Priola SA (2003) Multiple Amino Acid Residues within the Rabbit Prion Protein Inhibit Formation of Its Abnormal Isoform. J Virol 77: 2003-2009.

Vorberg I, Raines A, Priola SA (2004a) Acute formation of protease-resistant prion protein does not always lead to persistent scrapie infection in vitro. J Biol Chem.

Vorberg I, Raines A, Priola SA (2004b) Acute formation of protease-resistant prion protein does not always lead to persistent scrapie infection in vitro. J Biol Chem 279: 29218-29225.

Vorberg I, Raines A, Story B, Priola SA (2004d) Susceptibility of common fibroblast cell lines to transmissible spongiform encephalopathy agents. J Infect Dis 189: 431-439.

Vorberg I, Raines A, Story B, Priola SA (2004c) Susceptibility of common fibroblast cell lines to transmissible spongiform encephalopathy agents. J Infect Dis 189: 431-439.

Wadsworth JD, Joiner S, Fox K, Linehan JM, Desbruslais M, Brandner S, Asante EA, Collinge J (2006) Prion infectivity in vCJD rectum. Gut.

Wadsworth JDF, Joiner S, Hill AF, Campbell TA, Desbruslais M, Luthert PJ, Collinge J (2001) Tissue distribution of protease resistant prion protein in variant CJD using a highly sensitive immuno-blotting assay. Lancet 358: 171-180.

Wall NR, Shi Y (2003) Small RNA: can RNA interference be exploited for therapy? Lancet 362: 1401-1403.

Ward HJ, Everington D, Croes EA, Alperovitch A, Delasnerie-Laupretre N, Zerr I, Poser S, van Duijn CM (2002) Sporadic Creutzfeldt-Jakob disease and surgery: a case-control study using community controls. Neurology 59: 543-548.

Watt NT, Hooper NM (2003) The prion protein and neuronal zinc homeostasis. Trends Biochem Sci 28: 406-410.

Weiss S, Dunne C, Hewson J, Wohl C, Wheatley M, Peterson AC, Reynolds BA (1996) Multipotent CNS stem cells are present in the adult mammalian spinal cord and ventricular neuroaxis. J Neurosci 16: 7599-7609.

Weissmann C (1999) Knockout, Transgenics and Transplants in Prion Research. In: Prion Biology and Diseases (Prusiner SB, ed), pp 273-305. CSHL.

Weissmann C (1991) A 'unified theory' of prion propagation. Nature 352: 679-683.

Weissmann C (2004) The state of the prion2. Nat Rev Microbiol 2: 861-871.

Weissmann C, Aguzzi A (1997) Bovine spongiform encephalopathy and early onset variant Creutzfeldt-Jakob disease. Curr Opin Neurobiol 7: 695-700.

Weissmann C, Flechsig E (2003) PrP knock-out and PrP transgenic mice in prion research. Br Med Bull 66: 43-60.

White AR, Enever P, Tayebi M, Mushens R, Linehan J, Brandner S, Anstee D, Collinge J, Hawke S (2003) Monoclonal antibodies inhibit prion replication and delay the development of prion disease. Nature 422: 80-83.

Wilesmith JW, Wells GA, Cranwell MP, Ryan JB (1988) Bovine spongiform encephalopathy: epidemiological studies. Vet Rec 123: 638-644.

Will RG, Alpers MP, Dormont D, Schonberger LB (2004) Infectious and Sporadic Prion Diseases. In: Prion Biology and Disease (Prusiner SB, ed), pp 629-671. CSHL.

Will RG, Ironside JW, Zeidler M, Cousens SN, Estibeiro K, Alperovitch A, Poser S, Pocchiari M, Hofman A, Smith PG (1996) A new variant of Creutzfeldt-Jakob disease in the UK. Lancet 347: 921-925.

Williams BR (1997) Role of the double-stranded RNA-activated protein kinase (PKR) in cell regulation. Biochem Soc Trans 25: 509-513.

Windl O, Dempster M, Estibeiro JP, Lathe R, De Silva R, Esmonde T, Will R, Springbett A, Campbell TA, Sidle KCL, Palmer MS, Collinge J (1996) Genetic basis of Creutzfeldt-Jakob disease in the United Kingom: a systematic analysis of predisposing mutations and allelic variation in the *PRNP* gene. Hum Genet 98: 259-264.

Windl O, Dempster M, Estibeiro P, Lathe R (1995) A candidate marsupial *PrP* gene reveals two domains conserved in mammalian PrP proteins. Gene 159: 181-186.

Wong C, Xiong LW, Horiuchi M, Raymond L, Wehrly K, Chesebro B, Caughey B (2001) Sulfated glycans and elevated temperature stimulate PrP^{Sc}-dependent cell-free formation of protease-resistant prion protein. EMBO J 20: 377-386.

Wopfner F, Weidenhöfer G, Schneider R, Von Brunn A, Gilch S, Schwarz TF, Werner T, Schätzl M (1999) Analysis of 27 mammalian and 9 avian PrPs reveals high conservation of flexible regions of the prion protein. Journal of Molecular Biology 289: 1163-1178.

Wroe SJ, Pal S, Siddique D, Hyare H, Macfarlane R, Joiner S, Linehan JM, Brandner S, Wadsworth JD, Hewitt P, Collinge J (2006) Clinical presentation and pre-mortem diagnosis of variant Creutzfeldt-Jakob disease associated with blood transfusion: a case report. Lancet 368: 2061-2067.

Yedidia Y, Horonchik L, Tzaban S, Yanai A, Taraboulos A (2001) Proteasomes and ubiquitin are involved in the turnover of the wild-type prion protein. EMBO J 20: 5383-5391.

Yoo BC, Krapfenbauer K, Cairns N, Belay G, Bajo M, Lubec G (2002) Overexpressed protein disulfide isomerase in brains of patients with sporadic Creutzfeldt-Jakob disease. Neurosci Lett 334: 196-200.

Yu JY, DeRuiter SL, Turner DL (2002) RNA interference by expression of short-interfering RNAs and hairpin RNAs in mammalian cells. Proc Natl Acad Sci U S A 99: 6047-6052.

Zamore PD, Tuschl T, Sharp PA, Bartel DP (2000) RNAi: double-stranded RNA directs the ATP-dependent cleavage of mRNA at 21 to 23 nucleotide intervals. Cell 101: 25-33.

Zanata SM, Lopes MH, Mercadante AF, Hajj GN, Chiarini LB, Nomizo R, Freitas AR, Cabral AL, Lee KS, Juliano MA, De Oliveira E, Jachieri SG, Burlingame A, Huang L, Linden R, Brentani RR, Martins VR (2002) Stress-inducible protein 1 is a cell surface ligand for cellular prion that triggers neuroprotection27. EMBO J 21: 3307-3316.

Zhang CC, Steele AD, Lindquist S, Lodish HF (2006) Prion protein is expressed on long-term repopulating hematopoietic stem cells and is important for their self-renewal. Proc Natl Acad Sci U S A 103: 2184-2189.

Appendices

1 Appendix - Neural stem cell culture

1.1 Neural stem cell culture medium (500 ml)

483.5 ml	DMEM/F12
10 ml	50x B27
5 ml	L-Glutamine (200 mM)
1ml	Heparin sodium mucous (5000 I.U/ml; CP Pharmaceuticals Ltd.)
0.5 ml	Gentamycin (50 mg/ml)

1.2 Growth factors

1.2.1 Epidermal growth factor (EGF; Sigma): 10 µg/ml stock recipe

Aseptically reconstitute 0.2 mg EGF powder with 20 ml filter-sterilised 10mM acetic acid, containing 0.1% human serum albumin (HSA; Sigma). Store aliquots at -20°C for 3 months. Store defrosted aliquots at 4°C for 2 weeks. Use at 20 ng/ml final concentration.

1.2.2 Basic fibroblast growth factor (bFGF; Peprotech): 10 µg/ml stock recipe

Aseptically reconstitute 25 µg bFGF powder in 2.5 ml DMEM/F12 containing 0.1% HSA. Store aliquots at -20°C for 3 months. Store defrosted aliquots at 4°C for 2 weeks. Use at 10 ng/ml final concentration.

1.3 Trituration solution (100ml)

55 mg	soybean trypsin inhibitor (Sigma)
3.3 ml	30% HSA (Sigma)
96.7 ml	DMEM/F12

Sterilise by passing through 0.2 µm filter

2 Appendix - Bacterial culture

2.1 Luria Bertani (LB) medium (1L)

Tryptone	10g
Yeast Extract	5g
NaCl	10g

Gently shake the above ingredients and add

5N NaOH	0.2ml to adjust to pH7

Add ddH_2O to a final volume of 1L (in 2L flask)

Very briefly and gently stir (at setting 1 on magnetic stirrer)

Sterilise by autoclaving at 121°C

2.2 LB agar (1L)

Tryptone	10g
Yeast Extract	5g
NaCl	10g
5N NaOH	0.2ml
Bactoagar	15g

Adjust to 1L with ddH_2O in a 2L flask

Very briefly and gently stir (at setting 1 on magnetic stirrer)

Autoclave at 121°C

Put in oven @ 55-60°C to cool but not set

Add 100 µg/ml ampicillin

Pour into petri dishes

3 Appendix - Buffers

3.1 2x SDS-PAGE sample buffer

125mM	Tris-HCl
20% (v/v)	glycerol
4%	SDS
0.025% (w/v)	bromophenol blue
pH 6.8	

3.2 Deglycosylation buffer

4mM	AEBSF
1.25%	Nonidet -P40

Made up in sodium phosphate buffer, pH7 (see **appendix 3.3**)

3.3 Sodium phosphate buffer

50mM	Na_2HPO_4,
1mM	EDTA
pH7	

3.4 SDS-PAGE running buffer (National Diagnostics)

25 mM	Tris-HCl pH 8.0
192 mM	glycine
0.1%	SDS

3.5 Electroblotting buffer (National Diagnostics)

25 mM	Tris-HCl pH 8.0
192 mM	glycine
20%	methanol

3.6 TBST

10 mM	Tris-HCl, pH 8.0
150 mM	NaCl
0.1%	Tween 20

3.7 PBST

1x	PBS
0.05%	Tween 20

3.8 Tropix assay buffer

20mM	Tris-HCl
1mM	$MgCl_2$
pH 9.8	

3.9 Lysis buffer

50 mM	Tris.HCl, pH 8
150 mM	NaCl
0.5%	Na deoxycholate
0.5%	Triton X-100

Sterilise by passing through a 0.2µm filter for treatment of brain homogenate prior to cell infection

4 Appendix - Plasmid vectors

4.1 Human PrP expression vectors

Restriction sites used to clone the human PrP ORF into pCDNA 3.1 (**A**) and pLNCX2 (**B**) are shown in red.

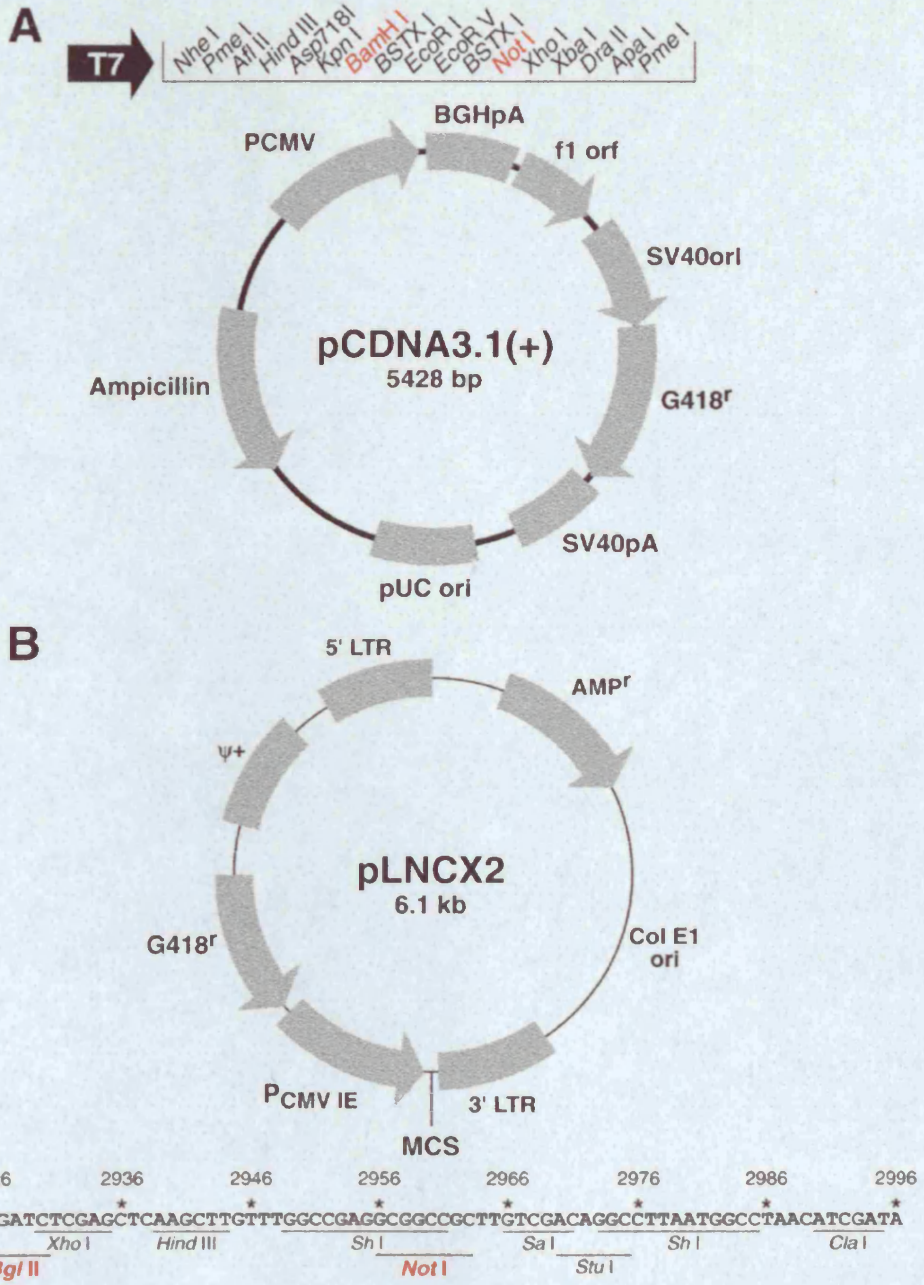

4.2 siRNA retroviral expression vectors

Restriction sites used to clone shRNA into pSuper.retro (**A**) and pMSCV (**B**) are shown in red.

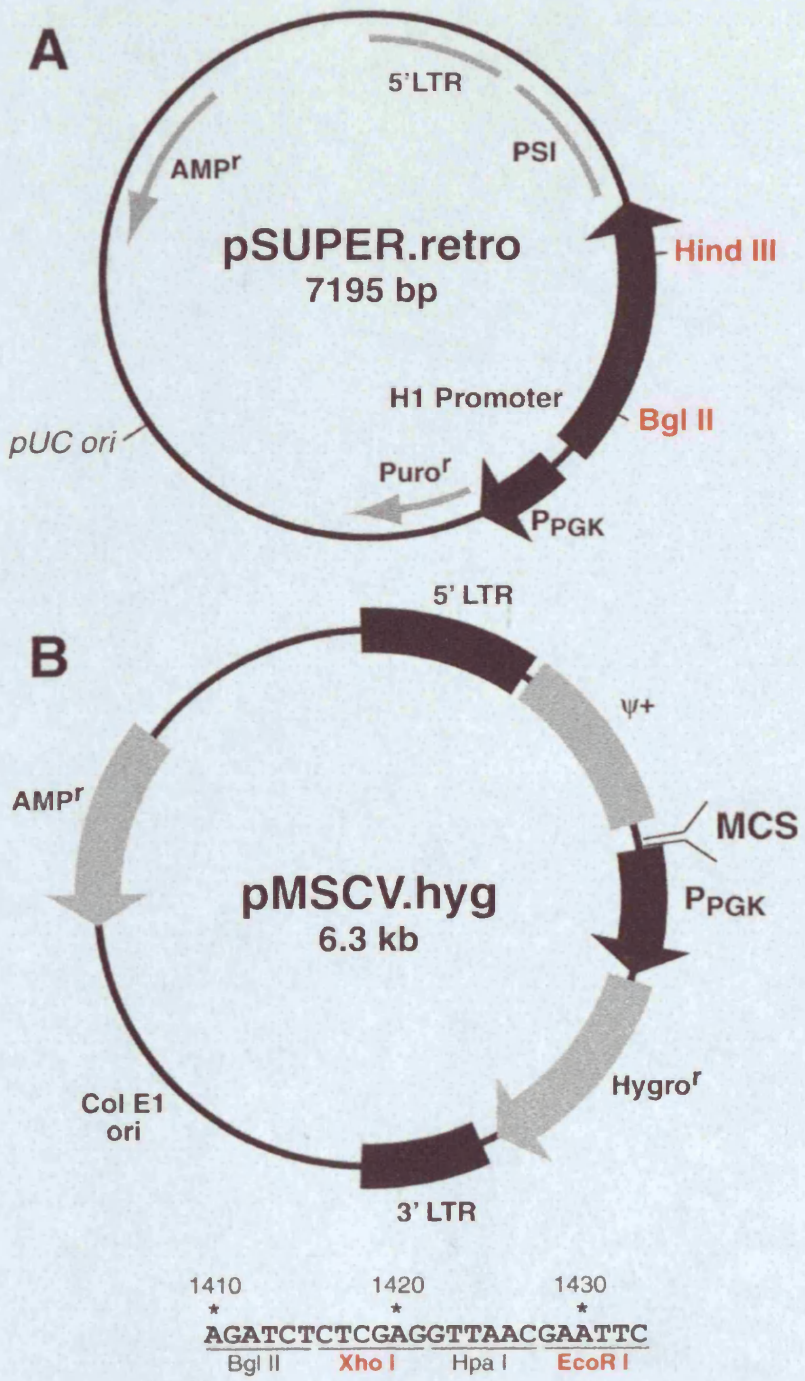

5 Human *PRNP* primers

Human *PRNP* DNA and amino acid sequence are shown; forward primers are shown by red arrows and reverse primers in blue arrows. For PCR amplification of genomic human *PRNP*, primers outside the open reading frame, 106 and 46 were used. Primers 3, 10, 122, 33 and 125 were used for sequencing.

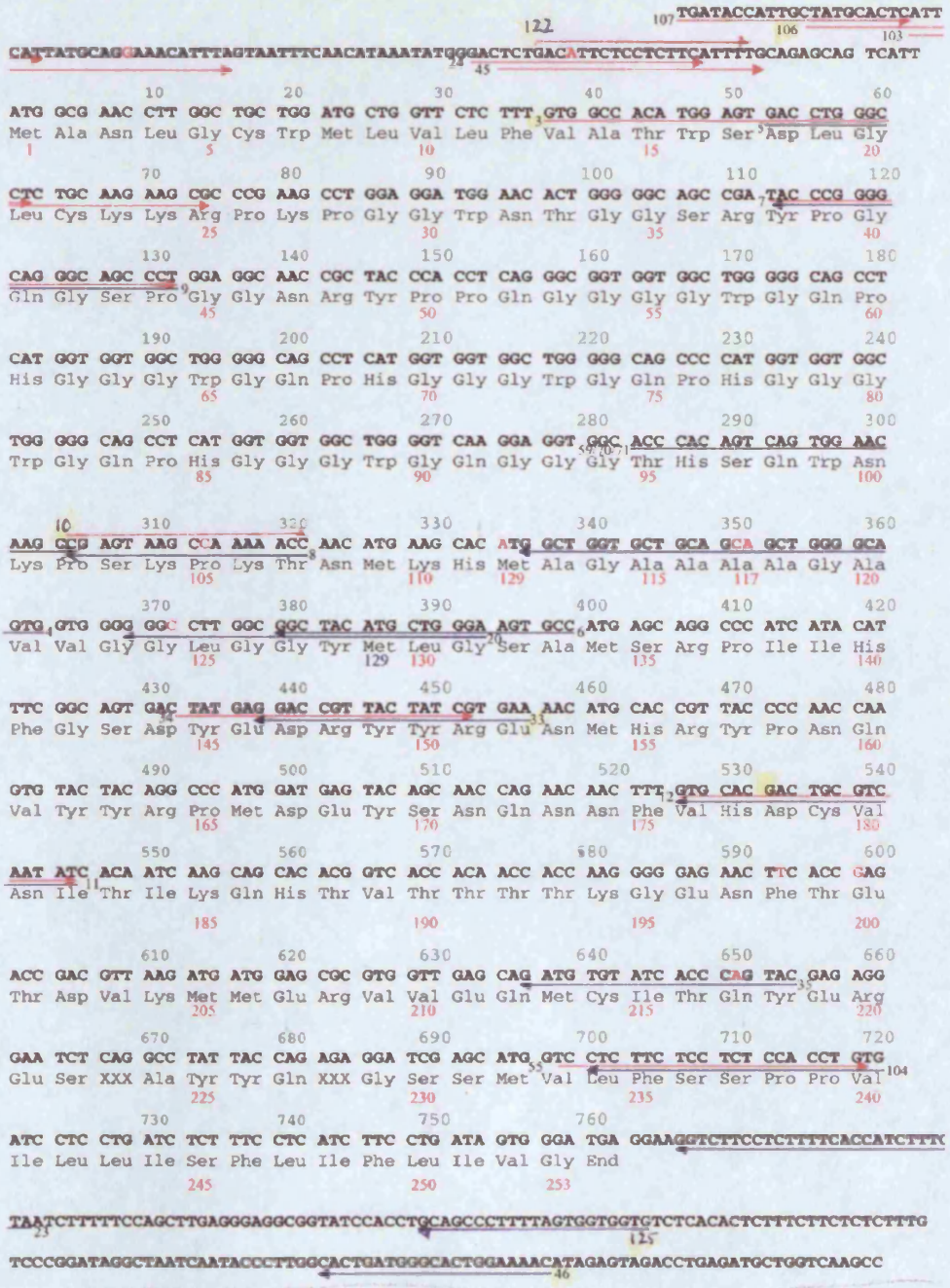

6 Transmissibility of vCJD inoculum (12811) to wild-type SJL mice

Brain section from mouse (SJL strain) infected with 1% 12811 vCJD inoculum 360 days post-infection.

A Haematoxylin and eosin staining

B GFAP staining demonstrating widespread gliosis

C Anti-PrP monoclonal antibody (ICSM35) staining demonstrating diffuse PrP^{Sc} staining

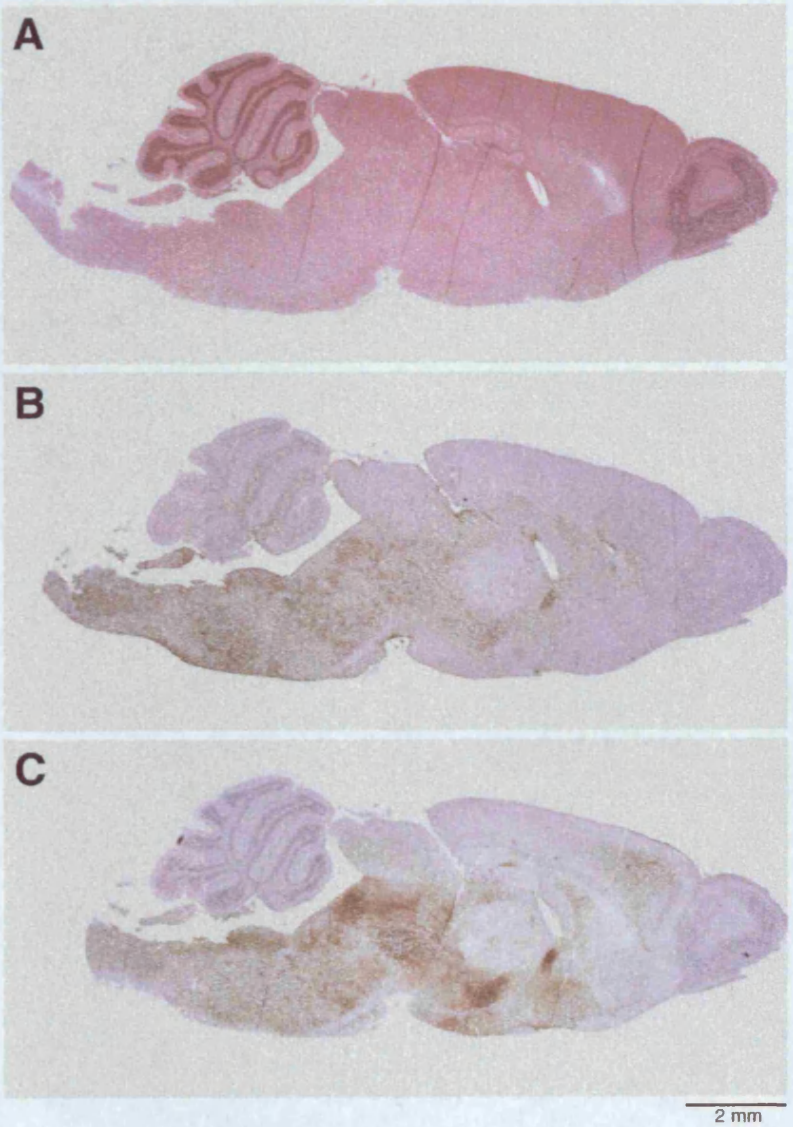

7 Human *PRNP* ORF sequence

Example electropherogram of human *PRNP* ORF construct to demonstrate no mutations and methionine homozygosity at codon 129 (red box).

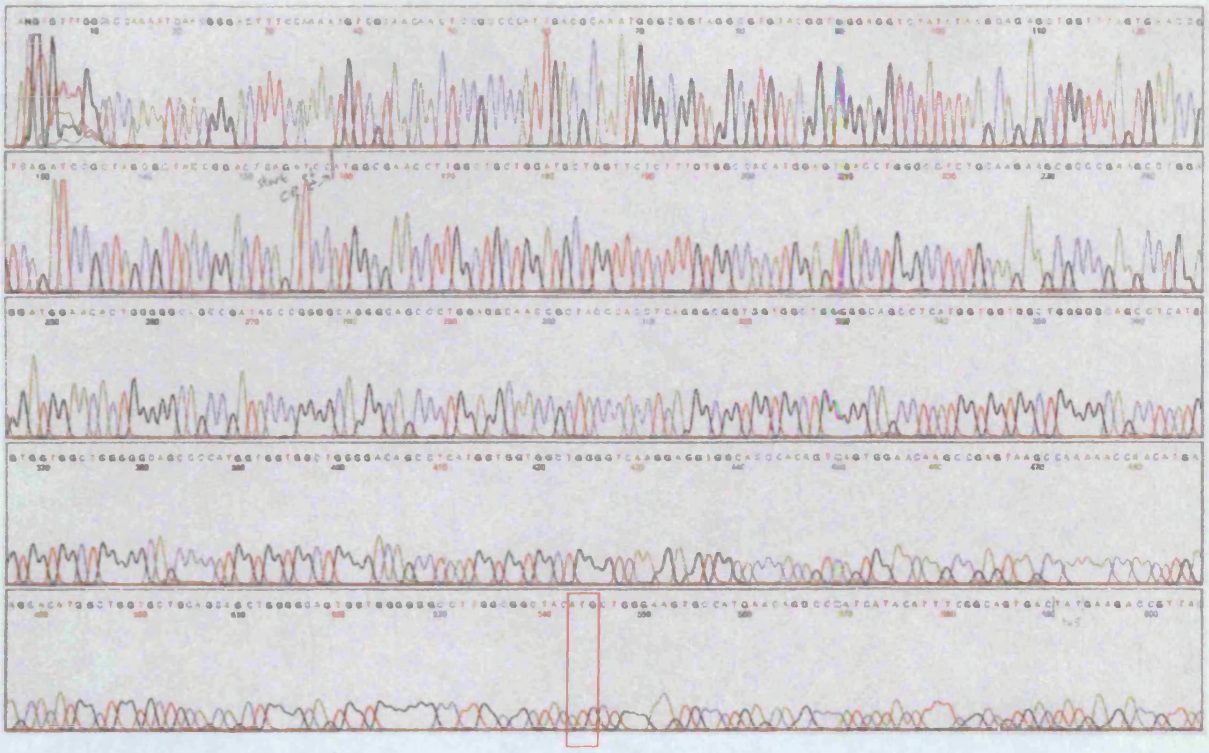

Codon129 Met